

MIT/WHOI 2007-10

**Massachusetts Institute of Technology  
Woods Hole Oceanographic Institution**



**Joint Program  
in Oceanography/  
Applied Ocean Science  
and Engineering**



---

**DOCTORAL DISSERTATION**

Geochemistry of Slow-Growing Corals:  
Reconstructing Sea Surface Temperature, Salinity and  
the North Atlantic Oscillation

by

Nathalie Fairbank Goodkin

June 2007

**20070927459**

MIT/WHOI

2007-10

**Geochemistry of Slow-Growing Corals:  
Reconstructing Sea Surface Temperature, Salinity and the North Atlantic Oscillation**

by

Nathalie Fairbank Goodkin

Massachusetts Institute of Technology  
Cambridge, Massachusetts 02139

and

Woods Hole Oceanographic Institution  
Woods Hole, Massachusetts 02543

June 2007

**DOCTORAL DISSERTATION**

Funding was provided by National Science Foundation grant OCE-0402728, Stanley W. Watson Foundation Fellowship, Paul M. Fye Teaching Fellowship, and the Ocean and Climate Change Institute Fellowship.

Reproduction in whole or in part is permitted for any purpose of the United States Government. This thesis should be cited as: Nathalie Fairbank Goodkin, 2007. Geochemistry of Slow-Growing Corals: Reconstructing Sea Surface Temperature, Salinity and the North Atlantic Oscillation. Ph.D. Thesis. MIT/WHOI. 2007-10.

Approved for publication; distribution unlimited.

Approved for Distribution:



Ken O. Buesseler, Chair

Department of Marine Chemistry and Geochemistry



Paola Malanotte-Rizzoli  
MIT Director of Joint Program



James A. Yoder  
WHOI Dean of Graduate Studies



Geochemistry of Slow-Growing Corals: Reconstructing Sea Surface Temperature, Salinity and  
the North Atlantic Oscillation

by

Nathalie Fairbank Goodkin

A. B. *cum laude* in Chemistry  
Harvard College, 2000

SUBMITTED TO THE DEPARTMENT OF EARTH ATMOSPHERIC AND  
PLANETARY SCIENCES IN PARTIAL FULFILLMENT OF THE REQUIREMENTS  
FOR THE DEGREE OF

*DOCTOR OF PHILOSOPHY* IN CHEMICAL OCEANOGRAPHY

at the

MASSACHUSETTS INSTITUTE OF TECHNOLOGY  
and  
WOODS HOLE OCEANOGRAPHIC INSTITUTION

June 2007

© Nathalie Fairbank Goodkin, 2007. All rights reserved.

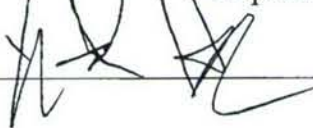
The author hereby grants MIT and WHOI permission to reproduce and distribute paper  
and electronic copies of this thesis document in whole or in part.

Signature of Author:



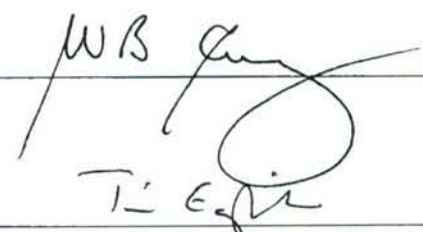
Department of Earth, Atmosphere and Planetary Sciences  
February 27, 2007

Certified by:



Konrad A. Hughen  
Associate Scientist  
Thesis Co-Supervisor

Certified by:



William B. Curry  
Senior Scientist  
Thesis Co-Supervisor

Accepted by:



Timothy Eglinton  
Chair, Joint Committee for Chemical Oceanography  
Woods Hole Oceanographic Institution



## Abstract

A 225-year old coral from the south shore of Bermuda (64°W, 32°N) provides a record of decadal-to-centennial scale climate variability. The coral was collected live, and sub-annual density bands seen in x-radiographs delineate cold and warm seasons allowing for precise dating. Coral skeletons incorporate strontium (Sr) and calcium (Ca) in relative proportions inversely to the sea surface temperature (SST) in which the skeleton is secreted.  $\delta^{18}\text{O}$  of the coral skeleton changes based on both temperature and the  $\delta^{18}\text{O}$  of sea water ( $\delta\text{O}_w$ ), and  $\delta\text{O}_w$  is proportional to sea surface salinity (SSS).

Understanding long-term climate variability requires the reconstruction of key climate parameters, such as sea surface temperature (SST) and salinity, in records extending beyond the relatively short instrumental period. The high accretion rates, longevity, and skeletal growth bands found in coral skeletons make them an ideal resource for well-dated, seasonal climate reconstructions. Growing between 2 and 6 mm/year and reaching more than 1m in length, slow-growing corals provide multi-century records from one colony. Additionally, unlike the fast growing (10-20 mm/year) species *Porites*, slow-growing species are generally found in both tropical and sub-tropical locations greatly expanding the geographical location of these records.

A high resolution record (HRR, ~11 samples per year) was drilled for the entire length of the coral record (218 years). Samples were split and Sr/Ca,  $\delta^{18}\text{O}$ , and  $\delta^{13}\text{C}$  were measured for each sample. Sr/Ca was used to reconstruct winter time and mean-annual SST. Oxygen isotopic measurements were used to determine directional salinity changes, in conjunction with Sr/Ca based SST reconstructions. Winter-time and mean annual SSTs show SSTs ~1.5 °C colder during the end of the Little Ice Age (LIA) relative to today. Simultaneously, SSS is fresher during that time.

Sr/Ca based climate reconstructions from coral skeletons have been met with some skepticism because some reconstructions show temperature changes back in time that are 2-4 times greater than the reconstructions of other marine proxies. In this study, we show that when using bulk-sampled, slow-growing corals, two steps are critical to producing accurate reconstructions: 1) incorporating growth rate into multi-variant regressions with SST and Sr/Ca and 2) using multiple colonies that grew at the same time with varying average growth rates and Sr/Ca. Application of these novel methods over the period of the instrumental record from Hydrostation S (monthly since 1954, 32°10'N, 64°30'W) reduces the root mean square of the residuals between the reconstructed SST and the instrumental SST by as much as 1.52°C to 0.46°C for three coral colonies.

Winter-time SSTs at Bermuda are correlated to phases of the North Atlantic Oscillation (NAO), a meridional oscillation in atmospheric mass. Much uncertainty remains about the relationship between the NAO and the ocean, and one critical outstanding question is whether anthropogenic changes are perturbing the system. Using winter Sr/Ca as a proxy for temperature, we show strong coherence to the NAO at multi-decadal and inter-annual frequencies. These coral records show significant changes in variance in the NAO during the late 20<sup>th</sup> century compared to the cooler LIA, but limited changes in the mean phase (positive or negative) of the NAO, implying that climate change may be pushing the NAO to extremes but not to a new mean position.



## Acknowledgements

Three WHOI fellowships supported my time in the Joint Program: Stanley W. Watson Foundation Fellowship, Paul M. Fye Teaching Fellowship and the Ocean and Climate Change Institute Fellowship (OCCI). Research funding from NSF (OCE-0402728) and WHOI to Konrad Hughen, Anne Cohen, and Michael McCartney supported this project. Research support was also awarded to the author from the OCCI and the education office Ditty Bag Fund.

The coral samples used in this project were collected with funding to Anne Cohen and Michael McCartney. The corals were collected by A. Cohen, S. R. Smith, G. Piniak, J. Pitt, and others at the Bermuda Institute of Ocean Science (BIOS, formerly BBSR). This coral has proved to have been an amazing reservoir of historical, geochemical proxies and I am grateful to have been given access to them.

Konrad Hughen, William Curry, Edward Boyle and Scott Doney all served as committee members for my thesis. Each of them proved to be an asset during this process. Konrad has contributed extensively to this work through his own ideas and through the enthusiastic encouragement of mine. Bill contributed significantly to my education by teaching me among other things how to methodically evaluate the quality of my data – leaving no stone unturned. Ed and Scott have generously contributed beyond the level of expectation for committee members, also exposing me to projects beyond my thesis.

The analysis in this thesis both measurements and quantitative analysis would not have been completed without help and guidance of Dorinda Ostermann, Andy Solow, Peter Huybers, Tom Farrar, and David Glover. Naomi Levine and Greg Gerbi patiently taught me how to use Matlab – from across the Atlantic. Mark Kurtz provided me with office space and a lot of patient advice over the four plus years, which I will always appreciate. Thank you to you all.

The technical and support staff at WHOI is truly unmatched and very generous to the students. On the fourth floor of Clark Josh Curtice and Dempsey Lott can identify and fix any instrument problem, with a smile. Chanda Bertrand was great company in the lab and helped enormously with the initial Sr/Ca measurements. Rick Kaiser and Peter Landry provided assistance in slicing the coral. Sheila Clifford made all the hard work look presentable. The WHOI academic programs office is unmatched in the support that they provide to students. Sheila Clifford, Donna Mortimer, and Alla Skorokhod at MIT have been good friends throughout my time in the Joint Program.

Elisabeth Sikes, John Wilkin and Daniel Schrag initially encouraged me down this path and provided much guidance and encouragement. Dorinda Ostermann and Peggy Smith provided advice and friendship that made all of the difference on many occasions. These five plus John Farrington, Ellen Druffel, Marty Jeglinski, Timothy Eglinton and Margaret Tivey have continued to provide encouragement and new windows of opportunity.

I have made some exceptionally good friends while in the Joint Program who have helped me in numerous ways, but none more than providing good company and laughter. Greg Gerbi, Rachel Stanley, Nick Drenzek, Sharon Hoffman, Carly Strasser, Regina Campbell-Malone, Naomi Levine, David Fike, and Helen White in particular have made this a wonderful time. Several other non-science friends have lent support during this time Nora Gilhooly (the only person in history to visit Falmouth in the winter), Charu Singh (my general exam czar), Scott Elkins, Heather Stanhaus, Dolly Geary, Audrey Lee, and Chana Zimmerman have provided distraction, entertainment and support

The sacrifices that were made for the completion of this thesis could not have been done without very strong support systems. On behalf of Amir and myself, I would like to thank both of our families for always supporting the decisions that we made to complete our educations. Without our parents, siblings, in-laws, nieces and nephew our lives would be much less fulfilling. I would also like to thank the Ostermann-Smith, the Levine et al., and the White-Huxol households in the States and the Hafts, the Glassmans, and the Inesis in Bermuda for friendship, housing, good food and good friends.

To my family, who certainly didn't expect this when emphasizing the importance of math, science and education, you have been amazing. Mom, Dad, Graham and Laura I would not be who or where I am today if it were not for your love, support, and honesty, combined with a great telephone plan. Thanks for all your time, advice, and particularly your humor. To my parents and Louise Smith Bross, Janet Kinney, and Nathalie Fairbank Bell whose lives taught me that I could be anything I wanted to be, anywhere I wanted to be. To my grandmothers who taught me never to do anything in moderation. And, finally, to Amir who has sacrificed so much for this dissertation. Thank for you believing in me and believing that the only obstacle to our dreams is our ability to imagine them.

# Table of Contents

<b>Abstract</b>	<b>3</b>
<b>Acknowledgements</b>	<b>4</b>
<b>Table of Contents</b>	<b>6</b>
<b>Table of Figures</b>	<b>9</b>
<b>Table of Tables</b>	<b>13</b>
 <b>Chapter 1: Introduction</b>	 <b>15</b>
1.1 Goals of Thesis	
1.2 Overview of Sr/Ca and $\delta^{18}\text{O}$ in Corals as Paleoceanographic Proxies	
1.2.1 Advantages of Coral Records from Slow Growing Corals	
1.2.2 Sr/Ca as a Temperature Proxy	
1.2.3 $\delta^{18}\text{O}$ as a Salinity and Temperature Proxy	
1.3 Climate Reconstructions	
1.3.1 Studying Climate at Bermuda	
1.3.2 Overview of the North Atlantic Oscillation	
1.3.3 Overview of the Little Ice Age	
1.4 Research Strategy	
1.5 References	
 <b>Chapter 2: Record of Little Ice Age Sea Surface Temperature at Bermuda Using a Growth-Dependent Calibration of Coral Sr/Ca</b>	 <b>43</b>
Abstract	
2.1 Introduction	
2.2 Methods	
2.2.1 Study Site	
2.2.2 Sub-sampling and Analysis of Coral	
2.3 Results	
2.3.1 Reproducibility of the Sr/Ca Record within the Colony	
2.3.2 Monthly Resolution Calibration	
2.3.3 Inter-annual Calibrations	
2.3.4 Application of Calibration Regression	
2.3.5 Temperature Trends at Bermuda	
2.4 Discussion	
2.5 Conclusions	
Acknowledgements	
2.6 References	



**Chapter 3: A Multi-Coral Calibration Method to Approximate a Universal Equation Relating Sr/Ca and Growth Rate to Sea Surface Temperature** 67

Abstract

3.1 Introduction

3.2 Methods

3.2.1 Study Site

3.2.2 Sub-sampling and Analysis of Corals

3.3 Results

3.3.1 Seasonal Cycle

3.3.2 Inter-annual Calibrations

3.4 Discussion: Testing the Multi-Colony Regression

3.5 Conclusions

Acknowledgements

3.6 References

**Chapter 4: Sea Surface Temperature and Salinity Variability at Bermuda during the End of the Little Ice Age** 93

Abstract

4.1 Introduction

4.1.1 Little Ice Age

4.1.2 Coral Based Proxy Records

4.2 Methods

4.2.1 Study Site

4.2.2 Sub-Sampling

4.2.3 Sr/Ca Analysis

4.2.4 Stable Oxygen Isotope Analysis

4.2.5 Age Model Development

4.3 Results

4.3.1 Sr/Ca – SST

4.3.2  $\delta^{18}\text{O}$  – SSS

4.4 Discussion

4.4.1 Climate and Ocean Trends at Bermuda

4.4.2 Influences on Observed Variability

4.5 Conclusions

4.6 References

**Chapter 5: North Atlantic Oscillation Reconstructed using Winter Strontium to Calcium Ratios in Bermuda Brain Coral** 143

Abstract

5.1 Introduction

5.2 Methods

5.3 Results

5.4 Discussion

5.5 Conclusions

## 5.6 References

<b>Chapter 6: Conclusions</b>	<b>173</b>
<b>Appendix A: Low Resolution (Biennial) Record Data</b>	<b>177</b>
<b>Appendix B: Sr/Ca Measurements</b>	<b>183</b>
B.1 Sr/Ca Long-Term Drift Correction	
B.2 References	
<b>Appendix C: Stable Oxygen and Carbon Isotope Measurements</b>	<b>187</b>
C.1 Introduction	
C.2 Small Sample Measurements	
C.3 Unbalanced Sample Measurements	
C.5 Conclusions	
C.6 References	
<b>Appendix D: High Resolution (Sub-Annual) Record Data</b>	<b>197</b>
<b>Appendix E: Low Resolution Record (Biennial) versus High Resolution Record (Sub-Annual) Sampling</b>	<b>253</b>
E.1 Introduction	
E.2 Complications of Biennial Sampling	
E.3 Unaccounted Growth Influence	
E.4 Inapplicability of Sub-Annual Based Calibration to Biennial Samples	
E.5 Results of Chapter 2	
E.6 Conclusions	
E.7 References	
<b>Appendix F: Oxygen Isotope – Salinity Relationship in Bermuda Waters</b>	<b>265</b>
Acknowledgements	
References	
<b>Appendix G: Methods of Error Propagation for Temperature Changes</b>	<b>269</b>
<b>Appendix H: BB 001 X-radiographs</b>	<b>271</b>
<b>Appendix I: Sr/Ca Calibration Data Sets</b>	<b>279</b>

## List of Figures

- Figure 1.1** Distribution of major coral reefs in the world's oceans.
- Figure 1.2** Instrumental record of the North Atlantic Oscillation from 1860-2000.
- Figure 1.3** Map of Bermuda.
- Figure 1.4** Correlation of SST anomalies and the NAO Index (NAOI).
- Figure 1.5** Winter-time SST anomaly from Hydrostation S and an instrumental record of the NAOI plotted versus year.
- Figure 2.1** Coral slabs cut from ~1m long coral to capture full growth axis.
- Figure 2.2** X-radiograph positive image of first 97mm of coral.
- Figure 2.3** Coral Sr/Ca and Hydrostation S SST plotted versus year and correlated using linear regression.
- Figure 2.4** Mean-annual growth rate compared to Sr/Ca and Sr/Ca based-SST residuals.
- Figure 2.5** Mean-annual instrumental SST from Hydrostation S compared to reconstructed mean-annual SST using the mean-annual regression and the growth-corrected model.
- Figure 2.6** Biennial-resolution SST reconstructed to 1780 using the monthly calibration and the growth-corrected model.
- Figure 2.7** Biennial averaged mean annual extension rate and Sr/Ca from 1780-1997.
- Figure 2.8** Biennial-resolution SST reconstructed to 1780 using the mean-annual regression and the growth corrected model.
- Figure 3.1** X-radiograph positive image of corals BER 003 and BER 004.
- Figure 3.2** Coral Sr/Ca and Hydrostation S SST at monthly resolution plotted versus year and correlated using linear regression for BB 001, BER 002, BER 003, and BER 004.
- Figure 3.3** Coral Sr/Ca and Hydrostation S SST at mean-annual resolution plotted versus year and correlated using linear regression for BB 001, BER 002, BER 003, and BER 004.
- Figure 3.4** Single-colony, growth-corrected model intercepts and slopes from each coral model plotted versus average growth (mm/year) of the individual coral colony.



- Figure 3.5** Hydrostation S and reconstructed mean-annual SST for BB 001, BER 002 and BER 003 from the monthly, mean-annual, growth-corrected, and multi-colony models plotted versus year.
- Figure 4.1** Sr/Ca (mmol/mol) and  $\delta^{18}\text{O}$  (‰) plotted versus year over the calibration period of 1976-1997.
- Figure 4.2** Mean-annual Sr/Ca, SST and five-year averaged SST from 1781-1998 reconstructed from Sr/Ca using a multi-colony, growth-corrected calibration.
- Figure 4.3** Coral winter-time (Dec., Jan., Feb. and March) Sr/Ca and Hydrostation S SST plotted versus year and linearly for BB 001, for BER 002, and for BER 003.
- Figure 4.4** BB 001 winter-time (Dec., Jan., Feb. and March) Sr/Ca and Hadley SST plotted versus year for inter-annual, five-year bins, and both time intervals plotted linearly.
- Figure 4.5** Winter-time Sr/Ca and five-year averaged winter-time SST plotted versus time from 1781-1999.
- Figure 4.6** Five-year average mean-annual SST (top) and winter-SST (bottom) from coral reconstruction and Hadley gridded data set.
- Figure 4.7** Coral mean-annual and winter-time  $\delta^{18}\text{O}$  and reconstructed SST.
- Figure 4.8** Monthly coral  $\delta^{18}\text{O}$  regressed against SST and SSS. Sr/Ca regressed against  $\delta^{18}\text{O}$ .
- Figure 4.9** Results of a multivariate regression of mean-annual  $\delta\text{O}_c$  versus SST and  $\delta\text{O}_w$ .
- Figure 4.10** Results of a single variate regression of mean-annual  $\delta\text{O}_c - \delta\text{O}_w$  versus SST.
- Figure 4.11** Two hundred year records of mean-annual data or derived records of  $\delta\text{O}_c$ , SST, and  $\delta\text{O}_w$ .
- Figure 4.12** Results of a multivariate regression of winter-time  $\delta\text{O}_c$  versus SST and  $\delta\text{O}_w$ .
- Figure 4.13** Results of a single variant regression of winter-time  $\delta\text{O}_c - \delta\text{O}_w$  versus SST.
- Figure 4.14** Two hundred year records of winter-time data or derived records of  $\delta\text{O}_c$ , SST, and  $\delta\text{O}_w$ .
- Figure 4.15** Coral based reconstructed mean-annual and winter SST from 1781-1999. Reconstructions shown in five year averages.
- Figure 4.16** Mean-annual reconstructed SST from coral Sr/Ca, Arctic land reconstructed record (Overpeck et al., 1997) and Northern Hemisphere land reconstructed record (Jones et al., 1998) (all shaded) and then filtered over 30 years (solid).

- Figure 4.17** Records of potential forcing influences temperature. Annual solar flux ( $\text{W/m}^2$ ), annual volcanic index ( $x(-1)$ ), mean-annual reconstructed SST ( $^{\circ}\text{C}$ ), and mean-annual reconstructed vertical mixing rates (per year) at Bermuda.
- Figure 5.1** Three year averaged winter-time Sr/Ca and observation based gridded SST (HadISST) versus time linearly. Northern hemisphere temperature plotted both mean-annually and as a 5-year running.
- Figure 5.2** Spectral analysis of the negative of winter Sr/Ca (equivalent to SST) and instrumental records of the NAOI from a) Hurrell (1995) and b) Jones et al. (1997).
- Figure 5.3** Spectral analysis of the negative of winter Sr/Ca (equivalent to SST) and proxy records of the NAOI from a) Luterbacher et al. (2001) and b) Cook et al. (2002).
- Figure 5.4** Cross correlation analysis for frequencies less than 0.1 cycles per year for negative winter Sr/Ca and NAO instrumental record [Hurrell, 1995] and the winter Sr/Ca and mean-annual Northern Hemisphere temperature record [Jones et al., 1998].
- Figure 5.5** Records filtered to frequencies of three to five years per cycle for winter Sr/Ca, instrumental and proxy records of the NAO.
- Figure 5.6** Covariance of three to five year frequency band filtered record of (-) Sr/Ca to the four instrumental and proxy records of NAO over the time interval of 1948-1997.
- Figure 5.7** Records filtered to frequencies of fifteen to fifty years per cycle for winter Sr/Ca, instrumental and proxy records of the NAO.
- Figure 5.8** Wavelet analysis based on Torrence and Compo (1998) using a morlet wavelet function with the raw winter coral Sr/Ca record.
- Figure B.1** Coral powder standard Sr/Ca (ppm/ppm) values are plotted versus digital day.
- Figure B.2** Sr/Ca anomaly versus digital day for each measurement and the daily average.
- Figure C.1** Oxygen anomaly versus sample voltage for each standard.
- Figure C.2** Carbon anomaly versus sample voltage for each standard.
- Figure C.3** Oxygen anomaly versus carbon anomaly for small sample voltages (0.4-0.8V) for each standard.
- Figure C.4** Corrected anomaly versus sample voltage for oxygen and carbon.
- Figure C.5** Oxygen anomaly versus sample/standard voltage for each standard.
- Figure C.6** Corrected oxygen anomaly versus sample/standard voltage.
- Figure C.7** Carbon anomaly versus sample/standard voltage for each standard.

- Figure C.8** Corrected carbon anomaly versus sample/standard voltage.
- Figure E.1** Sr/Ca (mmol/mol) for the sub-annual resolution (HRR) record and the biennial resolution (LRR) record from the 1780s to 1998.
- Figure E.2** Staining experiment conducted and published by Cohen et al. (2004) shows the cone shaped growth of a *Diploria labyrinthiformis* with varying extension in summer and winter throughout the theca-ambulacrum pairs.
- Figure E.3** Sr/Ca (mmol/mol) for the biennial record and the mean-annual values generated by the sub-annual resolution record filtered with three, five, and seven year windows.
- Figure E.4** The difference between the HRR binned biennially and the LRR compared to the mean-annual smoothed growth rate versus time and linearly.
- Figure E.5** SST reconstructed from the LRR Sr/Ca record using the biennial growth-corrected model and SST reconstructed from the HRR Sr/Ca record using the group model.
- Figure E.6** SST reconstructions from the HRR comparing the BB 001 growth-corrected model to BB 001 monthly calibration, the BB 001 mean-annual calibration, and the group, growth-corrected model.
- Figure F.1**  $\delta^{18}\text{O}$  plotted versus salinity for the global database, Surf Bay Beach, and BATs.



# List of Tables

<b>Table 1.1</b>	Table of reported Sr/Ca-SST relationships for monthly resolution sampling. $Sr/Ca = m * (SST) + b$ .
<b>Table 1.2</b>	Table of reported $\delta^{18}O$ -SST and Sr/Ca- $\delta^{18}O$ monthly relationships by species.
<b>Table 3.1</b>	Average extension rates for the colony and the period of calibration.
<b>Table 3.2</b>	Root mean squares of the residuals ( $^{\circ}C$ ) generated by each calibration/model applied to each coral and the group as a whole.
<b>Table 3.3</b>	Covariance ( $\sigma^2$ ) amongst the slopes and intercept of the multi-colony model.
<b>Table 3.4</b>	Difference between the mean of the reconstructed SST and the mean of the instrumental SST ( $^{\circ}C$ ) over the calibration period for each individual colony growth-corrected model and the multi-colony model.
<b>Table 4.1</b>	Winter-time Sr/Ca regressions at inter-annual and five year time scales for the equations of the form: $Sr/Ca = \beta + \gamma * SST$ .
<b>Table 5.1</b>	Correlation (r) between the winter Sr/Ca record and instrumental and proxy records.
<b>Table A.1</b>	Low resolution (biennial) data including Sr/Ca, $\delta^{18}O$ , $\delta^{13}C$ , and growth rate.
<b>Table F.1</b>	Seawater measurements from Surf Bay Beach, Bermuda (32° 20' N, 64° 45' W).
<b>Table F.2</b>	Seawater measurements from BATs (31° 40' N, 64° 10' W).
<b>Table F.3</b>	$\delta^{18}O$ and SSS measurements from global seawater oxygen-18 database.
<b>Table G.1</b>	Slope and intercept values of the multi-colony, growth-corrected, mean-annual Sr/Ca-SST relationship.
<b>Table G.2</b>	Covariance and error values of the multi-colony, growth-corrected, mean-annual Sr/Ca-SST relationship.
<b>Table G.3</b>	Slope and intercept values of the five-year, winter-time Sr/Ca-SST relationship.
<b>Table G.4</b>	Covariance and error values of the five-year, winter-time Sr/Ca-SST relationship.



# Chapter 1

## Introduction

### 1.1 Goals of Thesis

Understanding long-term climate variability requires the reconstruction of key climate parameters, such as sea surface temperature (SST) and salinity (SSS), in records extending beyond the relatively short instrumental period. The focus of this thesis is on the development of ocean paleoclimate reconstructions of temperature, salinity and the North Atlantic Oscillation (NAO) from the sub-tropical North Atlantic at Bermuda. These records are based on geochemical analyses of slow-growing brain corals (*Diploria labyrinthiformis*). The high accretion rates, longevity, and semi-annual growth bands found in coral skeletons make them an ideal resource for well-dated, seasonal-resolution climate reconstructions. Corals incorporate minor elements (Sr) and stable oxygen isotopes ( $^{18}\text{O}$  and  $^{16}\text{O}$ ) as a function of the environmental conditions they experience during growth. During calcification, relatively more Sr and more  $^{18}\text{O}$  are incorporated into the coral skeletons when temperatures are colder. The  $^{18}\text{O}$  variations (reported as a ratio of  $^{18}\text{O}/^{16}\text{O}$  relative to a standard in the form  $\delta^{18}\text{O}$ ) also depend on SSS, as the  $\delta^{18}\text{O}$



of sea increases with salinity. Measurements of each proxy in the same coral skeleton should therefore permit SST and SSS to be reconstructed simultaneously.

The goals of this thesis are: 1) to investigate the Sr/Ca (temperature) and  $\delta^{18}\text{O}$  (salinity/temperature) paleo-proxies in slow-growing (<6mm/yr) corals, including quantification of the influence of growth on these proxies; 2) to examine mean-annual and winter (Dec.-March) changes in temperature and salinity using these coral paleo-proxies, particularly to examine conditions during the Little Ice Age; and 3) to use the record of winter-time Sr/Ca to examine changes in the NAO through time. This introduction presents many of the issues related to these three goals, which will be discussed in depth in subsequent chapters.

## **1.2 Overview of Sr/Ca and $\delta^{18}\text{O}$ in Corals as Paleoceanographic Proxies**

### **1.2.1 Advantages of Coral Records from Slow Growing Corals**

Reef corals, sediment cores, tree rings and ice cores are among the many environmental archives that contain detailed information regarding the earth's climate history on inter-annual to millennial time-scales. Several coral geochemical attributes indicate skeletal aragonite to be one of the most reliable sources of inter-annual to multi-decadal paleoclimate reconstructions during the Holocene. Annual banding in corals identified through x-radiographs, as well as resolvable seasonal cycles in both temperature and salinity proxies, allows precise dating and sampling with monthly resolution [Alibert and McCulloch, 1997; Beck *et al.*, 1992; Gagan *et al.*, 1998]. Instrumental records during the time of coral growth allows for the calibration of climate proxies which can then be applied to reconstructions that extend beyond the instrumental

record. The sedentary nature of corals eliminates concerns regarding changes in habitats or lateral transportation (e.g. [Be, 1977; Ohkouchi *et al.*, 2002]). In addition, sampling of dense aragonite along growth transects greatly diminishes concerns of unobservable diagenetic influences, particularly with respect to Sr concentrations [Bar-Matthews *et al.*, 1993]. Because corals grow abundantly throughout the tropical and sub-tropical oceans (Fig. 1.1) [NOAA], they provide the potential to generate large scale spatial reconstructions of sea surface temperature (SST) and sea surface salinity (SSS).



**Figure 1.1:** Distribution of major coral reefs in the world's oceans as designated by red dots. Coral reefs are found throughout the tropical and sub-tropical oceans ranging primarily from 30°N to 30°S. Figure reproduced from a NOAA website

*Diploria labyrinthiformis*, commonly known as brain coral, is a slow growing coral species that can be found throughout the latitudes at which corals grow (Fig. 1.1). Brain corals have slow growth rates, 2-6 mm/yr [Cardinal *et al.*, 2001; Cohen *et al.*, 2004; Dodge and Thomson, 1974; Goodkin *et al.*, 2005; Kuhnert *et al.*, 2002], compared to *Porites*, the more commonly used coral genus for paleoclimate reconstructions, which has growth rates from 8-20 mm/yr [Alibert and McCulloch, 1997; deVilliers *et al.*, 1994; Hughen *et al.*, 1999]. In addition, brain corals have relatively long life-spans of several



hundred years. Therefore, examining brain coral Sr/Ca and  $\delta^{18}\text{O}$  proxies will enable the paleoclimate community to extract continuous, multi-century records from relatively small geological samples and geographically diverse regions.

Until recently, brain corals have been sparsely used for geochemical records [Cardinal *et al.*, 2001; Cohen *et al.*, 2004; Dodge and Thomson, 1974; Druffel, 1997; Kuhnert *et al.*, 2002; Reuer, 2001], due to the complicated growth structure of the skeletal elements. The coral thecal wall is the densest and most often sampled skeletal element. This area extends rapidly along a cone-shaped surface during the summer. The brain coral continues the extension of the thecal wall during the winter, while simultaneously thickening the wall segment deposited during the summer [Cohen *et al.*, 2004]. This complicates high-resolution sampling in that summer-time aragonite layers may have seen winter-time influences, and the sharp cone-shaped growth surface may lead to discrete samples encompassing a variety of months, depending on the width of the sample [Hart and Cohen, 1996]. However, the high density thecal wall ensures both ample material for sampling and diminishes concerns of diagenesis or secondary precipitation [Bar-Matthews *et al.*, 1993]. Concerns have been raised about coral paleoclimate reconstructions due to several complicating factors, including commonly used bulk sampling techniques [Marshall and McCulloch, 2002; Swart *et al.*, 2002], as well as environmental, biological, growth rate and symbiotic effects [Amiel *et al.*, 1973; Cohen *et al.*, 2002; deVilliers *et al.*, 1994; Ferrier-Pages *et al.*, 2002; Greegor *et al.*, 1997; McConnaughey, 1989a; McConnaughey, 1989b; Reynaud *et al.*, 2004]. In this study, efforts are made to account for some of these impacts by incorporating the use of inter-annual, rather than monthly, data and by quantitatively evaluating growth rate



influences on reconstructed SST.

### 1.2.2 Sr/Ca as a Temperature Proxy

Sea surface temperature (SST) is one of the climate parameters most often reconstructed in coral records and is a critical parameter for interpreting long-term climate variability. The Sr/Ca content of coral reef  $\text{CaCO}_3$  is one geochemical proxy used to reconstruct past SSTs. This technique is based on the premise that as temperature increases, corals incorporate relatively less Sr into their  $\text{CaCO}_3$  structures, thereby recording the temperature of surrounding water as they grow [Beck *et al.*, 1992; Smith *et al.*, 1979].

Despite the promise of the Sr/Ca thermometer, there are several outstanding concerns. While Sr and Ca are both relatively conservative elements in seawater, small changes in their concentration have been observed due to coral symbionts and other biological activity, as well as upwelling and other local effects (e.g. [Bernstein *et al.*, 1987; Cohen *et al.*, 2002; deVilliers *et al.*, 1994; MacKenzie, 1964; Shen *et al.*, 1996]). Other studies have indicated that significant levels of coral strontium are deposited as strontianite ( $\text{SrCO}_3$ ) onto crystal surfaces rather than in substitution for Ca into the lattice [Amiel *et al.*, 1973; Greegor *et al.*, 1997]. As previously mentioned, coral growth is not often a purely linear process, particularly in slow growth corals where seasonal changes influenced extension rate and in-filling in the coral skeleton [Barnes and Lough, 1993; Cohen *et al.*, 2004]. Influences unrelated to SST, such as growth rate [deVilliers *et al.*, 1995] and short term changes in Sr and Ca concentrations in water [deVilliers *et al.*, 1994], can also influence the monthly Sr/Ca relationship, demonstrating the importance

of investigating averaged or inter-annual periods.

**Table 1.1:** Table of reported Sr/Ca-SST relationships for monthly resolution sampling.  $\text{Sr/Ca} = m * (\text{SST}) + b$ .

Author	Year	Slope ( $\text{mmol}^1\text{mol}^{-1}\text{°C}^{-1}$ )	Intercept ( $\text{mmol}^1\text{mol}^{-1}$ )	Growth (mm/year)	SST Range (deg C)	Species
Marshall & McCulloch	2001	-0.0593	10.375		25 - 30	Porites
Gagan et al.	1998	-0.0660	10.78	24	20 - 30	Porites
		-0.0639	10.73	22 / 12.5	22 - 29	
		-0.0616	10.68	8	20 - 31	
Correge et al.	2000	-0.0657	10.73		20 - 26	Porites
Marshall & McCulloch	2001	-0.0575	10.40	7.5 - 10	23 - 29.5	Porites
		-0.0587	10.40	16.2-17.0	21 - 30	
Smith et al.	1979	-0.071	11.01		19 - 29	Multiple
deVilliers et al.	1994	-0.0795	10.956	11	23 - 27	Porites
		-0.0763	11.004	8	23.5 - 27	Pocillopora
		-0.0675	10.646	11	20 - 25	Pavona
Correge et al.	2004	-0.060	10.57		22 - 30	Diploastrea
		-0.062	10.51	2 - 5	22 - 30	Porites
Fallon et al.	1999	-0.063	10.76	5.3	14.5 - 28	Porites
Shen et al.	1996	-0.0528	10.356	15-16	22 - 28	Porites
		-0.0505	10.307	17-23	22 - 28	
Alibert & McCulloch	1997	-0.0505	10.21	8	22 - 29	Porites
		-0.0615	10.485	13	23 - 29	
		-0.0507	10.17	12	22.5 - 28.5	
		-0.0604	10.425	14	23 - 28.5	
		-0.0629	10.56	9	22 - 28	
deVilliers et al.	1995	-0.0417	10.25	6	19.5 - 25	Pavona
		-0.0388	10.11	12	19.5 - 25	
		-0.0331	9.92	14	20 - 24	
Cardinal et al.	2001	-0.045	10.03	3.2	19.5 - 28.5	Diploria
				2.8	19.5 - 28.5	
Swart et al.	2001	-0.0377	9.994	6 - 9	24 - 30	Montastrea
This Study		-0.0358	10.1	3-5	18-29	Diploria
		-0.0376	10.1	1-5	18-29	
		-0.0436	10.3	3-5.5	18-29	
		-0.0429	10.3	1.5-3.5	18-29	

Two key problems have continued to plague the acceptance and validity of coral Sr/Ca paleo-reconstructions: 1) Each modern coral calibrated to instrumental SST results in a different coral Sr/Ca-SST relationship in both slope and intercept, implying that this is not simply a thermodynamic temperature relationship (e.g. Table 1.1) [Lough, 2004; Marshall and McCulloch, 2002]; and 2) coral based SST reconstructions have shown 2-4

times greater temperature changes in the tropical oceans from today to the last glacial maximum (LGM) [Beck *et al.*, 1997; Corregge *et al.*, 2004; Guilderson *et al.*, 1994; McCulloch *et al.*, 1996] compared to other marine paleoproxies [Lea *et al.*, 2000; Pelejero *et al.*, 1999; Rosenthal *et al.*, 2003; Rühlemann *et al.*, 1999].

This thesis strives to demonstrate that growth rate influences may be accounting for some of the complexities observed in the literature. Incorporation of growth rate, multiple-coral colonies, and inter-annual averaged data generates more robust Sr/Ca-SST coral calibrations and reconstructions.

### 1.2.3 $\delta^{18}\text{O}$ as a Salinity and Temperature Proxy

The  $\delta^{18}\text{O}$  of coral skeleton can be used to reconstruct sea surface salinity in conjunction with a Sr/Ca based SST reconstruction. The relative concentration of stable oxygen isotopes in corals depends on the temperature of the surrounding sea water and the oxygen isotopic composition of that sea water at the time of coral growth. To first approximation, the isotopic composition of sea water is linearly related to sea surface salinity [Urey, 1947]. This relationship varies both between geographic locations and between depths in the water column.

Kinetic models predict that slow growing corals should incorporate oxygen isotopes relatively close to thermodynamic equilibrium compared to their fast growing counterparts [McConnaughey, 1989a; McConnaughey, 1989b]. The isotopic composition of biogenic aragonite from measurements of non-coral species (foraminifera, gastropods, and scaphopods) has been expressed as [Grossman and Ku, 1986]:



$$\delta O_c - \delta O_w = -0.23 * (SST) + 4.75 \quad \text{Eqn. (1)}$$

Slow growing corals are likely to exhibit enrichment in  $^{16}\text{O}$  relative to other marine organisms, but with fewer kinetic fractionation effects (growth effects) during calcification than faster growing corals. These kinetic effects are thus expected to have small impacts on the  $\delta^{18}\text{O}$ -SST slope, both within and between slow-growing colonies [deVilliers *et al.*, 1995; Guilderson and Schrag, 1999; Linsley *et al.*, 1999; Lough, 2004; McConnaughey, 1989b; McConnaughey, 2003], relative to faster growing colonies. Therefore, using the  $\delta^{18}\text{O}$  to reconstruct temperature and/or salinity should be feasible.

**Table 1.2:** Table of reported  $\delta^{18}\text{O}$ -SST and Sr/Ca-  $\delta^{18}\text{O}$  monthly relationships by species.

Author	Year	Oxygen - SST		Sr/Ca - Oxygen		Growth (mm/year)	SST Range (deg C)	Species
		Slope	Intercept	Slope	Intercept			
Bagnato <i>et al.</i>	2004	-0.15	-0.84				24.5 - 29.5	Porites
		-0.16	-0.26					
Cardinal <i>et al.</i>	2004	-0.14		0.30		3.2	19.5 - 28.5	Diploria
				0.18		2.8		
de Villiers <i>et al.</i>	1995	-0.174	0.22			6	19.5 - 25	Pavona
		-0.106	-1.56			12	19.5 - 25	
Smith <i>et al.</i>	2006	-0.101	-1.24	0.28	10.31	7	22 - 31	Montastrea
Dunbar <i>et al.</i>	1994	-0.122	-1.48			13	20 - 28	Pavona
Gagan <i>et al.*</i>	1998	-0.174	0.002			12.5	22 - 29	Porites
		-0.189	0.447			22.0	22 - 29	
Watanabe <i>et al.</i>	2003	-0.18	0.23			2.7	20 - 28	Diplorastrea
Beck <i>et al.</i>	1992			0.27			20 - 27	Porites
McCulloch <i>et al.</i>	1994	-0.203	0.577	0.30				Porites
This Study		-0.105	-1.17	0.28	10.3	3-5	18-29	Diploria

\* Regressions to Sr/Ca based reconstructed SST

Units on oxygen-SST slopes are ‰/°C and intercepts are ‰.

Units on Sr/Ca Oxygen slopes are mmol/mol/‰ and intercepts are mmol/mol.

Much like the Sr/Ca record, the  $\delta^{18}\text{O}$  of slow-growing corals may be further complicated by growth structure and smoothing during bulk sampling, [Cohen *et al.*, 2004; Goodkin *et al.*, 2005; Swart *et al.*, 2002]. The  $\delta^{18}\text{O}$  – SST relationships determined by previous studies are all based on monthly calibrations (Table 1.2). They

are not close to the expected values based on the laboratory measurements of aragonite formation (Eqn. 1.1), and slower growing corals are not more consistent between colonies than faster growing colonies (e.g. Table 1.2). These results are contradictory to expectations and may be due to smoothing during bulk sampling. In order to avoid previously discussed complications including growth regimes and bulk sampling, this study aims to develop accurate paleo-temperature and salinity reconstructions using inter-annual calibrations that incorporate potential non-equilibrium processes, including the evaluation of growth rate influences.

### **1.3 Climate Reconstructions**

Upon completion of the paleoclimate proxy calibrations, I will use multi-century long geochemical records to reconstruct and examine the interactions between two large scale climatic patterns: one spatial - the North Atlantic Oscillation (NAO) and the other temporal - the last century-scale event of the Little Ice Age (LIA). The NAO is an oscillation of atmospheric mass, commonly measured as a pressure difference between the Icelandic low and the Açores high regions [Hurrell, 1995; Jones *et al.*, 1997]. NAO variability can be defined on a wide range of time-scales including synoptic (10 days), seasonal and multi-century. The Little Ice Age, on the other hand, was a multi-century climate event believed to have ended in the late 1800s. It was a period of colder than normal temperatures recorded historically by many communities, particularly in the North Atlantic region [Grove, 1988]. Anthropogenic climate changes appear to be causing rapid warming of the earth's temperature, which is subsequently altering a range of climate dynamics. By examining the NAO during the time of the LIA, a better

understanding of how this system has behaved during times of rapid climate change and during times of a different mean-temperature than seen today is investigated. Therefore, I use the coral to reconstruct the NAO and ocean state at Bermuda prior to the instrumental record, including the LIA.

The NAO has wide reaching influence over weather and climate patterns across the North Atlantic, the United States and Europe [*Visbeck et al.*, 2001]. The NAO's influence on temperature, precipitation and other ocean conditions is important to society due to its location between the eastern United States and Europe, both large centers of industry and population. The NAO can have significant impacts on wave height in the Atlantic, which can drastically impact shipping, oil drilling, and coastal management [*Hurrell et al.*, 2003; *Kushnir et al.*, 1997]. Precipitation patterns impact agriculture, hydroelectric power generation, and tourism [*Hurrell et al.*, 2003]. Additionally, the negative impacts of the NAO on agriculture, fisheries, and ecosystems can threaten food sources for many regions [*Hurrell et al.*, 2003; *Thompson and Wallace*, 2001]. For example, Fromentin and Planque (2000) suggested that shifts in the NAO cause large fluctuations in plankton communities in the North Atlantic, which in turn can significantly impact pelagic communities such as herring and cod. Changes in precipitation can also have drastic agricultural effects from the mid-western United States to the Middle East [*Visbeck*, 2002]. Improving our ability to predict abrupt, annual shifts in the NAO could also improve our ability to anticipate the economic impacts of such short-term changes in climate. By linking NAO Index (NAOI) variability with events relevant to society, much like El Niño and maize crops in Zimbabwe [*Cane et al.*, 1994], significant improvements in human productivity and quality of life can be achieved.



Instrumental records of the NAOI from Iceland and the Açores [Hurrell, 1995] show an extended period of positive phase in the NAO beginning in the early 1970s that is unprecedented in the instrumental record in terms of duration and intensity (Fig. 1.2). The NAOI [Hurrell, 1995] is measured by differencing normalized sea level pressure measurements at Portugal ( $L_n$ ) and Iceland ( $S_n$ ). These data lend themselves to the hypothesis that the onset of global climate change resulting from anthropogenic forcing has already influenced the trend of the NAO [Shindell *et al.*, 1999]. Unfortunately, instrumental records are too short to provide information about the long-term behavior of the NAO beyond 1860. This hampers not only our ability to evaluate the importance of

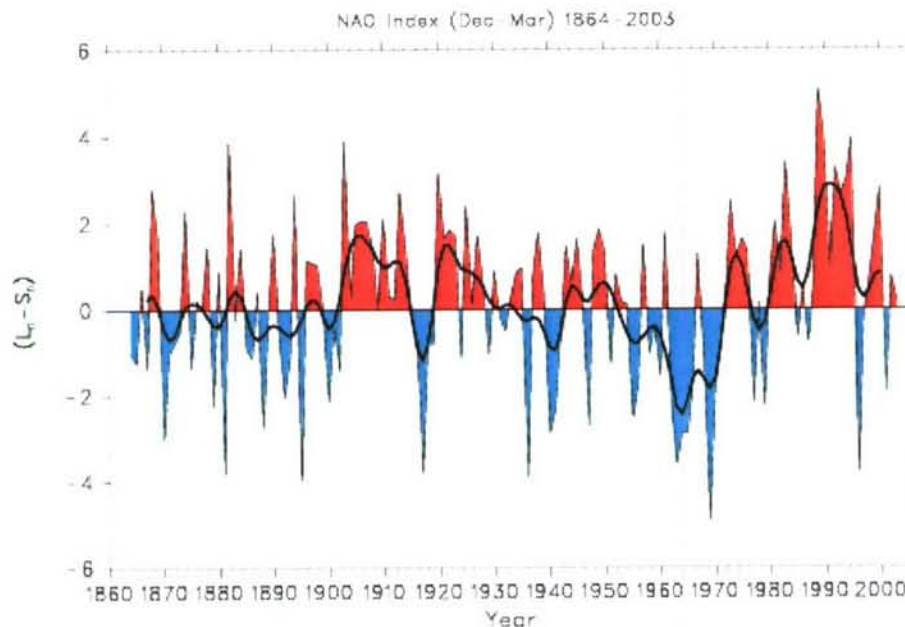


**Figure 1.2:** Instrumental record of the NAOI from 1860 to 2002 shows an unprecedented and extended positive trend for the past 30 years. (<http://www.cgd.ucar.edu/cas/jhurrell/nao.stat.winter.html>). The NAOI is calculated by differencing the normalized (over the length of the record) sea level pressure measurements at Portugal ( $L_n$ ) and Iceland ( $S_n$ ).

anthropogenic influences, but also our ability to predict the behavior of the NAO in the future. Annually resolved, multi-century records of natural background climate variability are therefore important not only for distinguishing recent anthropogenic impacts, but also for predicting potential future trends. In addition, such information is critical to identifying possible feedbacks, whereby changing NAO dynamics could amplify gradual climate change and introduce abrupt climate shifts, with consequences for the environment and society.

### 1.3.1 Studying Climate at Bermuda

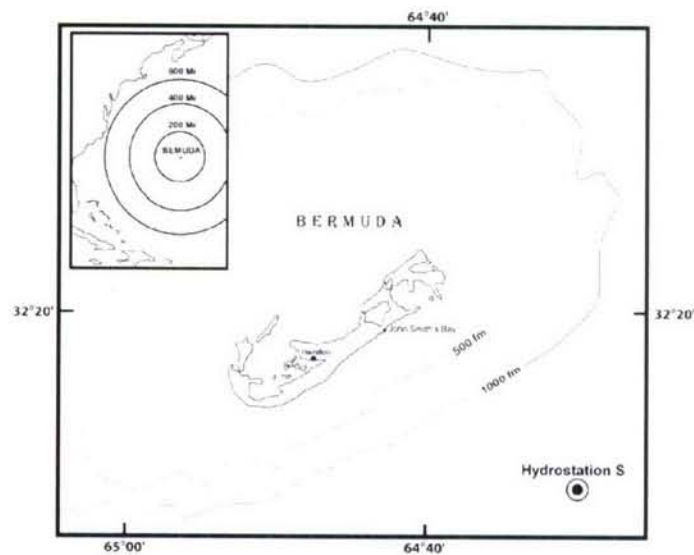


**Figure 1.3:** Map of Bermuda. Bermuda is located roughly 330 km off the coast of North Carolina. Hydrostation S is 30 km southeast of Bermuda and provides approximately 50 years of SST data in proximity to where the corals were taken along the southeastern edge of the platform off John Smith's Bay at 16m depth. (Figure adapted from World Ocean Circulation Experiment Newsletter, Number 8, October 1989)

The island of Bermuda (64°W, 32°N) (Fig. 1.3) located in the western subtropical Atlantic is an excellent location for examining long-term climate variability for

several reasons. This location is sensitive to the dominant atmospheric process in this region, the NAO [Visbeck *et al.*, 2001], and experiences SST anomalies coherent with the NAO at low (multi-decadal) and high (inter-annual) frequencies. In addition, the site is influenced by the Gulf Stream, the sub-tropical gyre and sub-polar waters of the North Atlantic. The Sargasso Sea, which encompasses Bermuda, is formed by recirculation of Gulf Stream waters [Hogg, 1992; Schmitz and McCartney, 1993], imprinting Bermuda paleoclimate records with a Gulf Stream signal. Changes in position and strength of the Gulf Stream will impact temperature and salinity properties at Bermuda [Schmitz and McCartney, 1993; Talley, 1996]. Waters in the Sargasso Sea are also influenced by the larger sub-tropical gyre. Strength in the circulation of this gyre is dependent on the strength of the westerlies and large scale atmospheric processes [Talley, 1996]. The sensitivity of this location to two major ocean circulation processes responsible for climatically important ocean heat transport – the Gulf Stream and the sub-tropical gyre – provides the possibility to further inform our knowledge of ocean circulation.

In addition, Bermuda is the site of extensive oceanographic research providing long instrumental SST and SSS records. Hydrostation S, (Fig. 1.3) founded and visited approximately bi-weekly since 1954, provides the longest SST record in the area. Over the history of Hydrostation S, monthly SST has ranged from 18.0 to 28.9°C with annual averages ranging from 22.4-24.3°C. The plethora of corals growing on the Bermuda shelf and the large sedimentary deposits along the Bermuda rise allow for many types of paleo-climate reconstructions [Draschba *et al.*, 2000; Keigwin, 1996; Kuhnert *et al.*, 2002; Sachs and Lehman, 1999] over an array of timescales, which can serve to strengthen the paleoclimate story at this location.



### 1.3.2 Overview of the North Atlantic Oscillation

Winter-time SST at Bermuda has been shown to correlate with the NAO on high (annual) and low (decadal) frequency time scales [Eden and Willebrand, 2001; Marshall *et al.*, 2001; Visbeck *et al.*, 2001], making Bermuda an ideal location to examine this climate system. Reconstructing the NAO requires sub-annual resolution, precisely dated records, which are unique to corals.

The NAO has a widespread impact, on weather affecting the Northern Hemisphere from the Eastern US to Western Europe. In a positive NAO Index (NAOI) phase, both the low (Iceland) and high (Açores) pressure zones are intensified. This leads to an increased frequency of strong winter storms crossing the Atlantic Ocean along a

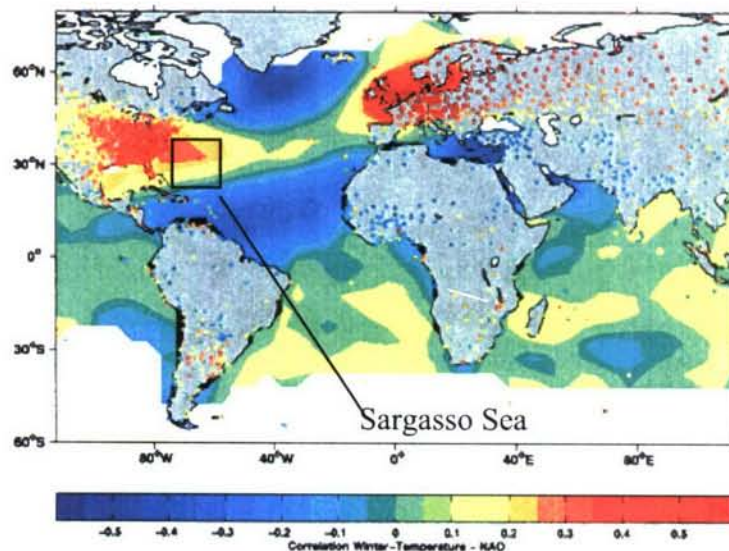


**Figure 1.4:** Correlation of mean winter (Dec., Jan., Feb., March) temperature against the NAOI from 1865-1930 (Visbeck *et al.*, 2001). Yellow-red shows positive correlation (0.1-0.6). Blues show negative correlation (-0.1- -0.6). Greens are approximately no correlation.

northeast transect toward the Icelandic low. The deflection of the winter storm track north into the intensified low pressure zone causes colder temperatures over the Northwestern Atlantic, and warmer and stormier conditions in the eastern United States extending to Bermuda, and to warmer and drier conditions in Southern Europe. In the negative phase of the NAOI, both pressure anomalies are diminished and the gradient weakened. Positive and negative phase NAOI years have a distinct influence on mean winter surface temperature anomalies (Fig. 1.4). On multi-decadal time-scales, extended negative periods lead to warming in the tropics and sub-tropics and cooling in the sub-polar gyre [Eden and Willebrand, 2001; Visbeck *et al.*, 2003]. The reverse SST anomaly patterns occur during extended positive NAO periods. The inter-annual patterns are influenced by changes in Ekman pumping and heat flux due to the latitudinal shift and changes in strength of the prevailing winds (trades and westerlies). The multi-decadal response may result either from gradual changes in the strength of meridional overturning circulation (MOC), resulting from prolonged change in location and strength of Ekman pumping and convection in the Labrador Sea or from long-term propagation of inter-annual anomalies [Eden and Willebrand, 2001; Visbeck *et al.*, 2003; Visbeck *et al.*, 2001].

Uncertainty remains regarding the relationship between the NAO and the ocean. Currently, during a positive NAO, the SST anomalies form a “tri-pole” pattern with colder than normal waters in the sub-arctic and tropics and warmer than normal temperatures in the subtropics (Fig. 1.4) [Visbeck *et al.*, 2003]. While it is clear that atmospheric processes drive changes in wind speed and subsequent Ekman currents and heat exchange that lead to the tri-pole SST pattern seen in the ocean, it is not clear how relative influences of heat flux and ocean circulation how the presence of this SST pattern

impacts the NAO [Czaja *et al.*, 2003]. Recent studies suggest that atmospheric feedbacks driven by SST anomalies may influence the NAO and these feedbacks could lead to enhanced prediction capabilities [Czaja and Frankignoul, 2002; Rodwell *et al.*, 1999]. However, short instrumental records make this difficult to assess.

A strong correlation within the tri-pole pattern seen in the North Atlantic between SST anomalies and the NAO has been established for the last 130 years [Visbeck *et al.*, 2003] (Fig. 1.3). However, one of the strongest periods of correlation occurs over the last 30 years when the NAO was already in its strong positive phase.

Joyce (2002) used an extended SST data set from off the coast of the eastern United States to show that over the past 130 years, there are periods between 1910-1930 and 1980-1985 when the correlation between the SST record and the NAO was weak or non-existent. The 1980-1985 period of weak-correlation is also captured in the Bermuda SST record from Hydrostation S, indicating its coherence with regional SST (Fig. 1.5).

Currently, there are several century-long reconstructions of the NAO from ice cores, tree rings, and snow accumulation rates [Appenzeller *et al.*, 1998a; Appenzeller *et al.*, 1998b; Cook *et al.*, 2002; Glueck and Stockton, 2001]. The only marine NAO reconstruction comes from the North and Norwegian Seas using mollusk calcification rates [Schone *et al.*, 2003]. This marine record shows a good correlation to NAO over the instrumental period ( $r=0.67$ ). But, beyond the instrumental period, the correlations between the mollusk NAO reconstruction and other proxy reconstructions are greatly diminished ( $r=0.44$ ). This decreased correlation supports the Joyce (2002) hypothesis that ocean-based reconstructions which include the last 30 years as a large portion of the calibration period may exaggerate NAO variability back in time. This reinforces the need



to fully examine the SST-NAO relationship over longer time scales, prior to the advent of anthropogenic influences. I present a new record of NAO variability from an important region adding a second marine reconstruction to the literature.

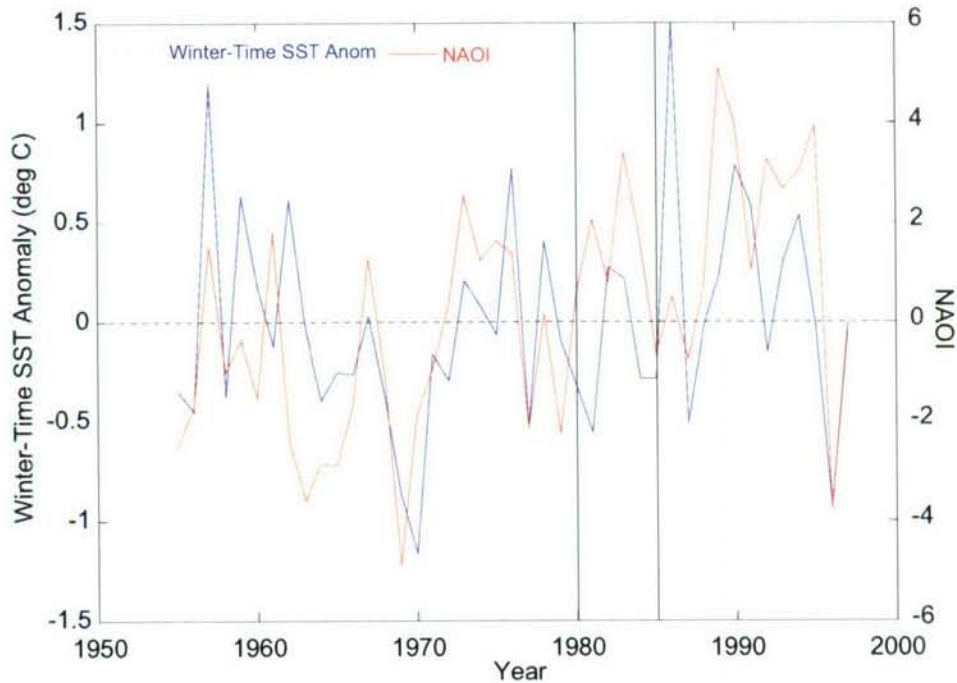


**Figure 1.5:** Winter-time SST anomaly from 1954-1997 average from Hydrostation S (blue) and an instrumental record of the NAOI (red) [Hurrell, 1995] plotted versus year. From 1980-1985 a disagreement between both phase and amplitude is seen as has been observed at other locations.

### 1.3.3 Overview of the Little Ice Age

The Little Ice Age (LIA) occurred from 1400s to the late 1800s following the Medieval warm period [Bradley and Jones, 1993; Jones *et al.*, 1998; Overpeck *et al.*, 1997]. This period is defined by a well documented series of extended centennial-scale cold periods. Currently, high-resolution records of the LIA exist from tree rings [Briffa *et al.*, 2001; Esper *et al.*, 2002; Jacoby and D'Arrigo, 1989], ice cores [Dahl-Jensen *et al.*,

1998; Dansgard *et al.*, 1975], and coral records from the Caribbean Sea [Druffel, 1982; Watanabe *et al.*, 2001; Winter *et al.*, 2000]. Proxy reconstructions from throughout the North Atlantic region show a large range of temperature changes, from 0.5 to 5 °C below current temperatures [deMenocal *et al.*, 2000; Druffel, 1982; Dunbar *et al.*, 1994; Glynn *et al.*, 1983; Keigwin, 1996; Lund and Curry, 2006].

The LIA has been proposed as the most recent example of decadal-to-centennial scale climate change during the Holocene. One question is how future anthropogenic climate change will alter climate behavior on short (100 year) periods (Abrupt Climate Change: Inevitable Surprises [NRC, 2002]). Two forcing mechanisms have been put forth as a possible cause for the LIA – solar and volcanic activity. Proxy reconstructions indicate that solar activity may have been low during this time [Crowley, 2000; Lean *et al.*, 1995; Wigley and Kelly, 1990], and volcanic activity may have been high [Crowley, 2000] both of which would have lead to cooling. Some studies have suggested that a 1500 year cycle in solar output may be another forcing of the LIA through the MOC [Bond *et al.*, 2001; Bond *et al.*, 1997]. Combined, solar and volcanic activity have the potential to produce wide spread cooling across the globe.

As previously discussed, another climate forcing mechanism in this region is the NAO. The direct influence of NAO processes is limited geographically to the Northern Hemisphere. In contrast to the volcanism and solar activity, the NAO will generate differing responses across the basin and at different frequencies [Keigwin and Pickart, 1999; Visbeck *et al.*, 2003]. Although instrumental and proxy reconstructions of this climate system show different results during the end of the LIA [Cook *et al.*, 2002; Glueck and Stockton, 2001; Luterbacher *et al.*, 2001; Schoene *et al.*, 2003], the

reconstruction by Luterbacher et al. (2001), a record based on historical and multiple proxy records over a large geographical area, shows either a weak positive or neutral NAO at this time. Similarly, our study shows that a low frequency (decadal-to-centennial scale) connection to a positive NAO at Bermuda would be cooling and this would be likely to occur over much of the North Atlantic [Visbeck et al., 2003].

## 1.4 Research Study

This project begins by contributing two new methods of calibrating coral paleoproxy data that quantify biases resulting from both sampling processes and varying growth rates through time. First, the biases introduced from the dampening of the seasonal cycle through bulk sampling on monthly calibrations are investigated and addressed by evaluating calibrations on inter-annual time scales rather than monthly calibrations which are impacted by seasonal biasing. Second, the ability of both inter-annual and long-term average growth rates to generate differences in the Sr/Ca-SST slopes is investigated using multiple coral colonies from the same location. The quantitative addition of growth rates first presented in Chapter 2 and further developed in Chapter 3 is critical to performing Sr/Ca-SST calibrations with these slow-growing corals. While growth rate is found to play a less significant role in the oxygen isotope proxies, bulk sampling effects still lead to the application of inter-annual, rather than monthly calibrations.

Ultimately, this thesis uses the methods and calibrations developed for both Sr/Ca and  $\delta^{18}\text{O}$  to generate multi-century records of mean-annual and winter-time SST and directional changes in SSS. The records are used to investigate changes in temperature



and salinity between today and the end of the LIA (Chapter 4) at Bermuda. Finally, winter Sr/Ca is found to represent the NAO at varying frequencies and a new marine based NAO reconstruction is presented and used to evaluate changes in NAO behavior and in the ocean-atmosphere NAO relationships during periods of different mean-climate (Chapter 5).

## 1.5 References

- Alibert, C., and M. T. McCulloch, Strontium/calcium ratios in modern Porites corals from the Great Barrier Reef as a proxy for sea surface temperature: Calibration of the thermometer and monitoring of ENSO, *Paleoceanography*, 12, 345-363, 1997.
- Amiel, A. J., G. M. Friedman, and D. S. Miller, Distribution and nature of incorporation of trace elements in modern aragonitic corals, *Sedimentology*, 20, 47-64, 1973.
- Appenzeller, C., J. Schwander, S. Sommer, and T. F. Stocker, The North Atlantic Oscillation and its imprint on precipitation and ice accumulation in Greenland, *Geophysical Research Letters*, 25, 1939-1942, 1998a.
- Appenzeller, C., T. F. Stocker, and M. Anklin, North Atlantic oscillation dynamics recorded in Greenland ice cores, *Science*, 282, 446-449, 1998b.
- Bar-Matthews, M., G. J. Wasserburg, and J. H. Chen, Diagenesis of Fossil Coral Skeletons - Correlation between Trace-Elements, Textures, and U-234/U-238, *Geochimica Et Cosmochimica Acta*, 57, 257-276, 1993.
- Barnes, D. J., and J. M. Lough, On the Nature and Causes of Density Banding in Massive Coral Skeletons, *Journal of Experimental Marine Biology and Ecology*, 167, 91-108, 1993.
- Be, A. W. H., An ecological, zoogeographic and taxonomic review of recent planktonic foraminifera. in *Oceanic Micropaleontology*, edited by Ramsay, A. T. S., pp. 1-100, Academic Press, San Diego, CA, 1977.
- Beck, J. W., R. L. Edwards, E. Ito, F. W. Taylor, J. Recy, F. Rougerie, P. Joannot, and C. Henin, Sea-Surface Temperature from Coral Skeletal Strontium Calcium Ratios, *Science*, 257, 644-647, 1992.
- Beck, J. W., J. Recy, F. Taylor, R. L. Edwards, and G. Cabioch, Abrupt changes in early Holocene tropical sea surface temperature derived from coral records, *Nature*, 385, 705-707, 1997.
- Bernstein, R. E., P. R. Betzer, R. A. Feely, R. H. Byrne, M. F. Lamb, and A. F. Michaels, Acantharian Fluxes and Strontium to Chlorinity Ratios in the North Pacific Ocean, *Science*, 237, 1490-1494, 1987.
- Bond, G., B. Kromer, J. Beer, R. Muscheler, M. N. Evans, W. Showers, S. Hoffman, R. Lottibond, I. Hajdas, and G. Bonani, Persistent Solar Influence on North Atlantic Climate During the Holocene, *Science*, 294, 2130-2136, 2001.

- Bond, G., W. Showers, M. Cheseby, R. Lotti, P. Almasi, P. deMenocal, P. Priore, H. M. Cullen, I. Hajdas, and G. Bonani, A Pervasive Millennial-Scale Cycle in North Atlantic Holocene and Glacial Climates, *Science*, 278, 1257-1266, 1997.
- Bradley, R. S., and P. D. Jones, Little Ice Age summer temperature variations: their nature and relevance to recent global warming trends, *The Holocene*, 3, 367-376, 1993.
- Briffa, K. R., T. J. Osborn, F. H. Schweingruber, I. C. Harris, P. D. Jones, S. G. Shiyatov, and E. A. Vaganov, Low-frequency temperature variations from a northern tree-ring density network, *Journal of Geophysical Research*, 106, 2929-2941, 2001.
- Cane, M. A., G. Eshel, and R. W. Buckland, Forecasting Zimbabwean Maize Yield Using Eastern Equatorial Pacific Sea-Surface Temperature, *Nature*, 370, 204-205, 1994.
- Cardinal, D., B. Hamelin, E. Bard, and J. Patzold, Sr/Ca, U/Ca and delta O-18 records in recent massive corals from Bermuda: relationships with sea surface temperature, *Chemical Geology*, 176, 213-233, 2001.
- Cohen, A. L., K. E. Owens, G. D. Layne, and N. Shimizu, The effect of algal symbionts on the accuracy of Sr/Ca paleotemperatures from coral, *Science*, 296, 331-333, 2002.
- Cohen, A. L., S. R. Smith, M. S. McCartney, and J. van Etten, How brain corals record climate: an integration of skeletal structure, growth and chemistry of *Diploria labyrinthiformis* from Bermuda, *Marine Ecology-Progress Series*, 271, 147-158, 2004.
- Cook, E. R., R. D. D'Arrigo, and M. E. Mann, A well-verified, multiproxy reconstruction of the winter North Atlantic Oscillation index since AD 1400, *Journal of Climate*, 15, 1754-1764, 2002.
- Correge, T., M. K. Gagan, J. W. Beck, G. S. Burr, G. Cabioch, and F. Le Cornec, Interdecadal variation in the extent of South Pacific tropical waters during the Younger Dryas event, *Nature*, 428, 927-929, 2004.
- Crowley, T. J., Causes of Climate Change Over the Past 1000 Years, *Science*, 289, 270-277, 2000.
- Czaja, A., and C. Frankignoul, Observed impact of Atlantic SST anomalies on the North Atlantic oscillation, *Journal of Climate*, 15, 606-623, 2002.
- Czaja, A., A. W. Robertson, and T. Huck, The Role of Atlantic Ocean-Atmosphere Coupling Affecting North Atlantic Oscillation Variability. in *The North Atlantic Oscillation: Climatic Significance and Environmental Impact*, edited by Hurrell, J., Y. Kushnir, G. Ottersen and M. Visbeck, pp. 147-172, American Geophysical Union, Washington, D. C., 2003.



- Dahl-Jensen, D., K. Mosegaard, N. Gunderstrup, G. D. Clow, A. W. Johnsen, A. W. Hansen, and N. Balling, Past Temperature Directly from the Greenland Ice Sheet, *Science*, 282, 268-271, 1998.
- Dansgaard, W., S. J. Johnsen, N. Reeh, N. Gunderstrup, H. B. Clausen, and C. U. Hammer, Climate changes, Norsemen, and modern man, *Nature*, 255, 24-28, 1975.
- deMenocal, P., J. Ortiz, T. Guilderson, and M. Sarnthein, Coherent high- and low-latitude climate variability during the holocene warm period, *Science*, 288, 2198-2202, 2000.
- deVilliers, S., B. K. Nelson, and A. R. Chivas, Biological-Controls on Coral Sr/Ca and Delta-O-18 Reconstructions of Sea-Surface Temperatures, *Science*, 269, 1247-1249, 1995.
- deVilliers, S., G. T. Shen, and B. K. Nelson, The Sr/Ca-Temperature Relationship in Coralline Aragonite - Influence of Variability in (Sr/Ca)Seawater and Skeletal Growth-Parameters, *Geochimica Et Cosmochimica Acta*, 58, 197-208, 1994.
- Dodge, R. E., and J. Thomson, The Natural Radiochemical and Growth Records in Contemporary Hermatypic Corals from the Atlantic and Caribbean, *Earth and Planetary Science Letters*, 23, 313-322, 1974.
- Draschba, J., J. Patzold, and G. Wefer, North Atlantic Climate Variability Since AD 1350 Recorded in  $\delta^{18}\text{O}$  and Skeletal Density of Bermuda Corals, *International Journal of Earth Sciences*, 88, 733-741, 2000.
- Druffel, E. M., Banded corals: changes in oceanic carbon-14 during the Little Ice Age, *Science*, 218, 13-19, 1982.
- Druffel, E. R. M., Pulses of Rapid Ventilation in the North Atlantic Surface Ocean During the Past Century, *Science*, 275, 1454-1457, 1997.
- Dunbar, R. B., G. M. Wellington, M. W. Colgan, and W. Peter, Eastern pacific sea surface temperature since 1600 AD: the  $\delta^{18}\text{O}$  record of climate variability in Galapagos corals, *Paleoceanography*, 9, 291-315, 1994.
- Eden, C., and J. Willebrand, Mechanisms of interannual to decadal variability of the North Atlantic circulation, *Journal of Climate*, 14, 2266-2280, 2001.
- Esper, J., E. R. Cook, and F. H. Schweingruber, Low-Frequency Signals in Long Tree-Ring Chronologies for Reconstructing Past Temperature Variability, *Science*, 295, 2250-2253, 2002.
- Ferrier-Pages, C., F. Boisson, D. Allemand, and E. Tambutte, Kinetics of strontium uptake in the scleractinian coral *Stylophora pistillata*, *Marine Ecology-Progress Series*, 245, 93-100, 2002.

- Gagan, M. K., L. K. Ayliffe, D. Hopley, J. A. Cali, G. E. Mortimer, J. Chappell, M. T. McCulloch, and M. J. Head, Temperature and surface-ocean water balance of the mid-Holocene tropical Western Pacific, *Science*, 279, 1014-1018, 1998.
- Glueck, M. F., and C. W. Stockton, Reconstruction of the North Atlantic Oscillation, *International Journal of Climatology*, 21, 1453-1465, 2001.
- Glynn, P. W., E. M. Druffel, and R. B. Dunbar, A dead Central American reef tract: possible link with the Little Ice Age, *Journal of Marine Research*, 41, 605-637, 1983.
- Goodkin, N. F., K. Hughen, A. C. Cohen, and S. R. Smith, Record of Little Ice Age sea surface temperatures at Bermuda using a growth-dependent calibration of coral Sr/Ca, *Paleoceanography*, 20, PA4016, doi:4010.1029/2005PA001140, 2005.
- Gregor, R. B., N. E. Pingitore, and F. W. Lytle, Strontianite in coral skeletal aragonite, *Science*, 275, 1452-1454, 1997.
- Grossman, E. L., and T. L. Ku, Oxygen and carbon isotope fractionation in biogenic aragonite: temperature effects, *Chemical Geology*, 59, 59-74, 1986.
- Grove, J. M., *The Little Ice Age*, 498 pp., Methuen & Co. Ltd., London, 1988.
- Guilderson, T. P., R. G. Fairbanks, and J. L. Rubenstone, Tropical Temperature-Variations since 20,000 Years Ago - Modulating Interhemispheric Climate-Change, *Science*, 263, 663-665, 1994.
- Guilderson, T. P., and D. P. Schrag, Reliability of coral isotope records from the western Pacific warm pool: A comparison using age-optimized records, *Paleoceanography*, 14, 457-464, 1999.
- Hart, S. R., and A. L. Cohen, An ion probe study of annual cycles of Sr/Ca and other trace elements in corals, *Geochimica Et Cosmochimica Acta*, 60, 3075-3084, 1996.
- Hogg, N. G., On the transport of the Gulf Stream between Cape Hatteras and the Grand Banks, *Deep Sea Research*, 39, 1231-1246, 1992.
- Hughen, K. A., D. P. Schrag, S. B. Jacobsen, and W. Hantoro, El Nino during the last interglacial period recorded by a fossil coral from Indonesia, *Geophysical Research Letters*, 26, 3129-3132, 1999.
- Hurrell, J., Y. Kushnir, G. Ottersen, and M. Visbeck, An Overview of the North Atlantic Oscillation. in *The North Atlantic Oscillation: Climatic Significance and Environmental Impact*, edited by Hurrell, J., Y. Kushnir, G. Ottersen and M. Visbeck, pp. 1-36, American Geophysical Union, Washington, D. C, 2003.
- Hurrell, J. W., Decadal Trends in the North-Atlantic Oscillation - Regional Temperatures and Precipitation, *Science*, 269, 676-679, 1995.



- Jacoby, G., and R. D. D'Arrigo, Reconstructed northern hemisphere annual temperature since 1671 based on high-latitude tree-ring data from North America, *Climatic Change*, 14, 39-59, 1989.
- Jones, P. D., K. R. Briffa, T. P. Barnett, and S. F. B. Tett, High-resolution palaeoclimatic records for the last millennium: interpretation, integration and comparison with General Circulation Model control-run temperatures, *Holocene*, 8, 455-471, 1998.
- Jones, P. D., T. Jonsson, and D. Wheeler, Extension to the North Atlantic Oscillation using early instrumental pressure observations from Gibraltar and south-west Iceland, *International Journal of Climatology*, 17, 1433-1450, 1997.
- Keigwin, L. D., The Little Ice Age and Medieval warm period in the Sargasso Sea, *Science*, 274, 1504-1508, 1996.
- Keigwin, L. D., and R. S. Pickart, Slope Water Current over the Laurentian Fan on Interannual to Millennial Time Scales, *Science*, 286, 520-523, 1999.
- Kuhnert, H., J. Patzold, B. Schnetger, and G. Wefer, Sea-surface temperature variability in the 16th century at Bermuda inferred from coral records, *Palaeogeography Palaeoclimatology Palaeoecology*, 179, 159-171, 2002.
- Kushnir, Y., V. J. Cardone, J. G. Greenwood, and M. A. Cane, The recent increase in North Atlantic wave heights, *Journal of Climate*, 10, 2107-2113, 1997.
- Lea, D. W., D. K. Pak, and H. J. Spero, Climate impact of the late Quaternary equatorial Pacific sea surface temperature variations, *Science*, 289, 1719-1724, 2000.
- Lean, J., J. Beer, and R. Bradley, Reconstruction of solar irradiance since 1610: implications for climate change, *Geophysical Research Letters*, 22, 3195-3198, 1995.
- Linsley, B. K., R. G. Messier, and R. B. Dunbar, Assessing between-colony oxygen isotope variability in the coral *Porites lobata* at Clipperton Atoll, *Coral Reefs*, 18, 13-27, 1999.
- Lough, J. M., A strategy to improve the contribution of coral data to high-resolution paleoclimatology, *Palaeogeography Palaeoclimatology Palaeoecology*, 204, 115-143, 2004.
- Lund, D. C., and W. B. Curry, Florida Current surface temperature and salinity variability during the last millennium, *Paleoceanography*, 21, doi:10.1029/2005PA001218, 2006.
- Luterbacher, J., E. Xoplaki, D. Dietrich, P. D. Jones, T. D. Davies, D. Portis, J. F. Gonzalez-Rouco, H. von Storch, D. Gyalistras, C. Casty, and H. Wanner, Extending the North Atlantic Oscillation reconstructions back to 1500, *Atmospheric Science Letters*, 2, 114-124, 2001.



- MacKenzie, F. T., Strontium content and variable strontium-chlorinity relationship of sargasso sea water, *Science*, 146, 517-518, 1964.
- Marshall, J., Y. Kushner, D. Battisti, P. Chang, A. Czaja, R. Dickson, J. Hurrell, M. McCartney, R. Saravanan, and M. Visbeck, North Atlantic climate variability: Phenomena, impacts and mechanisms, *International Journal of Climatology*, 21, 1863-1898, 2001.
- Marshall, J. F., and M. T. McCulloch, An assessment of the Sr/Ca ratio in shallow water hermatypic corals as a proxy for sea surface temperature, *Geochimica Et Cosmochimica Acta*, 66, 3263-3280, 2002.
- McConnaughey, T., C-13 and O-18 Isotopic Disequilibrium in Biological Carbonates .1. Patterns, *Geochimica Et Cosmochimica Acta*, 53, 151-162, 1989a.
- McConnaughey, T., C-13 and O-18 Isotopic Disequilibrium in Biological Carbonates .2. Invitro Simulation of Kinetic Isotope Effects, *Geochimica Et Cosmochimica Acta*, 53, 163-171, 1989b.
- McConnaughey, T. A., Sub-equilibrium oxygen-18 and carbon-13 levels in biological carbonates: carbonate and kinetic models, *Coral Reefs*, 22, 316-327, 2003.
- McCulloch, M., G. Mortimer, T. Esat, X. H. Li, B. Pillans, and J. Chappell, High resolution windows into early Holocene climate: Sr/Ca coral records from the Huon Peninsula, *Earth and Planetary Science Letters*, 138, 169-178, 1996.
- NOAA, About Coral Reefs: [www.coris.noaa.gov/about/welcome.html](http://www.coris.noaa.gov/about/welcome.html).
- NRC, *Abrupt Climate Change: Inevitable Suprises*, National Research Council, Washington, D. C., 2002.
- Ohkouchi, N., T. I. Eglinton, L. D. Keigwin, and J. M. Hayes, Spatial and Temporal Offsets Between Proxy Records in a Sediment Drift, *Science*, 298, 1224-1227, 2002.
- Overpeck, J., K. Hughen, D. Hardy, R. Bradley, R. Case, M. Douglas, B. Finney, K. Gajewski, G. Jacoby, A. Jennings, S. Lamoureux, A. Lasca, G. MacDonald, J. Moore, M. Retelle, S. Smith, A. Wolfe, and G. Zielinski, Arctic environmental change of the last four centuries, *Science*, 278, 1251-1256, 1997.
- Pelejero, C., J. O. Grimalt, S. Heilig, M. Kienast, and L. Wang, High resolution Uk37 temperature reconstruction in the South China Sea over the past 220 Kyr., *Paleoceanography*, 14, 224-231, 1999.
- Reuer, M. K., Centennial-Scale Elemental and Isotopic Variability in the Tropical and Subtropical North Atlantic, Doctoral, MIT/WHOI Joint Program, 2001.

- Reynaud, S., C. Ferrier-Pages, F. Boisson, D. Allemand, and R. G. Fairbanks, Effect of light and temperature on calcification and strontium uptake in the scleractinian coral *Acropora verweyi*, *Marine Ecology-Progress Series*, 279, 105-112, 2004.
- Rodwell, M. J., D. P. Rowell, and C. K. Folland, Oceanic forcing of the wintertime North Atlantic Oscillation and European climate, *Nature*, 398, 320-323, 1999.
- Rosenthal, Y., D. W. Oppo, and B. K. Linsley, The amplitude and phasing of climate change during the last deglaciation in the Sulu Sea, western equatorial Pacific, *Geophysical Research Letters*, 30, 1429, 2003.
- Rühlemann, C., S. Mulitza, P. J. Müller, G. Wefer, and R. Zahn, Warming of the tropical Atlantic Ocean and slowdown of thermohaline circulation during the last deglaciation, *Nature*, 402, 511-514, 1999.
- Sachs, J. P., and S. Lehman, Subtropical North Atlantic Temperatures 60,000 to 30,000 Years Ago, *Science*, 286, 756-759, 1999.
- Schmitz, W. J., and M. S. McCartney, On the North Atlantic Circulation, *Reviews of Geophysics*, 31, 29-49, 1993.
- Schoene, B. R., W. Oschmann, J. Rossler, A. D. F. Castro, S. D. Houk, I. Kroncke, W. Dreyer, R. Janssen, H. Rumohr, and E. Dunca, North Atlantic Oscillation dynamics recorded in shells of a long-lived bivalve mollusk, *Geology*, 31, 1037-1040, 2003.
- Schone, B. R., W. Oschmann, J. Rossler, A. D. F. Castro, S. D. Houk, I. Kroncke, W. Dreyer, R. Janssen, H. Rumohr, and E. Dunca, North Atlantic Oscillation dynamics recorded in shells of a long-lived bivalve mollusk, *Geology*, 31, 1037-1040, 2003.
- Shen, C. C., T. Lee, C. Y. Chen, C. H. Wang, C. F. Dai, and L. A. Li, The calibration of D Sr/Ca versus sea surface temperature relationship for Porites corals, *Geochimica Et Cosmochimica Acta*, 60, 3849-3858, 1996.
- Shindell, D. T., R. L. Miller, G. Schmidt, and L. Pandolfo, Simulation of recent northern winter climate trends by greenhouse-gas forcing., *Nature*, 399, 452-455, 1999.
- Smith, S. V., R. W. Buddemeier, R. C. Redalje, and J. E. Houck, Strontium-Calcium Thermometry in Coral Skeletons, *Science*, 204, 404-407, 1979.
- Swart, P. K., H. Elderfield, and M. J. Greaves, A high-resolution calibration of Sr/Ca thermometry using the Caribbean coral *Montastraea annularis*, *Geochemistry Geophysics Geosystems*, 3, 2002.
- Talley, L. D., North Atlantic circulation and variability, reviewed for the CNLS conference, *Physica D*, 98, 625-646, 1996.

- Thompson, D. W. J., and J. M. Wallace, Regional climate impacts of the Northern Hemisphere annular mode, *Science*, 293, 85-89, 2001.
- Urey, H. C., The thermodynamic properties of isotopic substances, *Journal of Chem. Soc.*, 562-581, 1947.
- Visbeck, M., Climate - The ocean's role in Atlantic climate variability, *Science*, 297, 2223-2224, 2002.
- Visbeck, M., E. Chassignet, R. Curry, T. Delworth, R. Dickson, and G. Krahmann, The Ocean's Response to North Atlantic Oscillation Variability. in *The North Atlantic Oscillation: Climate Significance and Environmental Impact*, edited by Hurrell, J., Y. Kushnir, G. Ottersen and M. Visbeck, pp. 113-145, American Geophysical Union, Washington, D. C., 2003.
- Visbeck, M. H., J. W. Hurrell, L. Polvani, and H. M. Cullen, The North Atlantic Oscillation: Past, present, and future, *Proceedings of the National Academy of Sciences of the United States of America*, 98, 12876-12877, 2001.
- Watanabe, T., A. Winter, and T. Oba, Seasonal changes in sea surface temperature and salinity during the Little Ice Age in the Caribbean Sea deduced from Mg/Ca and  $^{18}\text{O}/^{16}\text{O}$  ratios in corals, *Marine Geology*, 173, 21-35, 2001.
- Wigley, T. M. L., and P. M. Kelly, Holocene climatic change,  $^{14}\text{C}$  wiggles and variations in solar irradiance, *Philosophical Transactions of the Royal Society of London Series A*, 330, 547-560, 1990.
- Winter, A., H. Ishioroshi, T. Watanabe, T. Oba, and J. Christy, Caribbean sea surface temperatures: two-to-three degrees cooler than the present during the Little Ice Age, *Geophysical Research Letters*, 27, 3365-3368, 2000.



## Chapter 2

# Record of Little Ice Age Sea Surface Temperatures at Bermuda Using a Growth-Dependent Calibration of Coral Sr/Ca

Reprinted with permission of the American Geophysical Union.

Goodkin, N. F., K. A. Hughen, A. L. Cohen, and S. R. Smith (2005), Record of Little Ice Age sea surface temperatures at Bermuda using a growth-dependent calibration of coral Sr/Ca, *Paleoceanography*, 20, PA4016, doi:10.1029/2005PA001140.

### Abstract

Strontium to calcium ratios (Sr/Ca) are reported for a massive brain coral *Diploria labyrinthiformis* collected from the south shore of Bermuda and are strongly correlated with both sea surface temperature (SST) and mean annual skeletal growth rate. High Sr/Ca ratios correspond with cold SSTs and slow skeletal growth rate and vice versa. We provide a quantitative calibration of Sr/Ca to extension rate and SST along the axis of maximum growth and derive a growth-dependent Sr/Ca–SST calibration equation to reconstruct western subtropical North Atlantic SSTs for the past 223 years. When the influence of growth rate is excluded from the calibration, Sr/Ca ratios yield SSTs that are too cold during cool anomalies and too warm during warm anomalies. Toward the end of the Little Ice Age (~1850), SST changes derived using a calibration that is not growth-dependent are exaggerated by a factor of 2 relative to those from the growth-corrected model that yields SSTs ~1.5°C cooler than today. Our results indicate that incorporation of growth rate effects into coral Sr/Ca calibrations may improve the accuracy of SSTs derived from living and fossil corals.

## 2.1 Introduction

Accurate estimates of past SSTs, not captured in short instrumental records, are key to understanding long-term variability in Earth's climate system. One method of SST reconstruction is based on the inverse correlation between the Sr/Ca content of reef coral skeleton and ocean temperature [Smith *et al.*, 1979]. With this technique, Sr/Ca–SST calibrations derived from living corals are applied to ancient specimens to reconstruct SST [Beck *et al.*, 1992; Corregge *et al.*, 2004; Guilderson *et al.*, 1994; McCulloch *et al.*, 1999]. With high accretion rates, longevity, and skeletal annual growth bands, corals can potentially provide seasonally resolved, precisely dated records of SST spanning several centuries. Despite this potential, Sr/Ca–derived SSTs from ancient corals are often several degrees cooler than those derived from other marine proxies [Lea *et al.*, 2000; Pelejero *et al.*, 1999; Rosenthal *et al.*, 2003] and their accuracy has been questioned [Crowley, 2000].

There are several indications that growth or calcification rate may influence the Sr/Ca ratio of coral skeleton. Across coral taxa, faster growing species have lower Sr/Ca ratios than slow growing species [Corregge *et al.*, 2004; Weber, 1973]. Within a single species, fast growing colonies often have lower Sr/Ca ratios than slow growing colonies or slower growing parts within a colony [Alibert and McCulloch, 1997; Cohen and Hart, 2004; deVilliers *et al.*, 1995]. Corals whose calcification rates are enhanced by symbiont photosynthesis have lower Sr/Ca ratios than conspecifics without symbionts [Cohen *et al.*, 2002]. Culture studies demonstrate that differences in ion transport rates during calcification lead to reduced Sr uptake relative to Ca during periods of rapid calcification and vice versa [Cohen and McConnaughey, 2003; Ferrier-Pages *et al.*, 2002; Ip and

Krishnaveni, 1991]. Hypotheses regarding the mechanisms by which growth may influence coral Sr/Ca ratios include sampling artifacts linked to slow growth, convoluted skeletal architecture [Cohen *et al.*, 2004; Swart *et al.*, 2002], and kinetic effects [deVilliers *et al.*, 1994]. To date, effects related to calcification or growth rates have been examined between colonies of the same species [deVilliers *et al.*, 1995], between fast and slow growing axes of the same colony [deVilliers *et al.*, 1994] and between different times in the life of a coral polyp [Alibert and McCulloch, 1997].

Here we present data that demonstrate the impact of variability in skeletal extension rates on the accuracy of Sr/Ca-based SST reconstructed along a single, fast growing axis of a massive brain coral, *Diploria labyrinthiformis*. Growth rate changes of up to factors of 2–3 are associated with anomalously warm and cool Sr/Ca-derived SSTs, compared to recorded temperatures. A Sr/Ca–SST calibration that takes growth rate into account shows improved agreement with instrumental SST, and an application of the growth-corrected model yields late Little Ice Age (LIA), ~1850 AD, SSTs 1.5°C cooler than they are today. In contrast, SSTs derived from Sr/Ca while excluding growth rate effects were up to 3.0°C cooler than today.

## **2.2 Methods**

### **2.2.1 Study Site**

In May 2000, an ~230-year-old massive brain coral colony was sampled live off John Smith's Bay (JSB) on the southeastern edge of the Bermuda platform at 16-m depth. On Bermuda, growth rates of *Diploria labyrinthiformis* range from 2 to 6 mm/yr [Cohen *et al.*, 2004; Dodge and Thomson, 1974; Logan and Tomascik, 1991; Logan *et al.*, 1994],



compared to 8 mm/yr and up to 20 mm/yr in more widely used species such as *Porites* [Alibert and McCulloch, 1997; Hughen et al., 1999; Mitsuguchi et al., 1996; Shen et al., 1996]. *Diploria* spp. inhabit a wide range of water temperatures and are found in both the tropical and subtropical Atlantic. While *Diploria* spp. have not often been widely used for paleoclimate reconstruction [Cardinal et al., 2001; Cohen et al., 2004; Kuhnert et al., 2002] the long life spans and large geographic distribution indicate its promise as a tool for long paleoclimate records.

The south terrace of Bermuda was chosen because of its exposure to open ocean waters and proximity to Hydrostation S located 30 km to the southeast. SST from 0- to 16-m depth has been recorded at Hydrostation S biweekly since 1954. Over that time, monthly averaged SST ranged from 18.0° to 28.9°C with annual averages between 22.4° and 24.3°C. For the calibration period of this study (1976–1997), mean annual SST ranged from 22.8° to 23.5°C with a seasonal range of 18.3° to 28.9°C. The SST record is incomplete over different intervals including 2 or more months of missing data in the years 1978–1980, 1986 and 1989.

### **2.2.2 Sub-sampling and Analysis of Coral**

Three 5- to 10-mm-thick slabs were cut from the maximum growth axis of the coral using a diamond blade rock saw (Figure 2.1). The slabs were cleaned in an ultrasonic bath with deionized H<sub>2</sub>O 3 times for 10 min and dried in an oven at 50°C. X-radiographs were performed at Falmouth (Massachusetts) Hospital with machine settings of 50 kV and 1.6 mAs, a film focus distance of 1 m and an exposure time of 0.2 s.

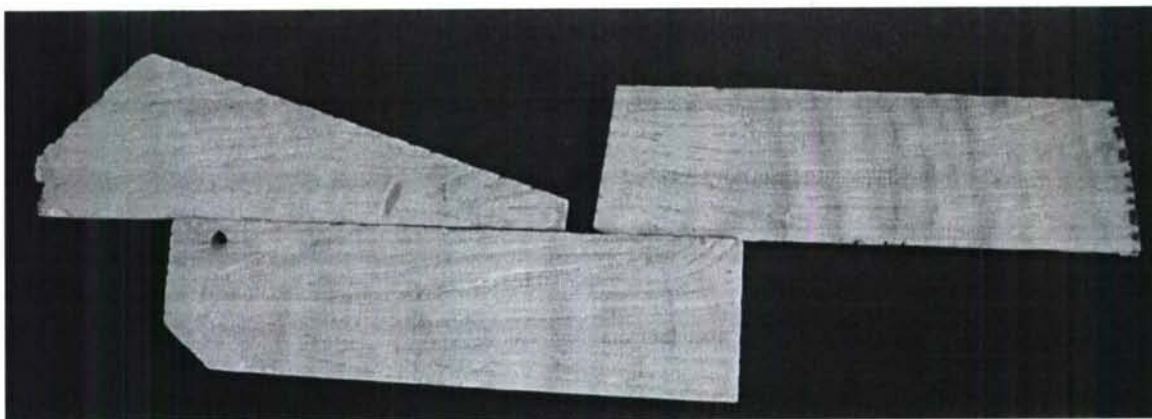


**Figure 2.1.** Three 5- to 10-mm-thick slabs were sliced from the ~1-m-long coral to capture the major growth axis through time. Slabs were cut in an overlapping fashion to ensure proper age model development and consecutive sampling of the entire record.

All samples were drilled from the solid thecal wall (the septotheca) that separates the calyx from the ambulacrum [Cohen *et al.*, 2004]. We targeted the theca to ensure that ample material could be extracted for analysis and to diminish the potential for diagenetic alteration or secondary aragonite precipitation due to the isolation of the center of the wall from skeletal pore spaces filled with seawater. In situ staining studies suggest that extension rates on the theca are higher in the summer (June through September) than they are in the winter [Cohen *et al.*, 2004].

Annual extension rates, calculated from the distance between successive high-density bands in the X-radiograph, indicate an average growth rate of 3.8 mm/yr. From 1976 to 1997, the thecal wall was sampled at 0.33 mm (approximately monthly resolution) with a drill press and micrometer-controlled stage. Approximately 200 mg of powder was collected for each Sr/Ca analysis. The years 1775–1997 were sampled biennially, using a diamond blade band saw. To generate the biennial record, samples were cut between every second high- low-density band interface, and two thecal walls and the ambulacrum were isolated by grinding away the calyx with a hand-held Dremel

tool. Thecal samples (~0.9 g) representing the full 2 years growth were cleaned in an ultrasonic bath with deionized H<sub>2</sub>O 3 times for 10 min, and dissolved in 1N HNO<sub>3</sub> for analysis.

Sr and Ca were measured using Inductively Coupled Plasma–Atomic Emission Spectrometry (ICP-AES) applying solution standards to correct for drift and matrix effects related to interference from varying Ca concentrations [Schrag, 1999]. The samples, blanks, and external standard (a homogenized, powdered *Porites* coral) were prepared simultaneously. Repeat measurements on the coral external standard over 12 months showed reproducibility ( $n = 96$ , standard deviation = 0.02 mmol/mol).

The age model was constructed from density banding visible in the X-radiographs and refined by tuning Sr/Ca to monthly averaged SSTs at inflection points. While this lessens the independence of the Sr/Ca–SST relationship, maximum and minimum values rather than median values at the inflection points drive the correlation of Sr/Ca to SST. The Sr/Ca data were resampled by linear interpolation at even monthly intervals equivalent to SST data.

Reported annual growth (extension) rates for the high-resolution record (approximately monthly sampling) were calculated from the distance between two successive Januarys in each annual cycle as defined by the Sr/Ca–derived age model. Growth rates for the biennial record were determined using X-radiographs (Figure 2.2) as follows; the distance between every other high- low-density band interface was measured and divided in two to calculate the average growth per year over the 2 years sampled.



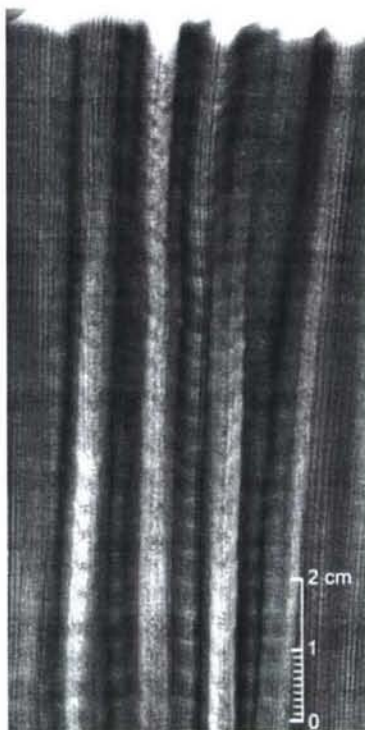


**Figure 2.2.** X-radiograph positive image of the first 97 mm of the top slab. X rays show clear annual banding made up of one low-density and one high-density band.

## 2.3 Results

### 2.3.1 Reproducibility of the Sr/Ca Record Within the Colony

As this *Diploria* colony grew, the position of the maximum growth axis changed relative to the center of the dome (Figure 2.1). Therefore it was difficult for the entire length of the coral to be sampled along one planar growth transect, mandating that sampling transects change between the theca from along the slabs. Parallel transects were drilled for the periods 1979–1986 and 1989–1992. A strong relationship exists between the multiple tracts ( $r^2 = 0.83$ ,  $p = 0$ , slope = 1.04, intercept = -0.000705), demonstrating the reproducibility of the Sr/Ca signal between parallel sample transects.

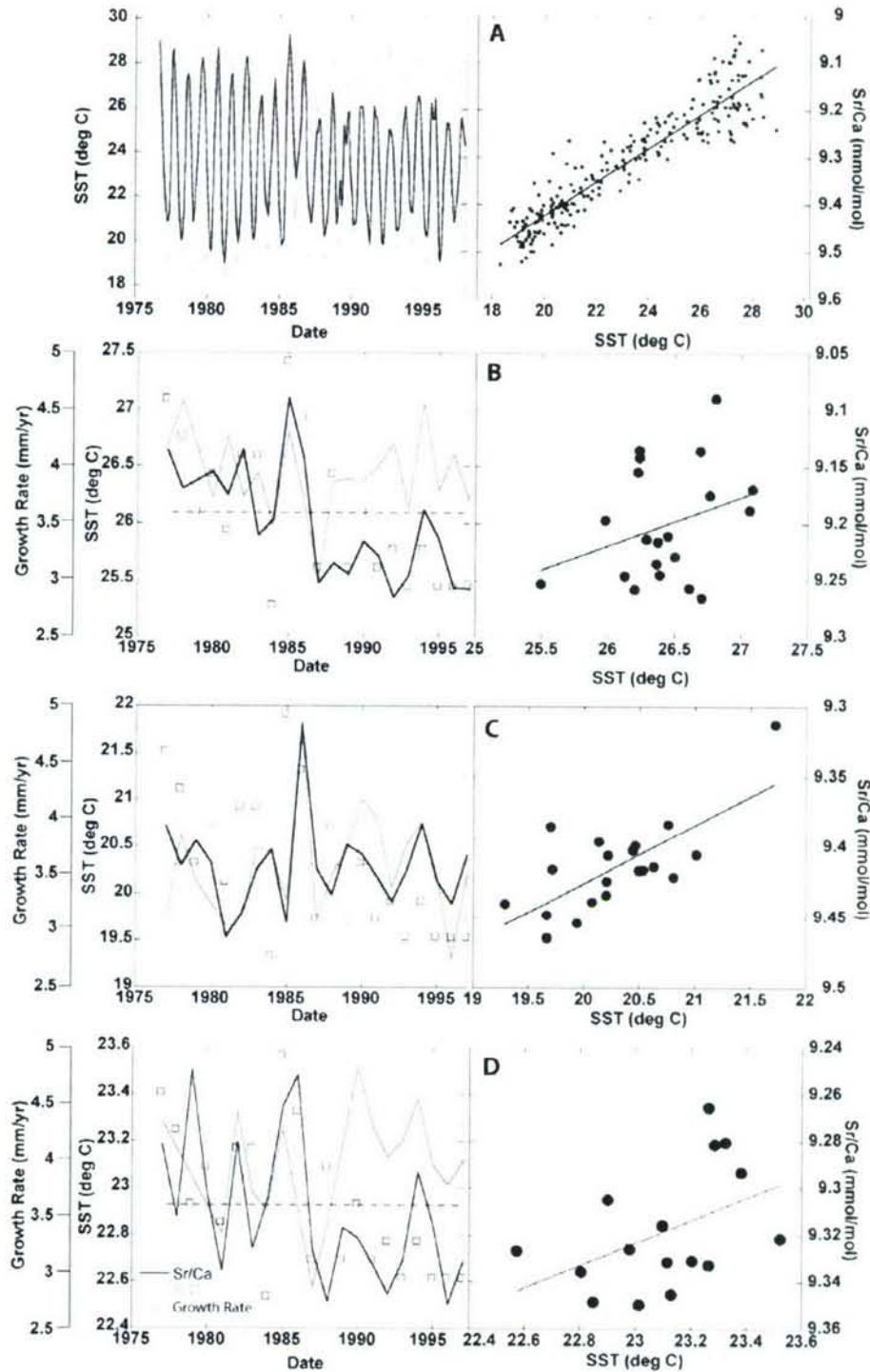


**Figure 2.3.** Coral Sr/Ca (solid line) and Hydrostation S sea surface temperature (SST) (shaded line) plotted versus year and correlated using linear regression. Calibration results for (a) monthly ( $r^2 = 0.86$ ,  $p < 0.0001$ ), (b) summer (June, July, August, September (JJAS)) ( $r^2 = 0.10$ ,  $p = 0.17$ ), (c) winter (December, January, February, March (DJFM)) ( $r^2 = 0.51$ ,  $p = 0.0004$ ), and (d) mean annual ( $r^2 = 0.21$ ,  $p = 0.077$ ) resolved data. Mean annual coral growth rates (squares) and average growth (dashed line) are shown for the calibration period. Size of circles represents  $2\sigma$  analytical error.

### 2.3.2 Monthly Resolution Calibration

A linear regression of monthly resolved Sr/Ca ratios to SST yields the following correlation (Figure 2.3a):

$$\text{Sr/Ca} = 10.1 (\pm 0.04) - 0.0358 (\pm 0.0018) * \text{SST} \\ (2\sigma, 95\% \text{ conf.}, r^2=0.86, p<<0.0001, \text{stdr}=1.2 \text{ } ^\circ\text{C}) \quad (1)$$

where stdr is the standard deviation of the residual. These results are consistent with previous studies of slow to moderately slow growing corals, including a colony of *Diploria* from Bermuda [Cardinal *et al.*, 2001], *Montastraea* from Florida [Swart *et al.*, 2002], and *Diploastrea* from Fiji [Bagnato *et al.*, 2004]. On the basis of results from Cohen *et al.* [2004] using microbeam measurements, our sampling resolution may dampen the full range of Sr/Ca variability over the annual cycle. Owing to this smoothing, the monthly calibration cannot be used to reconstruct interannual variability as the dampened slope would return overestimated changes in SST. For this reason, calibrations using interannual variability were derived.

### 2.3.3 Inter-annual Calibrations

To derive the Sr/Ca–SST calibrations based on interannual variability, 4-month summer (JJAS), 4-month winter (DJFM), and mean annual averages were calculated. Examination of the monthly Sr/Ca calibration (Figure 2.3a) indicates that summertime Sr/Ca reflects SST from 1977 to 1986 differently than from 1987 to 1997, while the wintertime signal continues to capture interannual SST variability. This can be seen clearly when the data are averaged for summer (Figure 2.3b) and winter (Figure 2.3c)



periods. Coincident with the change in the summer time Sr/Ca–SST relationship is a decrease in the mean annual extension rate from above average to below average for the calibration period (Figures 2.3b, 2.3c, and 2.3d). Average annual SSTs derived from coral Sr/Ca are essentially a combination of the summer and winter signals and also diverge from instrumental data at the same time as the decrease in mean annual extension rate (Figure 2.3d). Average summer Sr/Ca shows no relationship to SST when correlated over the entire 1977–1997 calibration interval ( $r^2 = 0.10$ ,  $p = 0.17$ ) (Figure 2.3b), and the mean annual record shows a poor correlation ( $r^2 = 0.21$ ,  $p = 0.077$ ) (Figure 2.3d). Average winter Sr/Ca does not show any discrepancy affiliated with growth rate (Figure 2.3c), and a winter linear least squares regression to SST shows a significant relationship:

$$\text{Sr/Ca} = 10.3 (\pm 0.4) - 0.0412 (\pm 0.0191) * \text{SST}$$

$$(2\sigma, 95\% \text{ conf.}, r^2=0.51, p=0.0004, \text{stdr}=0.54 \text{ } ^\circ\text{C}) \quad (2)$$

The winter correlation  $r^2$  value is diminished in comparison with the monthly calibration, because of the lower signal-to noise ratio (winter SST range = 19°–22°C, annual SST range = 18°–29°C).

Examination of the relationship between Sr/Ca and growth reveals that summer Sr/Ca correlates more strongly to annual skeletal extension rate ( $r^2 = 0.64$ ,  $p < 0.0001$ ) (Figure 2.4a) than to SST ( $r^2 = 0.10$ ,  $p = 0.17$ ). Mean annual Sr/Ca correlates relatively equally to growth rate ( $r^2 = 0.36$ ,  $p = 0.014$ ) and SST ( $r^2 = 0.21$ ,  $p = 0.077$ ), whereas winter Sr/Ca shows no relationship to growth rate ( $r^2 = 0.01$ ,  $p = 0.61$ ) (Figure 2.4a) and a strong relationship to SST ( $r^2 = 0.51$ ,  $p = 0.0004$ ). The impact of growth rate on summer, winter, and mean annual Sr/Ca–SST calibrations is further investigated by correlating growth rate with SST residuals (calculated by subtracting instrumental SST from

reconstructed monthly SST). Summer SST residuals are strongly correlated with growth rate ( $r^2 = 0.59$ ,  $p < 0.0001$ ), but no significant relationship is observed between growth rate and winter SST residuals ( $r^2 = 0.06$ ,  $p = 0.31$ ) (Figure 2.4b). Mean annual SST residuals show a correlation with growth rate ( $r^2 = 0.37$ ,  $p = 0.013$ ) that is better than the winter residual Sr/Ca regression but not as good as the summer residual Sr/Ca regression (Figure 2.4b). Thus averaging over the annual cycle does not eliminate the impact of growth rate on Sr/Ca signals, implying that a growth-corrected model must be employed to examine interannual variability.

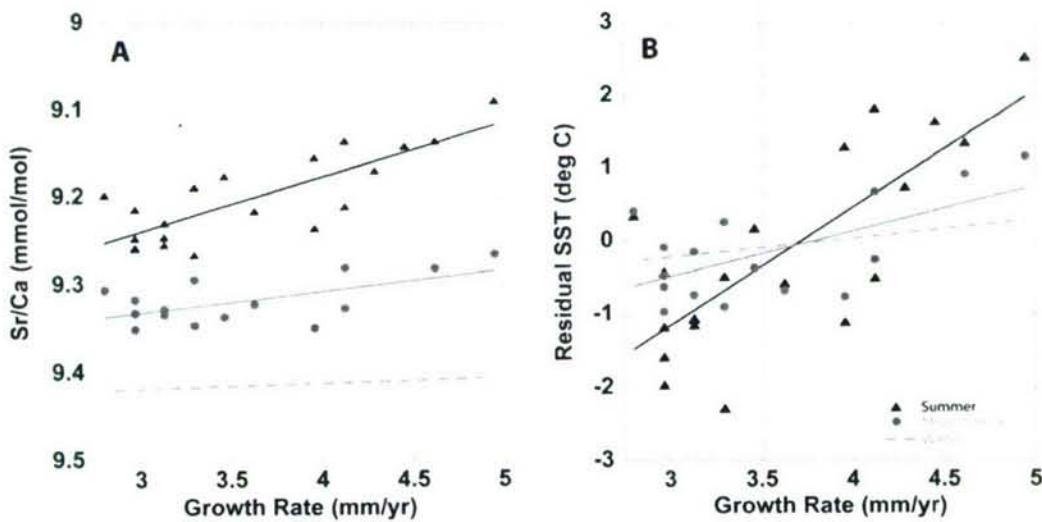


**Figure 2.4.** Mean annual growth rate compared to Sr/Ca and Sr/Ca-based SST residuals. (a) Sr/Ca to growth rate correlations for summer (JJAS) (triangles) ( $r^2 = 0.64$ ,  $p < 0.0001$ ), mean annual (circles) ( $r^2 = 0.36$ ,  $p = 0.014$ ), and winter (DJFM) (squares) ( $r^2 = 0.01$ ,  $p = 0.61$ ) resolved data. (b) Residual SST to growth rate correlations for summer ( $r^2 = 0.59$ ,  $p < 0.0001$ ), mean annual ( $r^2 = 0.36$ ,  $p = 0.013$ ), and winter ( $r^2 = 0.06$ ,  $p = 0.31$ ) resolved data. Residuals are calculated by converting monthly Sr/Ca to SST and then subtracting from instrumental SST.

In the mean annual Sr/Ca regression, mean annual Sr/Ca was linearly regressed on mean annual SST by the preceding equation (Figure 2.3d):

$$\text{Sr/Ca} = m * \text{SST} + b \quad (3)$$

This regression produced the following result:

$$\text{Sr/Ca} = 10.4 (\pm 1.2) - 0.0481 (\pm 0.0503) * \text{SST}$$

$$(2\sigma, 95\% \text{ conf.}, r^2=0.21, p=0.0766, \text{stdr}=0.46 \text{ } ^\circ\text{C}) \quad (4)$$

In the growth-corrected mean annual model, the slope (m) of the mean annual Sr/Ca–SST relationship (equation (3)) is hypothesized to change as a linear function of growth rate where

$$m = n * (\text{growth rate}) + c \quad (5)$$

and growth rate is the 3-year averaged linear extension rate. The net regressed equation is

$$\text{Sr/Ca} = c*(\text{SST}) + n*(\text{growth rate})*(\text{SST}) + b \quad (6)$$

For the purposes of the growth-corrected model, growth rates were averaged over 3-year periods, providing a more conservative estimate of the continuous calcification rates that occurred as the aragonite was formed by both extension and infilling for the time represented by sampling methods. The linear least squares multiple regression returns the following equation:

$$\text{Sr/Ca} = -0.0529 (\pm 0.0334) * (\text{SST}) - 0.00170 (\pm 0.00078) * (\text{growth rate}) * (\text{SST}) + 10.7 (\pm 0.8)$$

$$(2\sigma, 95\% \text{ conf.}, r^2=0.68, p_c=0.0074, p_n=0.00078, \text{stdr}=0.24 \text{ } ^\circ\text{C}) \quad (7)$$

where  $p_c$  is the significance on slope  $c$  from equation (6) and  $p_n$  is the significance on slope  $n$  from equation (6). The inclusion of this additional relationship into the growth-corrected model leads to a significant improvement in fit ( $r^2 = 0.68$ ,  $p_c = 0.0074$ ,  $p_n = 0.00078$ ) compared to the mean annual Sr/Ca–SST regression ( $r^2 = 0.21$ ,  $p = 0.077$ ). While the variance of the two fits are not comparable because of the change in the number of variables, mean annual Sr/Ca values over the calibration period were converted to SST using the mean annual Sr/Ca–SST regression and the growth-corrected



model to demonstrate the improved accuracy in reconstructing SST. SSTs reconstructed with the growth-corrected model agree more closely with instrumental data ( $r^2 = 0.49$ ,  $p = 0.0026$ ) than those with the mean annual Sr/Ca–SST regression ( $r^2 = 0.21$ ,  $p = 0.077$ ) (Figure 2.5). This improvement is exemplified by a decrease in the variance of the residual where the standard deviation equals  $0.46^\circ\text{C}$  in the Sr/Ca–SST regression compared to  $0.24^\circ\text{C}$  in the growth-corrected model (Figure 2.5).

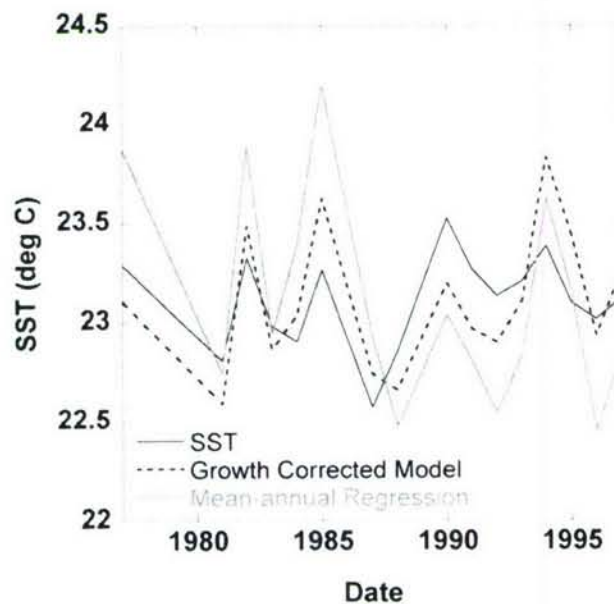


**Figure 2.5.** Mean annual instrumental SST from Hydrostation S (solid line) compared to reconstructed mean annual SST using the mean annual Sr/Ca–SST regression (shaded line) and growth-corrected model (dashed line). The growth-corrected model has a stronger fit to the instrumental records ( $r^2 = 0.49$ ,  $p = 0.0026$  compared to  $r^2 = 0.21$ ,  $p = 0.077$  for the non-growth dependent mean annual Sr/Ca–SST regression).

### 2.3.4 Application of Calibration Regression

In order to examine the potential effects of the different calibrations on paleotemperature reconstructions, the monthly, mean annual Sr/Ca–SST regression and growth-corrected mean annual model were used to quantify SST from the 223-year biennially sampled Sr/Ca record. Reconstructed SST shows distinct cooling during the

LIA, with an abrupt temperature drop in the 1840s and a gradual warming culminating in the 1960s. However, the amplitude of these changes varies significantly depending on which calibration is applied.

The reconstruction based on the monthly calibration shows that biennial SST changed nearly  $5^{\circ}\text{C}$  from 1960 to the end of the LIA in the late 1840s, 2.5 times the change found using the growth-corrected mean annual model (Figure 2.6). The use of a monthly resolved calibration which does not capture the full amplitude of the seasonal cycle clearly influences the magnitude of interannual SST change calculated back through time. The biennial record does not necessarily capture the exact same months in each sample through time which may lead to some seasonal biases. However, this effect is diminished by looking at 2-year periods and is likely not large enough to account for the changes in temperature seen in this record.

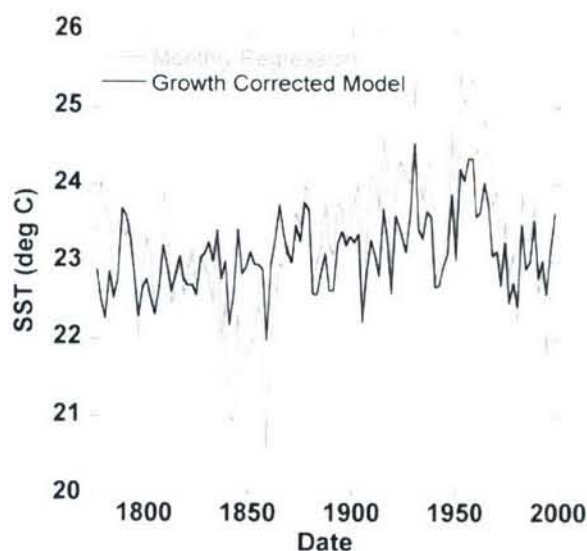


**Figure 2.6.** Biennial-resolution SST reconstructed to 1780. SST was reconstructed using the growth-corrected mean annual model (solid line) and the monthly regression (shaded line). By exaggerating both maximums and minimums, the monthly regression shows an SST change 2.5 times greater than the growth-corrected mean annual model reconstruction.

The mean annual extension rate of the coral is shown to covary with the Sr/Ca record over the length of the biennial record, supporting the initial observation that both growth and SST may influence the Sr/Ca record (Figure 2.7). The highest mean annual Sr/Ca values seen in the mid-to-late 1800s are also the periods of slowest growth. Use of the mean annual Sr/Ca–SST regression yields an SST change of 3.5°C from the 1960s to the 1840s, whereas the growth-corrected model shows a change of only 2°C over this same period (Figure 2.8).

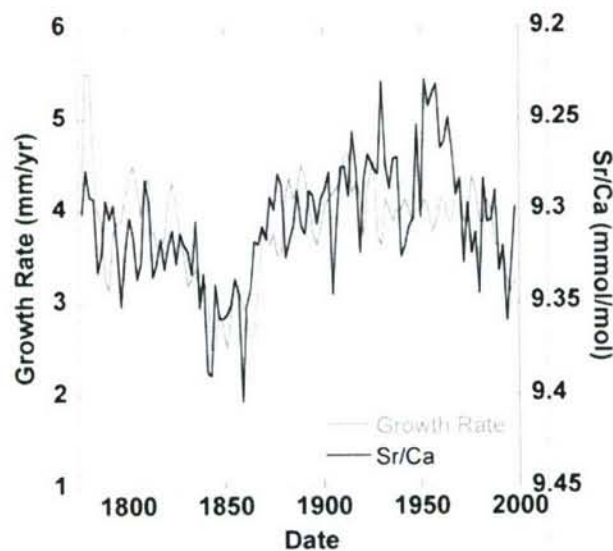


**Figure 2.7.** Biennially averaged mean annual extension (growth) rate (shaded line) and Sr/Ca (solid line) from 1780 to 1997. Extension rate and Sr/Ca have the same large-scale variability patterns over the entire 200-year period ( $r^2 = 0.32$ ,  $p < 0.0001$ ).



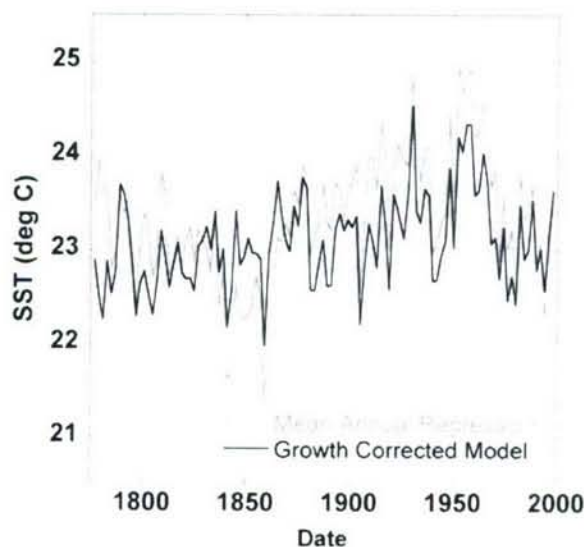


**Figure 2.8.** Biennial-resolution SST reconstructed to 1780. SST reconstructed using the growth-corrected model (solid line), as shown in Figure 4, compared to SST, reconstructed using the mean annual Sr/Ca–SST regression (shaded line). The mean annual Sr/Ca–SST regression exaggerates SST changes from maximum to minimum by a factor of 2.

### 2.3.5 Temperature Trends at Bermuda

The biennially growth-corrected reconstruction agrees with both Hydrostation S and other long coral records from this site. Hydrostation S shows a nearly 2°C cooling from the late 1950s to the late 1960s, simultaneous with the cooling in this record. In coral growth rate records from Bermuda [Patzold and Wefer, 1992], growth rate is correlated to SST and shows a >2°C temperature change from approximately the late 1800s to the 1950s consistent with the growth-corrected biennial Sr/Ca record over the same period. A coral  $\delta^{18}\text{O}$  record from Bermuda shows a similar trend, with an abrupt cooling around 1840 followed by a slow warming coming out of the end of the Little Ice Age [Draschba *et al.*, 2000].

LIA temperature changes at Bermuda have also been investigated using  $\delta^{18}\text{O}$  of foraminifera [Keigwin, 1996] and the alkenone unsaturation index,  $U_{37}^k$  [Ohkouchi *et al.*,

2002; *Sachs and Lehman*, 1999]. Unfortunately, foraminiferal  $\delta^{18}\text{O}$  is influenced both by temperature and the  $\delta^{18}\text{O}$  of water, which is a function of salinity. *Keigwin* [1996] addressed this problem by assuming that the modern salinity and temperature relationship remained constant back in time, and reconstructed an SST change in the Sargasso Sea back to the middle of the LIA of  $1^{\circ}\text{--}2^{\circ}\text{C}$ . The unsaturation index of alkenones provides an SST proxy that is unaffected by water chemistry [*Sikes and Sicre*, 2002] and has been used to reconstruct abrupt shifts in SST at this location [*Sachs and Lehman*, 1999]. However,  $U^{k'}_{37}$  reconstructions of LIA SSTs are much larger ( $4^{\circ}\text{--}6^{\circ}\text{C}$ ) than suggested by foraminiferal  $\delta^{18}\text{O}$ , and compound specific  $^{14}\text{C}$  dating of these alkenones shows they are susceptible to resuspension and long distance transport [*Ohkouchi et al.*, 2002], rendering  $U^{k'}_{37}$  LIA reconstructions at this location suspect. Our growth-corrected calibration also provides an SST reconstruction not influenced by salinity, yielding late LIA cooling of  $1.5^{\circ}\text{C}$ . Overall, our data show that application of a Sr/Ca–SST calibration that takes growth rate variations into account yields coral-based SSTs in good agreement with the instrumental record (Figure 2.5) and with foraminiferal  $\delta^{18}\text{O}$  SST estimates [*Keigwin*, 1996].

## 2.4 Discussion

While our data support previous observations of growth-related impacts on coral Sr/Ca, the underlying mechanism, a sampling artifact [*Swart et al.*, 2002], a growth regime [*Cohen et al.*, 2004], or a kinetic effect [*deVilliers et al.*, 1994], is not clear. Microscale analyses of *Diploria labyrinthiformis* reveal that the amplitude of the annual Sr/Ca cycle is greater than that derived by these sampling techniques [*Cohen et al.*,

2004]. Bulk sampling of insufficient resolution smoothes the record as previously suggested [Swart *et al.*, 2002], even though in this study relative winter variability is accurately captured. Examination of the high- and low-density bands in the coral X-rays and duration of summer and winter in the Sr/Ca seasonal cycle shows that winter skeletal extension is consistent from year to year, compared to more variable summer extension. This could lead to a consistent attenuation of the record during sampling of winter skeleton but variable attenuation of summer skeleton, creating the observed growth impact on the summer record but not the winter. Swart *et al.* [2002] show similar results in a 2-year calibration study in which one summer peak has an average growth rate (during the peak) of  $>8$  mm/yr and Sr/Ca values that match the SST maximum, but the second and third summers with lower summer growth rates ( $<7$  mm/yr and  $<6$  mm/yr during the peak) have Sr/Ca values that do not reflect the same magnitude summertime SST. These data clearly support an influence of growth rate on the summer Sr/Ca–SST relationship. Similarly, in studies by deVilliers *et al.* [1994] and Alibert and McCulloch [1997], Sr/Ca values associated with relatively slow growth and calcification rates are elevated relative to those from high growth rate and calcification rate intervals. However, in both studies, the records with slower growth or calcification rates appear offset rather than dampened, inconsistent with bulk-sample smoothing as the sole mechanism.

Another hypothesis for the impact of growth on coral Sr/Ca is that different growth mechanisms employed by this coral in the summer and winter may influence the Sr/Ca signal. Cohen *et al.* [2004] proposed that skeleton accreted during the summer is overlain by skeleton accreted during the following winter, dampening the summer peak in reconstructed SSTs. Thus the extent of dampening may differ from year to year



depending on whether summer extension is slow or fast and the ratio of summer to winter skeleton is shifted.

Coral culture studies indicate that uptake of Sr relative to Ca might increase at low calcification rates, increasing the Sr/Ca ratio of the skeleton [Ferrier-Pages *et al.*, 2002; Ip and Krishnaveni, 1991] which implies the existence of a kinetic effect. Potential evidence supporting a combined growth regime and kinetic effect is seen in the need to average extension rates over 3 years to fully capture the growth effect in our study. Because in-filling may occur within the skeleton for several years, aragonite laid down in the same location will reflect different calcification rates. By averaging the extension rates (effectively a measure of calcification through time) over 3 years, a better estimate of the average calcification rate over the period of skeletal accretion is achieved and allows for the development of the growth-corrected model. Further study of Sr/Ca measurements in conjunction with specific calcification rates could further elucidate the viability of this hypothesis. Independent of the mechanism by which coral growth rate affects Sr/Ca, our data show that changes in growth rate along the axis of maximum growth may cause large excursions in Sr/Ca that do not accurately reflect the SSTs experienced by the coral.

## **2.5 Conclusions**

The use of a monthly resolved Sr/Ca–SST calibration to reconstruct biennial temperature records appears to cause exaggeration of decadal SST variability over the end of the LIA by a factor of 2.5. This demonstrates the importance of using calibrations that are appropriate to the desired resolution of temperature reconstructions to prevent

such amplification of signals, especially if the full seasonal range of Sr/Ca variability is not captured by bulk sampling techniques. However, the mean annual Sr/Ca–SST regression also exaggerates SST variability by as much as a factor of 2, demonstrating that growth rate variability can also amplify variations in the Sr/Ca reconstructions of temperature. While growth effects are more often referenced for slower growing species such as *Diploria*, the more commonly studied genera *Porites* show that interannual growth rates between colonies and within single sampling transects, can vary by factors of 2–2.8 [Alibert and McCulloch, 1997; Hughen et al., 1999; Mitsuguchi et al., 1996; Shen et al., 1996], comparable to the range observed here. It is possible that the influence of growth rate effects on Sr/Ca–SST calibrations could explain previous coral-based SST reconstructions back in time showing larger SST changes [Beck et al., 1997; Corrége et al., 2004; Guilderson et al., 1994; McCulloch et al., 1996] than seen with other proxies [Lea et al., 2000; Pelejero et al., 1999; Rosenthal et al., 2003; Rühlemann et al., 1999]. The quantitative incorporation of growth rate information into coral Sr/Ca reconstructions could improve the thermometer and result in more accurate estimates of past SST changes and should therefore be considered when undertaking site and species specific calibrations where growth rate data are available.

## Acknowledgements

We are indebted to Mike McCartney (M.S.M.) for his support and to G. Webster, S. du Putron, G. Piniak, J. Pitt, A. Solow, D. Schrag, E. Boyle, C. Bertrand, P. Landry, and R. Kayser for logistical and technical help. The in-depth comments and suggestions of one anonymous reviewer and J. Cole significantly improved the original manuscript. A Stanley Watson Foundation Fellowship (N.F.G.), and grants from NSF (OCE-0402728) and WHOI (K.A.H., A.L.C., and M.S.M.) supported this work. This is WHOI contribution 11246.

## 2.6 References

- Alibert C. and McCulloch M. T. (1997) Strontium/calcium ratios in modern Porites corals from the Great Barrier Reef as a proxy for sea surface temperature: Calibration of the thermometer and monitoring of ENSO. *Paleoceanography* **12**(3), 345-363.
- Bagnato S., Linsley B. K., Howe S. S., Wellington G. M., and Salinger J. (2004) Evaluating the use of the massive coral *Diploastrea heliopora* for paleoclimate reconstruction. *Paleoceanography* **19**(1).
- Beck J. W., Edwards R. L., Ito E., Taylor F. W., Recy J., Rougerie F., Joannot P., and Henin C. (1992) Sea-Surface Temperature from Coral Skeletal Strontium Calcium Ratios. *Science* **257**(5070), 644-647.
- Beck J. W., Recy J., Taylor F., Edwards R. L., and Cabioch G. (1997) Abrupt changes in early Holocene tropical sea surface temperature derived from coral records. *Nature* **385**(6618), 705-707.
- Cardinal D., Hamelin B., Bard E., and Patzold J. (2001) Sr/Ca, U/Ca and delta O-18 records in recent massive corals from Bermuda: relationships with sea surface temperature. *Chemical Geology* **176**(1-4), 213-233.
- Cohen A. L. and Hart S. R. (2004) Deglacial SSTs of the Western Tropical Pacific: A New Look at Old Coral. *Paleoceanography* **19**(4), np.
- Cohen A. L. and McConnaughey T. A. (2003) Geochemical perspectives on coral mineralization. In *Biom mineralization*, Vol. 54, pp. 151-187. MINERALOGICAL SOC AMERICA.
- Cohen A. L., Owens K. E., Layne G. D., and Shimizu N. (2002) The effect of algal symbionts on the accuracy of Sr/Ca paleotemperatures from coral. *Science* **296**(5566), 331-333.
- Cohen A. L., Smith S. R., McCartney M. S., and van Etten J. (2004) How brain corals record climate: an integration of skeletal structure, growth and chemistry of *Diploria labyrinthiformis* from Bermuda. *Marine Ecology-Progress Series* **271**, 147-158.
- Correge T., Gagan M. K., Beck J. W., Burr G. S., Cabioch G., and Le Cornec F. (2004) Interdecadal variation in the extent of South Pacific tropical waters during the Younger Dryas event. *Nature* **428**, 927-929.
- Crowley T. J. (2000) CLIMAP SSTs Re-revisited. *Climate Dynamics* **255**(16), 241-255.
- deVilliers S., Nelson B. K., and Chivas A. R. (1995) Biological-Controls on Coral Sr/Ca and Delta-O-18 Reconstructions of Sea-Surface Temperatures. *Science* **269**(5228), 1247-1249.



- deVilliers S., Shen G. T., and Nelson B. K. (1994) The Sr/Ca-Temperature Relationship in Coralline Aragonite - Influence of Variability in (Sr/Ca)Seawater and Skeletal Growth-Parameters. *Geochimica Et Cosmochimica Acta* **58**(1), 197-208.
- Dodge R. E. and Thomson J. (1974) The Natural Radiochemical and Growth Records in Contemporary Hermatypic Corals from the Atlantic and Caribbean. *Earth and Planetary Science Letters* **23**, 313-322.
- Draschba J., Patzold J., and Wefer G. (2000) North Atlantic Climate Variability Since AD 1350 Recorded in  $\delta^{18}\text{O}$  and Skeletal Density of Bermuda Corals. *International Journal of Earth Sciences* **88**, 733-741.
- Ferrier-Pages C., Boisson F., Allemand D., and Tambutte E. (2002) Kinetics of strontium uptake in the scleractinian coral *Stylophora pistillata*. *Marine Ecology-Progress Series* **245**, 93-100.
- Guilderson T. P., Fairbanks R. G., and Rubenstone J. L. (1994) Tropical Temperature-Variations since 20,000 Years Ago - Modulating Interhemispheric Climate-Change. *Science* **263**(5147), 663-665.
- Hughen K. A., Schrag D. P., Jacobsen S. B., and Hantoro W. (1999) El Nino during the last interglacial period recorded by a fossil coral from Indonesia. *Geophysical Research Letters* **26**(20), 3129-3132.
- Ip Y. K. and Krishnaveni P. (1991) Incorporation of Strontium ( $^{90}\text{Sr}^{2+}$ ) into the Skeleton of the Hermatypic Coral *Galaxea-Fascicularis*. *Journal of Experimental Zoology* **258**(2), 273-276.
- Keigwin L. D. (1996) The Little Ice Age and Medieval warm period in the Sargasso Sea. *Science* **274**(5292), 1504-1508.
- Kuhnert H., Patzold J., Schnetger B., and Wefer G. (2002) Sea-surface temperature variability in the 16th century at Bermuda inferred from coral records. *Palaeogeography Palaeoclimatology Palaeoecology* **179**(3-4), 159-171.
- Lea D. W., Pak D. K., and Spero H. J. (2000) Climate impact of the late Quaternary equatorial Pacific sea surface temperature variations. *Science* **289**, 1719-1724.
- Logan A. and Tomascik T. (1991) Extension growth rates in two coral species from high-latitude reefs of Bermuda. *Coral Reefs* **10**, 155-160.
- Logan A., Yang L., and Tomascik T. (1994) Linear skeletal extension rates in two species of *Diploria* from high-latitude reefs in Bermuda. *Coral Reefs* **13**, 225-230.

- McCulloch M., Mortimer G., Esat T., Li X. H., Pillans B., and Chappell J. (1996) High resolution windows into early Holocene climate: Sr/Ca coral records from the Huon Peninsula. *Earth and Planetary Science Letters* **138**(1-4), 169-178.
- McCulloch M. T., Tudhope A. W., Esat T. M., Mortimer G. E., Chappell J., Pillans B., Chivas A. R., and Omura A. (1999) Coral record of equatorial sea-surface temperatures during the penultimate deglaciation at Huon Peninsula. *Science* **283**(5399), 202-204.
- Mitsuguchi T., Matsumoto E., Abe O., Uchida T., and Isdale P. J. (1996) Mg/Ca thermometry in coral-skeletons. *Science* **274**(5289), 961-963.
- Ohkouchi N., Eglinton T. I., Keigwin L. D., and Hayes J. M. (2002) Spatial and Temporal Offsets Between Proxy Records in a Sediment Drift. *Science* **298**(5596), 1224-1227.
- Patzold J. and Wefer G. (1992) Bermuda Coral Reef Record of the last 1000 years. *Fourth International Conference on Paleoceanography*, 224-225.
- Pelejero C., Grimalt J. O., Heilig S., Kienast M., and Wang L. (1999) High resolution Uk37 temperature reconstruction in the South China Sea over the past 220 Kyr. *Paleoceanography* **14**, 224-231.
- Rosenthal Y., Oppo D. W., and Linsley B. K. (2003) The amplitude and phasing of climate change during the last deglaciation in the Sulu Sea, western equatorial Pacific. *Geophysical Research Letters* **30**, 1429.
- Rühlemann C., Mulitza S., Müller P. J., Wefer G., and Zahn R. (1999) Warming of the tropical Atlantic Ocean and slowdown of thermohaline circulation during the last deglaciation. *Nature* **402**, 511-514.
- Sachs J. P. and Lehman S. (1999) Subtropical North Atlantic Temperatures 60,000 to 30,000 Years Ago. *Science* **286**(5440), 756-759.
- Schrag D. P. (1999) Rapid analysis of high-precision Sr/Ca ratios in corals and other marine carbonates. *Paleoceanography* **14**(2), 97-102.
- Shen C. C., Lee T., Chen C. Y., Wang C. H., Dai C. F., and Li L. A. (1996) The calibration of D Sr/Ca versus sea surface temperature relationship for Porites corals. *Geochimica Et Cosmochimica Acta* **60**(20), 3849-3858.
- Sikes E. L. and Sicre M.-A. (2002) Relationship of the tetra-unsaturated C37 alkenone to salinity and temperature: Implications for paleoproxy applications. *Geochem. Geophys. Geosyst.* **3**(11), 1063.
- Smith S. V., Buddemeier R. W., Redalje R. C., and Houck J. E. (1979) Strontium-Calcium Thermometry in Coral Skeletons. *Science* **204**(4391), 404-407.

- Swart P. K., Elderfield H., and Greaves M. J. (2002) A high-resolution calibration of Sr/Ca thermometry using the Caribbean coral *Montastraea annularis*. *Geochemistry Geophysics Geosystems* **3**.
- Weber J. N. (1973) Incorporation of Strontium into Reef Coral Skeletal Carbonate. *Geochimica Et Cosmochimica Acta* **37**(9), 2173-2190.



## Chapter 3

### A multi-coral calibration method to approximate a universal equation relating Sr/Ca and growth rate to sea surface temperature

Reprinted with permission of the American Geophysical Union.

Goodkin, N. F., K. A. Hughen, and A. L. Cohen, (in press), A multi-coral calibration method to approximate a universal equation relating Sr/Ca and growth rate to sea surface temperature, *Paleoceanography*, doi: 2006PA001312.

#### Abstract

Combining strontium-to-calcium ratios (Sr/Ca) with mean annual growth rates in Bermuda *Diploria labyrinthiformis* (brain corals) is shown to improve sea surface temperature (SST) calibrations relative to instrumental data. Growth-corrected Sr/Ca–SST calibrations based on single-coral colonies over the same calibration interval, however, are found to be poorly suited for application to data from different coral colonies. This raises concerns about the accuracy of SST reconstructions from fossil coral measurements that involve extrapolation beyond the range of values seen during the calibration period. Here we pursue a novel approach to this problem by incorporating data from multiple coral colonies into a single growth-corrected Sr/Ca–SST calibration equation, effectively expanding the range of modern values constraining the model. The use of a multiple-colony calibration model for reconstructing SST yields greater precision and accuracy relative to instrumental data than single-colony models, providing greater confidence for applications to fossil coral samples.

### 3.1. Introduction

Understanding long-term climate variability requires the reconstruction of key climate parameters, such as sea surface temperature (SST), in records extending beyond the relatively short instrumental period. The high accretion rates, longevity, and annual growth bands found in coral colonies make this an ideal resource for well-dated, seasonal resolution climate reconstructions. One method used for quantifying past temperature changes from corals involves the inverse relationship between SST and the strontium (Sr) to calcium (Ca) ratio in coral skeleton [Smith *et al.*, 1979]. Typically, this method relies on obtaining a linear regression of Sr/Ca on SST from a modern coral colony and then applying this calibration to Sr/Ca measurements from fossil samples [Beck *et al.*, 1992; Beck *et al.*, 1997; Correge *et al.*, 2004; McCulloch *et al.*, 1999]. However, in many cases reconstructions of past SST from coral Sr/Ca ratios are several degrees cooler than other marine proxies such as alkenones or foraminiferal Mg/Ca (e.g., [Lea *et al.*, 2000; Pelejero *et al.*, 1999; Rosenthal *et al.*, 2003]). Part of this discrepancy may be due to differences in seasonality, differences in the depth at which various proxies record SST, or influences from other environmental factors.

Nevertheless, it has been observed that correlations of coral Sr/Ca to SST vary between individual colonies, time periods, and species [Alibert and McCulloch, 1997; deVilliers *et al.*, 1995; Marshall and McCulloch, 2002; Swart *et al.*, 2002]. Differences between coral colony Sr/Ca-SST calibrations have been previously investigated, and proposed sources of error include: variations in Sr and Ca concentrations of seawater, particularly in areas of upwelling [Alibert and McCulloch, 1997; deVilliers *et al.*, 1994; Marshall and McCulloch, 2002; Shen *et al.*, 1996]; the veracity of the instrumental or

calibration SST record [Crowley *et al.*, 1999; Marshall and McCulloch, 2002]; imprecise age models [Swart *et al.*, 2002]; biological and symbiotic effects [Cohen *et al.*, 2002; deVilliers *et al.*, 1995; Ferrier-Pages *et al.*, 2002]; and the length of the calibration period [Goodkin *et al.*, 2005]. In addition, several studies have indicated that growth rate and/or calcification rate may act as an additional influence on Sr/Ca ratios [Alibert and McCulloch, 1997; Cohen and Hart, 2004; deVilliers *et al.*, 1995; Ferrier-Pages *et al.*, 2002; Goodkin *et al.*, 2005; Weber, 1973]. In a recent study of corals with slow growth rates, the use of a multi-variant regression of Sr/Ca to SST and extension (growth) rate was shown to improve SST reconstructions over the instrumental calibration period [Goodkin *et al.*, 2005]. In addition, applying this regression to a record back to 1775 AD resulted in SST changes consistent with other marine proxies (e.g., [Keigwin, 1996]). These studies indicate that growth rate can be an important factor to consider when examining Sr/Ca in modern and fossil corals. However, the concern remains that measurements of past coral growth rates often fall well outside the range seen during the instrumental interval, and thus require extrapolation beyond the constraints of the observed modern calibration relationship. One way to minimize uncertainties due to extrapolating beyond the calibration range is to utilize data simultaneously from several coexisting corals with different growth rates. In addition to extending the range of modern values for comparison, using multiple colonies for calibration can also serve to average away uncertainties due to dating errors and individual metabolic effects. For example, averaging Sr/Ca measurements from multiple corals prior to calibration [Stephans *et al.*, 2004] or averaging coefficients from two or



more single-colony calibrations [Alibert and McCulloch, 1997; Smith *et al.*, 1979] have previously been shown to reduce errors in reconstructed SSTs.

Here we present a unique approach to coral Sr/Ca-SST calibration, combining data from multiple corals into a single multivariate regression in an effort to derive a universal equation that can be applied with equal confidence to any modern or fossil coral from the same location. Combining multiple colonies into a single SST calibration expands the range of Sr/Ca and growth rate values applied to the calibration, minimizing extrapolation beyond modern coral values during reconstructions of past SST. We demonstrate that a calibration using multiple colonies results in increased accuracy and precision for Sr/Ca-based SST reconstructions. In this study, multivariate regressions of Sr/Ca to SST and growth rate ("single-colony" growth-corrected model) were performed on several colonies of massive *Diploria labyrinthiformis* from Bermuda, following the method of Goodkin *et al.* (2005). In addition, a similar multivariate regression was performed using measurements from multiple colonies simultaneously ("multi-colony" model) to provide a single calibration equation. The multi-colony and single-colony calibration models were applied to data from each individual colony, and reconstructed SST was compared to instrumental SST over the calibration interval to determine the method that provides the most accurate and precise reconstruction.

## **3.2. Methods**

### **3.2.1 Study Site**

In April 1999, three 30-50 year old brain corals (*Diploria labyrinthiformis*) (BER 002, BER 003, and BER 004) were sampled live off John Smith's Bay (JSB) on the

southeastern edge of the Bermuda platform at 16-meters depth. A fourth, ~230 year old coral (BB 001) was sampled live from the same location in May of 2000. *Diploria labyrinthiformis* was chosen for this study because slow growth rates combined with multi-century life spans and large geographical distribution from tropical to sub-tropical waters makes this species a promising source of paleoceanographic information. Growth rates from brain corals in this region vary from 2-6 mm/yr [Dodge and Thomson, 1974; Goodkin et al., 2005; Logan and Tomascik, 1991], much slower than more commonly used species such as *Porites*, which exhibits growth rates from 8-20 mm/yr [Alibert and McCulloch, 1997; Hughen et al., 1999; Shen et al., 1996].

The south terrace of Bermuda provides exposure to open ocean waters and proximity to instrumental data from Hydrostation S, located 30 km to the southeast. At Hydrostation S, SST from 0-16 m depth has been recorded bi-weekly since 1954. Over that time, monthly averaged SST ranged from 18.0 to 28.9 °C with annual averages between 22.4 and 24.3 °C. The calibration period of this study (1976-1997) has mean annual SST ranging from 22.8 to 23.5 °C with a seasonal range of 18.3 to 28.9 °C. The SST record is incomplete over different intervals including two or more months of missing data in the years 1978-1980, 1986, and 1989, and subsequently these years are omitted from the mean-annual calibrations.

### **3.2.2 Sub-sampling and Analysis of Coral**

Corals were sliced into ~1 cm thick slabs along the growth axis using a diamond blade rock saw and cleaned in an ultrasonic bath [Goodkin et al., 2005]. X-radiographs were performed at Falmouth Hospital (Falmouth, MA) with machine settings of 50kV

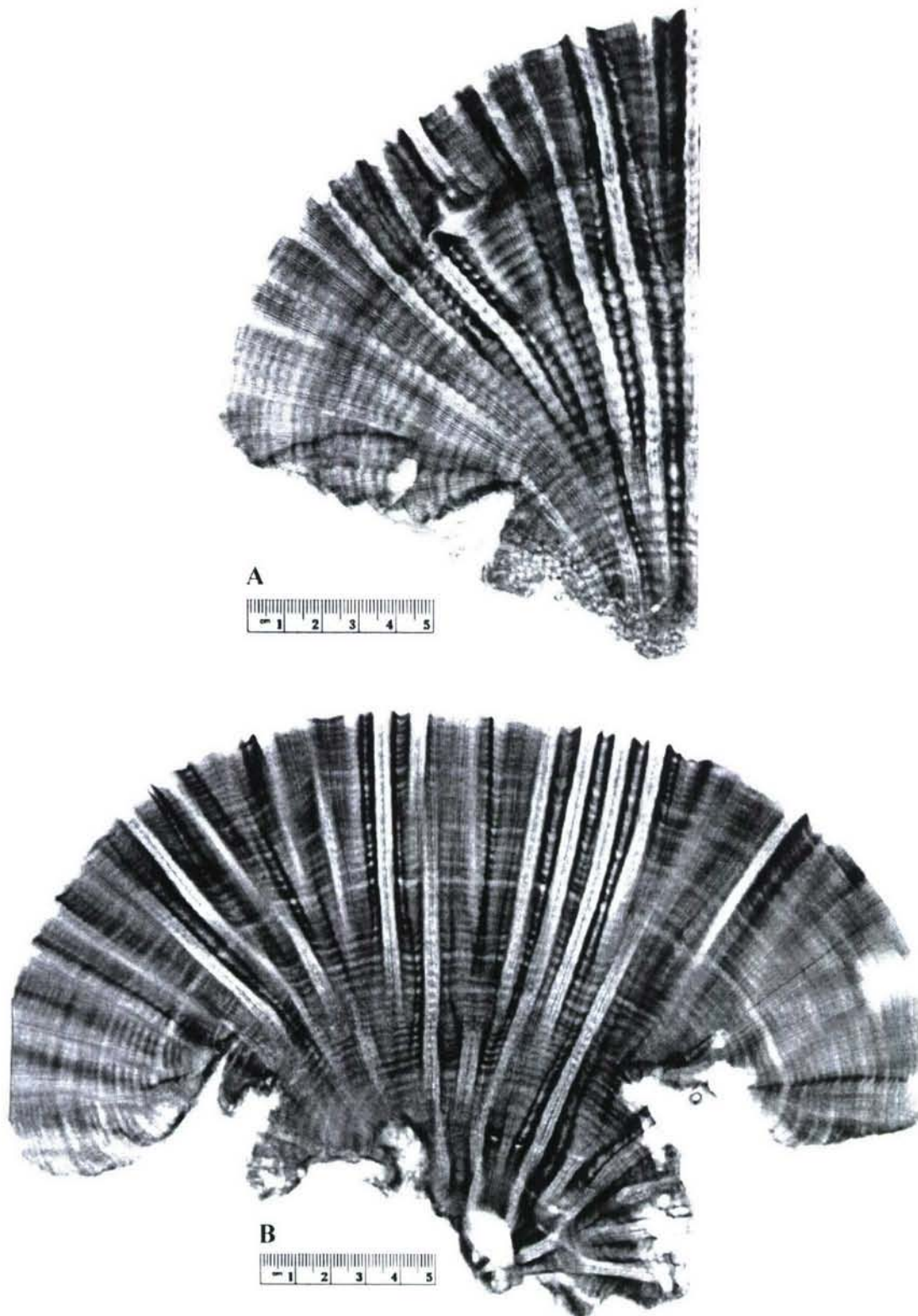


**Figure 3.1.** X-radiograph positive image of a) BER 003 and b) BER 004. X-rays show clear annual banding made up of a low and high density band.



and 1.6 mAs, a film focus distance of 1 m and exposure time of 0.2s. X-rays for BB 001 and BER 002 can be found in Goodkin et al. (2005) and Cohen et al. (2004), respectively. X-radiographs for BER 003 and BER 004 are shown in Fig. 3.1.

Samples for Sr/Ca analysis were drilled along the solid *thecal* wall separating the *ambulacrum* from the *calyx* following the methods of Goodkin et al. (2005). For the calibration period (1976-1997), BER 002, 003, and 004 were sampled every 0.25 mm and BB 001 was sampled every 0.33 mm, using a drill press and micrometer controlled stage.

An Inductively Coupled Plasma–Atomic Emission Spectrometer (ICP-AES) at the Woods Hole Oceanographic Institution (WHOI) was used to measure Sr and Ca simultaneously, applying solution standards to correct for drift and matrix effects related to interference from varying Ca concentrations following the methods of Schrag (1999). The unknowns, blanks and samples of external standard (a homogenized, powdered *Porites* coral) were prepared simultaneously. Repeat measurements on the coral external standard over 12 months showed good reproducibility (RSD = 0.3%, n=847).

Over the calibration interval, age models and annual extension rates for all corals were developed using density banding visible in the x-radiographs (Fig. 3.1), followed by assigning Sr/Ca to monthly averaged SSTs at maxima, minima and inflection points [Goodkin et al., 2005]. Sr/Ca was then interpolated in order to re-sample at even monthly increments, and mean-annual Sr/Ca was calculated by averaging the interpolated monthly values. Average extension rates for each colony used in the multi-colony correlation exercises were calculated based on the entire length of the colony (Table 3.1).

**Table 3.1.** Average extension rates for the colony and the period of calibration.

<b>Coral</b>	<b>Average Extension Rate (mm/yr)</b>	<b>Time Period of Calibration</b>
BB 001	3.8	1977-1997
BER 002	3.2	1976-1996
BER 003	4.2	1976-1997
BER 004	2.1	1976-1997

### 3.3. Results

#### 3.3.1 Seasonal Cycle

All four corals show strong seasonal cycles in Sr/Ca (Fig. 3.2). Type-I linear regressions of monthly-resolved Sr/Ca ratios to SSTs yield relatively consistent correlations among the four corals:

$$\text{BB 001: Sr/Ca} = 10.1 (\pm 0.04) - 0.0358 (\pm 0.0018) * \text{SST}$$

$$(2\sigma, 95\% \text{ conf.}, r^2 = 0.86, F_{\text{sig}} < 0.0001) \text{ [Goodkin et al., 2005]}$$

$$\text{BER 002: Sr/Ca} = 10.1 (\pm 0.07) - 0.0376 (\pm 0.0030) * \text{SST}$$

$$(2\sigma, 95\% \text{ conf.}, r^2 = 0.73, F_{\text{sig}} < 0.0001)$$

$$\text{BER 003: Sr/Ca} = 10.3 (\pm 0.06) - 0.0436 (\pm 0.0024) * \text{SST}$$

$$(2\sigma, 95\% \text{ conf.}, r^2 = 0.85, F_{\text{sig}} < 0.0001)$$

$$\text{BER 004: Sr/Ca} = 10.3 (\pm 0.07) - 0.0429 (\pm 0.0029) * \text{SST}$$

$$(2\sigma, 95\% \text{ conf.}, r^2 = 0.76, F_{\text{sig}} < 0.0001)$$

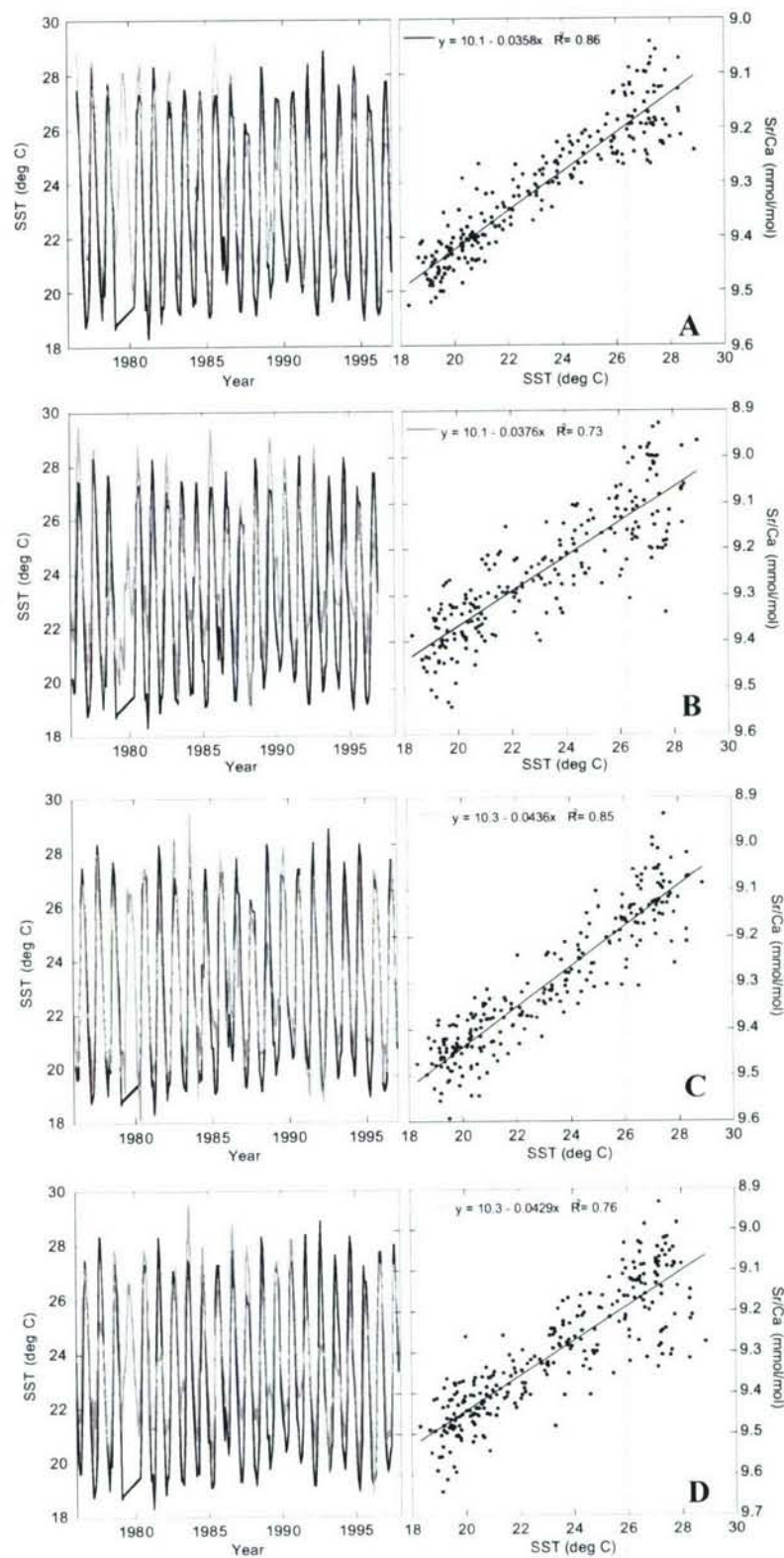


**Figure 3.2.** Coral Sr/Ca (shaded) and Hydrostation S SST (solid) at monthly resolution plotted versus year (left) and correlated using linear regression (right). Calibration results for a) BB 001 ( $r^2=0.86$ ), b) BER 002 ( $r^2=0.73$ ), c) BER 003 ( $r^2=0.85$ ), and d) BER 004 ( $r^2=0.76$ ).



These results are consistent to one another and to other slow to moderately growing corals [Bagnato *et al.*, 2004; Cardinal *et al.*, 2001; Swart *et al.*, 2002]. A larger variance in summer Sr/Ca values than in winter in all four corals suggests a growth effect on the summer Sr/Ca values, as previously found for BB 001 [Goodkin *et al.*, 2005]. Smoothing of the seasonal cycle, as previously identified for bulk sampling methods in slow growing corals, is seen in these colonies, rendering the seasonal calibration ineffective for reconstructing SST back through time [Cohen and Hart, 2004; Cohen *et al.*, 2004; Goodkin *et al.*, 2005].

### 3.3.2 Inter-annual Calibrations

Mean annual Sr/Ca regressed (type I) upon mean annual SST shows a significantly reduced correlation coefficient for all four corals relative to the seasonal correlations (Fig. 3.3):

$$\text{BB 001: Sr/Ca} = 10.4 (\pm 1.2) - 0.0481 (\pm 0.0503) * \text{SST} \\ (2\sigma, 95\% \text{ conf.}, r^2 = 0.21, F_{\text{sig}}=0.0766, \text{rmsr}=0.5 \text{ } ^\circ\text{C})$$

$$\text{BER 002: Sr/Ca} = 11.2 (\pm 1.5) - 0.0844 (\pm 0.0666) * \text{SST} \\ (2\sigma, 95\% \text{ conf.}, r^2 = 0.31, F_{\text{sig}}=0.0238, \text{rmsr}=0.4 \text{ } ^\circ\text{C})$$

$$\text{BER 003: Sr/Ca} = 10.3 (\pm 1.3) - 0.0451 (\pm 0.0544) * \text{SST} \\ (2\sigma, 95\% \text{ conf.}, r^2 = 0.15, F_{\text{sig}}=0.1180, \text{rmsr}=0.6 \text{ } ^\circ\text{C})$$

$$\text{BER 004: Sr/Ca} = 9.33 (\pm 2.23) - 0.00005467 (\pm 0.0964689) * \text{SST} \\ (2\sigma, 95\% \text{ conf.}, <<0.0001, F_{\text{sig}}=0.9991, \text{rmsr}= \text{not relevant})$$

where rmsr is the root mean square of the residual.

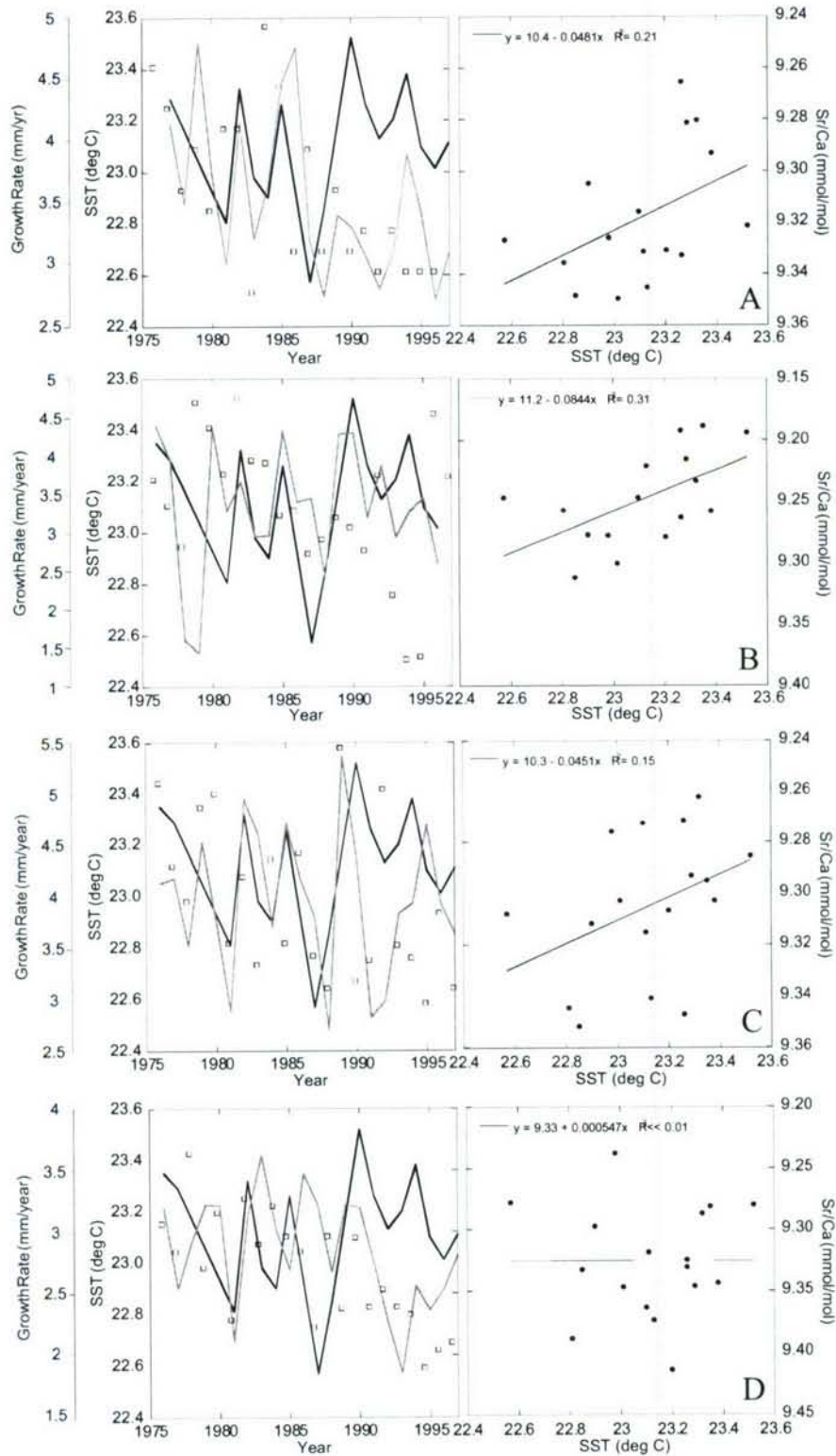


**Figure 3.3.** Coral Sr/Ca (shaded) and Hydrostation S SST (solid) at mean-annual resolution plotted versus year (left) and correlated using linear regression (right). Calibration results for a) BB 001 ( $r^2=0.21$ ), b) BER 002 ( $r^2=0.31$ ), c) BER 003 ( $r^2=0.15$ ), and d) BER 004 ( $r^2<0.01$ ).

Previous work has demonstrated that growth rate influences do not impact the summer and winter season equally [Goodkin *et al.*, 2005]. In that work, changes in mean-annual growth rates were shown to correlate strongly with anomalous summer and mean-annual Sr/Ca values. Incorporating annual growth rate data into a single-colony, multivariate regression of mean-annual Sr/Ca onto SST resulted in an improved calibration with reduced residual SSTs. The poor correlation observed here in the mean-annual calibrations for each of these corals, combined with the larger spread in summer Sr/Ca relative to winter Sr/Ca values (Fig. 3.2), implies that a similar effect may be impacting the Sr/Ca-SST relationship.

A growth corrected mean-annual model following the method of Goodkin *et al.* (2005), was therefore fit to each of the four corals to evaluate the influence of growth on the calibration of Sr/Ca versus SST. The following correlations were found:

$$\begin{aligned} \text{BB 001: } \text{Sr/Ca} = & -0.0529 (\pm 0.0334) * \text{SST} - 0.00170 (\pm 0.00078) * (\text{growth rate}) \\ & * \text{SST} + 10.7 (\pm 0.8) \\ & (2\sigma, 95\% \text{ conf.}, r^2 = 0.68, F_{\text{sig}} = 0.0006, \text{rmsr} = 0.2 \text{ } ^\circ\text{C}) \end{aligned}$$

$$\begin{aligned} \text{BER 002: } \text{Sr/Ca} = & -0.0906 (\pm 0.0679) * \text{SST} - 0.000522 (\pm 0.001060) * (\text{growth rate}) \\ & * \text{SST} + 11.4 (\pm 1.6) \\ & (2\sigma, 95\% \text{ conf.}, r^2 = 0.36, F_{\text{sig}} = 0.0538, \text{rmsr} = 0.3 \text{ } ^\circ\text{C}) \end{aligned}$$

$$\begin{aligned} \text{BER 003: } \text{Sr/Ca} = & -0.0502 (\pm 0.0573) * \text{SST} + 0.000543 (\pm 0.001584) * (\text{growth rate}) \\ & * \text{SST} + 10.4 (\pm 1.3) \\ & (2\sigma, 95\% \text{ conf.}, r^2 = 0.18, F_{\text{sig}} = 0.2441, \text{rmsr} = 0.5 \text{ } ^\circ\text{C}) \end{aligned}$$

$$\begin{aligned} \text{BER 004: } \text{Sr/Ca} = & -0.000201 (\pm 0.092689) * \text{SST} - 0.00194 (\pm 0.00259) * (\text{growth rate}) \\ & * \text{SST} + 9.4 (\pm 2.1) \\ & (2\sigma, 95\% \text{ conf.}, r^2 = 0.14, F_{\text{sig}} = 0.3525, \text{rmsr} = 8.2 \text{ } ^\circ\text{C}) \end{aligned}$$



BER 004 fails to show enough improvement in the growth corrected model to be used to reconstruct SST. BER 004 has the slowest average annual extension rate (2.1 mm/yr) by more than one mm/yr. A correlation of mean-annual Sr/Ca to average annual extension in BER 004, with an  $r^2$  of 0.21 and an  $F_{sig}$  of 0.0337, shows a stronger correlation than does Sr/Ca to SST, with an  $r^2$  of  $<<0.0001$  and an  $F_{sig}$  of 0.9991. The inability to model the Sr/Ca-SST thermometer at the mean-annual level in BER 004 is an indication that extremely slow growing corals are not suitable for bulk sampling of this resolution and should be avoided when both calibrating and reconstructing SST by this sampling method. These results warrant further study of corals growing consistently at or below 2mm/yr, as BER 004 does in the last 10 years of the calibration.

In contrast to BER 004, the growth-corrected models of BB 001, BER 002, and BER 003 more accurately reconstruct SST, decreasing the root mean squares of the residuals in all cases (Table 3.2). BB 001 shows increased significance for the relationship ( $F_{sig} = 0.0006$ , growth, and 0.0766, non-growth), an improved  $r^2$  (0.68 compared to 0.21) and a strong significance for the added term ( $p=0.00078$ ). For BER 002 and 003, the explained variance ( $r^2$ ) in Sr/Ca for the growth-corrected model increases slightly from 0.31 to 0.36 and 0.15 to 0.18, respectively. The significance of the equations, however, do not improve in either case from the mean-annual model to the growth-corrected model, and neither coral shows statistical significance for the added term accounting for inter-annual growth rate ( $p = 0.34$  and 0.50 for 002 and 003, respectively).

**Table 3.2.** Root mean squares of the residuals (°C) generated by each calibration/model applied to each coral and to the group as a whole. Values are reported to the 100<sup>th</sup> decimal place for comparison purposes.

<b>Calibration</b>	<b>BB 001</b>	<b>BER 002</b>	<b>BER 003</b>	<b>Group</b>
<b>Multi-Colony</b>	0.43	0.47	0.47	0.46
<b>BB 001</b>				
Growth-Corrected	0.24	1.53	0.53	0.94
Mean-Annual	0.46	1.59	0.58	1.00
Monthly	0.65	2.00	0.72	1.28
<b>BER 002</b>				
Growth-Corrected	0.81	0.32	0.77	0.67
Mean-Annual	0.88	0.43	0.74	0.71
Monthly	1.89	0.88	1.60	1.52
<b>BER 003</b>				
Growth-Corrected	0.65	1.24	0.51	0.86
Mean-Annual	0.56	1.45	0.55	0.95
Monthly	0.62	1.40	0.57	0.94

More importantly, the growth-corrected model, when applied to corals 001, 002, and 003, fails to establish a single equation that can be applied reliably for all modern and, by inference, fossil corals – i.e., the slopes and intercepts of the three equations are not consistent (Fig. 3.4). This leads to the conclusion that inter-annual growth rate is not accounting for all of the differences found between these individual corals. An alternate hypothesis is required in order to link the different corals together into a single relationship.

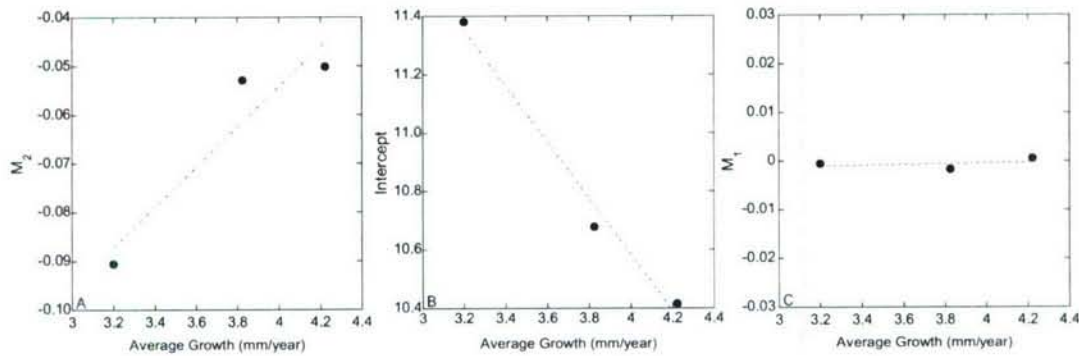


**Figure 3.4.** Single-colony, growth-corrected model intercepts and slopes from each coral model plotted versus average growth (mm/year) of the individual coral colony. (a)  $M_2$ , b) intercept ( $b_0$ ), and c)  $M_1$  versus average growth.

Following the general form of the growth-corrected model:

$$\text{Sr/Ca} = m_1 * (\text{inter-annual growth}) * \text{SST} + m_2 * \text{SST} + b_0 \quad \text{eqn. 1}$$

we observe that  $m_2$  (the SST slope) reveals a correlation to the average growth rate ( $r^2=0.89$ ) for the three colonies (Fig. 3.4a), which in turn influences the values of the intercepts ( $b_0$ ) (Fig. 3.4b). Thus, the intercept also shows a strong correlation to average growth rate ( $r^2=0.98$ ).  $M_1$ , which already accounts for a growth rate influence, shows relatively little correlation to average growth rates (Fig. 4c) ( $r^2=0.13$ ). Three points do not allow for a statistical evaluation of these observed relationships or determination of the nature (linear, exponential etc.) of these relationships. However, this illustrative result implies that developing a general model applicable to different coral colonies requires incorporation of the average growth rate of each colony. We therefore adopt the simplest hypothesis that a multi-colony calibration model will assume that  $m_2$  (the SST slope) changes as a linear function of growth rate, such that:



$$m_2 = d_0 * (\text{average growth}) + d_1 \quad \text{eqn. 2}$$

The net regressed equation is:

$$\text{Sr/Ca} = m_1 * (\text{ig}) * \text{SST} + d_0 * (\text{ag}) * (\text{SST}) + d_1 * (\text{SST}) + b_0 \quad \text{eqn. 3}$$

where (ig) is inter-annual growth and (ag) is average growth for each colony. The linear least square (type I) multiple regression performed on all three data sets simultaneously returns the following equation:

$$\begin{aligned} \text{Sr/Ca} = & -0.000697 (\pm 0.000751) * (\text{ig}) * \text{SST} + 0.00304 (\pm 0.00102) * (\text{ag}) * \text{SST} - \\ & 0.0738 (\pm 0.0374) * \text{SST} + 10.8 (\pm 0.9) \\ & (2\sigma, 95\% \text{ conf.}, r^2=0.51, F_{\text{sig}} < 0.0001, \text{rmsr}=0.5 \text{ } ^\circ\text{C}) \end{aligned}$$

Covariance amongst the slopes and intercepts are reported in Table 3.3. The inter-annual growth term ( $m_1$ ) which previously showed significance only in the individual colony model for coral BB 001, is now significant in this model including data from all three colonies ( $p=0.0800$ ). The inclusion of the average growth term and the utilization of all three colonies in one regression lead to a highly significant model ( $F_{\text{sig}} < 0.0001$ ), a strong significance of the added average growth term ( $p < 0.0001$ ), and a low root mean square of the residual ( $0.5 \text{ } ^\circ\text{C}$ ).

**Table 3.3:** Covariance ( $\sigma^2$ ) amongst the slopes and intercept of the multi-colony model.

	Intercept	SST	ag * SST
SST	$-8.01 \times 10^{-3}$		
ag * SST	$9.57 \times 10^{-6}$	$-1.09 \times 10^{-6}$	
ig * SST	$-1.66 \times 10^{-5}$	$5.48 \times 10^{-7}$	$-8.79 \times 10^{-8}$

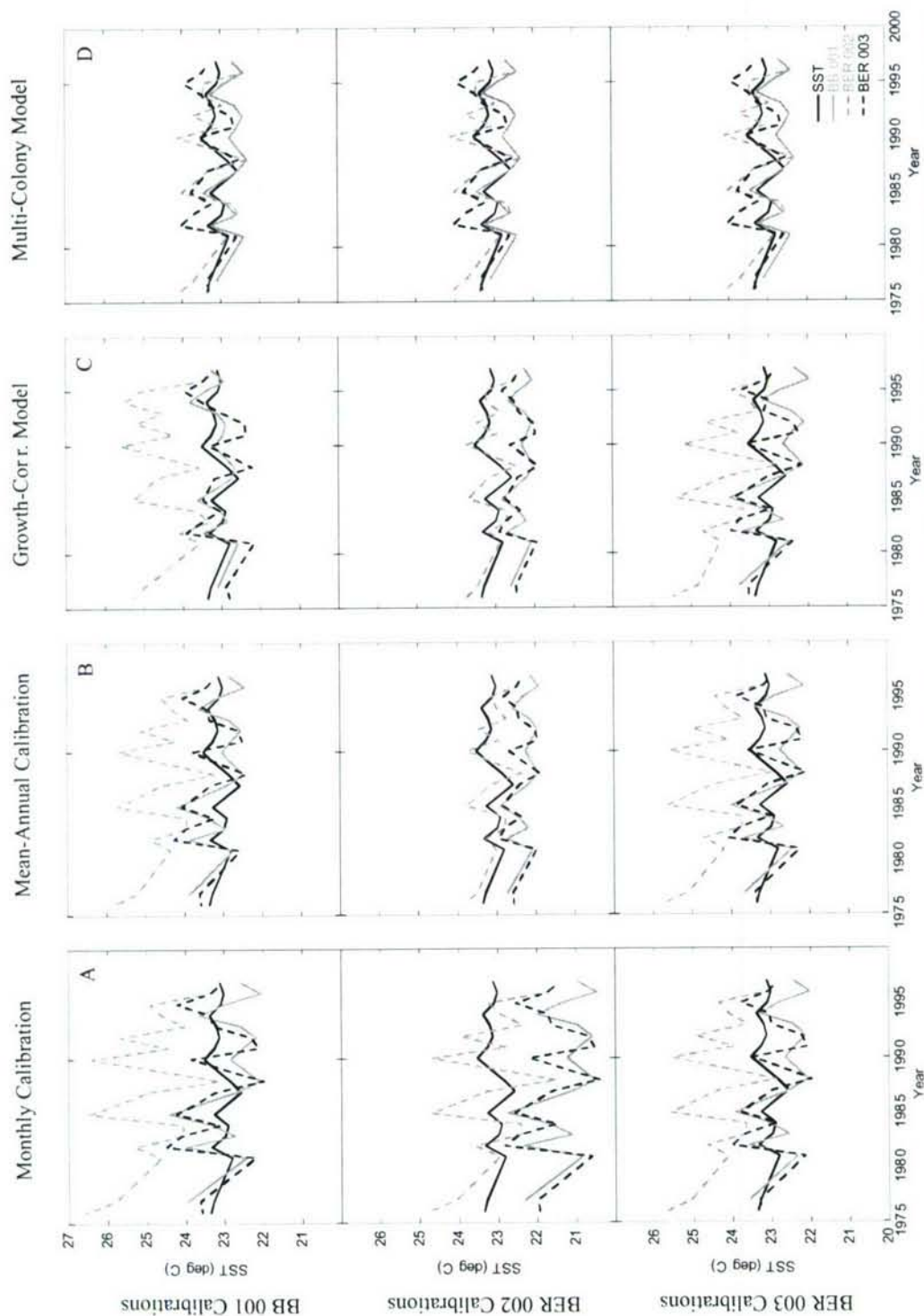


**Figure 3.5.** Hydrostation S (solid) and reconstructed mean-annual SST for BB 001 (shaded), BER 002 (shaded dashed) and BER 003 (solid dashed) plotted versus year. Reconstructed SSTs from (a) monthly calibration of BB 001 (top), BER 002 (middle) and BER 003 (bottom) b) mean-annual calibration of BB 001 (top), BER 002 (middle) and BER 003 (bottom) c) growth-corrected model of BB 001 (top), BER 002 (middle) and BER 003 (bottom) and d) the multi-colony model. The multi-colony model shows the most accurate reconstruction of SST for the colonies as a group with a rmsr of  $0.46^{\circ}\text{C}$  and a minimal off-set from the mean instrumental SST over the period of  $0.24^{\circ}\text{C}$ .

### 3.4 Discussion: Testing the Multi-Colony Regression

In order to evaluate the accuracy and precision of the different calibration methods presented here, each single-colony calibration (monthly, mean-annual, and growth-corrected) for the three corals, as well as the multi-colony calibration, was applied to all of the corals such that there are ten SST reconstructions for each coral (Fig. 3.5). In column A (Fig. 3.5), the monthly calibrations for coral 001, 002, and 003 (top to bottom) are applied to mean-annual Sr/Ca from each coral and compared to mean-annual instrumental SST. In these scenarios, neither the accuracy nor the precision are good. In a single year, the difference between the three records can be as large as 2.5 °C and the records on average are also significantly offset from one another and the instrumental record. In addition, the root mean squares of the SST residuals when applied to the group as a whole are 1.3, 1.5, and 0.9 °C (top to bottom, Table 3.2). If a reconstructed paleotemperature record was compiled from multiple corals using a monthly calibration from any single colony, it would be likely to significantly over- or under-estimate SST changes through time.

In panel B (Fig. 3.5), the mean-annual calibrations of 001, 002, and 003 (top to bottom) are applied to mean-annual Sr/Ca from each coral and compared to instrumental SST. Although minimizing the known artifacts of smoothing from bulk sampling of monthly calibrations (e.g., [Goodkin *et al.*, 2005]), the mean-annual calibrations still lead to significant offsets from the instrumental record (Fig. 3.5b). The mean-annual calibration from BER 003 performs as poorly as the monthly calibration when applied to all three corals, returning a root mean square of the residuals for the group of 1.0 °C,



while mean-annual calibrations for BB 001 and BER 002 show improvement (group rmsr of 1.0 and 0.7 °C respectively) (Table 3.2).

**Table 3.4.** Difference between the mean of the reconstructed SST and the mean of the instrumental SST (°C) over the calibration period for each individual colony growth-corrected model and the multi-colony model. Values are reported to the 100<sup>th</sup> decimal place for comparison purposes.

	BB 001	BER 002	BER 003	rmsr
<b>BB 001 Growth-Corrected Model</b>	0.00	1.38	-0.04	0.80
<b>BER 002 Growth-Corrected Model</b>	-0.78	0.00	-0.70	0.61
<b>BER 003 Growth-Corrected Model</b>	-0.35	-0.36	0.00	0.29
<b>Multi-Colony Model</b>	-0.34	0.13	0.20	0.24

In panel C (Fig. 3.5), the single-colony growth-corrected calibrations for corals 001, 002, and 003 (top to bottom) are again applied to mean-annual Sr/Ca from each coral and compared to mean annual SST. These models attempt to account for some of the variability between different coral colonies, but still result in significant errors in SST reconstructions (Fig 3.5c). The growth-corrected model for BB 001 reconstructs SST well for itself (rmsr = 0.2°C). However, it does relatively worse for BER 003 (rmsr = 0.5 °C), and it does poorly for BER 002 (rmsr = 1.5 °C; group rmsr = 0.8 °C). Similarly, single-colony growth-corrected models for BER 002 and 003 result in poor SST reconstructions when applied to other colonies. The BER 002 growth-corrected model provides the most precise reconstruction across the group (rmsr of 0.7 °C) of the three single-colony models, with rmsr of 0.8, 0.3 and 0.8 °C when applied to BB 001, BER 002, and BER 003, respectively. The growth-corrected model of BER 003 reconstructed SST with an rmsr of 0.7, 1.2 and 0.5 °C for the three colonies respectively, and a group rmsr of 0.9 °C. In general, the single-colony, growth-corrected models when applied to

other colonies still result in SST reconstructions with significant offsets of the mean from instrumental data (Fig 3.5c; Table 3.4), and demonstrate that reconstructions from fossil corals could possibly over- or under-estimate mean SST by as much as 1.4 °C (Table 3.4).

Finally, shown in triplicate along panel D (Fig. 3.5) and in the top row of Table 3.2 are the results of SST reconstructions using the multi-colony model. With the multi-colony model, both precision and accuracy of reconstructed SSTs are improved over the single-colony models. Although reconstructed SSTs for BB 001 and BER 002 (but not BER 003) fit best using their own single-colony growth-corrected model (Table 3.2), each single-colony model performs poorly when applied to the other colonies. The group rmsr of reconstructed SSTs for the three colonies equal 0.9, 0.7 and 0.9 °C for the single-colony models, compared to only 0.5 °C using the multi-colony model (Table 3.2). Similarly, the means for reconstructed SSTs using single-colony calibrations show greater offsets from instrumental SST (group offsets of 0.8, 0.6 and 0.3 °C) than the multi-colony model (average offset 0.2 °C) (Table 3.4). When reconstructing SST for the group as a whole, the best fit is clearly achieved using the multi-colony calibration. Applying the multi-colony calibration to all three corals shows reconstructed SSTs evenly distributed above and below the instrumental record, with diminished offsets and greatly reduced scatter compared to single-colony monthly, mean-annual, and growth-corrected methods (Fig. 3.5). This implies that the multi-colony calibration approximates a universal equation that may potentially be applied to any individual modern or fossil *Diploria labyrinthiformis* colony from this area with equal confidence.

### 3.5 Conclusion

Individual modern coral colonies often provide distinct independent calibrations of Sr/Ca to SST. Choosing an equation to apply to a fossil coral or even to the non-modern portion of a living coral can be problematic, as the variation in slopes from one calibration to another can have significant implications for reconstructed SST. The application of a single-colony Sr/Ca-SST calibration to different corals can lead to significant offsets between independent records covering the same time interval. Such discrepancies can pass unnoticed when a modern calibration is applied to a fossil coral, particularly if the fossil record shows no overlap with more recent values. In slow-to-moderate growing corals, growth rate can explain some of the differences in the calibrations of individual corals. However, even growth-corrected Sr/Ca-SST calibrations based on a single colony yield large anomalies in reconstructed SST when applied to other colonies.

For this study, data from multiple corals were used simultaneously in a multivariate regression to develop a single multi-colony growth-corrected Sr/Ca-SST calibration. Applying the multi-colony calibration for reconstructing SST reduces the root mean square of the residual as well as mean offsets for three colonies evaluated independently and together as a group, compared to single-colony growth-corrected calibration models. In general, incorporating quantitative interannual and average growth rate information and expanding the calibration range through the inclusion of multiple coral colonies improves the coral Sr/Ca thermometer and provides more accurate reconstructions of SST. Investigating growth influences on other slow-to-moderate growing corals and using multiple colonies in Sr/Ca-SST calibrations may improve the



reliability of past SST reconstructions and serve to diminish anomalies relative to other paleotemperature proxies.

## **Acknowledgements**

We are indebted to Mike McCartney (MSM) for his support: to S. Smith, G. Webster, S. du Putron, G. Piniak, J. Pitt, A. Solow, W. Curry, S. Doney, D. Schrag, E. Boyle, C. Bertrand, P. Landry, R. Kayser, and S. Clifford for logistical and technical help. The in-depth comments and suggestions of one anonymous reviewer, E. Rohling, and T. Guilderson significantly improved the original manuscript. A WHOI OCCI Fellowship (NFG), and grants from NSF (OCE-0402728) and WHOI (NFG, KAH, ALC, and MSM) supported this work.

### 3.6 References

- Alibert, C., and M. T. McCulloch, Strontium/calcium ratios in modern *Porites* corals from the Great Barrier Reef as a proxy for sea surface temperature: Calibration of the thermometer and monitoring of ENSO, *Paleoceanography*, 12, 345-363, 1997.
- Bagnato, S., B. K. Linsley, S. S. Howe, G. M. Wellington, and J. Salinger, Evaluating the use of the massive coral *Diploastrea heliopora* for paleoclimate reconstruction, *Paleoceanography*, 19, 2004.
- Beck, J. W., R. L. Edwards, E. Ito, F. W. Taylor, J. Recy, F. Rougerie, P. Joannot, and C. Henin, Sea-Surface Temperature from Coral Skeletal Strontium Calcium Ratios, *Science*, 257, 644-647, 1992.
- Beck, J. W., J. Recy, F. Taylor, R. L. Edwards, and G. Cabioch, Abrupt changes in early Holocene tropical sea surface temperature derived from coral records, *Nature*, 385, 705-707, 1997.
- Cardinal, D., B. Hamelin, E. Bard, and J. Patzold, Sr/Ca, U/Ca and delta O-18 records in recent massive corals from Bermuda: relationships with sea surface temperature, *Chemical Geology*, 176, 213-233, 2001.
- Cohen, A. L., and S. R. Hart, Deglacial SSTs of the Western Tropical Pacific: A New Look at Old Coral, *Paleoceanography*, 19, np, 2004.
- Cohen, A. L., K. E. Owens, G. D. Layne, and N. Shimizu, The effect of algal symbionts on the accuracy of Sr/Ca paleotemperatures from coral, *Science*, 296, 331-333, 2002.
- Cohen, A. L., S. R. Smith, M. S. McCartney, and J. van Etten, How brain corals record climate: an integration of skeletal structure, growth and chemistry of *Diploria labyrinthiformis* from Bermuda, *Marine Ecology-Progress Series*, 271, 147-158, 2004.
- Correge, T., M. K. Gagan, J. W. Beck, G. S. Burr, G. Cabioch, and F. Le Cornec, Interdecadal variation in the extent of South Pacific tropical waters during the Younger Dryas event, *Nature*, 428, 927-929, 2004.
- Crowley, T. J., T. M. Quinn, and W. T. Hyde, Validation of coral temperature calibrations, *Paleoceanography*, 14, 605-615, 1999.
- deVilliers, S., B. K. Nelson, and A. R. Chivas, Biological-Controls on Coral Sr/Ca and Delta-O-18 Reconstructions of Sea-Surface Temperatures, *Science*, 269, 1247-1249, 1995.
- deVilliers, S., G. T. Shen, and B. K. Nelson, The Sr/Ca-Temperature Relationship in Coralline Aragonite - Influence of Variability in (Sr/Ca)Seawater and Skeletal Growth-Parameters, *Geochimica Et Cosmochimica Acta*, 58, 197-208, 1994.

- Dodge, R. E., and J. Thomson, The Natural Radiochemical and Growth Records in Contemporary Hermatypic Corals from the Atlantic and Caribbean, *Earth and Planetary Science Letters*, 23, 313-322, 1974.
- Ferrier-Pages, C., F. Boisson, D. Allemand, and E. Tambutte, Kinetics of strontium uptake in the scleractinian coral *Stylophora pistillata*, *Marine Ecology-Progress Series*, 245, 93-100, 2002.
- Goodkin, N. F., K. Hughen, A. C. Cohen, and S. R. Smith, Record of Little Ice Age sea surface temperatures at Bermuda using a growth-dependent calibration of coral Sr/Ca, *Paleoceanography*, 20, PA4016, doi:4010.1029/2005PA001140, 2005.
- Hughen, K. A., D. P. Schrag, S. B. Jacobsen, and W. Hantoro, El Nino during the last interglacial period recorded by a fossil coral from Indonesia, *Geophysical Research Letters*, 26, 3129-3132, 1999.
- Keigwin, L. D., The Little Ice Age and Medieval warm period in the Sargasso Sea, *Science*, 274, 1504-1508, 1996.
- Lea, D. W., D. K. Pak, and H. J. Spero, Climate impact of the late Quaternary equatorial Pacific sea surface temperature variations, *Science*, 289, 1719-1724, 2000.
- Logan, A., and T. Tomascik, Extension growth rates in two coral species from high-latitude reefs of Bermuda, *Coral Reefs*, 10, 155-160, 1991.
- Marshall, J. F., and M. T. McCulloch, An assessment of the Sr/Ca ratio in shallow water hermatypic corals as a proxy for sea surface temperature, *Geochimica Et Cosmochimica Acta*, 66, 3263-3280, 2002.
- McCulloch, M. T., A. W. Tudhope, T. M. Esat, G. E. Mortimer, J. Chappell, B. Pillans, A. R. Chivas, and A. Omura, Coral record of equatorial sea-surface temperatures during the penultimate deglaciation at Huon Peninsula, *Science*, 283, 202-204, 1999.
- Pelejero, C., J. O. Grimalt, S. Heilig, M. Kienast, and L. Wang, High resolution Uk37 temperature reconstruction in the South China Sea over the past 220 Kyr., *Paleoceanography*, 14, 224-231, 1999.
- Rosenthal, Y., D. W. Oppo, and B. K. Linsley, The amplitude and phasing of climate change during the last deglaciation in the Sulu Sea, western equatorial Pacific, *Geophysical Research Letters*, 30, 1429, 2003.
- Schrag, D. P., Rapid analysis of high-precision Sr/Ca ratios in corals and other marine carbonates, *Paleoceanography*, 14, 97-102, 1999.



- Shen, C. C., T. Lee, C. Y. Chen, C. H. Wang, C. F. Dai, and L. A. Li, The calibration of  $\delta$  Sr/Ca versus sea surface temperature relationship for Porites corals, *Geochimica Et Cosmochimica Acta*, 60, 3849-3858, 1996.
- Smith, S. V., R. W. Buddemeier, R. C. Redalje, and J. E. Houck, Strontium-Calcium Thermometry in Coral Skeletons, *Science*, 204, 404-407, 1979.
- Stephans, C. L., T. M. Quinn, F. W. Taylor, and T. Corregge, Assessing the reproducibility of coral-based climate records, *Geophysical Research Letters*, 31, L18210, doi:10.1029/2004GL020343, 2004.
- Swart, P. K., H. Elderfield, and M. J. Greaves, A high-resolution calibration of Sr/Ca thermometry using the Caribbean coral *Montastraea annularis*, *Geochemistry Geophysics Geosystems*, 3, 2002.
- Weber, J. N., Incorporation of Strontium into Reef Coral Skeletal Carbonate, *Geochimica Et Cosmochimica Acta*, 37, 2173-2190, 1973.



## Chapter 4

# Sea Surface Temperature and Salinity Variability at Bermuda during the End of the Little Ice Age

### Abstract

A 225-year old coral from the south shore of Bermuda (64°W, 32°N) provides a record of decadal-to-centennial scale climate variability. The coral was collected live, and sub-annual density bands seen in x-radiographs delineate cold and warm seasons allowing for precise dating. Coral skeletons incorporate strontium (Sr) and calcium (Ca) in relative proportions inversely to the sea surface temperature (SST) in which the skeleton is secreted. Previous studies on this and other coral colonies from this region document the ability to reconstruct mean-annual and winter-time SST using Sr/Ca measurements [Goodkin *et al.*, in press; Goodkin *et al.*, 2005].  $\delta^{18}\text{O}$  of the coral skeleton changes based on both temperature and the  $\delta^{18}\text{O}$  of sea water ( $\delta\text{O}_w$ ), where  $\delta\text{O}_w$  is proportional to sea surface salinity (SSS). We show in this study that mean-annual and winter-time  $\delta^{18}\text{O}$  of the carbonate ( $\delta\text{O}_c$ ) are correlated to both SST and SSS, but a robust quantitative measure of SSS is not found. In combination, however, the Sr/Ca and  $\delta\text{O}_c$  qualitatively predict fresher salinities at the end of the LIA. The coral band records of SST for the past two centuries show abrupt shifts in both decadal and centennial time-scales. Our reconstruction at Bermuda suggests that SST at the end of the Little Ice Age period (between 1830 and 1860) was  $1.5 \pm 0.4$  °C colder than today, and the surface sea water was fresher.



## 4.1. Introduction

### 4.1.1 Little Ice Age

The Little Ice Age (LIA) was a series of extended cold periods which occurred from the mid-1400s to the late 1800s, documented primarily in the Northern Hemisphere [Bradley and Jones, 1993; Jones *et al.*, 1998; Overpeck *et al.*, 1997]. Currently, high-resolution paleoclimate records of the LIA exist from tree rings [Briffa *et al.*, 2001; Esper *et al.*, 2002; Jacoby and D'Arrigo, 1989], ice cores [Dahl-Jensen *et al.*, 1998; Dansgaard *et al.*, 1975], and coral records from the Caribbean Sea [Druffel, 1982; Watanabe *et al.*, 2001; Winter *et al.*, 2000]. These and other proxy reconstructions from around the North Atlantic show LIA temperatures to be 0.5 to 5 °C colder than today [deMenocal *et al.*, 2000; Druffel, 1982; Dunbar *et al.*, 1994; Glynn *et al.*, 1983; Keigwin, 1996].

The LIA is the most recent example of decadal-to-centennial scale climate change events during the late Holocene. These events are of interest, in part because it is believed that by improving our understanding of the mechanisms and patterns of such natural climate change, we will greatly improve our ability to anticipate and evaluate future changes on similar time scales. Two forcing mechanisms have been put forth as a possible cause of for the Little Ice Age. Solar activity was low during this time [Crowley, 2000; Lean *et al.*, 1995; Wigley and Kelly, 1990], whereas volcanic activity is observed to have been high [Crowley, 2000]. Solar activity has also been linked to changes in thermohaline circulation leading to a possible millennial paced climate signal [Bond *et al.*, 2001; Bond *et al.*, 1997]. Both solar and volcanic influences have the potential to produce widespread cooling across the globe.

In addition to global processes, regional climate processes will impact the North Atlantic as well. The North Atlantic Oscillation (NAO), measured as a pressure difference between the Icelandic high and Azores low [Hurrell, 1995; Jones *et al.*, 1997a], exerts an influence from the eastern United States to western Europe at several frequencies [Visbeck *et al.*, 2003]. The influence of this system, however, is limited geographically to the Northern Hemisphere and produces different responses on varying timescales and at varying locations [Keigwin and Pickart, 1999; Visbeck *et al.*, 2003].

#### 4.1.2 Coral Based Proxy Records

Coral skeletons provide high-resolution, long records of climate variability in the ocean. The strontium (Sr) to calcium (Ca) ratio of coral skeleton is inversely related to the SST in which the coral grew [Smith *et al.*, 1979] and provides a salinity independent record of local sea surface temperatures (SST) [Beck *et al.*, 1992; Beck *et al.*, 1997]. Skeletal  $\delta^{18}\text{O}$  ( $\delta\text{O}_c$ ) is governed by both SST and the  $\delta^{18}\text{O}$  of sea water ( $\delta\text{O}_w$ ), which is linearly related to sea surface salinity (SSS). Therefore, in combination,  $\delta\text{O}_c$  and Sr/Ca provide the means to estimate records of both SST and SSS back through time [Gagan *et al.*, 1998; Iijima *et al.*, 2005; Quinn and Sampson, 2002; Watanabe *et al.*, 2001].

Here we use Sr/Ca and  $\delta^{18}\text{O}$  from a slow-growing coral from Bermuda to reconstruct SST and SSS from 1781-1999. Over the past 218 years (1781-1999), we evaluate inter-annual and winter-time SST and SSS/ $\delta\text{O}_w$  variations based upon monthly resolution records of Sr/Ca and  $\delta^{18}\text{O}$  from a brain coral (*Diploria labyrinthiformis*). Growth rate, particularly in slow growing corals, has been shown to impact coral Sr/Ca [Alibert and McCulloch, 1997; Cardinal *et al.*, 2001; Cohen and Hart, 1997; Cohen *et al.*,

2004; *deVilliers et al.*, 1995; *deVilliers et al.*, 1994; *Goodkin et al.*, in press; *Goodkin et al.*, 2005]. Previous studies at Bermuda show how mean-annual and summer Sr/Ca values are impacted by both inter-annual growth rate and average growth rate over the lifespan of the coral used in this study [*Goodkin et al.*, in press; *Goodkin et al.*, 2005]. In contrast, winter (Dec.-March) Sr/Ca values show no correlation to growth rate [*Goodkin et al.*, 2005]. We use a previously developed mean-annual calibration to SST including growth rate and a newly developed non-growth dependent winter time Sr/Ca-SST calibration. Reconstructed mean-annual and winter SSTs are then compared to  $\delta^{18}\text{O}$  to evaluate directional changes in salinity.

## **4.2. Methods**

### **4.2.1 Study Site**

In 2000, a 225-year old brain coral species (BB 001) was collected alive from the southeastern edge of the Bermuda platform at 16-meters water depth. Two smaller corals (BER 002 and BER 003) were collected from the same location to examine reproducibility between coral colonies and are used in this work to evaluate winter Sr/Ca. The island of Bermuda (64°W, 32°N) is located in the Sargasso Sea in the sub-tropical North Atlantic. This site is oceanographically important because a large portion of the world's ocean heat transport from low to high latitudes occurs in the North Atlantic via the Gulf Stream. Sargasso Sea water interacts with both warmer tropical and cooler sub-arctic water [*Curry et al.*, 2003; *Talley*, 1996]. Bermuda, a northernmost location for surface coral growth and near a site of high, deep sea sedimentation rates, has been the location for several reconstructions of past climate from coral [*Draschba et al.*, 2000;



*Druffel, 1997; Kuhnert et al., 2005*], foraminifera [*Keigwin, 1996*] and alkenone based proxy reconstructions [*Ohkouchi et al., 2002; Sachs and Lehman, 1999*].

The southern platform of Bermuda is in close proximity to Hydrostation S, which lies 30km to the southeast (32°10'N, 64°30'W). Since 1954, Hydrostation S has been visited bi-weekly for on-going research including the measurement of SST and SSS. Coral geochemistry proxies from multiple coral colonies (including the multi-century coral used in this study) collected off southern Bermuda have previously shown correlations to Hydrostation S temperature averaged above 16 meters depth [*Goodkin et al., in press; Goodkin et al., 2005*] for the calibration period of 1976 to 1997. At Hydrostation S, monthly averaged SST ranges from 18.0-28.9 °C. Annually averaged SSTs vary between 22.4-24.3 °C. Monthly SSS varies from 36.1-36.8 ‰. Annually averaged SSS has a range of 36.3-36.6 ‰. The Hydrostation S SST and SSS records are incomplete over several intervals, with two or more months of SST and/or SSS missing in 1978-1981, 1986, and 1989. In this paper, we will also compare the coral records to regional, observational SST records (HadISST) from 1870-1997 from the gridded area 31-33° N and 295-296° E [*Rayner et al., 2003*].

#### **4.2.2 Sub-sampling**

Coral slabs were cut, cleaned and x-rayed according to methods previously presented [*Goodkin et al., 2005*]. Approximately monthly samples were drilled using a micro-meter controlled drill press every 0.33 mm along the dense thecal wall [*Cohen et al., 2004*]. Individual samples averaged 220 µg and were split into a small portion (~8-40 µg) for stable isotope analysis and the remaining portion for Sr/Ca analysis. The thecal

wall was chosen, despite complicated skeletal architecture [Cohen *et al.*, 2004], because it is the densest skeletal component with the least potential impact from diagenesis.

#### 4.2.3 Sr/Ca Analysis

Sr and Ca were analyzed simultaneously using Inductively Coupled Plasma-Atomic Emission Spectrometry (ICP-AES) at Woods Hole Oceanographic Institution (WHOI). Samples were dissolved in 1N HNO<sub>3</sub> to a concentration of ~80 ppm Ca based on mass in order to minimize matrix corrections. Solution standards were employed to evaluate and correct for drift and matrix effects [Schrag, 1999]. A homogenized coral (*Porites*) powder external standard was prepared simultaneous to unknowns and blanks to evaluate precision. Repeat measurements on the coral external standard (run at variable concentrations matching the range of unknowns) analyzed over more than a year showed good reproducibility (standard deviation (SD) = 0.0244 mmol/mol, relative SD (RSD) = 0.27%, n=1,493). A small long-term drift (over several months) in the homogenous coral standard was observed on the order of 0.011 mmol/mol and corrections were made to the unknowns as described in Appendix B.

#### 4.2.4 Stable Oxygen Isotope Analysis

Stable oxygen isotope analyses were measured on a Finnigan MAT 253 coupled to a Kiel III carbonate device at WHOI. Conversion to the Vienna Pee Dee Belemnite (VPDB) scale was completed using NBS19 ( $\delta^{18}\text{O} = -2.20\text{‰}$ ). Reproducibility based on Estremoz marble (WHOI internal standard;  $\delta^{18}\text{O} = -5.98\text{‰}$  relative to VPDB), which has values closest to the coral unknowns, were  $\pm 0.11\text{‰}$  (n = 660). Corrections for small

samples (<0.8 volts, 9% of total) and samples with poorly balanced gas pressure relative to the reference gas (unbalanced, sample/standard voltage > 1.1, 11% of total) samples were required. These corrections were up to 0.2 ‰ for  $\delta^{18}\text{O}$  and are described in Appendix C.

#### 4.2.5 Age Model Development

Age models were developed using density banding visible in the x-radiographs (Appendix H) to identify the annual growth, and then correlating Sr/Ca to monthly averaged SSTs at maxima, minima and inflection points [Goodkin *et al.*, 2005]. Over the length of the entire record, three slabs were cut to capture changes in the primary growth axis through time. Multiple tracks were drilled within each slab as well as across slabs to produce a continuous record along the growth axis. In this situation, x-radiographs and algal bands provided the needed information to overlap samples during transitions between slabs. Overlapping Sr/Ca and  $\delta^{18}\text{O}$  samples were averaged. The correlation coefficient of Sr/Ca between overlapping slabs (average  $r = 0.83$ ) is strong, as previously found [Goodkin *et al.*, 2005].

For the record extending beyond the time frame of Hydrostation S, Sr/Ca data were fitted to a monthly-climatology from SST values for the entire Hydrostation S record. All geochemical records were then interpolated to even monthly increments. Before interpolation, the record had an average of 10.5 samples per year and a median of 11 samples per year. Annual averages (January-to-January) were calculated from the interpolated values.



Some error is expected within this age model due to very slow or non-growing years not visible on the x-ray and also not clearly discernible in the Sr/Ca seasonal cycle. While there is potential for error generated by noise in the Sr/Ca or the annual band counting leading to the inappropriate addition of a year, the majority of estimated age error will arise because of missing years, generating a bias in which coral bands are assigned to be more recent than actual dates. For example, if the coral did not grow in 1950, 1949 would be inappropriately assigned the date 1950, generating a bias in all years previous to 1950 (1948, 1947 etc.). Age model bias is expected to increase during the early-to-mid 1800s when growth rates are extremely slow for an extended period of time and hiatuses in growth may be expected.

### **4.3 Results**

Sr/Ca and  $\delta^{18}\text{O}$  records show cyclical seasonal cycles throughout the calibration period (1976-1997, Fig. 4.1) and the length of the record. Sr/Ca and  $\delta^{18}\text{O}$  show a strong correlation over this period ( $r^2 = 0.70$ ), as they are both driven in large part by SST. An offset in the timing of  $\delta^{18}\text{O}$  and Sr/Ca cycles is evident, with  $\delta^{18}\text{O}$  reaching maxima and minima on average one month later than Sr/Ca. This difference in timing likely results from the added influence of SSS on oxygen isotopic values. Within the Hydrostation S record, a similar phase difference is seen between SST and SSS hydrographic properties.

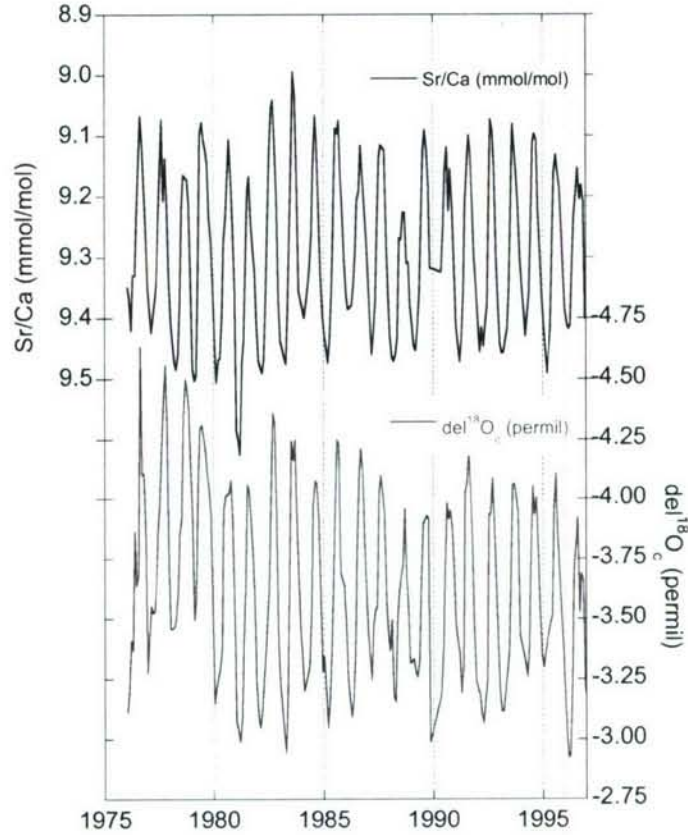


**Figure 4.1:** Sr/Ca (mmol/mol) and  $\delta^{18}\text{O}$  (‰) plotted versus year over the calibration period of 1976-1997. Both geochemical proxies show an inverse relationship to SST ( $r^2 = 0.86$  and  $0.69$  respectively).  $\delta^{18}\text{O}$  is additionally influenced by SSS ( $r^2 = 0.32$ ).

#### 4.3.1 Sr/Ca - SST

*Mean-Annual:* Sr/Ca in coral is known to be inversely related to SST [Smith *et al.*, 1979]. In addition, previous work has shown mean-annual SST in slow-growing corals to vary according to Sr/Ca (mmol/mol) as well as average mean-annual growth (mm/year) [Goodkin *et al.*, in press; Goodkin *et al.*, 2005]. For this work, mean-annual SST ( $^{\circ}\text{C}$ ) was calculated using a previously published, multi-coral growth corrected model [Goodkin *et al.*, in press]:

$$\text{Sr/Ca} = (-0.000697 * (\text{ig}) + 0.00304 * (\text{ag}) - 0.0738) * \text{SST} + 10.8$$

$$(2\sigma, 95\% \text{ conf.}, r^2=0.51, F_{\text{sig}} < 0.0001, \text{rmsr}=0.5 \text{ }^\circ\text{C}, \text{se}=0.031 \text{ mmol/mol})$$

eqn. (1)

where (ig) is interannual growth (mm/year) and (ag) is the average growth rate (mm/year) of the colony. RMSR is the root mean square of the residuals, when the regression was inverted and used to calculate SST. SE is the standard error on Sr/Ca predicted by the regression. The average growth rate is 3.8 mm/year and interannual growth rates are smoothed using a box window over three years according to Goodkin *et al.* (2005).

We compute error estimates on the application of the mean-annual SST regression to the 218-year Sr/Ca record beginning by inverting eqn. 1 to find SST as a function of Sr/Ca and growth rate. Standard methods of error propagation were used ([Bevington, 1969], detailed in Appendix G) including the slope and intercept errors shown with equation (1) and slope and intercept covariance values previously reported ([Goodkin *et al.*, in press], Appendix G). Error on Sr/Ca was based on the standard error of the regression (0.031 mmol/mol), which is larger than the measurement error (0.0244 mmol/mol), providing a more statistically conservative result. We have assumed no error in growth rate estimates. The  $1\sigma$  SST uncertainty for the mean-annual calibration has an average value of  $\pm 0.6 \text{ }^\circ\text{C}$  (max =  $1.0 \text{ }^\circ\text{C}$  and min =  $0.5 \text{ }^\circ\text{C}$ ) back to 1782 (Fig. 4.2).

Hydrostation S, Hadley, and the Sr/Ca based reconstructed SST agree well in absolute value until 1970, when the Sr/Ca reconstructed SST becomes on average higher than both the Hadley and Hydrostation S SST (Fig. 4.2). The error bars ( $1\sigma$ ) of the



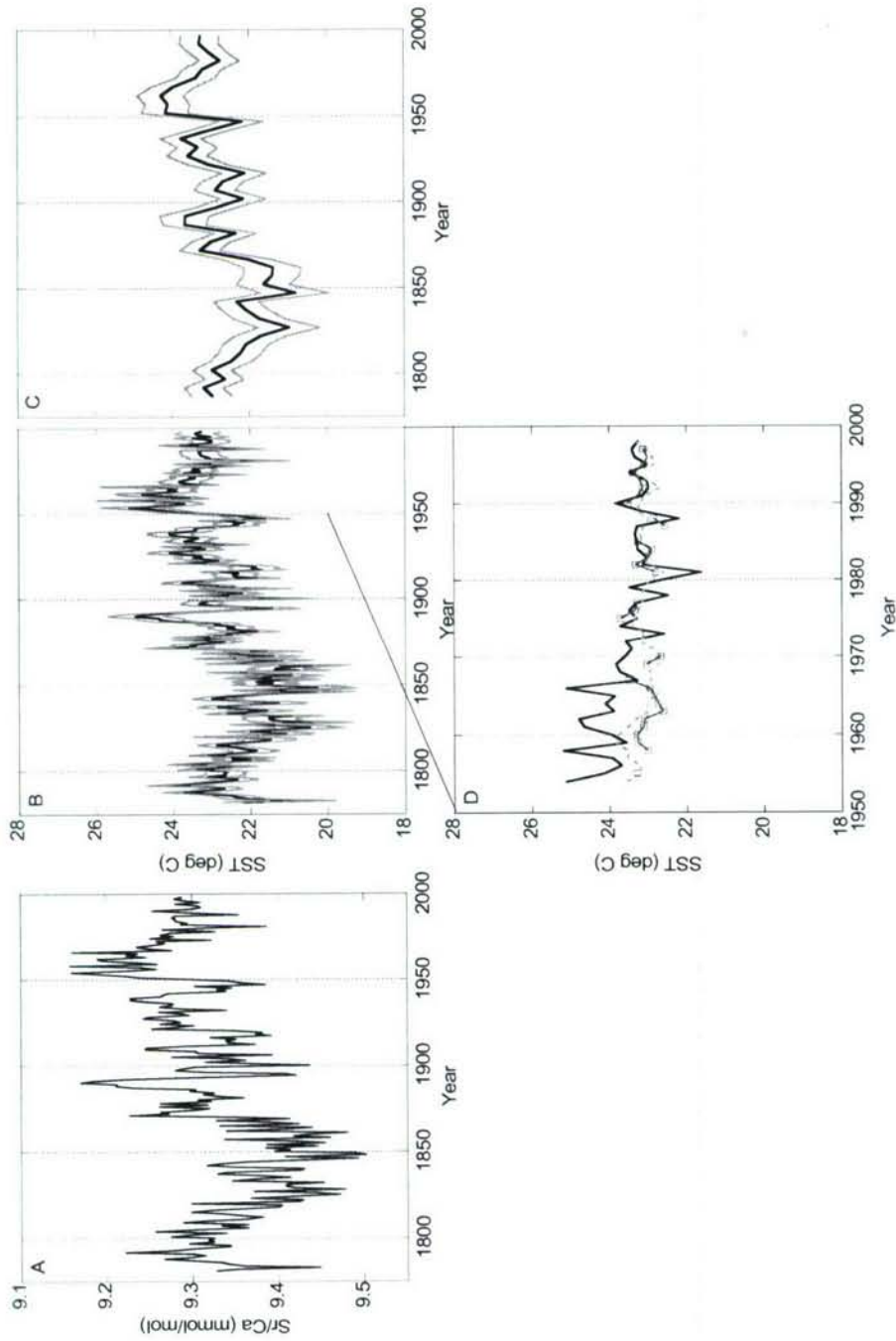


**Figure 4.2:** A) Mean-annual Sr/Ca shown versus time. B) Mean-annual SST generated from Sr/Ca (solid) ( $\pm 1\sigma$ ) using the multi-colony, growth corrected calibration (eqn. 1). Uncertainty resulting from error propagation shown with shaded lines. C) Mean-annual SST generated from Sr/Ca binned into five year averages (solid). Uncertainty shown with shaded lines. D) Mean-annual SST generated from Sr/Ca (solid), HadleySST (shaded-dashed), and Hydrostation S (solid with squares) for the period of 1954-1997.

reconstructed SST do overlap with the instrumental records for this period. Hydrostation S SST and Hadley SST also agree less well prior to 1970, with an  $r$  of 0.63 from 1970 to 1997 and an  $r$  of 0.37 from 1954-1970. The disagreement amongst all records prior to 1970 may be caused by several factors – for example less homogenous water in the region, changes in the shallow waters at Bermuda that are not representative of deeper waters, changes in SST measurements, or undiagnosed vital effects not present during calibration.

Mean-annual Sr/Ca values range from 9.16 mmol/mol to 9.50 mmol/mol (Fig. 4.2a) over the 218 year record. Reconstructed mean-annual temperature change at Bermuda exhibits both decadal and centennial scale variability with a 5 °C temperature range (20.3-25.2 °C). Temperature minima are found in the coral reconstruction at the end of LIA around 1840 and 1850 (Fig. 4.2b,c). Averaging annual samples into five year bins shows an SST range of 20.8–24.3 °C. Fig. 4.2 shows the Sr/Ca based reconstruction of SST to be cooler during the LIA than today, at a statistically certain level. The large temperature change ( $2.6\text{ °C} \pm 0.6\text{ °C}$ ) of the record occurs between the 1960s and 1840s. Temperatures during the LIA are  $1.6\text{ °C} \pm 0.6\text{ °C}$  cooler than the 1990s instrumental average.

*Winter Sr/Ca:* All three corals (BB 001, BER 002, BER 003) show a statistically significant ( $F_{\text{sig}} = 0.0004, 0.0938, \text{ and } 0.0106$  respectively) inverse relationship between winter-time (Dec-March) Sr/Ca and Hydrostation S SST over the calibration period (1976-1997) (Fig. 4.3). Linear regressions of winter Sr/Ca to SST for each coral yield statistically equivalent ( $1\sigma$ ) slopes and intercepts with an average slope of -0.039

mmol/mol/°C and an intercept of 10.2 mmol/mol. Unlike previous work done on mean-annual calibrations for these corals, adding growth rate either through inter-annual changes [Goodkin *et al.*, 2005] or colony averages [Goodkin *et al.*, in press] does not improve these calibrations, confirming the previous conclusion that growth rate is not impacting the winter Sr/Ca [Goodkin *et al.*, 2005]. Winter-time Sr/Ca appears to reflect SST in a linear fashion.

The short calibrations shown in Fig. 4.3, however, do not provide a realistic SST reconstruction over the length of the multi-century record. The BB 001-Hydrostation S winter-time calibration applied to the long record shows winter SSTs as high as 27 °C in the 1960s and as low as 15 °C in the 1850s, a range that is greater than the current seasonal cycle. This result implies a possible problem with the above calibration in that the noise is overwhelming the signal and biasing the regression.

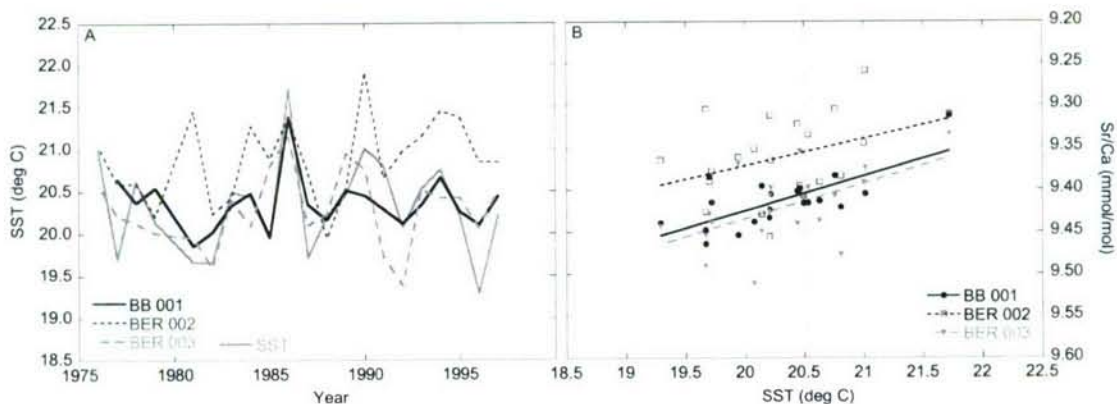


**Figure 4.3:** Coral winter-time (Dec., Jan., Feb. and March) Sr/Ca and Hydrostation S (solid, grey) SST plotted versus year (a) and linearly (b) for BB 001 (solid line, circles), for BER 002 (small dashes, squares), and for BER 003 (large dashes, triangles).



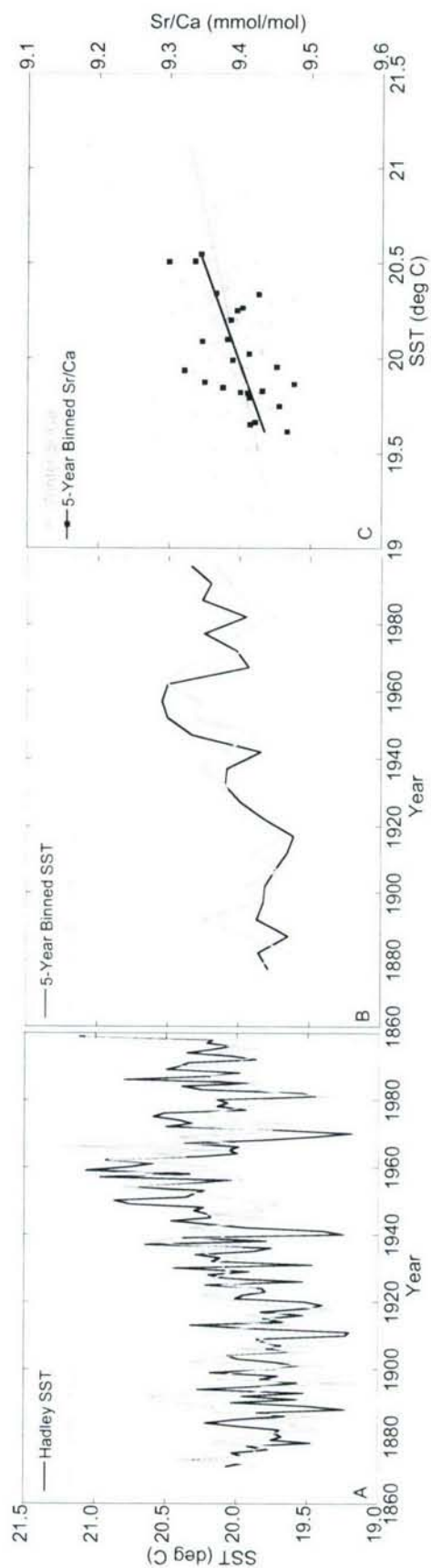


**Figure 4.4:** BB 001 winter-time (Dec-March) Sr/Ca (shaded) and Hadley SST (solid) plotted versus year for a) inter-annual ( $r^2 = 0.13$ ,  $\text{rmsr} = 1.03^\circ\text{C}$ ), b) five-year bins ( $r^2 = 0.36$ ,  $\text{rmsr} = 0.36^\circ\text{C}$ ), and c) linearly with inter-annual (shaded, circles), and five year bins (solid, squares).

In order to address this influence, the long record from BB 001 was correlated to Hadley SST from 1870-1999 both yearly and in five year bins to increase the length and range of signal of the calibration period (Fig. 4.4)<sup>1</sup>. Hadley SST is a compilation of regional observational SST measurements (HadISST, [Rayner *et al.*, 2003]). This study uses the gridded area 31-33° N and 64-65° W. The results are shown in table 4.1.

Table 4.1: Winter-time Sr/Ca regressions at inter-annual (eqn. 2) and five year (eqn. 3) time scales for the equations of the form:  $Sr/Ca = \beta + \gamma * SST$ .  $\sigma^2_{\beta-\gamma}$  is the covariance on the slope and intercept with units of  $(mmol/mol)^2(^{\circ}C)$ .  $\beta$  has units of  $mmol/mol$  and  $\gamma$  has units of  $mmol/mol/^{\circ}C$ .

Time Frame	$\beta$	2 $\sigma$ Er.	$\gamma$	2 $\sigma$ Er.	$r^2$	$F_{sig}$	rmsr ( $^{\circ}C$ )	se (mmol/mol)	$\sigma^2_{\beta-\gamma}$
Inter-Annual (2)	10.6	0.6	-0.0615	0.0279	0.13	<0.0001	1.05	0.0064	-0.004
Five Year Bin (3)	11.3	1.1	-0.0972	0.0531	0.36	0.0012	0.36	0.0036	-0.014

Increasing the length of the calibration data sets and then diminishing noise through averaging the SST records into 5-year bins succeeds at increasing the significance of the reconstructions and decreasing the root mean square of the residuals (rmsr) and standard error (se). The increase in slope confirms the hypothesis that the 25-year Hydrostation S calibration period contains too small a signal given the signal-to-noise ratio.

Error propagation was performed for the five year binned winter-time reconstruction (eqn. 3), as applied to the 218 year winter-time Sr/Ca record in five year bins. The equation was first inverted and then standard error propagation methods were

<sup>1</sup> A type I regression minimizes the distance between the dependent variable and the regressed line, whereas the type II regression minimizes the distance between the line and both the dependent and independent variables. Both type I and II linear regressions were performed. Type II regressions were examined to account for the error in Hadley SST, which is reconstructed using varying types and distributions of instrumental records. Type I and II regressions do not return statistically independent results, and therefore, type I regressions are used for consistency.

used (Appendix G). Propagating error returns an average error of  $\pm 0.4$  °C (max = 0.5 °C and min = 0.3 °C) over the long record (Fig. 4.5b).

Comparing the most-recent 50-years of winter-time Sr/Ca based reconstructed SST to Hadley and Hydrostation S winter-time SSTs for 5-year binned averages shows different results than seen with the mean-annual record (Fig. 4.5c). Between 1970 and 1997 both the Hadley instrumental SST (and the coral reconstructed SST which is

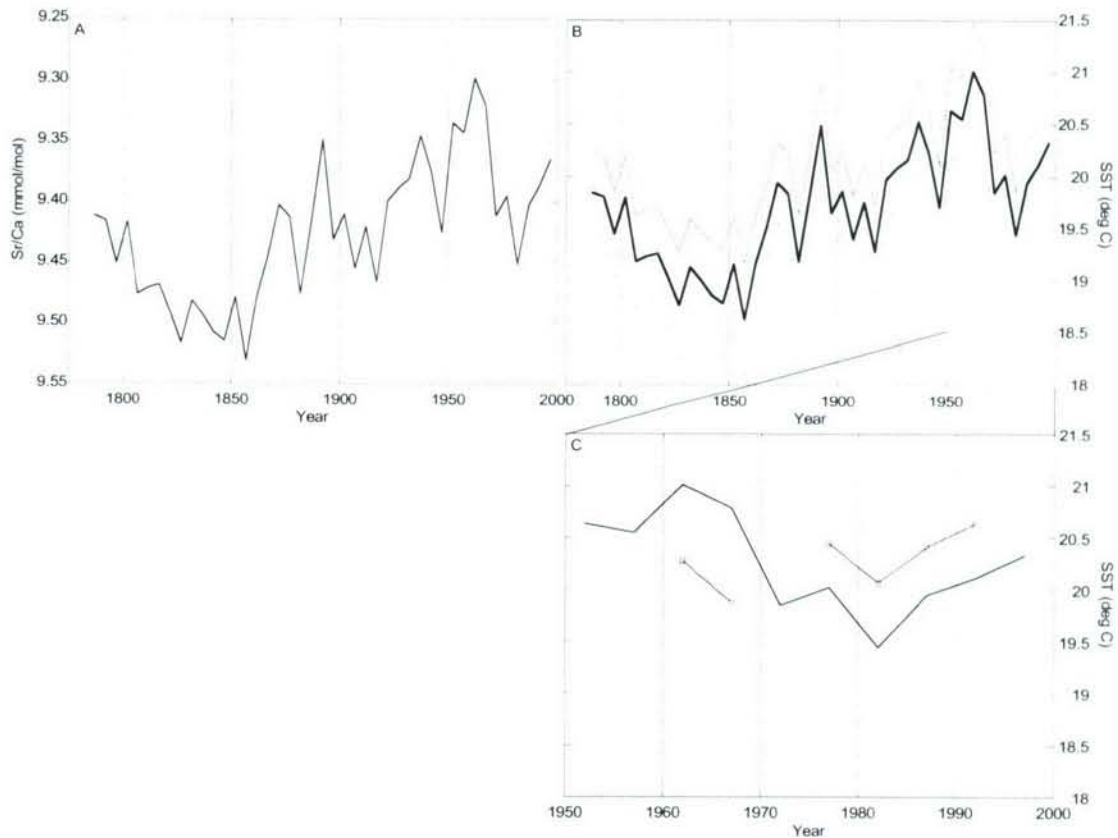


**Figure 4.5:** A) Five-year winter-time Sr/Ca and B) five-year averaged winter-time SST from 1781-1999. C) five-year averaged winter-time SST from 1950-1999 for winter-time SST (solid), Hadley SST (dashed) and Hydrostation S SST (solid, squares). Coral SSTs are reconstructed from Sr/Ca using five year averaged calibration (eqn. 3). Uncertainty resulting from error propagation ( $1\sigma$ ) is shown by shaded lines (b).



calibrated to Hadley) agree with the trends of Hydrostation S ( $r = 0.97$  and  $0.81$  respectively) though all three records are offset from one another. The coral record prior to the 1970s is still the warmest of the three records by more than  $0.5\text{ }^{\circ}\text{C}$ .

Applying eqn. 3 (Table 4.1) to the Sr/Ca record averaged in five-year bins reconstructs SST at the end of the LIA to be  $18.6\text{ }^{\circ}\text{C}$  and to be  $21\text{ }^{\circ}\text{C}$  during the time of late 20<sup>th</sup> century warming (Fig. 4.5a,b). Reconstructed winter-time SST changes between late 20<sup>th</sup> century warming and the end of the LIA by  $2.4 \pm 0.4\text{ }^{\circ}\text{C}$ , a statistically significant result. The LIA (1840s) is also shown to be  $1.5 \pm 0.4\text{ }^{\circ}\text{C}$  colder than today (1990s instrumental average). Much like the mean-annual record, the warmest temperatures are seen in the 1960s and the coldest temperatures are seen between 1840 and 1860 (Fig. 4.5b).

*Comparison to Instrumental Hadley SST Record:* Comparing both the mean-annual reconstructed SST and the winter-time coral reconstructed SST to Hadley SST ( $1^{\circ} \times 2^{\circ}$  grid) with five-year bins shows similar results (Fig. 4.6). For both the mean-annual and winter-time periods, reconstructed SSTs show largely increased temperature variability relative to the gridded data set throughout the duration of the instrumental record, implying that the bias in our record is to overestimate not underestimate temperature change. In the mean-annual comparison, five year binned instrumental temperature variability from 1871-1997 shows a range of  $1\text{ }^{\circ}\text{C}$  whereas the reconstructed SST shows a range slightly greater than  $2\text{ }^{\circ}\text{C}$  change ( $r = 0.48$ ). The gridded data and the coral reconstructed SST show no overall trend in temperature from 1871 to 1900, with the reconstructed SST showing much greater variability. Beginning in the early

1900s, both records show increasing temperatures, with the gridded data set peaking in 1959. The reconstructed SST shows a sharper temperature increase in the early 1900s with a distinct cooling during the 1940s and a larger and more extended period of warming in the 1950s and 1960s. Since the 1970s, the records show strong coherence. The periods of greatest disagreement in not only absolute temperature but in temperature trends are during the 1940s to the 1960s, when a disagreement to Hydrostation S is also seen.

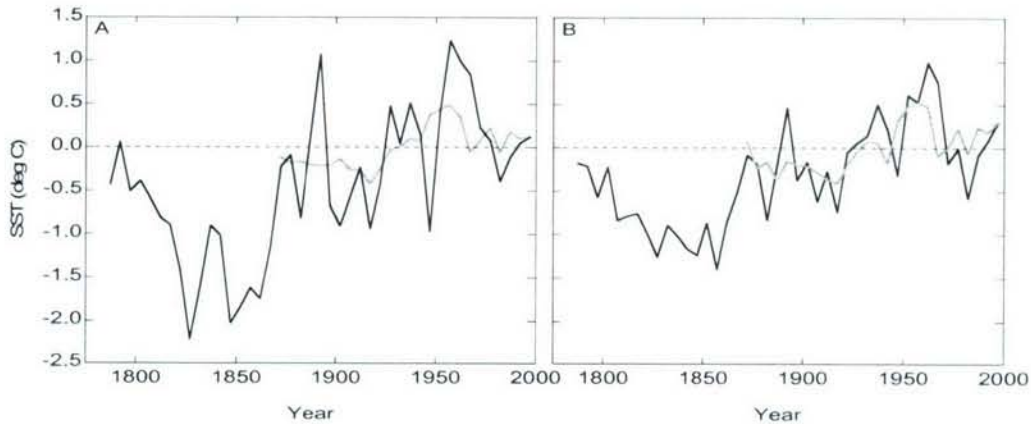


**Figure 4.6:** Five-year average mean-annual SST (a) and winter-SST (b) from coral reconstruction (solid) and Hadley gridded data set (shaded). All four SST records are normalized around each records' 1872-1997 mean.

While not independent because the calibration uses the Hadley instrumental data set, the winter comparison does show similar results as the mean-annual comparison. Five-year binned winter temperature records show a coral based SST range just under 2 °C relative to a 1 °C range for the gridded data set ( $r = 0.60$ ). The instrumental data set shows a slight trend of decreasing temperature from 1871 to 1900, consistent with the

coral data set which still shows much greater variability during this time. Similar to the mean-annual records, the winter-time records show generally rising temperatures during the 1900s, with maxima in the 1950s. The winter coral record also peaks later than the winter instrumental data set. Additionally, from 1960s onward the coral is showing cooler temperatures than the instrumental data set, though with similar trends.

There are several factors that could explain some of the temperature differences observed between the Hadley instrumental data product and the reconstructed coral SST records. The first factor is the difference between averaging over many points from a 2° by 1° grid compared to a one point temperature reconstruction. The large scale instrumental record has several sources of error typical of such data sets some of which will serve to dampen variability within its record [*Jones et al.*, 1997b; *Jones et al.*, 2001; *Rayner et al.*, 2003]. The error introduced from changing technology through time is one source of varying error through time with a larger impact the older the data. Non-equal distribution of the number and location of measurements made through out each year and through out the grid can serve to bias the record either seasonally or geographically. Finally, a varying number of samples within the grid through time will produce another source of error.

In addition, the instrumental data are generally collected from off-shore waters rather than shallow coastal where the coral grew. An off-shore water column will average out variability at specific locations, including not only site specific but micro-environmental information. This includes variability from the shallower, well-stratified water, as well as factors such as upwelling at the coral site due to close proximity to a land mass. Additionally, meso-scale eddy processes exert a large influence in this region [*Doney*, 1996; *Sweeney*, 2003]. Three types of eddies are found in the vicinity of



Bermuda supplying both positive and negative temperature anomalies. A 2° by 1° grid box could average eddy temperature anomalies, whereas eddies passing by the coral site over a several months would produce greater variability in SST recorded by the coral.

Although there are concerns as discussed above, we believe that the Sr/Ca-SST calibrations used in this study are robust. Research has shown that calibration error tends to exaggerate temperature change rather than minimize it [Goodkin *et al.*, 2005; Swart *et al.*, 2002]. This is reinforced by the increased variability seen in the coral reconstructions relative to the gridded data. Both the mean-annual and winter-time records show similar variability and similar differences relative to the instrumental data set, following a very different calibration. The coral reconstructed SSTs show changes between the LIA and today of ~2.5 °C between the 1960s and the end of the LIA and of 1.5 °C colder than modern instrumental records. Error propagation suggests these changes are statistically significant. This result implies that some of these discrepancies may result from differences between what the coral experienced locally and what the ocean experienced regionally. This distinction is important for interpreting these results climatologically.

#### 4.3.2 $\delta^{18}\text{O}$ – SSS

$\delta^{18}\text{O}$  of the coral aragonite ( $\delta\text{O}_c$ ) is expected to have a negative correlation to SST and a positive correlation to SSS (Fig. 4.8, eqn. 4.4). Trends in mean-annual (-0.0003 ‰/year) and winter-time (<0.0001 ‰/year)  $\delta\text{O}_c$  are effectively flat over the course of the two hundred year record (Fig. 4.7a,c). Simultaneously, both mean-annual and winter-time Sr/Ca based reconstructed SST show increasing temperatures through time (0.008 °C/year and 0.009 °C/year, respectively) (Fig. 4.7b,d). If  $\delta\text{O}_c$  were purely a record of

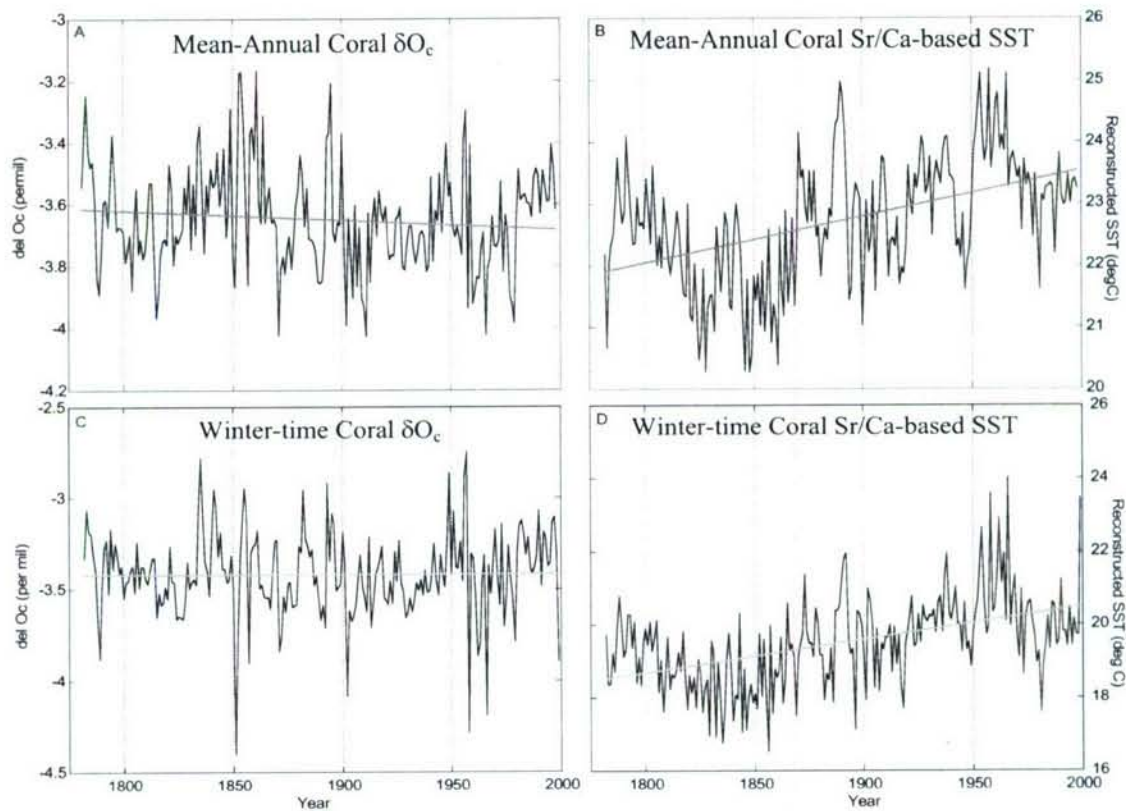


**Figure 4.7:** a) Coral measured mean-annual  $\delta O_c$  versus time. b) Coral Sr/Ca based mean-annual reconstructed SST (eqn. 1) versus time. c) Coral measured winter-time  $\delta O_c$  versus time. d) Coral Sr/Ca based winter-time reconstructed SST (yearly, eqn. 2) versus time. Linear regressions of each parameter versus time are shown by shaded lines.

SST, a stronger negative trend (more than order of magnitude steeper as predicted by eqn. 1 in Chapter 1) would be visible in the  $\delta O_c$  records. In addition, a strong LIA cooling is seen in both Sr/Ca generated SST records, whereas the mean-annual  $\delta O_c$  shows minimal indication of this cooling and winter-time shows no indication of this cooling. Therefore, to a first order approximation, Fig. 4.7 implies that both mean-annual and winter-time yearly SSS was lower (fresher) during the end of the LIA than it is today. Because  $\delta O_c$  is directly related to SSS, a salinity signal will serve to oppose the expected SST based trend in the  $\delta O_c$ . The lack of a strongly decreasing trend in the mean-annual record and

the presence of a slightly increasing trend in the winter-time  $\delta\text{O}_c$  measurements imply that  $\delta\text{O}_c$  is being impacted by increasing SSS over the length of the record.

In the following three sub-sections, we show that with the present coral record and calibration data set, we are unable to derive a robust quantitative estimate of paleo-salinity. There are several reasons that may prevent the quantification of these relationships. The most likely cause is the lack of instrumental data documenting large enough changes in SSS. Over the length of Hydrostation S, salinity (mean-annual and winter) has a range of 0.3 psu and inter-annual temperatures have a range of 2 °C. The SSS range is a very small range over which to establish a significant relationship that is impacted by more than one variable.

There are also several parameters that may be adding variability to the system, which given the small SSS signal makes calibration more difficult. As previously discussed with regards to regional SST records, eddy activity in the region can also alter salinity [Doney, 1996]. Eddies could lead to differences between SSS at the coral and Hydrostation S thus adding unexplained variability over the limited calibration period. Furthermore, vital effects and growth rates may be causing varying fractionation of  $\delta\text{O}_c$  during the calibration. While we were unable to model such effects, if they exist they could further convolve the SSS signal. In the end, we are unable to quantitatively reconstruct salinity. However, the raw data give a strong indication that Bermuda's sea water was fresher during the LIA.

*Monthly Relationships:* Growth rate and bulk sampling effects limit our ability to evaluate  $\delta^{18}\text{O}$  as an SSS proxy on monthly time-scales. However, for proper comparison to the literature we examine the  $\delta^{18}\text{O}$  data on monthly time-scales. The  $\delta^{18}\text{O}$  of the coral



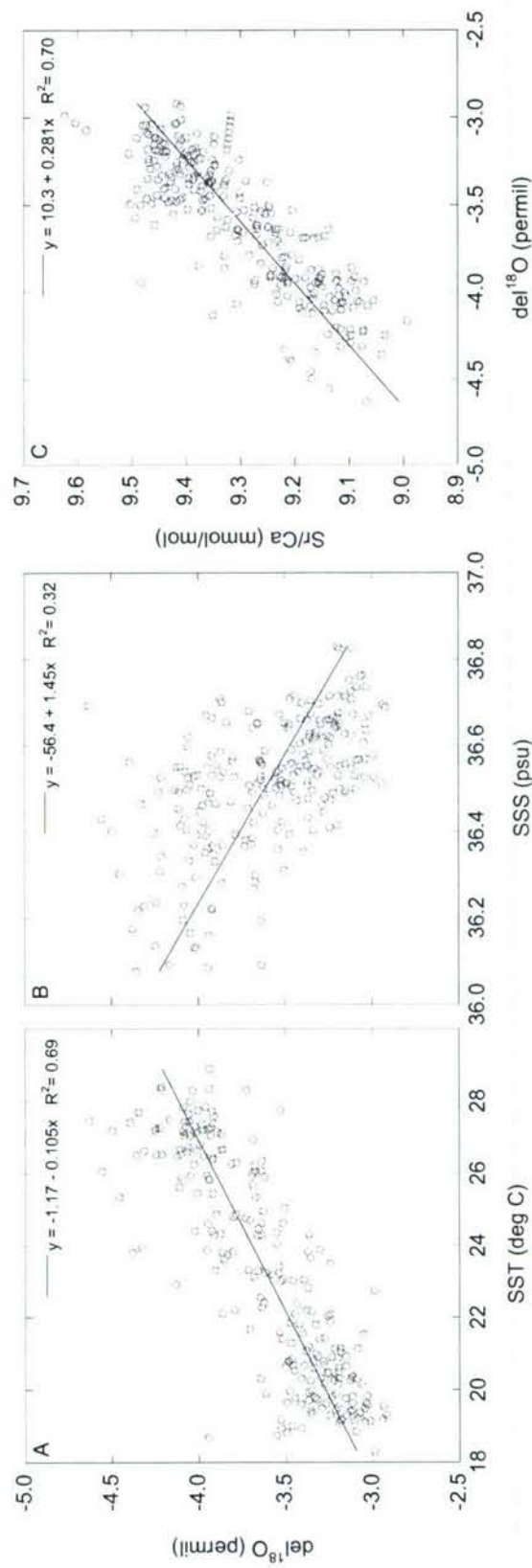


**Figure 4.8:** Monthly BB 001 measurements from 1976-1997. a)  $\delta^{18}\text{O}$  regressed linearly against monthly Hydrostation S SST and b) SSS. Monthly BB 001 Sr/Ca regressed against  $\delta^{18}\text{O}$ .

( $\delta\text{O}_\text{c}$ ) is shown to be negatively correlated to SST and positively correlated to SSS at Hydrostation S (Fig. 4.8). Over the calibration period, monthly coral  $\delta^{18}\text{O}$  values range from -4.63 to -2.92 ‰. The correlation coefficient ( $r^2$ ) of  $\delta\text{O}_\text{c}$  to SST is 0.69. The correlation coefficient ( $r^2$ ) of  $\delta\text{O}_\text{c}$  to salinity is 0.32. The correlation between SST and SSS ( $r^2 = 0.31$ ) over this time period is likely to impact these correlations making them less independent. The correlation of  $\delta^{18}\text{O}$  to Sr/Ca ( $r^2 = 0.70$ ) is strong, as expected from both proxies' dependence on SST.

Regressions of monthly  $\delta^{18}\text{O}$  to SST and monthly Sr/Ca to  $\delta^{18}\text{O}$  are regularly reported in the literature. Reported  $\delta^{18}\text{O}$  to SST slopes range from -0.101 to -0.179 ‰/°C [Bagnato *et al.*, 2004; Cardinal *et al.*, 2001; deVilliers *et al.*, 1995; Dunbar *et al.*, 1994; Gagan *et al.*, 1998; Guilderson *et al.*, 1994; McCulloch *et al.*, 1994; Smith *et al.*, 2006; Watanabe *et al.*, 2003]. The slope of -0.105 ‰/°C found in this study is at the low end of reported results. Reported Sr/Ca to  $\delta^{18}\text{O}$  slopes range from 0.27 to 0.30 mmol/mol/‰ (with one reported value of 0.18 [Cardinal *et al.*, 2001] from a coral growing less than 3 mm/year) [Beck *et al.*, 1992; Cardinal *et al.*, 2001; McCulloch *et al.*, 1994; Smith *et al.*, 2006], equivalent to our slope of 0.28 mmol/mol/‰.

Kinetic disequilibrium models indicate that slow growing corals should more closely approach thermodynamic equilibrium than faster growing corals [McConnaughey, 1989a; McConnaughey, 1989b]. While slow growing corals will exhibit enrichment in  $^{16}\text{O}$  relative to other marine organisms, fewer growth (kinetic) effects during calcification are expected to impact the  $\delta^{18}\text{O}$  of these slow-growing coral species. This should include effects found within and between colonies [deVilliers *et al.*, 1995; Guilderson and Schrag, 1999; Linsley *et al.*, 1999; McConnaughey, 1989b; McConnaughey, 2003]. However, in

addition to kinetic effects, the  $\delta^{18}\text{O}$  of slow-growing corals will be further complicated by growth structure and smoothing during bulk sampling [Cohen *et al.*, 2004; Goodkin *et al.*, 2005; Swart *et al.*, 2002]. Therefore, when examining oxygen isotopes to investigate salinity, consideration of inter-annual changes (rather than monthly changes) is critical.

*Mean-Annual Relationship:* The relationship between  $\delta^{18}\text{O}$ , SST, and SSS is analyzed over the same time period as Sr/Ca, from 1976-1997 with the exclusion of years missing instrumental data. First,  $\delta^{18}\text{O}$  of the water ( $\delta\text{O}_w$ ) was calculated using Hydrostation S SSS instrumental data and the following thermocline equilibrium equation [Schmidt, 1999]:

$$\delta\text{O}_w = 0.49 * (\text{SSS}) - 17 \quad \text{eqn. (4)}$$

A limited set of measurements of  $\delta\text{O}_w$  (‰) and salinity (psu) from the Bermuda Atlantic Time Series (BATS) and from Surf Bay Beach, Bermuda indicate this to be a sound assumption (Appendix F).

Mean-annual  $\delta\text{O}_c$  has the expected negative relationship to SST and positive correlation to  $\delta\text{O}_w$  (SSS) (Fig. 4.9a,b). Therefore, we began by using a multivariate model in which  $\delta\text{O}_c$  (‰) was linearly regressed against SST (°C) and  $\delta\text{O}_w$  (‰):

$$\delta\text{O}_c = -0.138 (\pm 0.250) * \text{SST} + 0.990 (\pm 1.35) * \delta\text{O}_w - 1.26 (\pm 5.47)$$

$$(2\sigma, 95\% \text{ conf.}, r^2 = 0.17, F_{\text{sig}} = 0.3092, \text{rmsr of } \delta\text{O}_w = 0.098 \text{ ‰},$$

$$\text{se on } \delta\text{O}_c = 0.108 \text{ ‰}) \quad \text{eqn. (5)}$$

Statistically this regression is insignificant ( $F_{\text{sig}} > 0.01$ ). In examining Fig. 4.9, we can see the impacts of using this regression to reconstruct salinity. Equation 5 does not sufficiently describe the  $\delta\text{O}_c$ , underestimating the range seen during the calibration period,



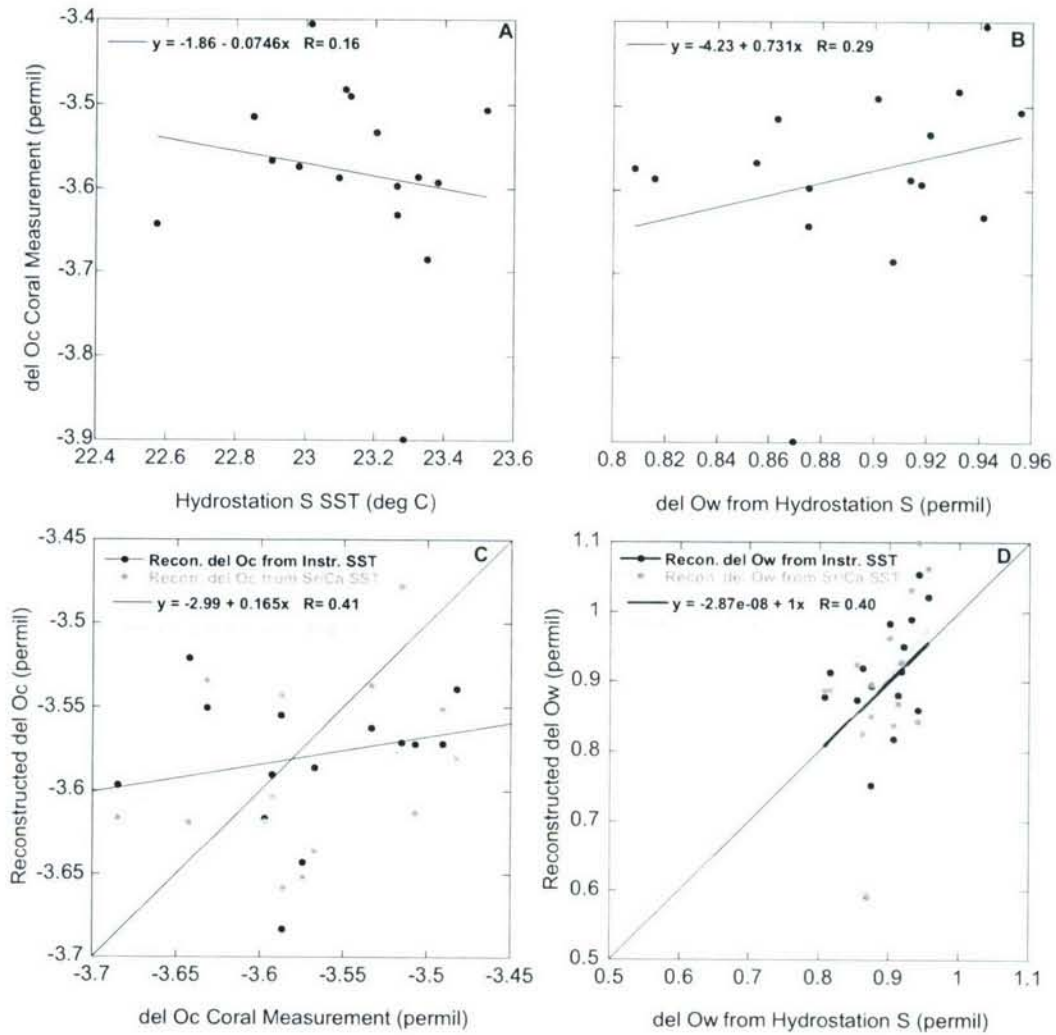


**Figure 4.9:** Results of a multivariate regression of mean-annual  $\delta O_c$  versus SST and  $\delta O_w$ . a) Coral measured  $\delta O_c$  versus Hydrostation S SST. b) Coral measured  $\delta O_c$  versus Hydrostation S  $\delta O_w$  (SSS). c) Reconstructed  $\delta O_c$  using eqn. 5 and both Hydrostation S SST (solid) and coral Sr/Ca reconstructed SST (shaded) versus measured  $\delta O_c$ . d) Reconstructed  $\delta O_w$  using eqn. 5 and both Hydrostation S SST (solid) and coral Sr/Ca reconstructed SST (shaded) versus measured  $\delta O_w$ .

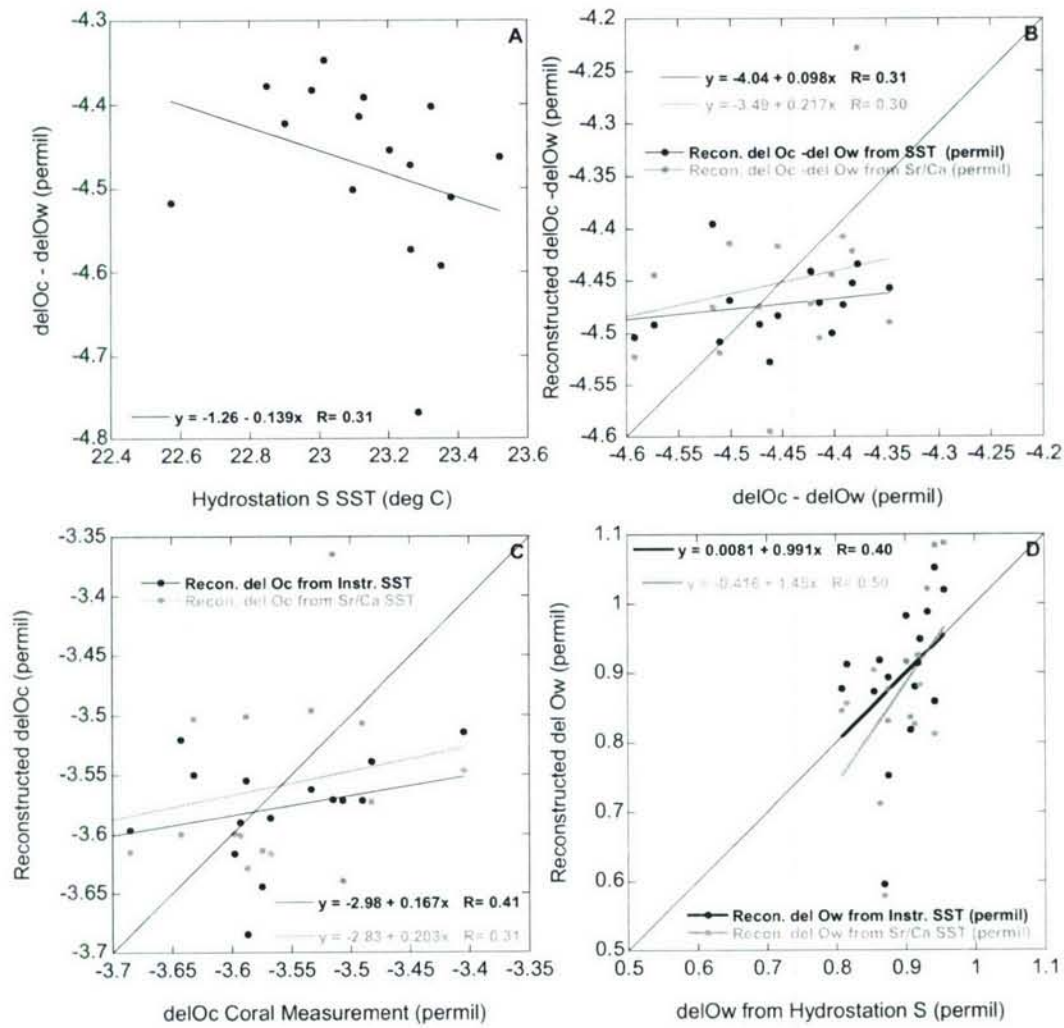


**Figure 4.10:** Results of a single variate regression of mean-annual  $\delta O_c - \delta O_w$  versus SST. a) Coral measured  $\delta O_c - \delta O_w$  versus Hydrostation S SST. b) Reconstructed  $\delta O_c - \delta O_w$  using eqn. 6 and both Hydrostation S SST (solid) and coral Sr/Ca reconstructed SST (shaded) versus measured  $\delta O_c$ . c) Reconstructed  $\delta O_c$  using eqn. 6 and both Hydrostation S SST (solid) and coral Sr/Ca reconstructed SST (shaded) versus measured  $\delta O_c$ . d) Reconstructed  $\delta O_w$  using eqn. 6 and both Hydrostation S SST (solid) and coral Sr/Ca reconstructed SST (shaded) versus measured  $\delta O_w$ .

when either Hydrostation S or Sr/Ca-based SST is used with Hydrostation S  $\delta O_w$  (Fig. 4.9c).  $\delta O_w$  is also calculated by inverting equation 5 and using both Hydrostation S and Sr/Ca-based SST with the measured  $\delta O_c$ . The model dictates that reconstructed  $\delta O_w$  over the calibration period will have a 1:1 relationship with the instrumental based  $\delta O_w$  (Fig. 4.9d). However, the range of reconstructed  $\delta O_w$  (0.6 – 1.1 ‰) overestimates the range seen at Hydrostation S (0.8 – 1.1‰) by a factor of 3 and the RMSR error of the reconstructed  $\delta O_w$  is very large.

Therefore, we developed a second model. In this model, instead of regressing  $\delta O_c$  vs both SST and  $\delta O_w$ , we subtracted  $\delta O_w$  (‰) from  $\delta O_c$  (‰) and linearly regressed the difference against SST (°C). Linear regression of  $\delta O_c - \delta O_w$  versus SST returns the following result:

$$\delta O_c - \delta O_w = -0.139 (\pm 0.226) * (SST) - 1.26 (\pm 5.22)$$

$$(2\sigma, 95\% \text{ conf.}, r^2 = 0.10, F_{\text{sig}} = 0.2378, \text{rmsr of } \delta O_w = 0.10\text{‰},$$

$$\text{se on } \delta O_c - \delta O_w = 0.104\text{‰}) \quad \text{eqn. (6)}$$

At a 95% confidence interval, this equation is also insignificant, and has a larger rmsr of  $\delta O_w$  than does eqn. 5. One potential problem with this method is that we are differing two large values ( $\delta O_c$  and  $\delta O_w$ ) to calculate a small residual, and if the errors in  $\delta O_c$  and  $\delta O_w$  are large, then we have little constraint on the resulting difference.

Figure 4.10 shows that switching to a single variant regression of  $\delta O_c - \delta O_w$  vs. SST does not improve the relationship. As shown in Fig. 4.10d,  $\delta O_w$  variability is still overestimated and error in reconstructed  $\delta O_w$  remains large. It is important to mention that the inclusion of growth rate in either of these regressions (eqns. 5 or 6) does not



improve the significance. In addition, the added growth rate term is never statistically significant ( $p$  is never  $<0.1$ ). This result implies that either growth rate has a much smaller impact on  $\delta^{18}\text{O}$  relative to SST and SSS than it does on Sr/Ca relative to SST or that the added noise of the  $\delta^{18}\text{O}_c$  coral record from salinity or vital effects cannot be fully described by growth.

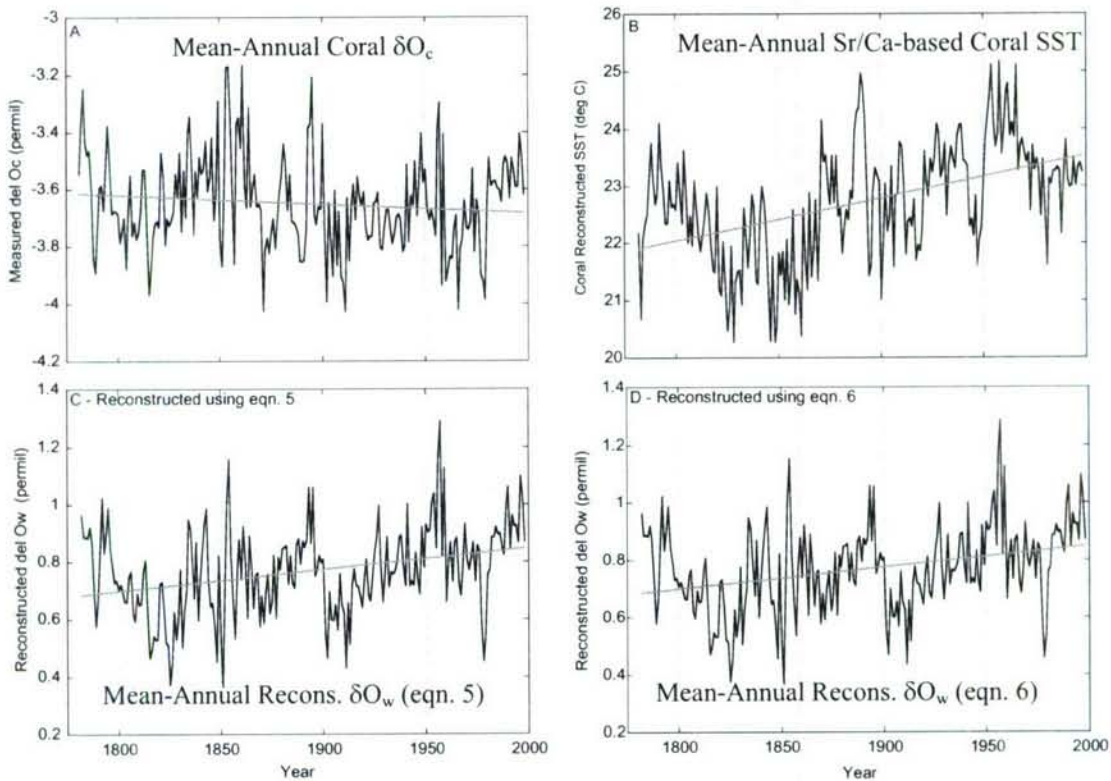


**Figure 4.11:** Two hundred year records of mean-annual data or derived records of a) Coral measured  $\delta\text{O}_c$ , b) Coral-based Sr/Ca reconstructed SST, c) Reconstructed  $\delta\text{O}_w$  using eqn. 5 and coral-based Sr/Ca reconstructed SST, d) Reconstructed  $\delta\text{O}_w$  using eqn. 6 and coral-based Sr/Ca reconstructed SST. Linear trends with time are shown by shaded lines.

As previously described, mean annual  $\delta O_c$  shows a flat or slightly decreasing trend ( $-0.0003 \text{ ‰/year}$ ) from 1782-1998, and coral Sr/Ca-based reconstructed SST shows an increasing trend (Fig. 4.11). Because the  $\delta O_c$  does not show a strong trend opposing the SST trend, the two records imply that historical mean-annual SSS ( $\delta O_w$ ) should be fresher than today. Both equations 5 and 6, which return very similar results, applied to the 218 year record of  $\delta O_c$  using coral SST estimates demonstrate a trend of increasing SSS ( $\delta O_w$ ) from the late 1700s to today. However, due to the lack of significance in either regression model, we are unable to robustly transform the results into a quantitative salinity change over this period.

*Winter Relationship:* The relationship between winter-time (Dec.-March)  $\delta^{18}O$ , SST and SSS is evaluated over the same calibration time period as mean-annual  $\delta^{18}O$  (1976-1997). Winter trace element ratios have shown no growth impacts, and therefore, are expected to have less vital and or sampling effects than the mean-annual reconstruction. The same two models are used as for the mean-annual calibrations. Beginning by describing  $\delta O_c$  (‰) as a function of both SST ( $^{\circ}C$ ) (Fig. 4.12a) and  $\delta O_w$  (Fig. 4.12b). The multi-variant regression returns the following result:

$$\delta O_c = -0.117 (\pm 0.100) * (SST) + 1.48 (\pm 1.42) * (\delta O_w) - 2.28 (\pm 2.26)$$

$$(2\sigma, 95\% \text{ conf.}, r^2 = 0.34, F_{\text{sig}} = 0.0299, \text{rmsr of } \delta O_w = 0.08\text{‰},$$

$$\text{se} = 0.125 \text{ ‰})$$

eqn. (7)

The winter-time results for the multi-variant regression are comparable to the mean-annual results. The relationship described by eqn. 7 is statistically significant.  $\delta O_c$ , calculated with Hydrostation S  $\delta O_w$  and either Hydrostation S and Sr/Ca-based reconstructed SST with Hydrostation S both underestimate variability relative to the  $\delta O_c$  of the coral (Fig. 4.12c). Reconstructed  $\delta O_w$  both with SST records and the coral  $\delta O_c$  show the expected (or close to expected) ratio of 1:1 relative to the Hydrostation S  $\delta O_w$ . However, the  $\delta O_w$  reconstructed range of 0.7-1.1 ‰ is close to three times the instrumental range of 0.8-1.0 ‰ (Fig. 4.12d) and size of the error is substantial relative to the signal. The winter-time multi-variant regression fails to describe the  $\delta O_c$ -SST- $\delta O_w$  relationship.

We also investigated the single variant model in which  $\delta O_c - \delta O_w$  is regressed against SST. A linear regression of  $\delta O_c - \delta O_w$  (‰) versus winter-time SST (°C) returns the following results (Fig. 4.13):

$$\delta O_c - \delta O_w = -0.112 (\pm 0.097) * (SST) - 1.93 (\pm 1.98)$$

$$(2\sigma, 95\% \text{ conf.}, r^2 = 0.23, F_{\text{sig}} = 0.0331, \text{rmsr of } \delta O_w = 0.12 \text{ ‰},$$

$$\text{se of } \delta O_c = 0.123 \text{ ‰}) \quad \text{eqn. (8)}$$

At a 95% confidence interval, this equation is significant, with a large amount of noise amongst the data (Fig. 4.13a). Using either the instrumental or Sr/Ca-based reconstructed SST, the  $\delta O_w$  is still not accurately reconstructed with a range of 0.6-1.2 ‰ compared to the Hydrostation S  $\delta O_w$  range of 0.8-1.0 ‰ (Fig. 4.13d). All of the  $\delta O_c$  regressions serve to underestimate variability in  $\delta O_c$  and overestimate variability in  $\delta O_w$ .



Ideally, we could examine these data over average periods as was done with the winter Sr/Ca to reduce the influence of noise. However, due to limited salinity data this will reduce the number of points in the regression, diminishing statistical evaluations.

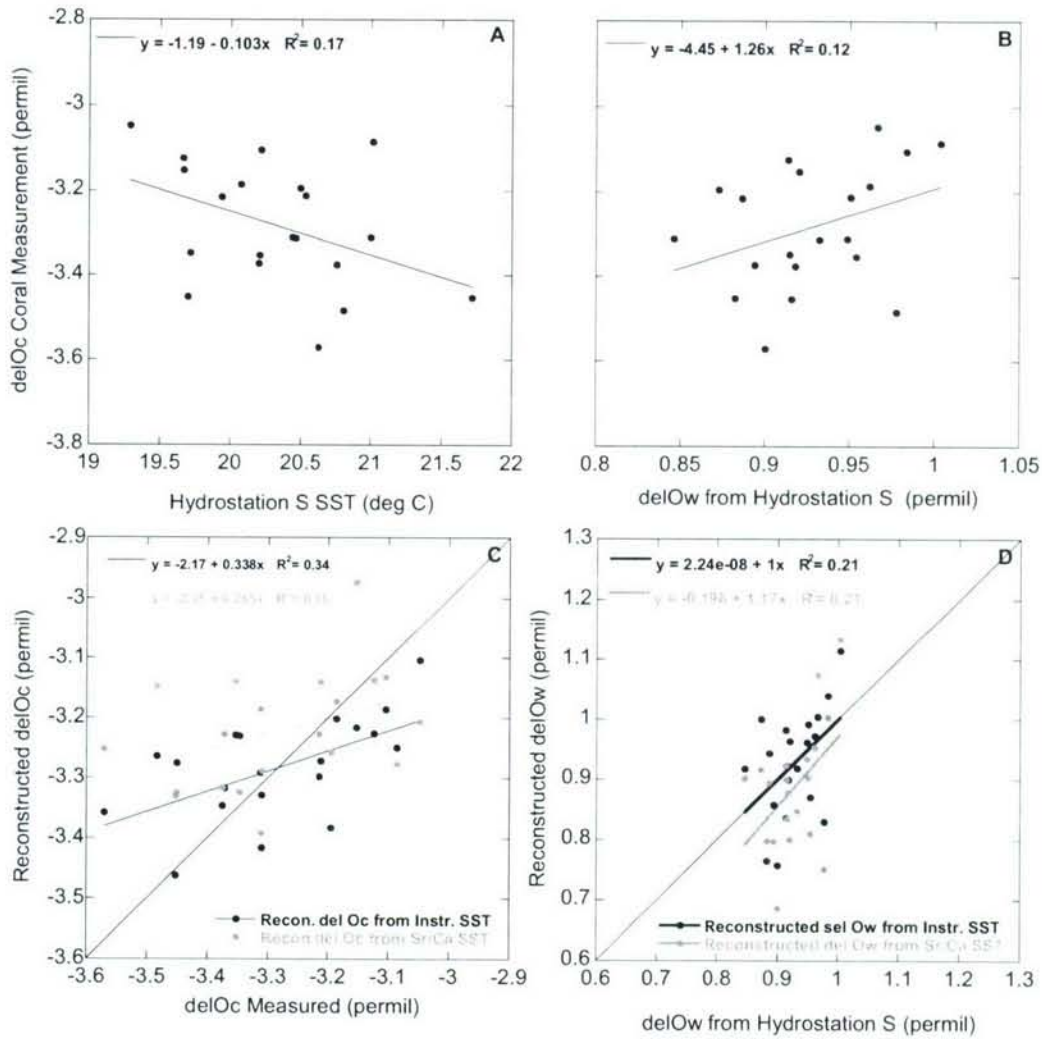


**Figure 4.12:** Results of a multivariate regression of winter-time  $\delta O_c$  versus SST and  $\delta O_w$ . a) Coral measured  $\delta O_c$  versus Hydrostation S SST. b) Coral measured  $\delta O_c$  versus Hydrostation S  $\delta O_w$ . c) Reconstructed  $\delta O_c$  using eqn. 7 and both Hydrostation S SST (solid) and coral Sr/Ca reconstructed SST (shaded) versus measured  $\delta O_c$ . d) Reconstructed  $\delta O_w$  using eqn. 7 and both Hydrostation S SST (solid) and coral Sr/Ca reconstructed SST (shaded) versus measured  $\delta O_w$ .

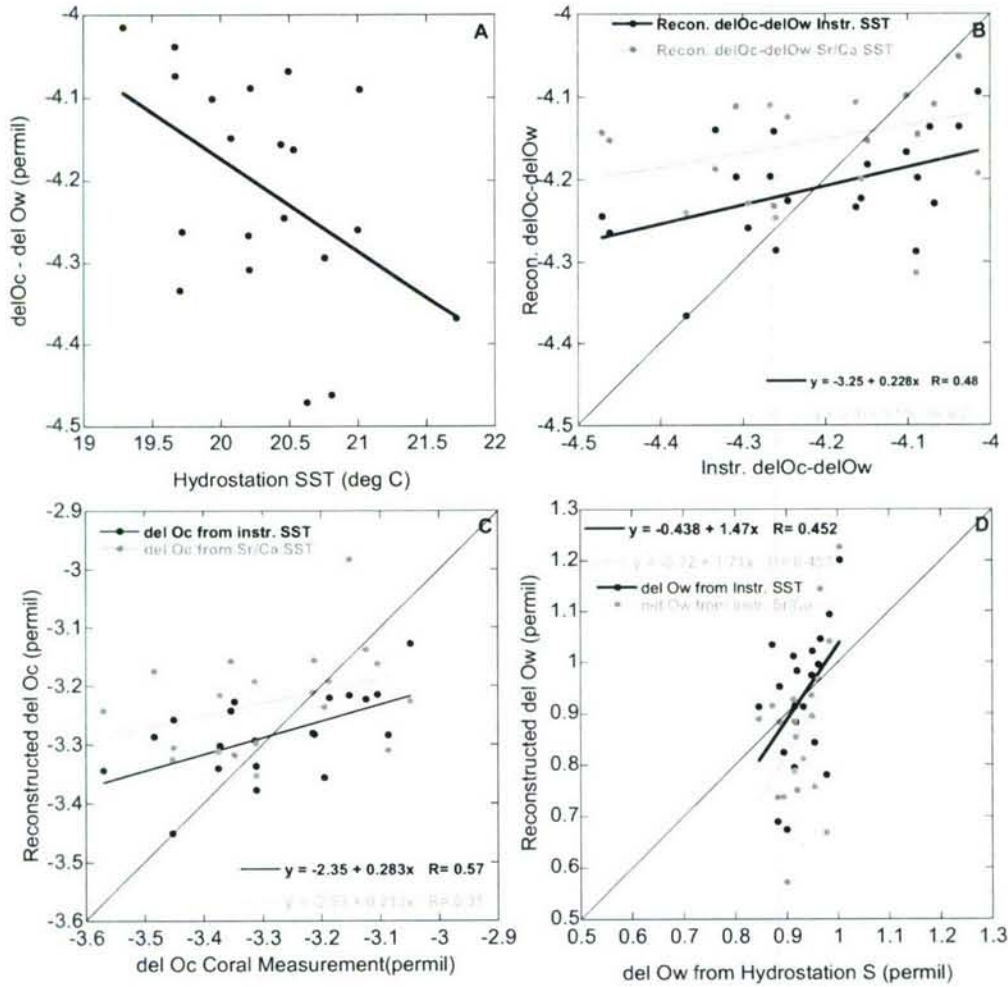


**Figure 4.13:** Results of a single variant regression of winter-time  $\delta O_c - \delta O_w$  versus SST. a) Coral measured  $\delta O_c - \delta O_w$  versus Hydrostation S SST. b) Reconstructed  $\delta O_c - \delta O_w$  using eqn. 8 and both Hydrostation S SST (solid) and coral Sr/Ca reconstructed SST (shaded) versus measured  $\delta O_c$ . c) Reconstructed  $\delta O_c$  using eqn. 8 and both Hydrostation S SST (solid) and coral Sr/Ca reconstructed SST (shaded) versus measured  $\delta O_c$ . d) Reconstructed  $\delta O_w$  using eqn. 8 and both Hydrostation S SST (solid) and coral Sr/Ca reconstructed SST (shaded) versus measured  $\delta O_w$ .

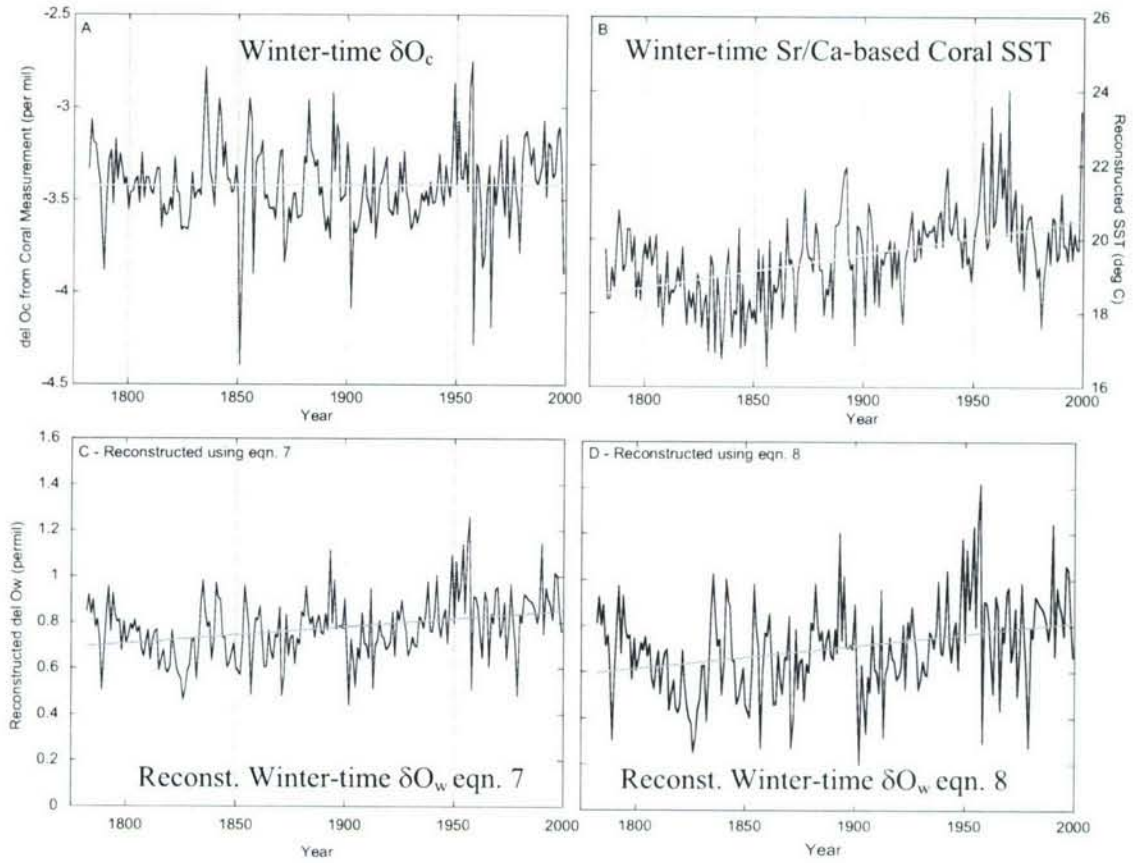


**Figure 4.14:** Two hundred year records of winter-time data or derived records of a) Coral measured  $\delta O_c$ , b) Coral-based Sr/Ca reconstructed SST, c) Reconstructed  $\delta O_w$  using eqn. 7 and coral-based Sr/Ca reconstructed SST, d) Reconstructed  $\delta O_w$  using eqn. 8 and coral-based Sr/Ca reconstructed SST. Linear trends with time are shown by shaded lines.

The winter-time 218 year long record shows strong qualitative results in agreement with mean-annual record.  $\delta O_c$  shows a slightly increasing or no trend through time (Fig. 4.14a) which combined with an increasing trend in the Sr/Ca-based reconstructed SST implies an increasing salinity ( $\delta O_w$ ) from the late 1700s until today. Both models overestimate variability in  $\delta O_w$ , and therefore, cannot be used as a



quantitative tool for reconstructing SSS. However, both models do return the expected result of increasing salinity, confirming the first order interpretation of the data.

## 4.4 Discussion

### 4.4.1 Climate and Ocean Trends at Bermuda

The Bermuda coral record shows temperature at the end of the LIA to be 1.6 °C cooler than the end of the twentieth century instrumental record. Simultaneous to the LIA cooling and 1950s-1960s warming,  $\delta^{18}\text{O}_c$  suggests fresher and saltier water, respectively (Fig. 4.7).

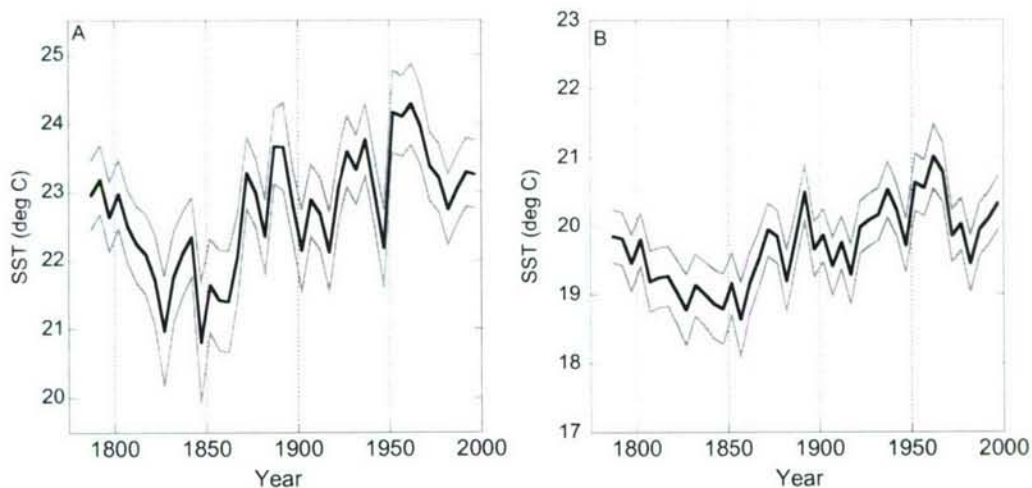


**Figure 4.15:** A) Coral based reconstructed mean-annual SST. B) Coral based reconstructed winter-time SST. Both reconstructions shown in five year averages (solid) with propagated error (shaded).

Temperature trends at Bermuda from this study are in good agreement with trends from other Bermuda coral records. Draschba et al. (2000) show maximum coral  $\delta^{18}\text{O}$  of  $\sim 3.2$  ‰ (minimum temperature) from 1840-1845 and around  $\sim 1855$  and minimum  $\delta^{18}\text{O}$

of  $\sim 3.7$  ‰ (maximum temperature) at  $\sim 1870$  [Draschba *et al.*, 2000], in agreement with trends and mean-annual  $\delta^{18}\text{O}$  values seen in this study (Fig. 4.7). A foraminifera  $\delta^{18}\text{O}$  Bermuda temperature reconstruction shows a temperature increase of  $1.5$  °C from the LIA to today [Keigwin, 1996], in agreement with the statistically significant change ( $1.6$  °C) found here for both the mean-annual and winter-time SST reconstructions (Fig. 4.15).

The temperature and salinity trends are similar to trends found from sclerosponges collected off the Bahamas (140m depth) that show both increasing temperature ( $1.6 - 2.0$  °C) and salinity ( $\sim 1$  psu) from 1890-1990 [Rosenheim *et al.*, 2005]. Another study from the Bahamas using foraminifera to reconstruct salinity records from the eastern side of the Florida current generally show increasing salinity since the LIA [Lund and Curry, 2006].

Several records of SST from proxy reconstructions exist from a variety of locations across the Atlantic. Two coral records near Puerto Rico show temperature changed in the Caribbean Sea between  $2$  to  $3$  °C from the LIA to present day [Watanabe *et al.*, 2001; Winter *et al.*, 2000]. A foraminifera based reconstruction in the eastern sub-tropical Atlantic shows larger SST changes (on the order of  $3-4$  °C) from the LIA to present [deMenocal *et al.*, 2000]. Surface temperature proxy reconstructions based on arctic ice cores show a temperature minimum around 1850 with a rapid increase of  $\sim 1$  °C immediately following the minimum [Dahl-Jensen *et al.*, 1998]. Combined, all of these single location records show that the sub-tropical gyre in the mid-latitudes experienced a large temperature increase between the end of the LIA and today.

Regional surface temperature records from the Northern Hemisphere [Jones *et al.*, 1998] and Arctic [Overpeck *et al.*, 1997], all smoothed over 30-years using a running

mean, show a lower magnitude of total temperature change from the temperature minimum in the 1850s to today ( $\sim 1^\circ\text{C}$ ) compared to the coral record ( $1.5^\circ\text{C}$ ) (Fig. 4.16). However, these records and the coral record all show very similar patterns of increasing temperature with time from the LIA to present. Correlation coefficients between the Sr/Ca-derived mean-annual SST record and the Arctic and Northern Hemisphere records are 0.40 and 0.47 respectively for the mean-annual records. Each of the records achieves minimum temperatures at the end of the LIA (between 1800 and 1850), followed by warming to maximum averaged temperatures in the 1950s and 60s. Two cool periods are seen in the early 1800s in all records, with an offset of  $\sim 10$  years in timing between the coral record and the atmospheric records. We believe this is possibly related to a combination of age model error in the coral record and a delayed ocean response to atmospheric cooling. The offset may provide an upper limit of 10-15 years on the error of the age model. A pronounced drop in temperature in the 1970s following the peak warmth (1960) is apparent, primarily in the Bermuda and Arctic records (Fig. 4.16).

Smoothing the records with a 30-year box filter reveals strong coherence in the timing of temperature changes of the past 200 years among all of the proxy records (Fig. 4.16). One large discrepancy between the records occurs between 1870 and 1900, when the Bermuda record shows warming not seen in the other records. The agreement between the smoothed regional records and coral reconstruction is highly significant, with correlation coefficients of 0.86 between the coral record and each regional synthesis.



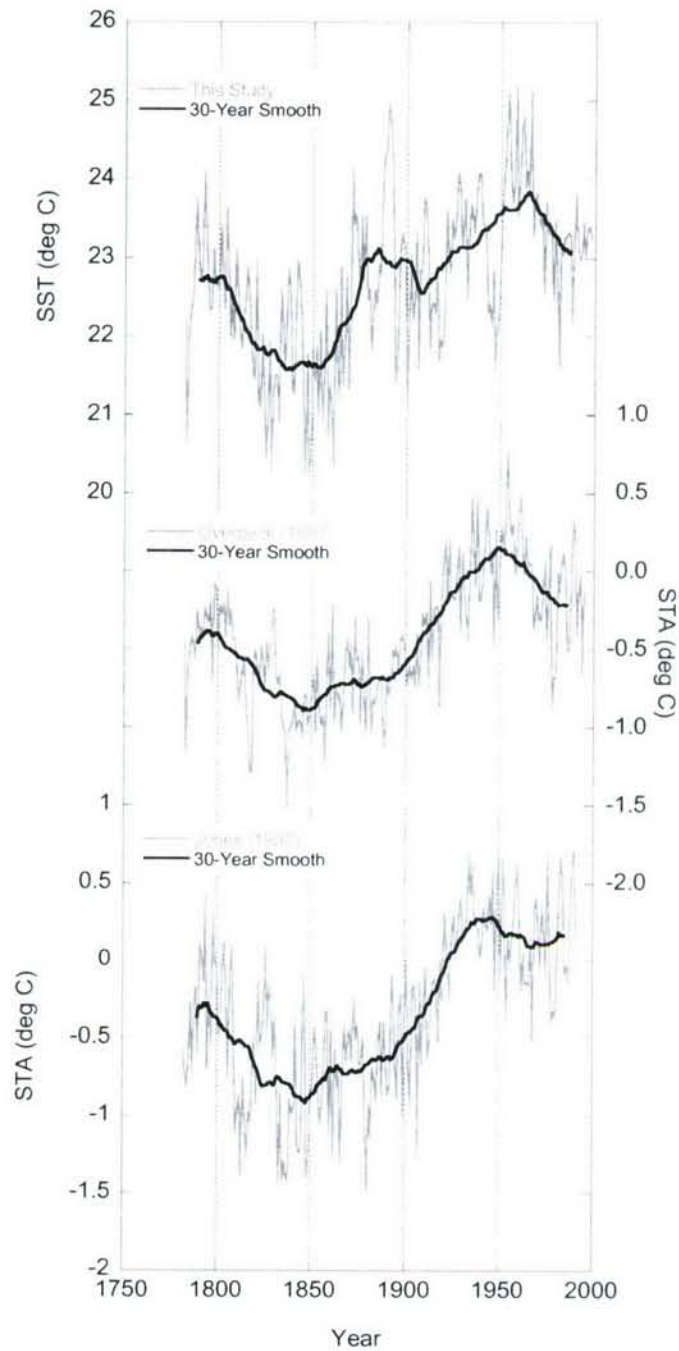


**Figure 4.16.** Mean-annual reconstructed SST from coral Sr/Ca, Arctic land reconstructed record (Overpeck et al., 1997) and Northern Hemisphere land reconstructed record (Jones et al., 1998) (all shaded) and then filtered over 30 years (solid). Coral reconstruction (top) compared to Overpeck et al. (1997) (middle,  $r = 0.40$ ) and to Jones et al. (1998) (bottom,  $r = 0.47$ ). The structure of the coral reconstruction as defined by the 30-year running average agrees with Overpeck (1997) ( $r = 0.86$ ) and Jones (1998) ( $r = 0.86$ ) after the low-pass filter, despite a difference in the magnitude of the temperature change (2.5 °C vs. 1.5 °C).

While all of the records (regional and local) show cooling in the mid-1800s consistent with a northern hemisphere response mostly due to radiative forcing, the range of temperature changes suggest differing local responses that may be due to process such as changing ocean circulation and the North Atlantic Oscillation (NAO).

#### **4.4.2 Influences on Observed Variability**

Temperature and salinity changes at Bermuda are likely due to a combination of atmospheric forcing and ocean circulation changes. The largest events over the past 200 years are the end of LIA cooling and 20<sup>th</sup> century warming, coupled with changes in salinity interpreted from the  $\delta O_c$ . Several possible influences may have contributed to these changes, including anthropogenic, solar and volcanic forcing. Changes in the strength of the Gulf Stream and the relative influence of tropical, sub-polar, and subtropical gyre waters may also be a factor [Lund *et al.*, 2006; Talley, 1996]. Additionally, the NAO has been hypothesized to have large influences on the climate of the North Atlantic Basin from the time of the LIA to the modern day [Luterbacher *et al.*, 1999], and may contribute to the differences in reconstructed temperature patterns seen throughout the Atlantic (see also Chapter 5). Local changes in ocean vertical mixing rates may also be a critical factor affecting SST at Bermuda [Druffel, 1997].

With respect to records of atmospheric and ocean forcing, multiple mechanisms appear to have a potential influence on temperature at Bermuda. Coral reconstructed SST is positively correlated to a global proxy reconstruction of solar activity [Lean *et al.*, 1995] ( $r = 0.34$ ) (Fig. 4.17). Cross-spectral analysis performed using a multi-taper method with 10 windows [Huybers, 2003] shows significant correlation at sub-decadal and multi-

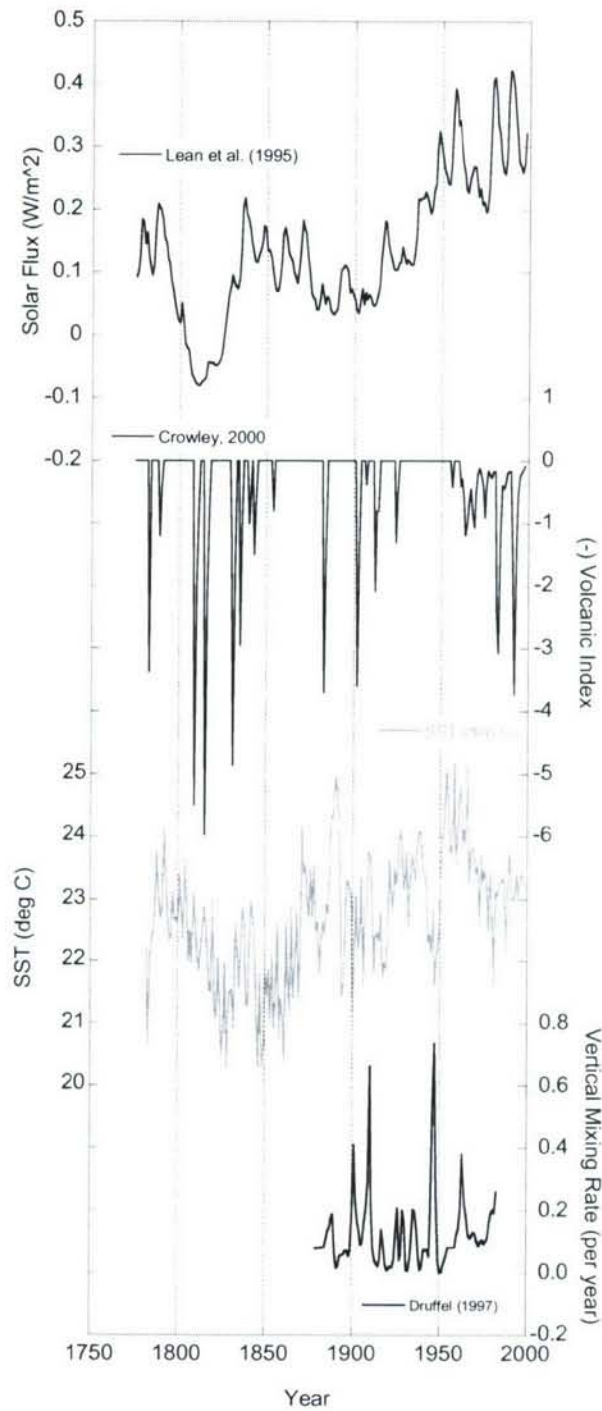


**Figure 4.17:** Records of potential forcing influences on temperature. Annual solar flux (W/m<sup>2</sup>) proxy [*Lean et al.*, 1995] (top), annual volcanic index (x(-1)) [*Crowley*, 2000] (second), mean-annual reconstructed SST (this record) (°C) (third), and mean-annual reconstructed vertical mixing rates (per year) at Bermuda [*Druffel*, 1997].



decadal frequencies (2.5 years per cycle,  $r = 0.55$  and  $>20$  years per cycle,  $r > 0.45$  respectively). At high frequencies the two records are in phase with one another, whereas at low frequencies, reconstructed SST lags estimated solar forcing. The lag at low frequencies is likely a combination of the heat capacity of water, ocean mixing and circulation, which could serve to dampen the oceanic response to atmospheric forcing, as well as potential bias in the coral age model.

A sharp decline in estimated solar forcing which begins in the 1790s and continues until the 1830s, coincides with the beginning of late LIA cooling seen in the coral record. However, the lowest SST temperatures are seen after the decline in solar flux has begun to return to pre-1790 values. Estimated solar activity and SST both reach maximum values in the late 1950s, although solar activity shows two more maxima in the 1980s-1990s, and SSTs do not reach maximum values during these periods [Crowley, 2000] (Fig. 4.17).

Volcanic activity is believed to cause decreased surface temperatures for 2-4 years post eruption depending on size and location, due to ash and  $\text{SO}_2$  in the atmosphere blocking solar activity from reaching earth (e.g. [Wigley *et al.*, 2005]). Minimum temperatures at Bermuda are seen during and following times of increased volcanic activity (Fig. 4.17). At the end of the 20<sup>th</sup> century, anomalously cool temperatures occur at a time of increased anthropogenic forcing and increased estimated solar activity, when relatively warmer temperatures would be expected. During this time an extended period of high to moderate volcanic activity is observed and may have contributed to decreased temperatures at this time [Crowley, 2000]. An increased volcanic index value [Crowley, 2000] also precedes sharp inter-annual temperature changes and occurs during extended

decadal cooling at the end of the LIA from 1820 to 1860. The lack of exact synchronicity of these periods may be due to errors in the age model, which would lead to the actual temperature drops occurring earlier in time and in closer proximity to the volcanic events. Atmospheric forcing in the form of solar flux and volcanic activity is impacting the ocean at this site. Strong correlations are seen between solar, volcanic and atmospheric temperature records and the Bermuda SST record, indicating an atmospheric influence on this location.

There is also evidence that increased vertical mixing rates at this location may contribute to ocean temperature trends (Fig. 4.17). Increased mixing will serve to entrain deeper, colder water at the surface [Druffel, 1997] and is reconstructed using  $\Delta^{14}\text{C}$  in corals. A high frequency correlation is seen between periods of extended increased vertical mixing and similarly long periods of decreased temperatures (Fig. 4.17), including the 1940s and late 20<sup>th</sup> century. However, corresponding changes in salinity and SST implied by the  $\delta\text{O}_c$  variability suggest that large-scale circulation changes are occurring as well, even if these are also atmospherically driven. At Bermuda, this could be caused by shifting positions in the Gulf Stream or by variable strength in sub-tropical gyre circulation [Talley, 1996; Worthington, 1976].

The NAO may be another influence on sea water property variability [Cayan, 1992; Dickson *et al.*, 1996; Reverdin *et al.*, 1996; Talley, 1996] (see Chapt. 5). During the end of the LIA from 1830 to 1860, the NAO has been shown to be in an extended positive phase (large difference between the pressure centers at Iceland and the Açores) [Luterbacher *et al.*, 1999], which at low frequencies causes decreased temperatures at this location [Visbeck *et al.*, 2003]. Winter-time SST remains relatively low throughout

this period but mean-annual SST shows larger variability. Filtering the Luterbacher et al. (1999) NAO record with a five year box window shows a period of extended weak, positive NAO from the mid-1840s to ~1880, coincident with the second extended cooling of the 1800s. This positive phase NAO may also help to explain the varying temperature changes seen across the Atlantic basin. The NAO SST anomaly pattern [Visbeck et al., 2001] dictates positive inter-annual temperature anomalies at Bermuda and the western Caribbean and negative anomalies off the coast of Africa during a positive NAO, consistent with the relatively lower temperature anomalies seen off the coast of Africa at this time.

## 4.5 Conclusions

Quantitative calibration of coral skeletal Sr/Ca to SST from the south shore of Bermuda resulted in long reconstruction of the variability in mean-annual and winter SST for the past two centuries. The records of SST document the end of the LIA event (~1850) with a drop in temperature on the order of ~1.5 °C compared to today. The mean-annual and winter-time SST records combined with  $\delta O_e$  imply generally increasing salinity from the end of the LIA to today. Radiative and atmospheric changes explain some of the SST variability, but implied changes in SST and SSS, not explained by atmospheric forcing, indicate circulation impacts as well. The circulation changes may be related to long-term variability in winds and shifts in the NAO.



## 4.6 References

- Alibert, C., and M. T. McCulloch, Strontium/calcium ratios in modern Porites corals from the Great Barrier Reef as a proxy for sea surface temperature: Calibration of the thermometer and monitoring of ENSO, *Paleoceanography*, 12, 345-363, 1997.
- Bagnato, S., B. K. Linsley, S. S. Howe, G. M. Wellington, and J. Salinger, Evaluating the use of the massive coral *Diploastrea heliopora* for paleoclimate reconstruction, *Paleoceanography*, 19, 2004.
- Beck, J. W., R. L. Edwards, E. Ito, F. W. Taylor, J. Recy, F. Rougerie, P. Joannot, and C. Henin, Sea-Surface Temperature from Coral Skeletal Strontium Calcium Ratios, *Science*, 257, 644-647, 1992.
- Beck, J. W., J. Recy, F. Taylor, R. L. Edwards, and G. Cabioch, Abrupt changes in early Holocene tropical sea surface temperature derived from coral records, *Nature*, 385, 705-707, 1997.
- Bevington, P. R., Chapter 4: Propagation of Error. in *Data Reduction and Error Analysis for the Physical Sciences*, pp. 56-65, McGraw Hill, United States of America, 1969.
- Bond, G., B. Kromer, J. Beer, R. Muscheler, M. N. Evans, W. Showers, S. Hoffman, R. Lottibond, I. Hajdas, and G. Bonani, Persistent Solar Influence on North Atlantic Climate During the Holocene, *Science*, 294, 2130-2136, 2001.
- Bond, G., W. Showers, M. Cheseby, R. Lotti, P. Almasi, P. deMenocal, P. Priore, H. M. Cullen, I. Hajdas, and G. Bonani, A Pervasive Millennial-Scale Cycle in North Atlantic Holocene and Glacial Climates, *Science*, 278, 1257-1266, 1997.
- Bradley, R. S., and P. D. Jones, Little Ice Age summer temperature variations: their nature and relevance to recent global warming trends, *The Holocene*, 3, 367-376, 1993.
- Briffa, K. R., T. J. Osborn, F. H. Schweingruber, I. C. Harris, P. D. Jones, S. G. Shiyatov, and E. A. Vaganov, Low-frequency temperature variations from a northern tree-ring density network, *Journal of Geophysical Research*, 106, 2929-2941, 2001.
- Cardinal, D., B. Hamelin, E. Bard, and J. Patzold, Sr/Ca, U/Ca and delta O-18 records in recent massive corals from Bermuda: relationships with sea surface temperature, *Chemical Geology*, 176, 213-233, 2001.
- Cayan, D., Latent and sensible heat flux anomalies over the northern oceans: the connection to monthly atmospheric circulation, *Journal of Climate*, 5, 355-369, 1992.
- Cohen, A. L., and S. R. Hart, The effect of colony topography on climate signals in coral skeleton, *Geochimica Et Cosmochimica Acta*, 61, 3905-3912, 1997.

- Cohen, A. L., S. R. Smith, M. S. McCartney, and J. van Etten, How brain corals record climate: an integration of skeletal structure, growth and chemistry of *Diploria labyrinthiformis* from Bermuda, *Marine Ecology-Progress Series*, 271, 147-158, 2004.
- Crowley, T. J., Causes of Climate Change Over the Past 1000 Years, *Science*, 289, 270-277, 2000.
- Curry, R., R. Dickson, and I. Yashayaev, A change in the freshwater balance of the Atlantic Ocean over the past four decades, *Nature*, 426, 826-829, 2003.
- Dahl-Jensen, D., K. Mosegaard, N. Gunderstrup, G. D. Clow, A. W. Johnsen, A. W. Hansen, and N. Balling, Past Temperature Directly from the Greenland Ice Sheet, *Science*, 282, 268-271, 1998.
- Dansgaard, W., S. J. Johnsen, N. Reeh, N. Gunderstrup, H. B. Clausen, and C. U. Hammer, Climate changes, Norsemen, and modern man, *Nature*, 255, 24-28, 1975.
- deMenocal, P., J. Ortiz, T. Guilderson, and M. Sarnthein, Coherent high- and low-latitude climate variability during the holocene warm period, *Science*, 288, 2198-2202, 2000.
- deVilliers, S., B. K. Nelson, and A. R. Chivas, Biological-Controls on Coral Sr/Ca and Delta-O-18 Reconstructions of Sea-Surface Temperatures, *Science*, 269, 1247-1249, 1995.
- deVilliers, S., G. T. Shen, and B. K. Nelson, The Sr/Ca-Temperature Relationship in Coralline Aragonite - Influence of Variability in (Sr/Ca)Seawater and Skeletal Growth-Parameters, *Geochimica Et Cosmochimica Acta*, 58, 197-208, 1994.
- Dickson, R., J. R. N. Lazier, J. Meincke, P. B. Rhines, and J. Swift, Long-term coordinated changes in the convective activity of the North Atlantic, *Progress in Oceanography*, 38, 241-295, 1996.
- Doney, S. C., A synoptic atmospheric surface forcing data set and physical upper ocean model for the U. S. JGOFS Bermuda Atlantic Time-Series Study site, *Journal of Geophysical Research*, 101, 25615-25634, 1996.
- Draschba, J., J. Patzold, and G. Wefer, North Atlantic Climate Variability Since AD 1350 Recorded in  $\delta^{18}\text{O}$  and Skeletal Density of Bermuda Corals, *International Journal of Earth Sciences*, 88, 733-741, 2000.
- Druffel, E. M., Banded corals: changes in oceanic carbon-14 during the Little Ice Age, *Science*, 218, 13-19, 1982.
- Druffel, E. R. M., Pulses of Rapid Ventilation in the North Atlantic Surface Ocean During the Past Century, *Science*, 275, 1454-1457, 1997.
- Dunbar, R. B., G. M. Wellington, M. W. Colgan, and W. Peter, Eastern pacific sea surface temperature since 1600 AD: the  $\delta^{18}\text{O}$  record of climate variability in Galapagos corals, *Paleoceanography*, 9, 291-315, 1994.



- Esper, J., E. R. Cook, and F. H. Schweingruber, Low-Frequency Signals in Long Tree-Ring Chronologies for Reconstructing Past Temperature Variability, *Science*, 295, 2250-2253, 2002.
- Gagan, M. K., L. K. Ayliffe, D. Hopley, J. A. Cali, G. E. Mortimer, J. Chappell, M. T. McCulloch, and M. J. Head, Temperature and surface-ocean water balance of the mid-Holocene tropical Western Pacific, *Science*, 279, 1014-1018, 1998.
- Glynn, P. W., E. M. Druffel, and R. B. Dunbar, A dead Central American reef tract: possible link with the Little Ice Age, *Journal of Marine Research*, 41, 605-637, 1983.
- Goodkin, N. F., K. Huguen, and A. C. Cohen, Multi-Coral Calibration of Sr/Ca and Growth Rate to Sea Surface Temperature, *Paleoceanography*, in press.
- Goodkin, N. F., K. Huguen, A. C. Cohen, and S. R. Smith, Record of Little Ice Age sea surface temperatures at Bermuda using a growth-dependent calibration of coral Sr/Ca, *Paleoceanography*, 20, PA4016, doi:4010.1029/2005PA001140, 2005.
- Guilderson, T. P., R. G. Fairbanks, and J. L. Rubenstone, Tropical Temperature-Variations since 20,000 Years Ago - Modulating Interhemispheric Climate-Change, *Science*, 263, 663-665, 1994.
- Guilderson, T. P., and D. P. Schrag, Reliability of coral isotope records from the western Pacific warm pool: A comparison using age-optimized records, *Paleoceanography*, 14, 457-464, 1999.
- Hurrell, J. W., Decadal Trends in the North-Atlantic Oscillation - Regional Temperatures and Precipitation, *Science*, 269, 676-679, 1995.
- Huybers, P., Multi-taper method coherence using adaptive weighting and correcting for the bias inherent to coherence estimates. <http://web.mit.edu/~phuybers/www/Mfiles/index.html>, 2003.
- Iijima, H., H. Kayanne, M. Morimoto, and O. Abe, Interannual sea surface salinity changes in the western Pacific from 1954 to 2000 based on coral isotope analysis, *Geophysical Research Letters*, 32, doi:10.1029/2004GL022026, 2005.
- Jacoby, G., and R. D. D'Arrigo, Reconstructed northern hemisphere annual temperature since 1671 based on high-latitude tree-ring data from North America, *Climatic Change*, 14, 39-59, 1989.
- Jones, P. D., K. R. Briffa, T. P. Barnett, and S. F. B. Tett, High-resolution palaeoclimatic records for the last millennium: interpretation, integration and comparison with General Circulation Model control-run temperatures, *Holocene*, 8, 455-471, 1998.



- Jones, P. D., T. Jonsson, and D. Wheeler, Extension to the North Atlantic Oscillation using early instrumental pressure observations from Gibraltar and south-west Iceland, *International Journal of Climatology*, 17, 1433-1450, 1997a.
- Jones, P. D., T. J. Osborn, and K. R. Briffa, Estimating Sampling Errors in Large-Scale Temperature Averages, *Journal of Climate*, 10, 2548-2568, 1997b.
- Jones, P. D., T. J. Osborn, K. R. Briffa, C. K. Folland, E. B. Horton, L. V. Alexander, D. E. Parker, and N. A. Rayner, Adjusting for sampling density in grid-box land and ocean surface temperature time series, *Journal of Geophysical Research*, 102, 835-860, 2001.
- Keigwin, L. D., The Little Ice Age and Medieval warm period in the Sargasso Sea, *Science*, 274, 1504-1508, 1996.
- Keigwin, L. D., and R. S. Pickart, Slope Water Current over the Laurentian Fan on Interannual to Millennial Time Scales, *Science*, 286, 520-523, 1999.
- Kuhnert, H., T. Cruger, and J. Patzold, NAO signature in a Bermuda coral Sr/CA record, *Geochemistry Geophysics Geosystems*, 6, Q04004, doi:04010.01029/02004GC000786, 2005.
- Lean, J., J. Beer, and R. Bradley, Reconstruction of solar irradiance since 1610: implications for climate change, *Geophysical Research Letters*, 22, 3195-3198, 1995.
- Linsley, B. K., R. G. Messier, and R. B. Dunbar, Assessing between-colony oxygen isotope variability in the coral *Porites lobata* at Clipperton Atoll, *Coral Reefs*, 18, 13-27, 1999.
- Lund, D. C., and W. B. Curry, Florida Current surface temperature and salinity variability during the last millennium, *Paleoceanography*, 21, doi:10.1029/2005PA001218, 2006.
- Lund, D. C., J. Lynch-Stieglitz, and W. B. Curry, Gulf Stream density structure and transport during the past millennium, *Nature*, 444, 601-604, 2006.
- Luterbacher, J., C. Schmutz, D. Gyalistras, E. Xoplaki, and H. Wanner, Reconstruction of monthly NAO and EU indices back to AD 1675, *Geophysical Research Letters*, 26, 2745-2748, 1999.
- McConnaughey, T., C-13 and O-18 Isotopic Disequilibrium in Biological Carbonates .1. Patterns, *Geochimica Et Cosmochimica Acta*, 53, 151-162, 1989a.
- McConnaughey, T., C-13 and O-18 Isotopic Disequilibrium in Biological Carbonates .2. Invitro Simulation of Kinetic Isotope Effects, *Geochimica Et Cosmochimica Acta*, 53, 163-171, 1989b.
- McConnaughey, T. A., Sub-equilibrium oxygen-18 and carbon-13 levels in biological carbonates: carbonate and kinetic models, *Coral Reefs*, 22, 316-327, 2003.

- McCulloch, M. T., M. K. Gagan, G. E. Mortimer, A. R. Chivas, and P. J. Isdale, A High-Resolution Sr/Ca and Delta-O-18 Coral Record from the Great-Barrier-Reef, Australia, and the 1982-1983 El-Nino, *Geochimica Et Cosmochimica Acta*, 58, 2747-2754, 1994.
- Ohkouchi, N., T. I. Eglinton, L. D. Keigwin, and J. M. Hayes, Spatial and Temporal Offsets Between Proxy Records in a Sediment Drift, *Science*, 298, 1224-1227, 2002.
- Overpeck, J., K. Hughen, D. Hardy, R. Bradley, R. Case, M. Douglas, B. Finney, K. Gajewski, G. Jacoby, A. Jennings, S. Lamoureux, A. Lasca, G. MacDonald, J. Moore, M. Retelle, S. Smith, A. Wolfe, and G. Zielinski, Arctic environmental change of the last four centuries, *Science*, 278, 1251-1256, 1997.
- Quinn, T. M., and D. E. Sampson, A multiproxy approach to reconstructing sea surface conditions using coral skeleton geochemistry, *Paleoceanography*, 17, 2002.
- Rayner, N. A., D. E. Parker, E. B. Horton, C. K. Folland, L. V. Alexander, D. P. Rowell, W. C. Kent, and A. Kaplan, Global analyses of sea surface temperature, sea ice, and night marine air temperature since the late nineteenth century, *Journal of Geophysical Research*, 108, 4407, 2003.
- Reverdin, G., D. Cayan, and Y. Kushnir, Decadal variability of hydrography in the upper northern North Atlantic 1948-1990, *Journal of geophysical Research - Oceans*, 102, 8505-8531, 1996.
- Rosenheim, B., P. K. Swart, S. Thorrold, A. Eisenhauer, and P. Willenz, Salinity change in the subtropical Atlantic: Secular increase and teleconnections to the North Atlantic Oscillation, *Geophysical Research Letters*, 32, doi:10.1029/2004GL021499, 2005.
- Sachs, J. P., and S. Lehman, Subtropical North Atlantic Temperatures 60,000 to 30,000 Years Ago, *Science*, 286, 756-759, 1999.
- Schmidt, G. A., Global Seawater oxygen-18 database, 1999.
- Schrag, D. P., Rapid analysis of high-precision Sr/Ca ratios in corals and other marine carbonates, *Paleoceanography*, 14, 97-102, 1999.
- Smith, J. M., T. M. Quinn, K. P. Helmle, and R. B. Halley, Reproducibility of geochemical and climatic signals in the Atlantic coral *Montastrea faveolata*, *Paleoceanography*, 21, doi:10.1029/2005PA001187, 2006.
- Smith, S. V., R. W. Buddemeier, R. C. Redalje, and J. E. Houck, Strontium-Calcium Thermometry in Coral Skeletons, *Science*, 204, 404-407, 1979.
- Swart, P. K., H. Elderfield, and M. J. Greaves, A high-resolution calibration of Sr/Ca thermometry using the Caribbean coral *Montastraea annularis*, *Geochemistry Geophysics Geosystems*, 3, 2002.



- Sweeney, E. N. M., D. J.; Buesseler, K. O., Biogeochemical impacts due to mesoscale eddy activity in the Sargasso Sea as measured at the Bermuda Atlantic Time-series Study (BATS), *Deep Sea Research Part II: Topical Studies in Oceanography*, 50, 3017-3039, 2003.
- Talley, L. D., North Atlantic circulation and variability, reviewed for the CNLS conference, *Physica D*, 98, 625-646, 1996.
- Visbeck, M., E. Chassignet, R. Curry, T. Delworth, R. Dickson, and G. Krahmann, The Ocean's Response to North Atlantic Oscillation Variability. in *The North Atlantic Oscillation: Climate Significance and Environmental Impact*, edited by Hurrell, J., Y. Kushnir, G. Ottersen and M. Visbeck, pp. 113-145, American Geophysical Union, Washington, D. C., 2003.
- Visbeck, M. H., J. W. Hurrell, L. Polvani, and H. M. Cullen, The North Atlantic Oscillation: Past, present, and future, *Proceedings of the National Academy of Sciences of the United States of America*, 98, 12876-12877, 2001.
- Watanabe, T., M. K. Gagan, T. Corregge, H. Scott-Gagan, J. Cowley, and W. Hantoro, Oxygen isotope systematics in *Diploastrea heliopora*: New coral archive of tropical paleoclimate, *Geochimica Et Cosmochimica Acta*, 67, 1349-1358, 2003.
- Watanabe, T., A. Winter, and T. Oba, Seasonal changes in sea surface temperature and salinity during the Little Ice Age in the Caribbean Sea deduced from Mg/Ca and  $^{18}\text{O}/^{16}\text{O}$  ratios in corals, *Marine Geology*, 173, 21-35, 2001.
- Wigley, T. M. L., R. A. Ammann, B. D. Santer, and S. C. B. Raper, Effect of climate sensitivity on the response to volcanic forcing, *Journal of Geophysical Research*, 110, doi:10.1029/2004JD005557, 2005.
- Wigley, T. M. L., and P. M. Kelly, Holocene climatic change,  $^{14}\text{C}$  wiggles and variations in solar irradiance, *Philosophical Transactions of the Royal Society of London Series A*, 330, 547-560, 1990.
- Winter, A., H. Ishioroshi, T. Watanabe, T. Oba, and J. Christy, Caribbean sea surface temperatures: two-to-three degrees cooler than the present during the Little Ice Age, *Geophysical Research Letters*, 27, 3365-3368, 2000.
- Worthington, L. V., On the North Atlantic circulation, *Johns Hopkins Oceanographic Studies*, 6, 1976.





## **Chapter 5**

# **North Atlantic Oscillation Reconstructed using Winter Sr/Ca Ratios in Bermuda Brain Coral**

### **Abstract**

The North Atlantic Oscillation (NAO) is an important mode of climate variability impacting atmospheric and North Atlantic ocean circulation. Here we reconstruct a marine based NAO signal using 218 years of annually resolved winter-time Sr/Ca ratios, a proxy of sea surface temperature (SST), from a brain coral collected from the south shore of Bermuda. Observed differences between the marine winter-Sr/Ca NAO record and Northern Hemisphere based, atmospheric proxy records from broad geographical regions imply that both NAO behavior and the NAO-ocean relationship have changed through time. In the ocean record, we see coherent changes in both the amplitude and phase at two frequencies - inter-annual (3-5 years per cycle) and multi-decadal (20-100 years per cycle). Changes in the strength of the multi-decadal NAO signal coincide with changes in a mean-hemispheric proxy based temperature record [Jones *et al.*, 1998]. At multi-decadal frequencies, the Sr/Ca-based NAO record exhibits greater variability and spectral power during late 20<sup>th</sup> century warming (1940-1998) than during the end of the Little Ice Age (LIA, 1800-1850). However, the Sr/Ca-based NAO record shows an extended positive state during the LIA similar to the late 20<sup>th</sup> century instrumental record. This indicates that changes in mean climate may alter the magnitude and type of variability, but not necessarily the phase of the NAO. At low frequencies, NAO variance increases through time coincident to anthropogenic warming but a positive or negative NAO state does not become dominant.

## 5.1. Introduction

The North Atlantic Oscillation (NAO), a meridional oscillation in atmospheric mass, is commonly measured by surface pressure differences between Iceland (65°N, 23°W) and the Açores (38°N, 26°W) and is reported as the NAO Index (NAOI) [Hurrell *et al.*, 2003; Hurrell, 1995]. The NAO is strongest during the boreal winter and identified as the dominant mode of winter pressure variability over the North Atlantic [Hurrell and VanLoon, 1997; Jones *et al.*, 2003]. The NAO is connected to the Arctic Oscillation (AO) [Rogers and McHugh, 2002], and together, these two systems are sometimes referred to as the Northern Hemisphere Annular Mode (NHAM). The NAO directly impacts surface wind speed and direction, leading to changes in surface temperature, evaporation and precipitation. In a positive NAOI, both the low pressure zone over Iceland and the high pressure zone over the Açores are intensified, resulting in increased strength and incidence of winter storms crossing the Atlantic Ocean. These storms are deflected northward by the intensified pressure gradient, causing warmer and drier conditions in Southern Europe. In addition, a positive NAOI results in warmer and stormier conditions in the eastern United States. In a negative NAOI, the pressure gradient is weakened, and the climate patterns are reversed.

The NAO's influence extends from the eastern United States across the North Atlantic to eastern Europe [Hurrell *et al.*, 2003]. The altered surface wind speed, wave heights and storm tracks, impact human activities such as shipping, oil drilling, fisheries, and coastal management [Fromentin and Planque, 2000; Hurrell *et al.*, 2003; Kushnir *et al.*, 1997; Ottersen and Stenseth, 2001]. Altered precipitation patterns influence



agriculture and hydroelectric power from the mid-western United States to the Middle East. Improving our ability to predict shifts in the phase of the NAO is therefore a prerequisite to anticipating the economic impacts of inter-annual changes in climate [Hurrell *et al.*, 2001; Rodwell, 2003].

Beginning in the early 1970s, the North Atlantic has experienced an extended period of positive NAO index that is unprecedented in the instrumental records in terms of duration and intensity (Fig. 5.1) [Hurrell, 1995] [see also: <http://www.cgd.ucar.edu/cas/jhurrell/indices.html>]. This anomalous period has been hypothesized to be linked to anthropogenic forcing [Hurrell, 1996; Shindell *et al.*, 1999]. However, our current knowledge of the system does not allow for a complete understanding of the relationship between the NAO and SST, nor an accurate prediction of NAO behavior in the future [Czaja *et al.*, 2003; Joyce, 2002]. By expanding the geographical and temporal distribution of NAO reconstructions [Schmutz *et al.*, 2000; Schone *et al.*, 2003], a better understanding of the NAO and its interactions with the ocean can be achieved.

Currently there are two instrumental reconstructions of the NAO [Hurrell, 1995; Jones *et al.*, 1997] dating back to 1870 and 1821, respectively. Two records using early measurements of sea level pressure, temperature, and precipitation, as well as proxy data, extend NAO records as far back as 1500 [Luterbacher *et al.*, 2001; Rodrigo *et al.*, 2001]. Finally, several terrestrial based proxy reconstructions exist from ice cores [Appenzeller *et al.*, 1998], tree rings [Cook *et al.*, 2002], snow accumulation rates [Glueck and Stockton, 2001] and other multi-proxy combinations [Cullen *et al.*, 2001]. While there are several evaluations of NAO forcing on marine systems (eg. [Gil *et al.*, 2006; Kuhnert

*et al.*, 2005]), there is only one published marine based reconstruction [*Schoene et al.*, 2003]. This record extends to 1780 (missing years from 1862-1865) and is generated from growth rates of mollusk shells from the Norwegian and North Seas, providing a proxy for nutrient supply and thus mixed layer depth. Additional marine records from the North Atlantic basin could further our understanding of ocean and land responses to the NAO and improve our ability to evaluate model and proxy reconstruction results.

Here we present a new marine based reconstruction of the winter-time NAO index from a 218-year long, continuous brain coral (*Diploria labyrinthiformis*) collected from Bermuda (64°W, 32°N). NAO reconstruction is based on the inverse relationship of winter time (Dec., Jan., Feb., and March) strontium (Sr) to calcium (Ca) ratio to winter-time SST [*Smith et al.*, 1979] (Fig. 5.1a,b). Winter-time SST at Bermuda shows a correlation to the NAO [*Visbeck et al.*, 2003; *Visbeck et al.*, 2001]; thus, the coral Sr/Ca (an SST proxy) can be directly related to the NAO. By filtering the Sr/Ca record to frequencies with significant coherence to the NAO, we can isolate the NAO-SST signal from the hemispheric and global temperature signals. There are two critical questions addressed in this paper. 1) Is the NAO-SST relationship consistent through time, or is it altered by anthropogenic influences as previously hypothesized [*Joyce*, 2002]? 2) Do variations in the amplitude and phase of the NAO correlate to the shift from cool (1800-1849) to warm (1950-1999) conditions in the northern hemisphere, as defined by a multi-proxy record from Jones *et al.* (1998) (here after JSTA) (Fig. 5.1c)? These questions will be addressed by isolating two distinct frequency bands of the NAO and over these two frequencies comparing the new marine based record at Bermuda to instrumental, atmospheric proxy, and marine proxy records [*Cook et al.*, 2002; *Hurrell*, 1995; *Jones et*

*al.*, 1997; *Luterbacher et al.*, 2001; *Schoene et al.*, 2003] (*Jones et al.*, 1997 here after JNAO).

## 5.2. Methods

### *Generation of the Coral NAO Record from Bermuda*

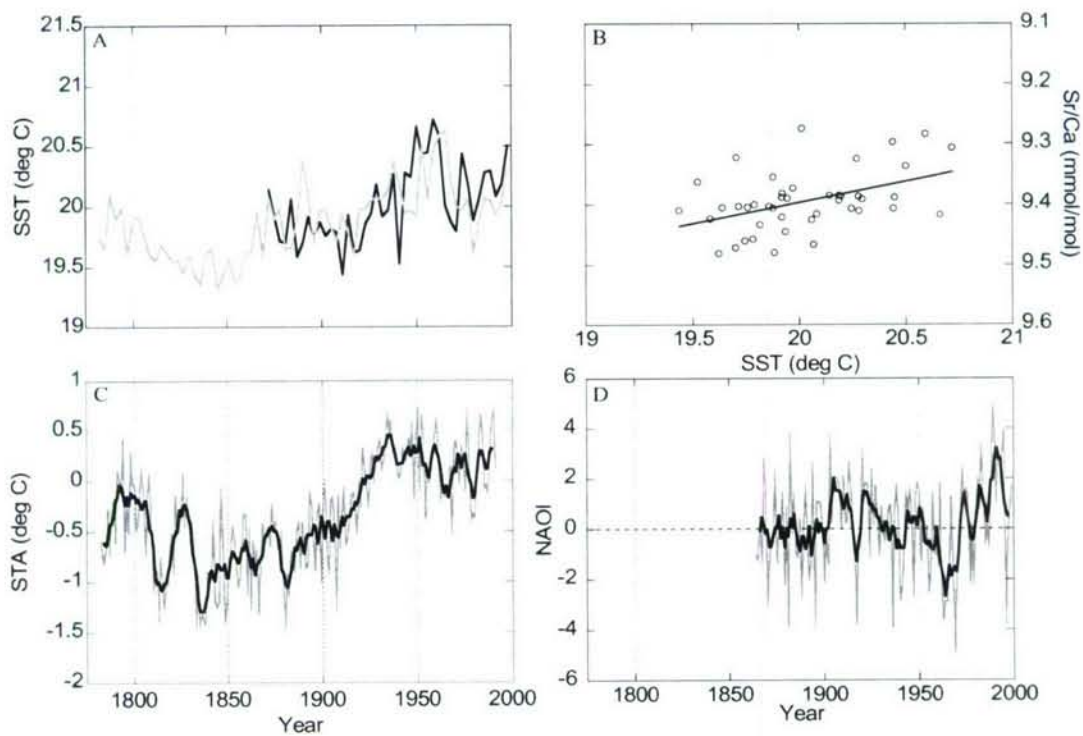


**Figure 5.1:** A) Three year averaged winter-time Sr/Ca (shaded) and observation based instrumental SST (solid) (HadISST, [Rayner *et al.*, 2003]) versus time and B) plotted linearly versus one another. Three year averages are shown as this is the shortest time period of coherence between the winter Sr/Ca and the instrumental NAO. A significant coherence ( $>95\%$ ) is found between the winter Sr/Ca and SST ( $F_{sig} = 0.0030$ ). C) A multi-proxy record of Northern hemisphere surface temperature anomalies (STA) [Jones *et al.*, 1998; JSTA] mean-annual (shaded) and with a 5-year running mean (solid). 1940-1998 shows the longest period of warm temperatures and 1800-1849 encompasses the two extended cold periods marking the end of the LIA. D) Instrumental record of the NAO [Hurrell, 1995] annually (shaded, and with a 5-year running mean (solid). 1950-2000 shows the largest variability during the record with both an extended positive and negative phase.



A ~230 year old brain coral (*Diploria labyrinthiformis*) was collected live off John Smith's Bay from the southeastern edge of the Bermuda platform at 16-meters depth in May 2000. Due to its location in the Atlantic, the island of Bermuda (64°W, 32°N) is well suited for an ocean based study of the NAO. Winter-time SST at Bermuda has been shown to correlate with the NAOI on inter-annual (positive correlation) and multi-decadal (negative correlation) frequencies [Eden and Willebrand, 2001; Visbeck *et al.*, 2003; Visbeck *et al.*, 2001]. Both responses are impacted by changes in Ekman pumping and heat flux due to the latitudinal wind shift. The multi-decadal response is either caused by gradual changes in the strength of meridional overturning circulation (MOC) [Eden and Willebrand, 2001] or by long-term propagation of the inter-annual SST anomalies [Krahmann *et al.*, 2001; Visbeck *et al.*, 1998]. The MOC hypothesis suggests that the observed temperature anomalies results from prolonged change in location and strength of Ekman pumping and intensified winds increasing heat flux from the ocean to atmosphere thus increasing Labrador Sea convection [Eden and Willebrand, 2001; Visbeck *et al.*, 2003; Visbeck *et al.*, 2001].

Coral Sr/Ca is inversely related to SST [Smith *et al.*, 1979], and Sr and Ca are both relatively conservative elements in seawater, with small changes in concentration due to coral symbionts and other biological and physical processes (eg. [Alibert and McCulloch, 1997; Bernstein *et al.*, 1987; Culkin and Cox, 1966; deVilliers *et al.*, 1994; Marshall and McCulloch, 2002]). In our previous work, we have shown that winter coral Sr/Ca at Bermuda is inversely correlated to SST at Hydrostation S, located 30 km to the southeast [Cohen *et al.*, 2004; Goodkin *et al.*, 2005], and to regional observational SST

measurements (HadISST, [Rayner *et al.*, 2003]) from 1870 to 1997 from the gridded area 31-33 °N and 64-65 °W [Goodkin *et al.*, in prep] (Fig. 5.1).

X-radiographs of 5mm-thick slabs cut along the axis of maximum growth of the brain coral reveal well-defined annual growth bands. Using the x-radiographs as a guide, samples were drilled down the length of the solid septotheca (calyx wall) at 0.33 mm intervals to achieve approximately monthly resolution from 1872 to 1999. Sr and Ca were measured simultaneously on an Inductively Coupled Plasma Atomic Emission Spectrometer (ICP-AES at WHOI). Materials and methods can be found in more detail in Goodkin *et al.* (2005), Goodkin *et al.* (in press), and Goodkin *et al.* (in prep).

Density banding from x-rays was used to construct an annual age model that was refined by correlating Sr/Ca to monthly averaged SSTs measured at Hydrostation S. Beyond the instrumental record, months were assigned based on an average climatology of the Hydrostation S data. The coral data were then re-sampled at evenly spaced monthly intervals to identify winter months (Dec.-March). Age model error is anticipated. Some age model error will be generated from noise in the Sr/Ca record and in counting the annual bands, which could either serve to add or eliminate years inappropriately. However, it is more likely that the coral record (and age model) will be biased because of missing years, resulting from years of no growth. This will lead to the reported date being younger (more recent) than the actual date [Goodkin *et al.*, (in prep)]. For example, if the coral did not grow in 1950, 1949 would be inappropriately assigned the date 1950, generating a bias in all years prior to 1950 (1948, 1947 etc.). This bias is likely to reach a maximum between 1830 and 1865 when growth rates are lowest [Goodkin *et al.*, 2005].

### *Comparison of the Coral Record to Other Records of the NAO*

Cross-spectral analysis comparing the negative of the winter Sr/Ca record to the other instrumental and proxy NAO records is completed using 10 multi-taper windows [Huybers, 2003] without detrending the records. Error estimates on phase relationships were generated using a Monte Carlo simulation in which 50 probable solutions were generated. Wavelet analysis was performed on the raw winter-time Sr/Ca record, using a morlet basis function, following previously published methods [Torrence and Compo, 1998a; Torrence and Compo, 1998b; Torrence and Webster, 1999].

### **5.3. Results and Discussion**

Cross-spectral analysis comparing the negative of winter Sr/Ca (equivalent to SST) to instrumental (Fig. 5.2) and proxy (Fig. 5.3) winter NAO records from 1864-1999 show two frequency intervals of significant coherence, one at periodicities less than 15 years (frequency of  $0.07 \text{ year}^{-1}$ ) and, the other at periodicities between  $\sim 3$  to 5 years (frequency of  $0.18\text{-}0.28 \text{ year}^{-1}$ ). Coherence to the two NAO instrumental records [Hurrell, 1995; Jones *et al.*, 1997] deteriorates at periodicities shorter than 3 years ( $0.33 \text{ year}^{-1}$ ). This limitation would be expected from single-geographic point proxy records [Huybers, submitted], for which site specific and proxy noise can overwhelm regional signals. At multi-decadal frequencies the negative of winter Sr/Ca and the NAO are anti-phase, whereas at inter-annual frequencies, the negative of winter Sr/Ca is within error of being in phase (Fig. 5.2). The coral Sr/Ca record's phase relationships to the instrumental and proxy records are consistent with the SST-NAO analysis from model and instrumental results [Eden and Willebrand, 2001; Visbeck *et al.*, 2003].

The comparison of the coral Sr/Ca data to the historical and proxy based records



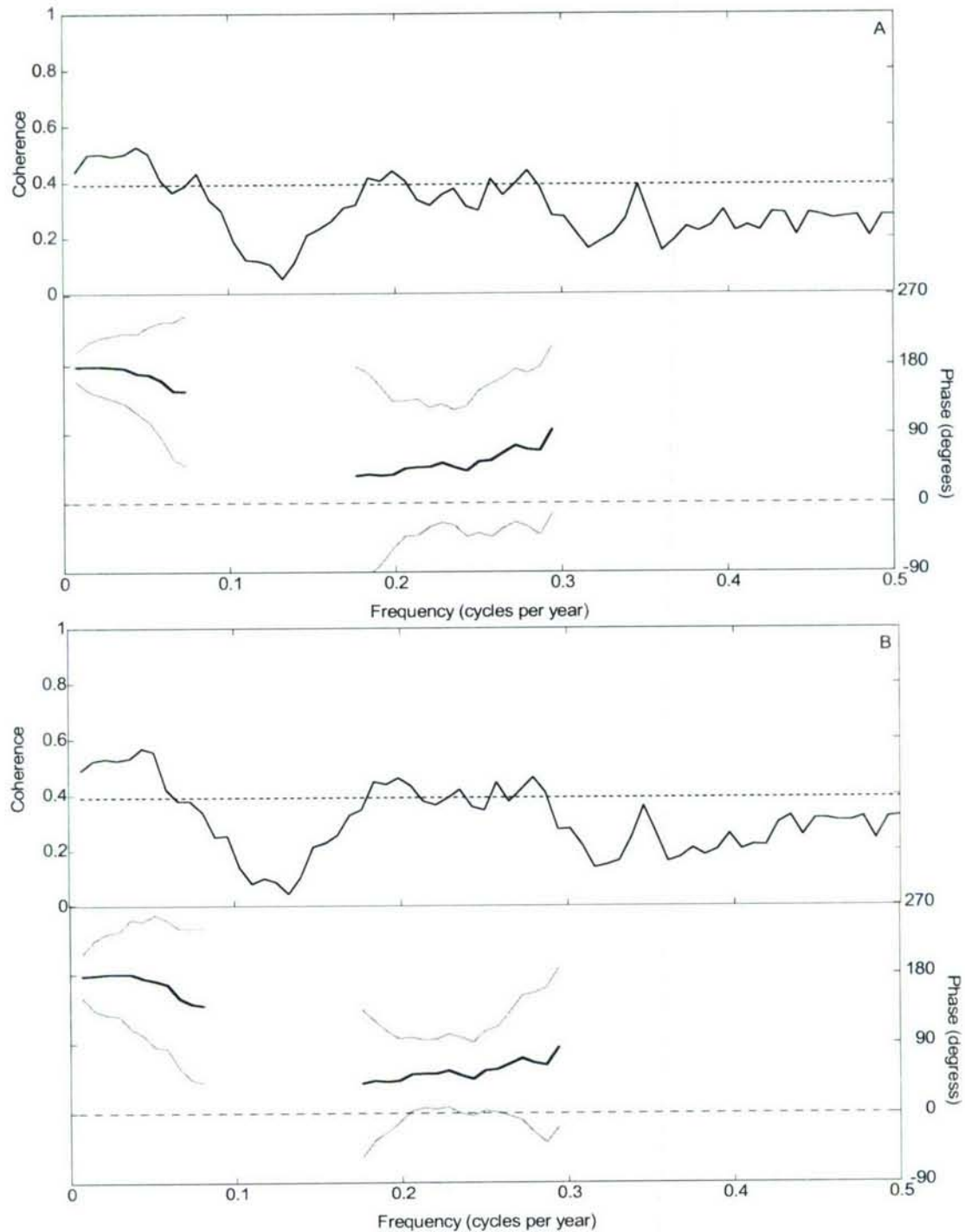


**Figure 5.2:** Spectral analysis of the negative of winter Sr/Ca (equivalent to SST) and instrumental records of the NAOI from a) Hurrell (1995) and b) Jones et al. (1997) (JNAO). Top panel of the a and b subplots shows the coherence ( $r$ ) (solid) including the 95% confidence interval (dashed). Bottom panels show the phase relationship (solid), including Monte Carlo based error calculation (grey), surrounding periods of significant coherence. Analysis completed using multi-taper method with 10 windows and 50 iterations on Monte Carlo error estimates [Huybers, 2003].

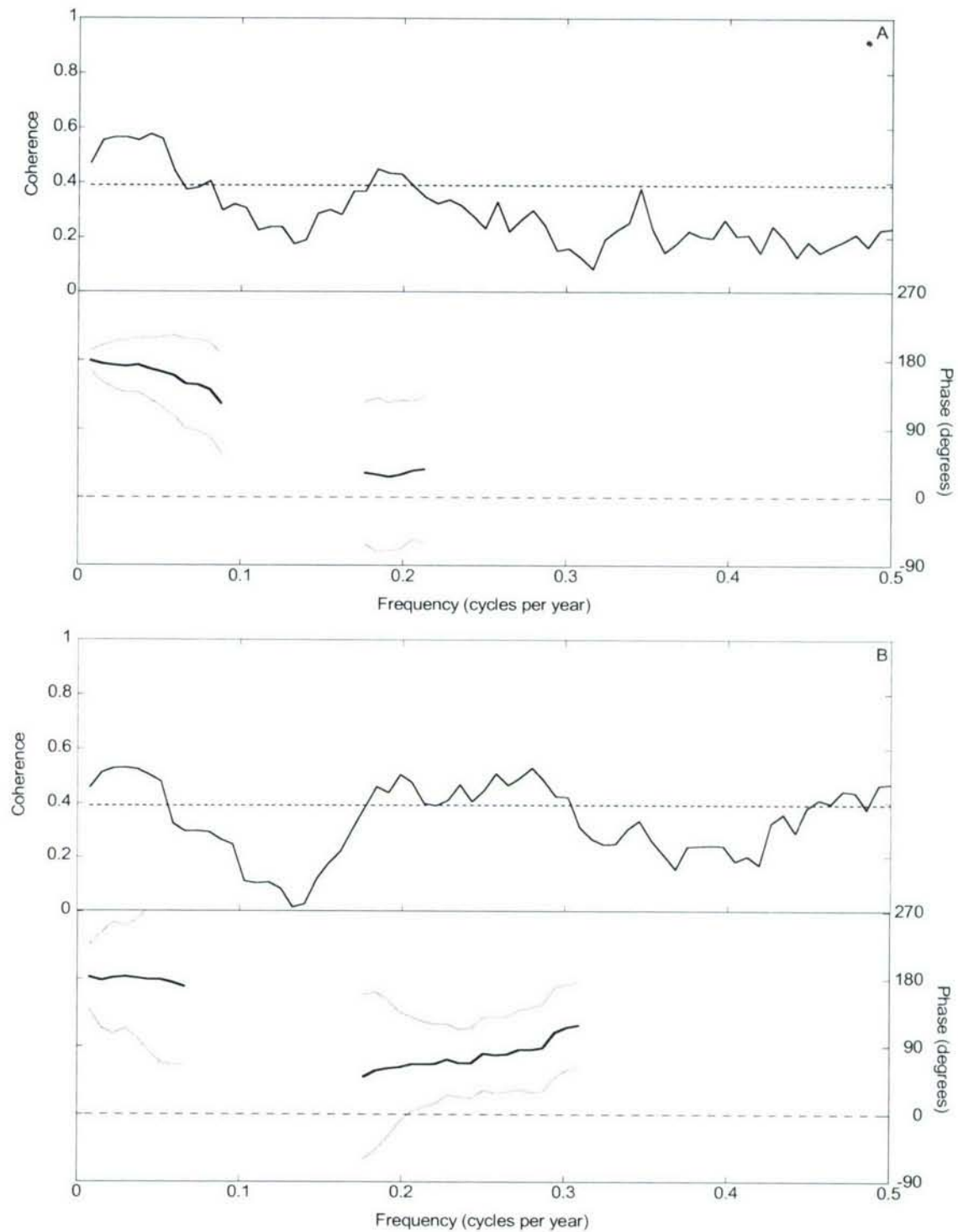


**Figure 5.3:** Spectral analysis of the negative of winter Sr/Ca (equivalent to SST) and proxy records of the NAOI from a) Luterbacher et al. (2001) and b) Cook et al. (2002). Top panel of the a and b subplots shows the coherence ( $r$ ) (solid) including the 95% confidence interval (dashed). Bottom panels show the phase relationship (solid), including Monte Carlo based error calculation (grey), surrounding periods of significant coherence. Analysis completed using multi-taper method with 10 windows and 50 iterations on Monte Carlo error estimates [Huybers, 2003].

show similar results as compared to the instrumental records. Luterbacher *et al.* (2001) and Cook *et al.* (2002) were chosen due to the large geographical distribution of the proxy records used in the reconstructions. The size of the coherent inter-annual frequency band for Sr/Ca and Luterbacher *et al.* (2001) records is narrower than those found in the other NAO comparisons (Fig. 5.3a). At inter-annual frequencies, comparison to the record of Cook *et al.* (2002) shows the longest and most coherent frequency band of all three records, with significant coherence spanning from 3.3 to 5.5 years per cycle (Fig. 5.3b). However, for this frequency band, Sr/Ca appears to lag the NAO reconstruction by 50 degrees, with the error bounds excluding the zero-lag at frequencies higher than 5 years per cycle.

Given these results, two coral Sr/Ca based NAO reconstructions were calculated by filtering the negative of the Sr/Ca record to isolate the two frequency bands where the coral data are coherent with the NAO. For the frequency reconstruction, the data were treated with Hanning window band-pass filters selecting frequencies between 3 and 5 years per cycle and 20 and 100 years per cycle. The multi-decadal reconstruction was performed by shortening the window on each end of the record such that the 100-year pass has averages of at least 50 years averaged at the record ends executed by shortening the Hanning window.

At low frequencies, the winter-time Sr/Ca record shows significant coherence with the hemispheric STA [*JSTA*] (Fig. 5.4). However, if the winter Sr/Ca and *JSTA* records are each linearly detrended (from 1781-1999) before cross-correlation analysis, then no low-frequency coherence is found (Fig. 5.4). The strongest agreement between the Sr/Ca and the STA record is marked by a generally increasing trend from the earliest



part of the record (1800) to today (Fig. 5.1). We therefore attempted to remove this very low frequency signal in the Sr/Ca record that may be dominated by processes other than the NAO. In choosing a 20-100 year band pass, we balanced 1) capturing a long enough trend to evaluate the prolonged coherence between the coral data and the instrumental NAO [Hurrell, 1995] beginning at ~15 years per cycle and 2) removing a lower

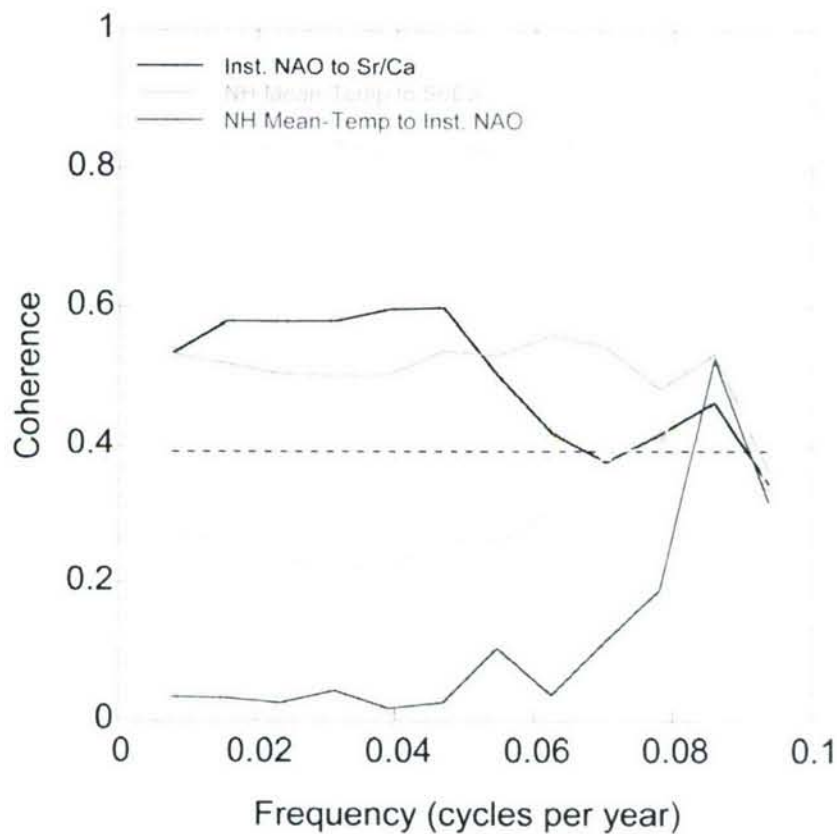


**Figure 5.4:** Cross correlation analysis for frequencies less than 0.1 cycles per year from 1864-1991, the maximum period of overlap for records of the NAO, negative winter Sr/Ca and NH temperature proxies. The negative winter Sr/Ca is compared to the NAO instrumental record [Hurrell, 1995] (solid, circles). The negative winter Sr/Ca is also compared to both the mean-annual Northern Hemisphere temperature proxy record (JSTA, [Jones *et al.*, 1998]) with neither record detrended (shaded, circles) and with both records detrended (shaded, squares). The instrumental NAO record and the mean-annual NH proxy record are also compared to one another (solid, squares). The dashed line represents coherence with 95% confidence.

frequency signal correlating to mean temperature. The correlation coefficient of the negative Sr/Ca record to the entire length of the NAO instrumental record [Hurrel, 1995] both filtered just with a 15-year Hanning window is -0.60 compared to -0.77 with the 20-100 year filter, which has also removed the secular hemispheric temperature driven trend in the Sr/Ca record. The NAO and hemispheric STA have no correlation over this frequency band, further implying the two signals should be separable.

A critical question to be evaluated from the filtered records is how the characteristics of the NAO-ocean relationship evolve with changes in the mean climate state of the Northern Hemisphere. A reconstruction of Northern Hemisphere surface temperature (JSTA, [Jones *et al.*, 1998]) shows intervals of relatively cold temperatures from 1800-1875, with two strong cooling events between 1800 and 1850 demarking the end of the LIA, and relatively warm temperatures from 1940-today (Fig. 5.1c). These two periods will be used to evaluate how the power and amplitude of the NAO changes between periods of different atmospheric temperature.

The inter-annual band passed Sr/Ca records are coherent, as expected, to similarly filtered instrumental and proxy records [Hurrel, 1995; Jones *et al.*, 1997; Luterbacher *et al.*, 2001; Cook *et al.*, 2002; Schoene *et al.*, 2003] (Fig. 5.5). In the three-to-five year frequency band, the winter Sr/Ca has the strongest coherence from 1950-2000 with Sr/Ca lagging the NAO proxy records by one year - in four of the five records - implying either that the NAO leads Bermuda SST by one year or that our age-model accounts for one year too few during this period (Fig. 5.6). The strongest coherence to Cook *et al.* (2002) occurs when Sr/Ca lags the atmospheric record by three years. The most coherent leads

and lags between the Sr/Ca and all proxy and instrumental records other than Cook *et al.* (2002) change through time ranging from Sr/Ca lagging by one year (1950-1997) to leading by two years (1850-1899) (Table. 5.1). The 3-5 year frequency band returns periodicities within our age model error which back in time could exceed five years; therefore, the Sr/Ca and atmospheric records cannot be used to evaluate changes between the timing of NAO events and resulting SST anomalies at inter-annual frequencies. The fact that Cook *et al.* (2002) is consistently coherent with a different lead or lag than the other records suggest some age model uncertainty in the tree ring record relative to the other instrumental and proxy records independent of the uncertainty in the Sr/Ca age model.

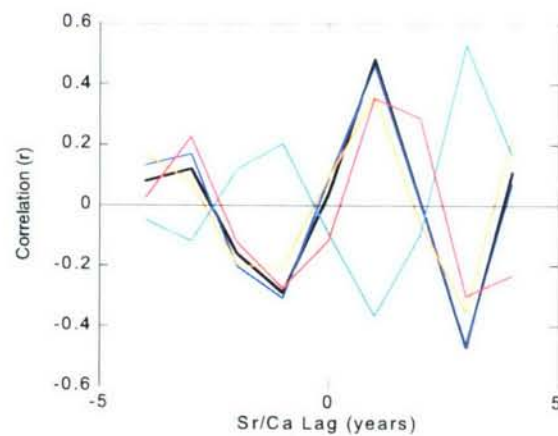


**Figure 5.6:** Covariance of three to five year frequency band filtered record of (-) Sr/Ca to the records of NAO over the time interval of 1948-1997. Comparisons to Hurrell (black), Jones (dark blue), Luterbacher (orange) and Schoene (red) show the strongest covariance with Sr/Ca lagging the other by one year. Comparisons to Cook (light blue) show the strongest correlation with a three year lag.



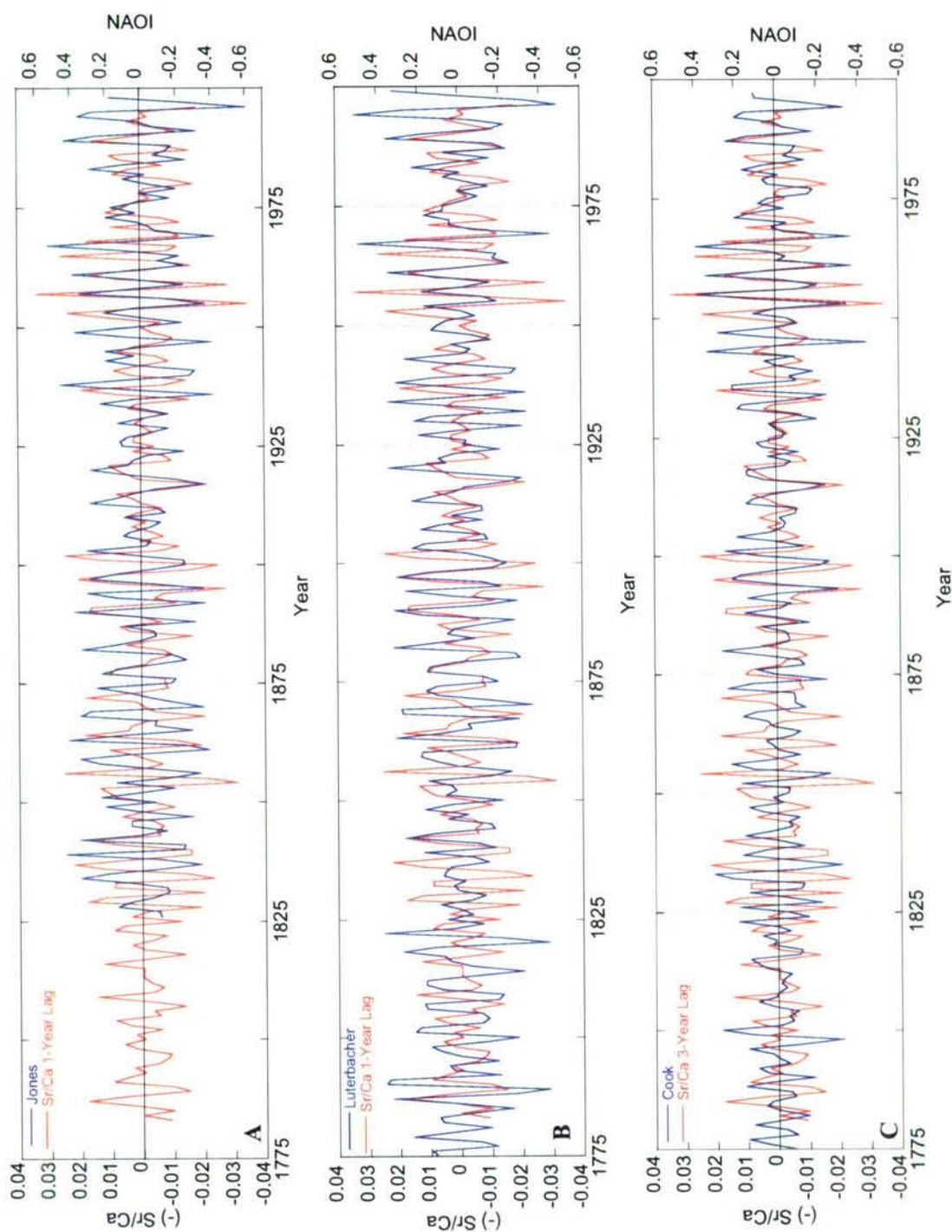


**Figure 5.5:** Band-passed filtered records to frequencies of three to five years per cycle for the negative of winter Sr/Ca (red) compared to Jones et al. (1997) (JNAO) (A), Luterbacher et al. (2001) (B), and Cook et al. (2002) (C) all in blue. Jones and Luterbacher are shown with winter Sr/Ca lagging by one year and Cook is shown with winter Sr/Ca lagging by three years. Prior to 1900, amplitude changes continue to be captured, but winter Sr/Ca goes in and out of phase with the other proxy records. At inter-annual frequencies, it is not possible to distinguish between the two potential causes – changes in the NAO-SST response or error in the coral age model.

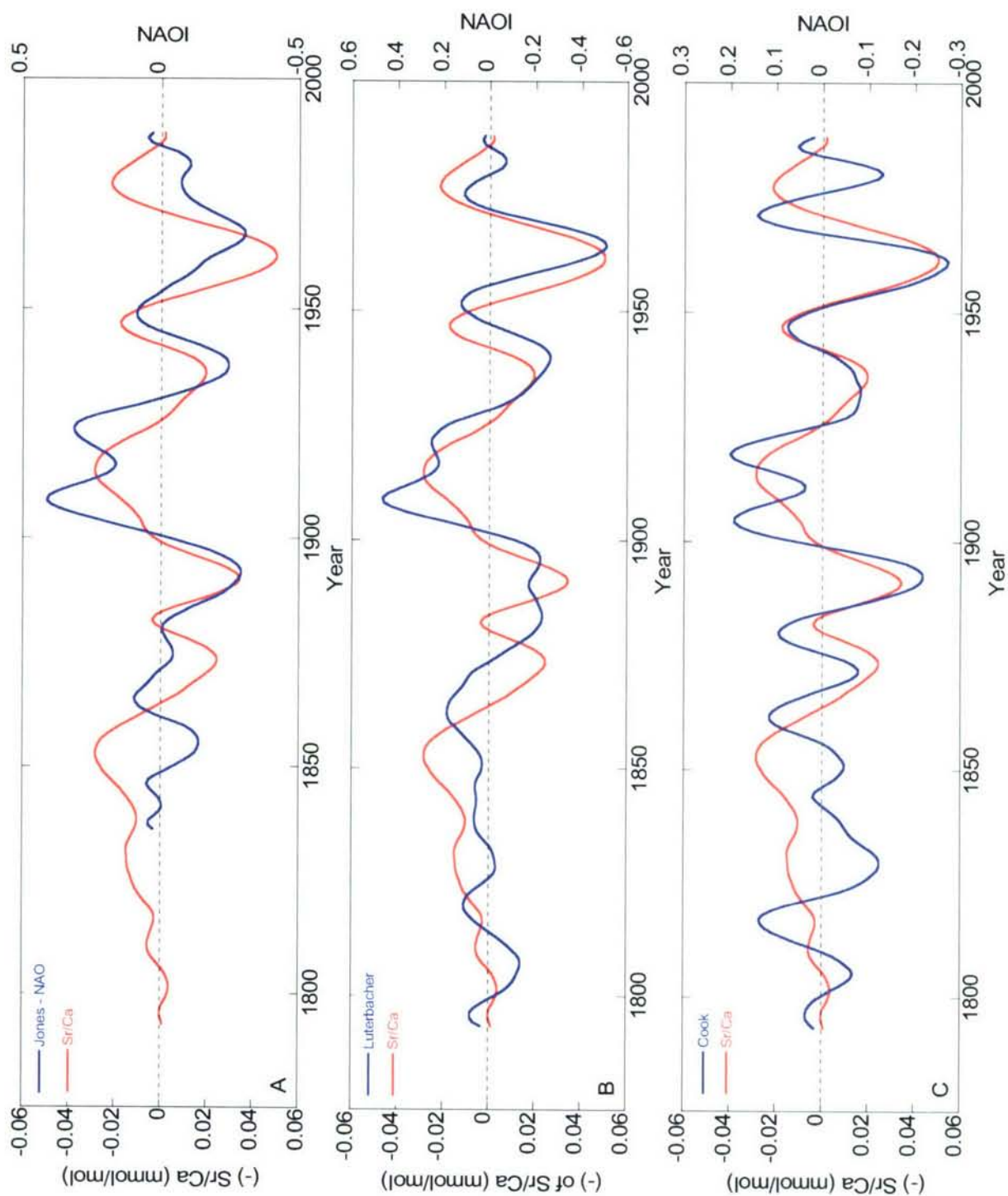


**Figure 5.7:** Band passed filtered records to frequencies of twenty to one hundred years per cycle for the negative of winter Sr/Ca (red) compared to Jones et al. (1997) (JNAO) (A), Luterbacher et al. (2001) (B), and Cook et al. (2002) (C) (all in blue).

**Table 5.1:** Correlation ( $r$ ) between the negative of winter Sr/Ca record and instrumental and proxy records at 3-5 year frequency bands (top) and 20-100 year frequency band (bottom).

		Instrumental and Proxy Records					Lead/Lag Description for Inter-Ann. Freq.
		Hurrel	Jones	Luterbacher	Cook	Schoene	
<b>Inter-Annual Correlations</b>							
<b>1950-1997</b>	0.48		0.46	0.36	0.53	0.35	Sr/Ca lags 1 year for all but Cook which lags 3 years.
<b>1900-1949</b>	0.44		0.45	0.46	0.32	0.35	Sr/Ca at zero lag for all but Cook which lags three years.
<b>1850-1899</b>	0.32		0.15	0.16	0.23	0.19	Sr/Ca leads by 2 years for Jones and Schoene, and lags by two years for Cook and Luterbacher. Sr/Ca lags Hurrel by one year and only goes back to 1866.
<b>1800-1849</b>				0.29	0.40	0.33	Sr/Ca leads by 1 year for Luterbacher and Jones and lags by one year for Cook.
<b>1900s Average</b>	0.46		0.45	0.41	0.42	0.35	
<b>1800s Average</b>				0.23	0.32	0.26	
<b>Multi-decadal Correlations</b>							
<b>1950-1992</b>	-0.82		-0.50	-0.80	-0.65	-0.06	
<b>1900-1949</b>	-0.53		-0.72	-0.77	-0.78	-0.37	
<b>1850-1899</b>	-0.76		-0.27	-0.46	-0.57	-0.39	
<b>1800-1849</b>				-0.52	0.23	-0.42	
<b>1900s Average</b>	-0.67		-0.61	-0.78	-0.72	-0.22	
<b>1800s Average</b>				-0.49	-0.17	-0.41	



We investigated the agreement between inter-annual filtered NAO reconstructions in fifty year increments to assess how the marine coral reconstruction performs for time periods of different mean-temperature. The maximum lagged correlation coefficients between the Sr/Ca and each record from 1950 to the end of the record are above or close to 95% significance as determined by spectral analysis ( $r = 0.39$ ) (Table 5.1). Maximum correlation coefficients are similar for the periods 1900-1947 and 1950-1997 (Table 5.1), and during the 20<sup>th</sup> century as a whole, the winter Sr/Ca record represents well both the phase and amplitude of inter-annual variability in the NAO.

Comparing the 19<sup>th</sup> and 20<sup>th</sup> century inter-annual results between the warmest periods of the 20<sup>th</sup> century (1950-1997) and the end of the LIA (1800-1849) shows minimal difference in correlation between Sr/Ca and the other NAO records. The maximum lagged correlations between Sr/Ca and the atmospheric proxy and instrumental records are relatively unchanged (Table 5.1). In addition, the variance does not differ between the two time periods with statistical significance (variance (1950-1997) = 0.0002, variance (1800-1849) = 0.0001,  $p = 0.0704$ ). During the end of the 19<sup>th</sup> century (1850-1899), when hemispheric temperature records are both colder relative to today and fairly constant, the coral Sr/Ca record shows the weakest correlation to all other records of the NAO (Fig. 5.1c). However, this will also be the time of largest potential age model bias which could serve to weaken coherence through temporal offsets over a 50-year period.

The correlation of the two marine records (coral Sr/Ca and Schoene *et al.*, 2003) during the end of the LIA (1800-1849) is similar to the correlation for the 20<sup>th</sup> century (Table 5.1). The lowest correlation between the marine records occurs from 1850 to

1899, much like the atmospheric record comparisons. The relative consistency of the correlation through time implies that if changes are occurring in the ocean's inter-annual response to the NAO they are consistent between these two locations. However, the marine records are not particularly well correlated with each other during the calibration period (1950-1997), with a lower correlation than found between the Sr/Ca and instrumental NAO records. This could occur for multiple reasons. The two locations do not have identical responses to the NAO even if the relative responses are consistent through time. NAO process are shifting geographically changing responses at each location, or error in both record's age models are impacting their correlation. However, the Schoene *et al.* (2003) record shows a much larger ( $p < 0.0001$ ) variance in amplitude during the cold interval at the end of the LIA, in contrast to a relatively flat or opposing variance trends in the Bermuda record, implying a larger impact than age model error.

In the twenty to one hundred year periodicity band, strong correlations are found between the negative of winter Sr/Ca record and the other proxy and instrumental records during the 20<sup>th</sup> century (Fig. 5.7, Table 5.1). The Sr/Ca deviates from the other records from 1900-1930. All five instrumental and proxy records show two maxima whereas the Sr/Ca record shows only one maximum. There are changes in coherence between the first and second half of the 20<sup>th</sup> century; however, depending on which proxy or instrumental record is examined, the interval with stronger (or positive) coherence differs. Low-frequency ocean behavior has been observed in models to lag the atmospheric records by 6-8 years [Eden and Willebrand, 2001]. Our record doesn't show consistent behavior of leading or lagging either through time or between the different atmospheric records. A larger geographic distribution of marine records could help to evaluate how

the NAO signal propagates through time, whereas a single point location does not provide enough information about possible spatial displacement.

The 19<sup>th</sup> century shows less consistent results at multi-decadal frequencies than does the 20<sup>th</sup> century. The Sr/Ca based record has a period of inverse correlation to the Cook *et al.* (2002) record. The winter Sr/Ca shows an interval of positive NAOI in the early 1800s, like the Luterbacher *et al.* (2001). While Cook *et al.* (2002) and Schoene *et al.* (2003) show periods of both positive and negative NAOI at this time. Similar to its inter-annual record, and unlike other records, the Schoene *et al.* (2003) record shows more amplitude variability in the early 1800s than in the 20<sup>th</sup> century (variance 1800-1849 = 0.041 and 1945-1994 = 0.002,  $p < 0.0001$ ) (Fig. 5.7)

Comparing the beginning of the 19<sup>th</sup> century (1800-1849) and the end of the 20<sup>th</sup> century (1939-1988) shows that during times of warm hemispheric mean temperatures (Fig. 5.2) the multi-decadal coral record has a stronger coherence to the atmospheric records (Table 5.1). Between these two time periods of mean-cold and mean-warm temperatures, a larger variance in the Sr/Ca record is also seen during warmer hemispheric temperatures (variance (1800-1849)  $< 0.0001$  and (1939-1998) = 0.0005,  $p < 0.0001$ ). In contrast, during the end of the LIA, a mean hemispheric cold period, the two atmospheric proxy records show varying agreement both with one another and with the coral Sr/Ca record. These results suggest at a minimum that multi-decadal variability in the NAO response at Bermuda was relatively weak during the end of the LIA relative to the warmest part of the 20<sup>th</sup> century.



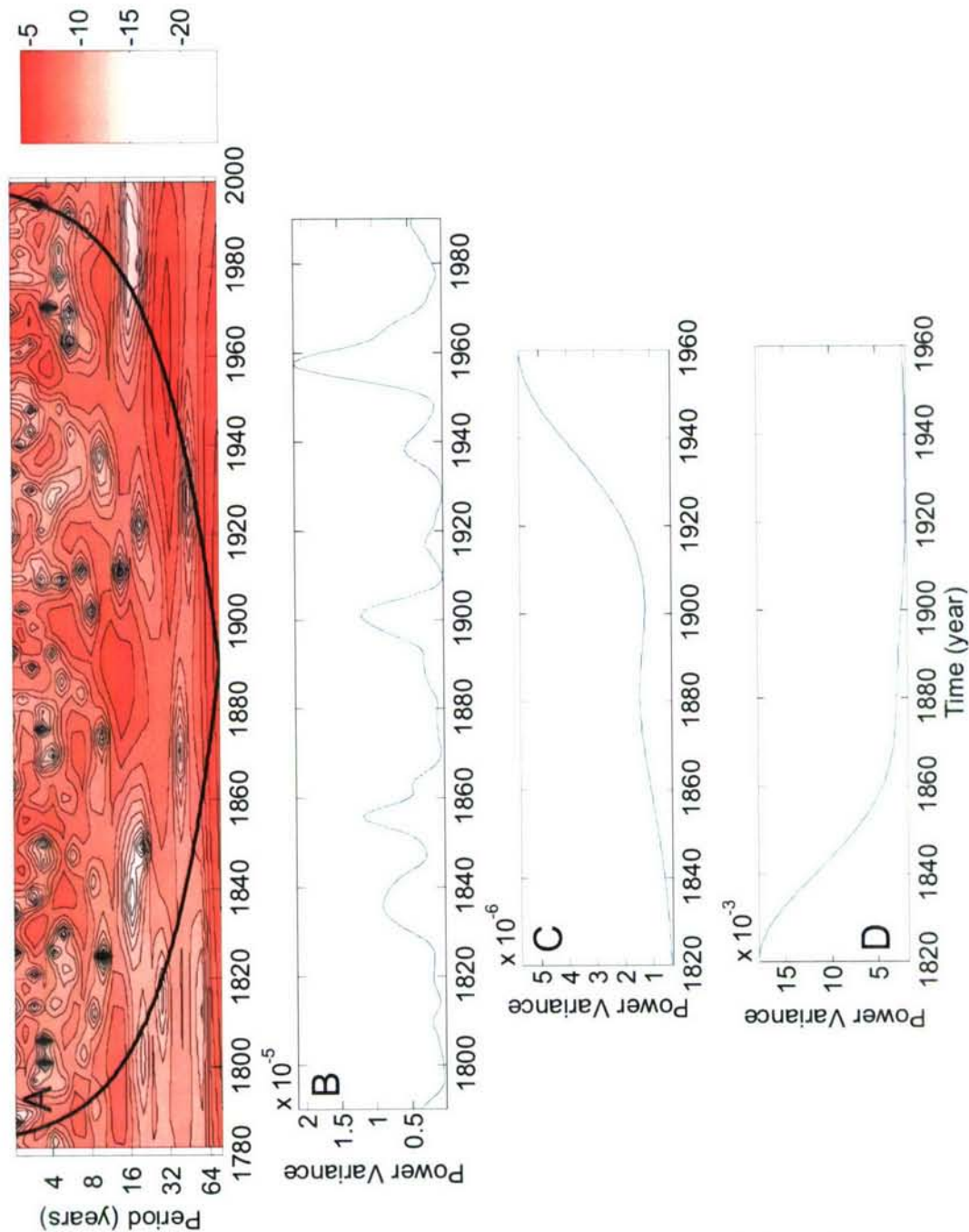


**Figure 5.8:** Wavelet analysis based on Torrence and Compo (1998) using a morlet wavelet function with the raw winter coral Sr/Ca record. A) Spectral power through time at varying frequencies. B) Spectral power through time over a 3-5 year frequency band. C) Spectral variance through time over a 20-50 year frequency band. Results are only useful above the cone of influence shown by black semi-circle, below which the results are not robust due to the windowing effects. D) Spectral variance results of the same analysis on the JSTA record over 20-50 year frequency band. The focus of power at the end of the LIA is in contrast to the results of the Sr/Ca record indicating separation from mean-hemisphere temperature at this frequency.

Wavelet analysis of the raw winter Sr/Ca record is used to examine the timing and strength of individual periodicities over different time intervals [Torrence and Compo, 1998a,b]. Spectral power is examined for the 3-5 year frequency band and a 20-50 year frequency band, which allows us to look at the multi-decadal power through time within the confidence limits of the analysis. The strongest spectral power in both bands occurs during the latest portion of the record (Fig. 5.8a). While the strongest spectral power in the 3-5 year frequency band is centered on the 1960 temperature maximum, three other clear peaks exist at 1830, 1850, and 1900 (Fig. 5.8b). These are all times of average or cooler than normal temperatures (Fig. 5.1c), and preclude a relation between NAO variance and mean hemispheric temperature.

The multi-decadal signal, however, does appear to be tied to hemispheric temperatures. For frequencies between 20 and 50 years, the power in the Sr/Ca and temperature records are not similarly distributed (Fig. 5.8c,d), supporting the successful separation of the hemispheric STA signal in the Sr/Ca. The Sr/Ca power is also not equally distributed through time. The power of the Sr/Ca record is greatest during the warmest part of the record (1820-1860). This result is consistent with the amplitude variance results and is visible in the low frequency records (Fig. 5.7). The differences amongst the marine and terrestrial proxies imply that the ocean, the land or both appear to respond differently (in amplitude or direction) to the NAO through time, and may be influenced by anthropogenic changes. This could result from a change in behavior in the NAO system or a change in oceanic response to the current system. Model and observational results also suggest variations in the strength of the MOC on centennial and inter-annual timescales (ex. [Bryden *et al.*, 2005; Villenga and Wu, 2004]). The

differences in amplitude and mean-value observed amongst the multi-decadal records could imply changes in MOC as well as the NAO during mean-warm versus mean-cool hemispheric conditions.

## 5.5 Conclusions

On inter-annual time scales, the NAO influences SST via atmospheric processes which drive changes in wind speed and subsequent Ekman currents. These changes can result in a positive NAO-positive SST (negative Sr/Ca) connection at Bermuda [Visbeck *et al.*, 2001]. At multi-decadal frequencies, it is believed that the MOC is enhanced following extended positive NAO conditions leading to a positive NAO-negative SST (positive Sr/Ca) connection at Bermuda [Eden and Willebrand, 2001]. The expected relationships are confirmed by this record through coral Sr to Ca records and found to occur for a longer time interval than previously known.

This new marine record of the NAO provides an insight into the SST-NAO relationship from the center of the Atlantic Basin. The mean-state of the NAOI does not show a clear shift into either a prolonged positive or negative state with extended warm or cold air temperatures. In fact, a prolonged positive NAOI is seen both during the end of the LIA and during the late 20<sup>th</sup> century warming. The inter-annual ocean response to the NAO does change through time. Coherence between the marine and atmospheric records decreases as power at this frequency diminishes in the Bermuda record. However, inter-annual changes in ocean behavior do not correlate with changes in mean atmospheric temperatures. At multi-decadal frequencies behavior is correlated to shifts in atmospheric mean-temperature, with greatly increasing power in the marine record at warmer temperatures. Anthropogenic influences do not appear to be altering the mean-



state of the NAOI, but maybe acting to increase multi-decadal variability and the connection between the NAO and SST at Bermuda. In essence, hemispheric warming may be pushing the NAO to higher variability but not to a new mean position. An increased number of marine records from a broad geographical distribution will help to further our understanding of this identified behavior and the role of anthropogenic activity in the state of the NAO.

## 5.6 References

- Alibert, C., and M. T. McCulloch, Strontium/calcium ratios in modern Porites corals from the Great Barrier Reef as a proxy for sea surface temperature: Calibration of the thermometer and monitoring of ENSO, *Paleoceanography*, 12, 345-363, 1997.
- Appenzeller, C., J. Schwander, S. Sommer, and T. F. Stocker, The North Atlantic Oscillation and its imprint on precipitation and ice accumulation in Greenland, *Geophysical Research Letters*, 25, 1939-1942, 1998.
- Bernstein, R. E., P. R. Betzer, R. A. Feely, R. H. Byrne, M. F. Lamb, and A. F. Michaels, Acantharian Fluxes and Strontium to Chlorinity Ratios in the North Pacific Ocean, *Science*, 237, 1490-1494, 1987.
- Bryden, H. L., H. R. Longworth, and S. A. Cunningham, Slowing of the Atlantic meridional overturning circulation at 25degrees N, *Nature*, 438, 655-657, 2005.
- Cohen, A. L., S. R. Smith, M. S. McCartney, and J. van Etten, How brain corals record climate: an integration of skeletal structure, growth and chemistry of *Diploria labyrinthiformis* from Bermuda, *Marine Ecology-Progress Series*, 271, 147-158, 2004.
- Cook, E. R., R. D. D'Arrigo, and M. E. Mann, A well-verified, multiproxy reconstruction of the winter North Atlantic Oscillation index since AD 1400, *Journal of Climate*, 15, 1754-1764, 2002.
- Culkin, F., and R. A. Cox, Sodium, potassium, magnesium, calcium and strontium in seawater, *Deep-Sea Research*, 13, 789-804, 1966.
- Cullen, H. M., R. D. D'Arrigo, E. R. Cook, and M. E. Mann, Multiproxy reconstructions of the North Atlantic Oscillation, *Paleoceanography*, 16, 27-39, 2001.
- Czaja, A., A. W. Robertson, and T. Huck, The Role of Atlantic Ocean-Atmosphere Coupling Affecting North Atlantic Oscillation Variability. in *The North Atlantic Oscillation: Climatic Significance and Environmental Impact*, edited by Hurrell, J., Y. Kushnir, G. Ottersen and M. Visbeck, pp. 147-172, American Geophysical Union, Washington, D. C., 2003.
- deVilliers, S., G. T. Shen, and B. K. Nelson, The Sr/Ca-Temperature Relationship in Coralline Aragonite - Influence of Variability in (Sr/Ca)Seawater and Skeletal Growth-Parameters, *Geochimica Et Cosmochimica Acta*, 58, 197-208, 1994.
- Eden, C., and J. Willebrand, Mechanisms of interannual to decadal variability of the North Atlantic circulation, *Journal of Climate*, 14, 2266-2280, 2001.

- Fromentin, J. M., and A. Planque, North Atlantic Oscillation and year-to-year plankton fluctuations, *The Sir Alister Hardy Foundation for Ocean's Science's Continuous Plankton Recorder Survey*, 2000.
- Gil, I. M., F. Abrantes, and D. Hebbeln, The North Atlantic Oscillation forcing through the last 2000 years: Spatial variability as revealed by high-resolution marine diatom records from N and SW Europe, *Marine Micropaleontology*, 60, 113-129, 2006.
- Glueck, M. F., and C. W. Stockton, Reconstruction of the North Atlantic Oscillation, *International Journal of Climatology*, 21, 1453-1465, 2001.
- Goodkin, N. F., K. Huguen, and A. C. Cohen, Multi-Coral Calibration of Sr/Ca and Growth Rate to Sea Surface Temperature, *Paleoceanography*, in press.
- Goodkin, N. F., K. Huguen, A. C. Cohen, and S. R. Smith, Record of Little Ice Age sea surface temperatures at Bermuda using a growth-dependent calibration of coral Sr/Ca, *Paleoceanography*, 20, PA4016, doi:4010.1029/2005PA001140, 2005.
- Goodkin, N. F., K. A. Huguen, A. C. Cohen, W. B. Curry, and D. R. Ostermann, Sea Surface Temperature and Salinity Variability at Bermuda during the End of the Little Ice Age, *Paleoceanography*, in prep.
- Hurrell, J., Y. Kushnir, G. Ottersen, and M. Visbeck, An Overview of the North Atlantic Oscillation. in *The North Atlantic Oscillation: Climatic Significance and Environmental Impact*, edited by Hurrell, J., Y. Kushnir, G. Ottersen and M. Visbeck, pp. 1-36, American Geophysical Union, Washington, D. C, 2003.
- Hurrell, J. W., Decadal Trends in the North-Atlantic Oscillation - Regional Temperatures and Precipitation, *Science*, 269, 676-679, 1995.
- Hurrell, J. W., Influence of variations in extratropical wintertime teleconnections on Northern Hemisphere temperature, *Geophysical Research Letters*, 23, 665-668, 1996.
- Hurrell, J. W., Y. Kushnir, and M. Visbeck, Climate - The North Atlantic oscillation, *Science*, 291, 603, 2001.
- Hurrell, J. W., and H. VanLoon, Decadal variations in climate associated with the north Atlantic oscillation, *Climatic Change*, 36, 301-326, 1997.
- Huybers, P., Multi-taper method coherence using adaptive weighting and correcting for the bias inherent to coherence estimates. <http://web.mit.edu/~phuybers/www/Mfiles/index.html>, 2003.
- Huybers, P., On the frequency dependence of hemispheric-scale paleo-temperature reconstructions, *Geophysical Research Letters*, submitted.



- Jones, P. D., K. R. Briffa, T. P. Barnett, and S. F. B. Tett, High-resolution palaeoclimatic records for the last millennium: interpretation, integration and comparison with General Circulation Model control-run temperatures, *Holocene*, 8, 455-471, 1998.
- Jones, P. D., T. Jonsson, and D. Wheeler, Extension to the North Atlantic Oscillation using early instrumental pressure observations from Gibraltar and south-west Iceland, *International Journal of Climatology*, 17, 1433-1450, 1997.
- Jones, P. D., T. J. Osborn, and K. R. Briffa, Pressure-based measures on the North Atlantic Oscillation (NAO): A comparison and an assessment of changes in the strength of the NAO and in its influence on surface climate parameters. in *The North Atlantic Oscillation: Climatic Significance and Environmental Impact*, edited by Hurrell, J., Y. Kushnir, G. Ottersen and M. Visbeck, American Geophysical Union, Washington, D.C., 2003.
- Joyce, T. M., One hundred plus years of wintertime climate variability in the Eastern United States, *Journal of Climate*, 15, 1076-1086, 2002.
- Krahmann, G., M. Visbeck, and G. Reverdin, Formation and propagation of temperature anomalies along the North Atlantic Current, *J. Phys. Oceanogr.*, 31, 1287-1303, 2001.
- Kuhnert, H., T. Cruger, and J. Patzold, NAO signature in a Bermuda coral Sr/CA record, *Geochemistry Geophysics Geosystems*, 6, Q04004, doi:04010.01029/02004GC000786, 2005.
- Kushnir, Y., V. J. Cardone, J. G. Greenwood, and M. A. Cane, The recent increase in North Atlantic wave heights, *Journal of Climate*, 10, 2107-2113, 1997.
- Luterbacher, J., E. Xoplaki, D. Dietrich, P. D. Jones, T. D. Davies, D. Portis, J. F. Gonzalez-Rouco, H. von Storch, D. Gyalistras, C. Casty, and H. Wanner, Extending the North Atlantic Oscillation reconstructions back to 1500, *Atmospheric Science Letters*, 2, 114-124, 2001.
- Marshall, J. F., and M. T. McCulloch, An assessment of the Sr/Ca ratio in shallow water hermatypic corals as a proxy for sea surface temperature, *Geochimica Et Cosmochimica Acta*, 66, 3263-3280, 2002.
- Ottersen, G., and N. C. Stenseth, Atlantic climate governs oceanographic and ecological variability in the Barents Sea, *Limnology and Oceanography*, 46, 1774-1780, 2001.
- Rayner, N. A., D. E. Parker, E. B. Horton, C. K. Folland, L. V. Alexander, D. P. Rowell, W. C. Kent, and A. Kaplan, Global analyses of sea surface temperature, sea ice, and night marine air temperature since the late nineteenth century, *Journal of Geophysical Research*, 108, 4407, 2003.

- Rodrigo, F. S., D. Pozo-Vazquez, M. J. Esteban-Parra, and Y. Castro-Diez, A reconstruction of winter North Atlantic Oscillation index back to A.D. 1501 using documentary data in Southern Spain, *Journal of Geophysical Research*, 106, 14805-14818, 2001.
- Rodwell, M. J., On the predictability of North Atlantic Climate. in *The North Atlantic Oscillation: Climatic Significance and Environmental Impact*, edited by Hurrell, J., Y. Kushnir, G. Ottersen and M. Visbeck, pp. 173-192, American Geophysical Union, Washington, D. C., 2003.
- Rogers, J. C., and M. J. McHugh, On the predictability of the North Atlantic Oscillation and the Arctic Oscillation, *Climate Dynamics*, 19, 599-608, 2002.
- Schmutz, C., J. Luterbacher, D. Gyalistras, E. Xoplaki, and H. Wanner, Can we trust proxy-based NAO index reconstructions?, *Geophysical Research Letters*, 27, 1135-1138, 2000.
- Schoene, B. R., W. Oschmann, J. Rossler, A. D. F. Castro, S. D. Houk, I. Kroncke, W. Dreyer, R. Janssen, H. Rumohr, and E. Dunca, North Atlantic Oscillation dynamics recorded in shells of a long-lived bivalve mollusk, *Geology*, 31, 1037-1040, 2003.
- Schoene, B. R., W. Oschmann, J. Rossler, A. D. F. Castro, S. D. Houk, I. Kroncke, W. Dreyer, R. Janssen, H. Rumohr, and E. Dunca, North Atlantic Oscillation dynamics recorded in shells of a long-lived bivalve mollusk, *Geology*, 31, 1037-1040, 2003.
- Shindell, D. T., R. L. Miller, G. Schmidt, and L. Pandolfo, Simulation of recent northern winter climate trends by greenhouse-gas forcing., *Nature*, 399, 452-455, 1999.
- Smith, S. V., R. W. Buddemeier, R. C. Redalje, and J. E. Houck, Strontium-Calcium Thermometry in Coral Skeletons, *Science*, 204, 404-407, 1979.
- Torrence, C., and G. P. Compo, A Practical Guide to Wavelet Analysis, *Bulletin of the American Meteorological Society*, 79, 61-78, 1998a.
- Torrence, C., and G. P. Compo, Wavelet Software available at <http://paos.colorado.edu/research/wavelets/>. 1998b.
- Torrence, C., and P. J. Webster, Interdecadal Changes in the ENSO-Monsoon System, *Journal of Climate*, 12, 2679-2690, 1999.
- Villenga, M., and P. Wu, Low-latitude freshwater influence on centennial variability of the Atlantic thermohaline circulation, *Journal of Climate*, 17, 4498-4511, 2004.
- Visbeck, M., E. Chassignet, R. Curry, T. Delworth, R. Dickson, and G. Krahmann, The Ocean's Response to North Atlantic Oscillation Variability. in *The North Atlantic Oscillation: Climate Significance and Environmental Impact*, edited by Hurrell, J., Y. Kushnir, G. Ottersen and M. Visbeck, pp. 113-145, American Geophysical Union, Washington, D. C., 2003.

- Visbeck, M., H. Cullen, G. Krahmann, and N. Naik, An oceans model's response to North Atlantic Oscillation like wind forcing., *Geophys. Res. Lett.*, 25, 4521–4524, 1998.
- Visbeck, M. H., J. W. Hurrell, L. Polvani, and H. M. Cullen, The North Atlantic Oscillation: Past, present, and future, *Proceedings of the National Academy of Sciences of the United States of America*, 98, 12876-12877, 2001.





## Chapter 6

### Conclusion

Professor Edward Boyle, in his course work at the Massachusetts Institute of Technology, presents his view of the life cycle of a paleoclimate proxy. Boyle suggests that a paleoproxy is first met with a euphoric response, followed by extended work on developing the proxy. After some time, disillusionment with the proxy sets in as complications are uncovered. Ultimately, a manageable way to use the proxy within a set of boundaries is found. Geochemical climate proxies from corals have befallen this path. Initially, there was much excitement over the application of elemental ratios in corals to generate SST records. Corals yielded high-resolution, long climate records from relatively short archives (up to 3m cores). The shallow depths at which corals grow and the uplifted corals on island atolls meant that sample collection was relatively inexpensive.

However, some disillusionment set in as proxy calibrations changed with each colony, and corals appeared to have significant biological effects complicating the inorganic precipitation. This realization made applying modern calibrations to fossil corals suspect, and combined with coral results showing much larger SST changes back in time compared to other marine proxies, led to criticism of the proxy's reliability.

Compounded with these concerns was the difficulty in sampling and analyzing slow-growing corals (e.g. *Diploria*.), which are the only corals to grow outside of the tropics. Without the incorporation of slow-growing coral records, this paleo-proxy would be very geographically limited.

Slow-growing corals appear to exacerbate some of the problems seen with coral SST reconstructions. Bulk-sampling clearly generates smoothing in the seasonal record, and changes in growth (calcification) rates can further alter this signal back through time. Smoothing of the calibration data can lead to exaggerated SST changes in the past with both mean-annual and winter time SST reconstructions showing inter-annual ranges larger than the modern seasonal cycle. Different seasonal calcification processes can lead to additional biasing in how seasons are resolved through time, further complicating even a mean-annual reconstruction.

In this thesis, I have tried to move beyond some of the disillusionment, and I have found that several of these problems are not insurmountable. Careful calibrations should include consideration of how growth rates have influences both within and between colonies. Multiple colonies regressed simultaneously into one calibration have also greatly improved the calibrations and accuracy of reconstructions, as evaluated by residuals and mean SST values. The use of sub-annual samples averaged into longer (mean-annual, winter-time and multi-year) periods has led to statistically significant reconstructions (temperature changes are larger than zero with uncertainty) with full error propagation that are within the range of many other sea surface temperature reconstructions from around the Atlantic between today and the end of the Little Ice Age. In essence, acknowledging the caveats of the methods – biology is a complicating factor,



sub-sampling must occur at resolutions higher than the reconstructions – as well as the level of significance of these reconstructions, both from the statistical measures of uncertainty and from the evaluation of the regional versus local significance of the record, will allow for robust reconstructions of temperature and salinity.

In this thesis, I was able to reconstruct both mean-annual and winter-time SST. These records show a statistically significant change in temperature between today and the end of the LIA of  $1.6 \pm 0.5$  °C. While this value is within the range of LIA temperature changes generated throughout the Atlantic, proxy reconstructions return temperature changes as varying as 0.5 to 5.0 °C. The range seen throughout the Atlantic implies that regional processes and ocean circulation changes may be at work, serving to amplify and to modify global forcing at specific locations.

Reconstructing salinity proved to be a greater challenge. There is much evidence that the study coral has recorded both temperature and salinity changes within the record of  $\delta^{18}\text{O}$ . The most basic support for this is the large secular trend in the Sr/Ca record which is absent in the  $\delta^{18}\text{O}$ . However, I was unable to quantify the amount of total salinity change with statistical significance. The biggest hurdle to quantifying the salinity impacts may be the limited range of salinity seen at Bermuda during the modern calibration period.

In addition to local conditions, coral geochemistry can also be used to reconstruct records of larger scale climate variability such as the NAO. Coral is one of the best ways in which marine based reconstructions of the NAO can be generated due to the required sub-annual scale. Spectral analysis appears to be a robust tool for evaluating these geochemical records. Our coral record reconstructs the NAO at two frequencies (3-5

years per cycle and 20+ years per cycle). Analysis of this record for time intervals of regionally high and low temperatures shows that while the inter-annual (3-5 years per cycle) behavior does not appear to be changing with increasing temperatures, multi-decadal (20+ years per cycle) behavior appears to exhibit greater amplitude variability during warmer periods, though not a change in the dominant phase of the NAO. In addition, our record shows an increased coherence with atmospheric records during warmer Northern Hemisphere temperatures, which may indicate changing ocean-atmosphere dynamics as the mean climate warms. Unfortunately, with only one ocean record, any conclusion about changes in ocean-atmosphere processes is limited.

The most successful terrestrial based proxy records of the NAO have been generated over large geographical areas and the same will be required to achieve the best marine based record. The record generated in this thesis and that of mollusks collected from the North and Norwegian Seas are a good starting point for generating a larger scale NAO marine reconstruction. Continuing this process with more corals from Bermuda and throughout the Caribbean, as well as mollusk shells and other potential archives from regions beyond coral growth, could lead to a detailed spatial reconstruction of the same caliber of the NAO over the ocean and a better understanding of ocean-atmosphere interactions as a function of different time scales and mean climates.

## Appendix A

### Low Resolution Record Data

Date	Sr/Ca (mmol/mol)	Oxygen Isotope (permil)	Carbon Isotope (permil)	Growth Rate (mm/year)
Top Piece Shown in Fig. 2.1				
1998	9.2979			3.0
1996	9.3292	-3.8893	-2.9911	3.5
1994	9.3597	-3.8397	-3.4800	3.0
1992	9.3192	-3.6193	-3.8701	3.0
1990	9.3328	-3.8947	-3.5190	4.0
1988	9.2888	-3.8743	-3.0571	3.5
1986	9.3053	-3.8717	-3.3430	3.5
1984	9.3064	-3.8663	-3.7201	4.0
1982	9.2820	-3.9817	-3.1140	4.5
1980	9.3450	-3.8833	-3.0621	3.5
1978	9.3121	-3.8387	-3.1290	4.0
1976	9.3234	-3.7833	-2.6311	4.0
1974	9.2956	-3.7687	-2.4520	5.0
1972	9.3285	-3.6043	-2.3511	3.5
1970	9.2825	-3.9737	-2.0860	3.5
1968	9.2913	-3.8613	-2.1351	5.0
1966	9.2668	-3.9253	-2.0051	4.0
1964	9.2489	-3.4195	-1.9811	4.0
1962	9.2624	-4.1607	-2.6560	3.5
1960	9.2660	-3.7843	-1.9181	4.5
1958	9.2305	-3.6517	-1.3560	4.0
1956	9.2358			4.0
1954	9.2431	-3.7907	-2.2820	3.5
1952	9.2282	-3.7553	-2.3141	4.0
1950	9.3042	-3.3297	-2.0040	4.5



<b>Date</b>	<b>Sr/Ca (mmol/mol)</b>	<b>Oxygen Isotope (permil)</b>	<b>Carbon Isotope (permil)</b>	<b>Growth Rate (mm/year)</b>
1948	9.2532	-3.6883	-2.5546	3.5
1946	9.3047	-3.8437	-2.1200	4.5
1944	9.3091	-3.7953	-2.1961	3.5
1942	9.3192	-3.7077	-2.3370	4.0
1940	9.3251	-3.6233	-2.1271	4.5
1938	9.2708	-3.8697	-1.8410	3.5
1936	9.2715	-3.8373	-1.7541	4.5
1934	9.2880	-3.7287	-1.7550	3.5
1932	9.2755	-3.7749	-1.7207	4.0
1930	9.2294	-3.6707	-1.3460	4.5
1928	9.2801	-3.8593	-2.0631	3.5
1926	9.2770	-3.3837	-1.1030	3.0
1923	9.2691	-3.5083	-1.5551	5.3
1921	9.2673	-3.7867	-1.9940	4.5
1919	9.3128	-3.6693	-1.3031	3.0
1917	9.2841	-3.6345	-1.3696	4.5
1915	9.2635	-3.4567	-1.3380	4.0
1913	9.2636	-3.6203	-1.7021	4.0
1911	9.2597	-3.5777	-2.0150	6.0
1909	9.2478	-3.5543	-1.5141	4.0
1907	9.2670	-3.6167	-1.9760	4.0
1905	9.3128	-3.7003	-1.3941	4.0
1903	9.2778	-3.6627	-1.5950	5.0
1901	9.2974	-3.7043	-1.4881	3.5
1899	9.2664	-3.7043	-1.4881	4.0
1897	9.3082	-3.5577	-1.3570	3.5
1895	9.2954			3.5
1893	9.2835			4.0

Middle piece seen in Fig. 2.1

1921	9.2979	2.5
1919	9.3337	5.0
1917	9.2710	5.0
1915	9.2499	3.0
1913	9.3213	4.5
1911	9.2916	5.0
1909	9.3048	4.5
1907	9.3442	4.5

Date	Sr/Ca (mmol/mol)	Oxygen Isotope (permil)	Carbon Isotope (permil)	Growth Rate (mm/year)
1905	9.3783			3.5
1903	9.2801			4.5
1901	9.2793	-3.7865	-1.6076	4.5
1899	9.3204	-3.0363	-0.7451	4.0
1897	9.3076	-3.3477	-0.8870	3.5
1895	9.2885	-3.6623	-1.4211	3.5
1893	9.2945	-3.4297	-1.2630	4.0
1891	9.3133	-3.4393	-1.6501	4.5
1889	9.3088	-3.5367	-1.7250	4.5
1887	9.2890	-3.5673	-1.6271	4.5
1885	9.3089	-3.1147	-1.3490	3.5
1883	9.3167	-3.4843	-1.5481	5.0
1881	9.3258	-3.4467	-1.6290	4.0
1879	9.2863	-3.5523	-1.3461	3.5
1877	9.2798	-3.4087	-1.3490	3.0
1875	9.3000	-3.4983	-1.6431	4.5
1873	9.2926	-3.3447	-2.2560	3.0
1871	9.3162	-3.4683	-2.0141	4.0
1869	9.3089	-3.4670	-1.7426	4.0
1867	9.3187	-3.5737	-1.7230	3.0
1865	9.3169	-3.4953	-1.8301	2.5
1863	9.3431	-3.5277	-1.4910	2.5
1861	9.3517	-3.3083	-1.8811	3.0
1859	9.4036	-3.5857	-1.6420	3.0
1857	9.3456	-3.3153	-1.4941	3.0
1855	9.3370	-3.3947	-1.7110	3.5
1853	9.3513	-2.9393	-1.3841	3.0
1851	9.3567	-3.7517	-2.4050	2.0
1849	9.3588	-3.2325	-1.1601	3.0
1847	9.3585	-3.4853	-1.0641	3.0
1845	9.3400	-3.4037	-1.6090	2.5
1843	9.3896	-3.4723	-1.2661	2.0
1841	9.3877	-3.4847	-1.2990	3.5
1839	9.3341	-3.6533	-1.2621	3.5
1837	9.3660	-3.3297	-0.9610	3.0
1835	9.3064	-3.3613	-0.8331	5.0
1833	9.3541	-3.7287	-0.8780	3.0
1831	9.2950	-3.2393	-1.3471	3.0

Date	Sr/Ca (mmol/mol)	Oxygen Isotope (permil)	Carbon Isotope (permil)	Growth Rate (mm/year)
1829	9.3146	-3.5835	-1.0366	4.0
1827	9.3420	-3.6957	-1.3730	4.0
1825	9.3390	-3.3313	-1.2261	4.0
1823	9.3405	-3.3997	-1.7790	4.5
1821	9.3332	-3.6103	-1.3051	4.5
1819	9.3420			3.0
1817	9.3371			3.0

Bottom piece seen in Fig. 2.1

1837	9.3405			2.0
1835	9.3048			3.0
1833	9.3153			3.0
1831	9.3503			3.0
1829	9.3228			3.5
1827	9.2835			3.0
1825	9.3193			4.5
1823	9.2815			4.0
1821	9.3049	-3.4517	-1.3030	4.5
1819	9.3218	-3.5400	-1.3641	3.5
1817	9.2942	-3.5993	-1.1221	4.5
1815	9.3288	-3.5927	-1.5010	4.0
1813	9.3362	-3.3733	-1.2041	3.5
1811	9.2955	-3.5117	-1.4410	4.5
1809	9.2829	-3.4083	-1.0371	4.5
1807	9.3284	-3.4937	-1.2280	3.5
1805	9.3374	-3.3903	-1.1911	4.5
1803	9.3147	-3.6247	-1.5080	4.5
1801	9.3042	-3.7073	-1.3591	4.5
1799	9.3213	-3.6070	-0.7661	4.0
1797	9.3524	-3.5427	-0.8120	4.0
1795	9.3202	-3.7033	-1.3031	3.5
1793	9.2970	-3.7407	-1.1690	4.5
1791	9.3049	-3.3933	-1.1161	2.5
1789	9.2944	-3.3957	-1.2240	3.0
1787	9.3240	-3.0413	-1.0611	4.5
1785	9.3336	-3.5527	-1.2840	3.5
1783	9.2934	-3.5843	-1.3161	4.5



<b>Date</b>	<b>Sr/Ca (mmol/mol)</b>	<b>Oxygen Isotope (permil)</b>	<b>Carbon Isotope (permil)</b>	<b>Growth Rate (mm/year)</b>
1781	9.2929	-3.5967	-1.1150	5.5
1779	9.2775	-3.6037	-1.3600	6.5
1777	9.3021	-3.5513	-1.3011	3.5



## Appendix B

### Sr/Ca Measurements

#### B.1 Sr/Ca Long-Term Drift Correction

Strontium and calcium measurements were made simultaneously on an Inductively Coupled Plasma – Atomic Emission Spectrometer (ICP-AES). The measurement of the high resolution (~monthly) record (HRR) from coral BB 001 presented in Chapters four and five took place from September 2005 to February 2006. Corrections were applied to raw data each day for error stemming from drift during the run and matrix interference, using solution standards (Schrag, 1999). Additionally, samples from a *Porites* coral (powder standard) which had been crushed and homogenized were prepared simultaneously with unknowns and measured randomly throughout each run to evaluate precision of the instrumentation through time.

During the measurements of the HRR, six hundred and seventy-three powder standard measurements were made with an average value of 0.01951 ppm Sr / ppm Ca (8.9231 mmol Sr / mol Ca), a standard deviation of 0.00004585 ppm Sr / ppm Ca or a relative standard deviation of 0.24% (n=646). On average, 16 powder standards were run



for every 100 unknowns. In addition, entire runs of powder standard were measured in advance of a series of days on which unknowns were measured.

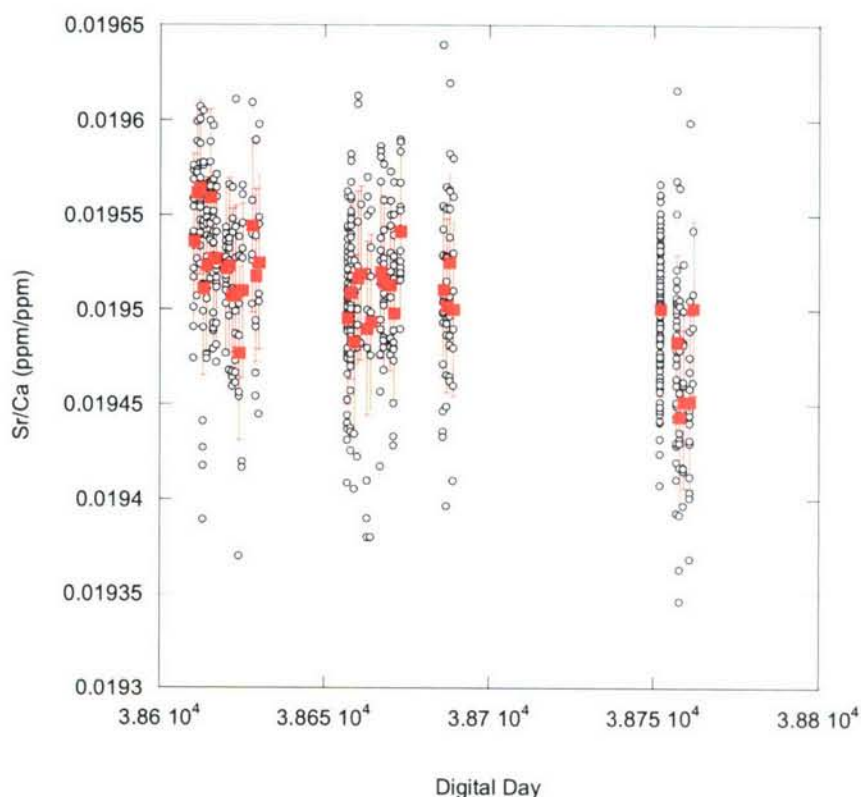


**Figure B.1:** Coral powder standard Sr/Ca (ppm/ppm) values are plotted versus digital day, with each measurement (circle) and the daily average (square) with one standard deviation error bars. The range of Sr/Ca seen on any given day remains relatively consistent through time, while the daily average shows a distinct drop in the last group of days.

Over the six months during which measurements occurred, there appears to be a slight drift in the Sr/Ca value (Fig. B.1). Primarily, this drift is driven by a drop in the average value seen in the last runs during February 2006. The first two hundred and twelve samples of the HRR were re-sampled and re-measured after completion of the measurements, and therefore, unlike the other measurements of this record, the first set was not fully randomized into the measuring sequence with the rest of the record. While

the range of powder standard values measured in Feb. is equivalent to those seen throughout the measurements and the offset in these measurements is small ( $\sim 0.00004$ ), on order of one standard deviation, the re-measurement of the first samples at this time may have contributed to an offset or bias in the HRR record.

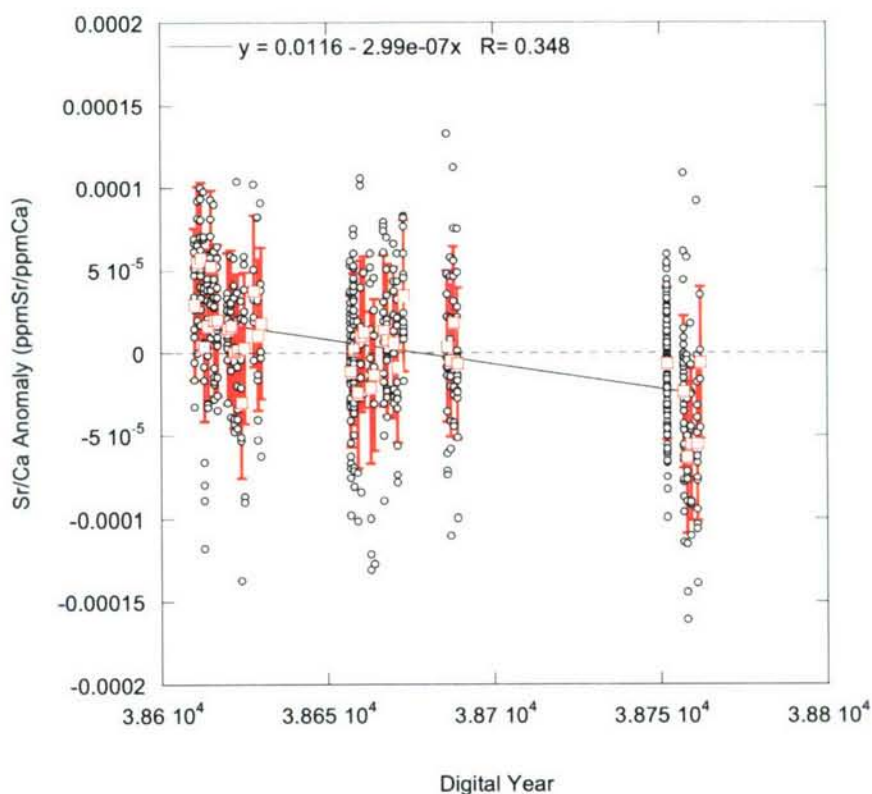


**Figure B.2:** Sr/Ca anomaly versus digital day for each measurement (circles) and the daily average (square) with one standard deviation error bars on daily average. A linear regression of Sr/Ca on time shows a trend of decreasing anomalies with time.

In order to eliminate an artifact from this drift in the standards, a correction was applied to all data which were run from Sept. 2005-Feb. 2006. The correction is defined by a Sr/Ca anomaly calculated by subtracting the average Sr/Ca (ppm/ppm) values from

each individual value, which is linearly regressed against time (Fig. B.2). The linear regression returned the following result:

$$\text{Sr/Ca Anom.} = -2.99\text{E-}7 (\pm 3.17\text{E-}8) * (\text{digital day}) - 0.0116 (\pm 0.0012) \\ (\sigma, 95\% \text{ confidence, } F_{\text{sig}}=7.85\text{E-}20, r^2=0.12) \quad (1)$$

This calculated Sr/Ca anomaly per day was then used to correct for the long-term drift in the standards. While this correction is two orders of magnitude smaller than our seasonal signal and generally smaller than the standard deviation, I believe that it removes any questions that may have arisen from lack of randomization of the first 200 samples from the rest of the record.

## B.2 References

Schrag D. P. (1999) Rapid analysis of high-precision Sr/Ca ratios in corals and other marine carbonates. *Paleoceanography* **14**(2), 97-102.



## Appendix C

# Stable Oxygen and Carbon Isotope Measurements

### C.1 Introduction

Stable isotopic data was measured on relatively small samples ranging from 10-30  $\mu\text{g}$ . Under these conditions, the mass spectrometer system is performing at its stability limits. As the sample size and subsequent voltage decreases, the flow through the capillaries can be altered impacting the isotopic measurement in the source. Additionally, the adjustable standard bellows malfunctioned during the generation of this record which led to significantly unbalanced sample/standard voltage on measurements on several days of runs. Unbalanced voltages between the sample and standard scans, which primarily occurred at relatively large voltages, appear to have impacted the isotopic values. Therefore, an analysis of external powder standards was conducted to evaluate the influence of these two effects – small sample size and sample-standard imbalance – on the measurements of unknowns.

Three external standards were used for this analysis: B1-2 (a Pee Dee Belemnite), carrara marble, and estremoze marble. Estremoze has a  $\delta^{18}\text{O}$  value of -5.98‰ relative to Vienna Pee Dee Belemnite (VPDB) with a standard deviation of 0.11‰ and a  $\delta^{13}\text{C}$  value of 1.63‰ relative to VPDB with a standard deviation of 0.07‰. These values are close

in isotopic composition to corals used in this study. B1-2 has a  $\delta^{18}\text{O}$  value of 0.17‰ relative to VPDB with a standard deviation of 0.14‰ and a  $\delta^{13}\text{C}$  of 0.66‰ relative to VPDB with a standard deviation of 0.15‰. Finally, carrara marble has  $\delta^{18}\text{O}$  value of -1.99‰ relative to VPDB with a standard deviation of 0.12‰ and  $\delta^{13}\text{C}$  value of 2.01‰ relative to VPDB with a standard deviation of 0.14‰.

## C.2: Small Sample Measurements

Small samples are defined as those analyses producing source pressure voltages of less than 0.800V (Ostermann and Curry, 2000), a signal intensity that results from ~15µg of  $\text{CaCO}_3$ . All samples generating a voltage of <0.400V are considered too small for inclusion in the dataset. As can be seen in Figure C.1, the oxygen isotope measurements show a large range (0.8‰) for all three standards (Fig. C.1a,b,c) with a group standard deviation of 0.18‰. As voltage decreases all three standards show trends of increasing isotopic values and in looking at all the measurements as a group (Fig C.1d) the same trend is found. Fitting a least squares regression on the data as a group (Fig. C.1d) returns the following equations:

$$\text{Oxygen Anomaly} = -0.565 (\pm 0.182) * (\text{sample voltage}) + 0.444 (\pm 0.116)$$

$$(\sigma, 95\% \text{ confidence, } F_{\text{sig}}=0.0027, r^2=0.12, n=73) \quad (1)$$

Carbon measurements show decreased scatter relative to oxygen and in general a diminished trend of increasing anomalies relative to decreasing voltages (Fig. C.2). The measurements show a spread of 0.5‰ with a standard deviation of 0.10‰. B1-2 (Fig. C.2a) shows an increasing trend of the same magnitude as the oxygen measurements (Fig. C.1a), but carrara (Fig. C.2b), estremoza (Fig. C.2c) and the group as a whole (Fig.

C.2d) all show a reduced trend relative to oxygen. Fitting a least squares regression on the data as a group (Fig. C.2d) returns the following equations:

$$\text{Carbon Anomaly} = -0.339 (\pm 0.106) * (\text{sample voltage}) + 0.223 (\pm 0.068)$$

$$(\sigma, 95\% \text{ confidence, } F_{\text{sig}}=0.0020, r^2=0.13, n=71) \quad (2)$$

Finally, if mass fractionation was occurring at these small voltages a 2:1 relationship of oxygen:carbon would be expected. The expected impact of mass fractionation on carbon and oxygen measurements is not found (Fig. C.3). B1-2 (Fig. C.3a) shows no relationship between the carbon anomaly and the oxygen anomaly. A very similar relationship is found for carrara and estremoiz with an oxygen:carbon ratio of ~1.5 (Fig. C.2b,c). Carrara and estremoiz fall short of this 2:1 ratio as does the group fit (Fig. C.2d) and the lack on any relationship for B1-2 do not provide an strong indication that mass fractionation is occurring.

In conclusion, while there is limited evidence for mass fractionation, the clear trends in the small standard data allow for correction of small samples. Therefore, all sample data with voltage >0.400V and <0.800V are corrected by calculating the anomaly relative to zero as predicted by the sample voltage in equations 1 & 2 and adding it to the isotope value.. Applying these corrections to the standard data minimally improve the standard deviation for the oxygen anomalies to 0.17‰ from 0.18‰, while successfully removing the trend found in the anomalies (Fig. C.4a). A similar result is found for the carbon anomalies with a standard deviation improvement to 0.095‰ from 0.102‰ with a successful removal of the trend (Fig. C.4b). Two hundred and nine samples out of 2,332 total samples or 9.0% of the long, high-resolution record have voltages that are less than 0.800 V and greater than 0.400 V.



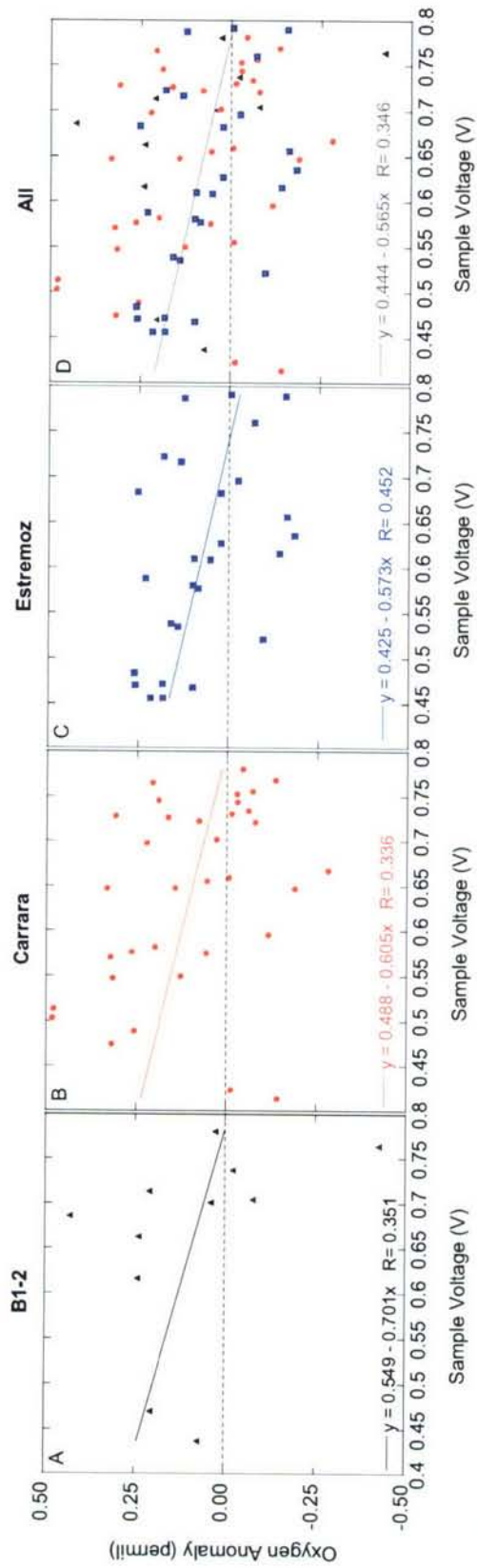


**Figure C.1:** Oxygen anomaly versus sample voltage (0.4-0.8V) for a) B1-2, b) carrara, c) estremoz, and d) all.

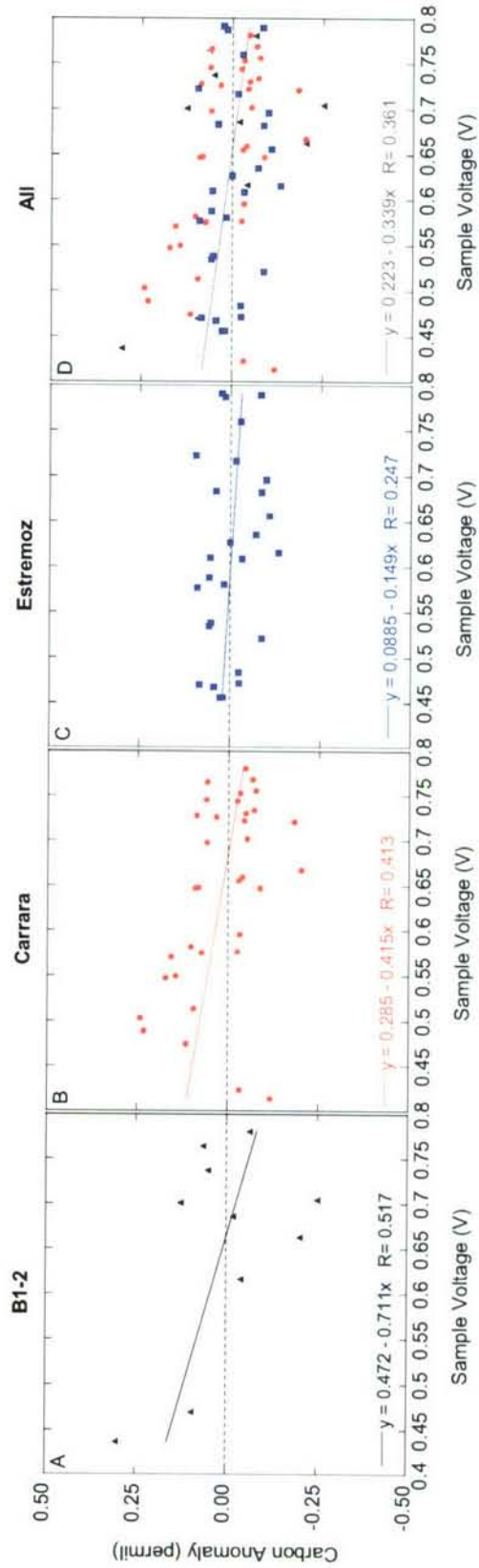


**Figure C.2:** Carbon anomaly versus sample voltage (0.4-0.8V) for a) B1-2, b) carrara, c) estremoz, and d) all.

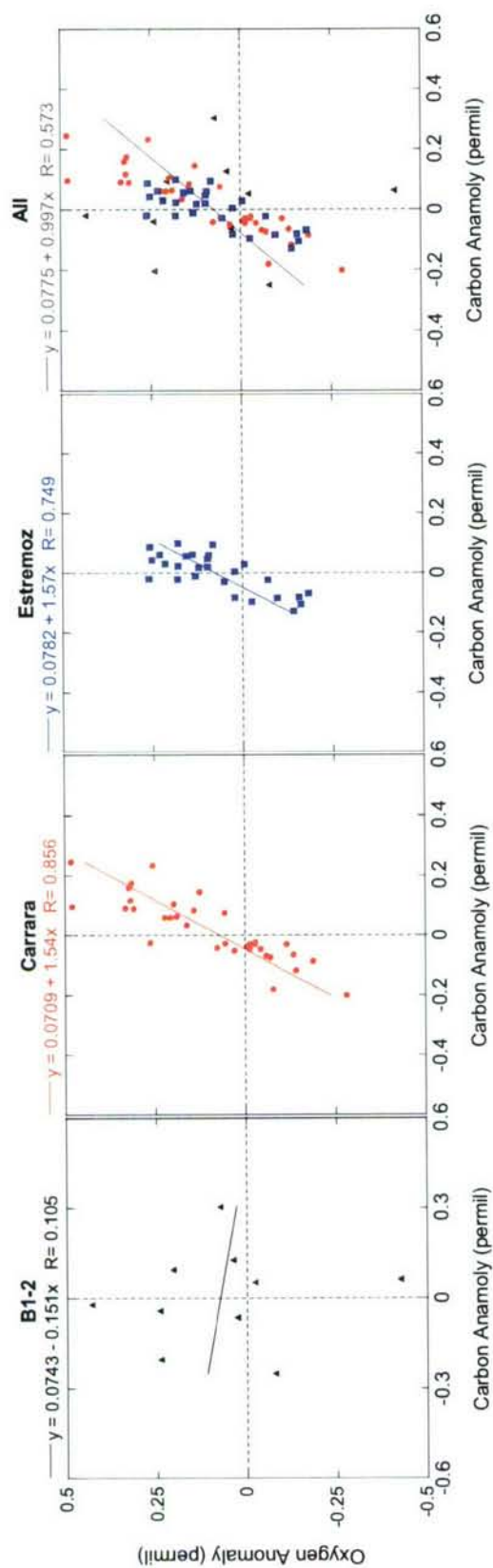


**Figure C.3:** Oxygen anomaly versus carbon anomaly for sample voltage (0.4-0.8V) for a) B1-2, b) carrara, c) estremoz, and d) all.

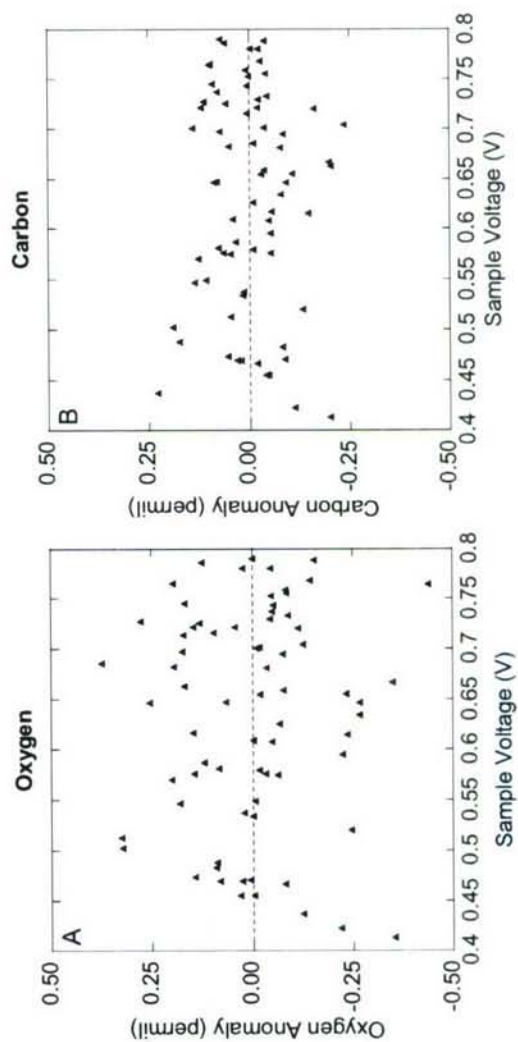


**Figure C.4:** Corrected anomaly versus sample voltage for a) oxygen and b) carbon.

### C.3: Unbalanced Sample Measurements

The second source of an increased standard deviation in the dataset is unbalanced sample/standard voltage data. Unbalanced data resulted from two causes. The majority resulted from a jammed pin in the bellows preventing the bellows from properly adjusting for larger voltage samples. The second source of error was samples larger than  $\sim 35\mu\text{g}$  that were run using a sample method optimized for samples smaller than  $30\mu\text{g}$  (lower maximum reference gas pressure, greater balancing accuracy and small voltage correction).

The standard deviation on all of the “non-small” oxygen anomalies for B1-2, carrara, and estremoza is  $0.10\text{‰}$  and for carbon is  $0.11\text{‰}$ . As can be seen in Fig. C.5, there is an increasing trend in oxygen measurements that have a sample/standard voltage ratio of  $>1.1$ , the normal cut off for an acceptable measurement. B1-2 (Fig. C.5a) and estremoza (Fig. C.5c) show similar trends with slopes in proximity to  $0.1$  (permil/(sample/standard voltage)). Carrara (Fig. C.5b) does not show as strong a trend, but the measurements are still positively offset from mean values. As a group (Fig. C.5d), the data does show an upward trend as samples become increasingly unbalanced. Beyond a sample standard voltage ratio of  $2.5$  these relationships fall apart. Therefore, measurements with an unbalance of greater than  $2.5$  have been removed from the dataset. Fitting a least squares regression to the remaining data returns the following equation:

$$\text{Oxy. Anom.} = 0.0967 (\pm 0.0148) * (\text{sample voltage/standard voltage}) - 0.0547 (\pm 0.0225)$$

$$(\sigma, 95\% \text{ confidence, } F_{\text{sig}}=8.02\text{E-}10, r^2=0.21, n=164)(3)$$



After applying this correction equation to all the non-small data the standard deviation is reduced from 0.10 to 0.09 and as can be seen in Fig. C.6 removes the trend from the unbalanced anomalies. Therefore, this correction is applied to the unknowns by calculating the expected anomalies based on the sample/standard voltage and then adding it to the measured value.

Similar results are found for carbon measurements (Fig. C.7). Each standard has an increasing trend as the sample/standard voltage increases. B1-2 (Fig. C.7a) has the sharpest slope at 0.135, but the largest spread of both positive and negative anomalies. Carrara (Fig. C.7b) and estremoza (Fig. C.7c) show all positive anomalies with slopes of 0.0361 and 0.0603 respectively. Fitting a least squares regression on the data as a group (Fig. C.7d) returns the following equations:

$$\text{Carbon Anom.} = 0.0620 (\pm 0.0108) * (\text{sample voltage/standard voltage}) - 0.0374 (\pm 0.0164) \\ (\sigma, 95\% \text{ confidence, } F_{\text{sig}}=4.54\text{E-}8, r^2=0.17, n=174) \quad (4)$$

After applying this correction equation to the data the standard deviation on all non-small carbon measurements is reduced from 0.11 to 0.10 and as can be seen in Fig. C.8 removes the trend from the unbalanced anomalies. Therefore, this correction is applied to the unknowns by calculating the expected anomalies based on the sample/standard voltage and then adding it to the measured value. .

These corrections were applied to 267 out of 2,332 samples or 11% of the record.

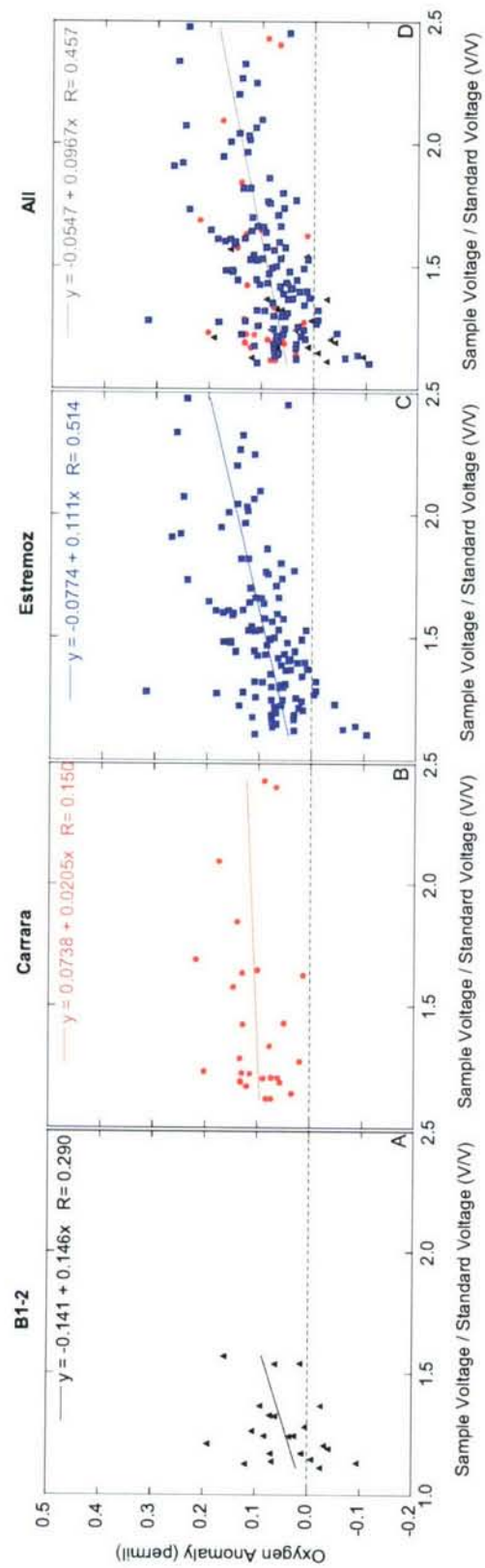


**Figure C.5:** Oxygen anomaly versus sample/standard voltage for a) B1-2, b) carrara, c) estremoz, and d) all.

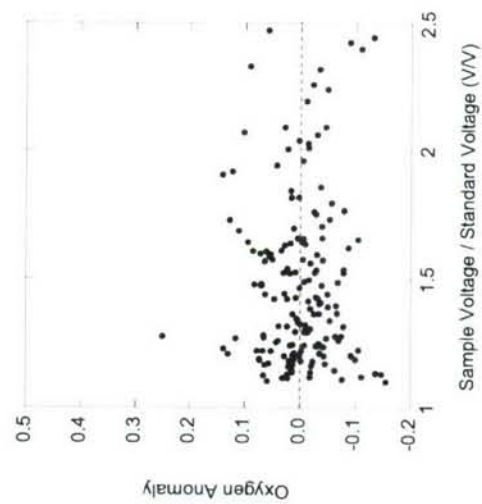


**Figure C.6:** Corrected oxygen anomaly versus sample/standard voltage.

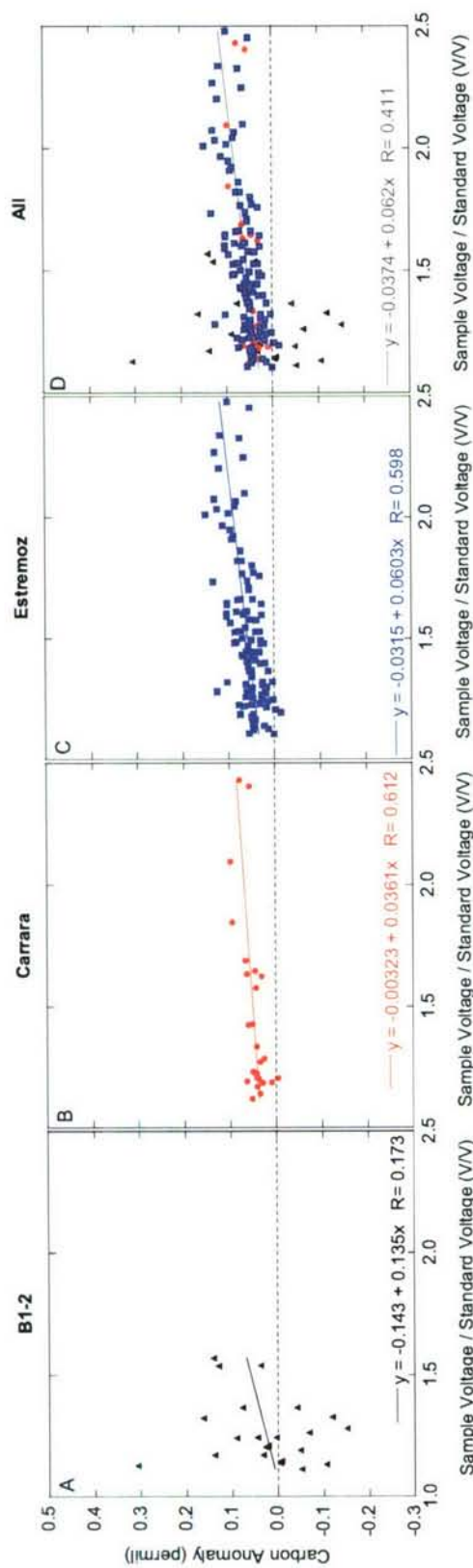


**Figure C.7:** Carbon anomaly versus sample/standard voltage for a) B1-2, b) carrara, c) estremoz, and d) all.

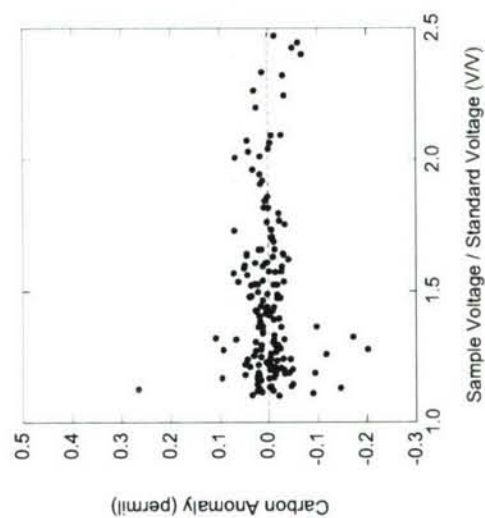


**Figure C.8:** Corrected carbon anomaly versus sample/standard voltage.



## **C.5: Conclusion**

In conclusion, before corrections all (n=660) of the oxygen standards have a standard deviation of 0.11‰. After both the small voltage and imbalance correction the standard deviation of the oxygen anomalies is 0.10‰. The carbon anomalies as a group have a lower standard deviation of 0.098‰ compared to an initial standard deviation of 0.105‰. While these changes are small, successful removal of trends in the standards which may be introduced due to measurements based on sample size or voltage imbalances (Figs. C.4, C.6, & C.8).

## **C.6: References**

Ostermann D. R. and Curry W. B. (2000) Calibration of stable isotopic data: An enriched  $\delta^{18}\text{O}$  standard used for source gas mixing detection and correction. *Paleoceanography* 15(3), 353-360.

## Appendix D

### High Resolution Record Data

Depth from Top of Coral (mm)	Sr/Ca (mmol/mol)	Oxygen Isotope (permil)	Carbon Isotope (permil)	Date
Top Piece Shown in Fig. 2.1				
0.0	9.2182			1999.67
0.3	9.1727	-3.6895	-3.4854	1999.58
0.7	9.1668	-3.7770	-3.1513	1999.50
1.0	9.0830	-4.0976	-3.5943	1999.42
1.3	9.0325	-4.4030	-3.8533	1999.33
1.7	9.0764	-4.2346	-3.9273	1999.25
2.0	9.1053	-4.2117	-3.4747	1999.17
2.3	9.1677	-3.9966	-3.0993	1999.08
2.7	9.2170	-3.6615	-2.6552	1999.00
3.0	9.4285	-3.2186	-2.0723	1998.92
3.3	9.3930	-3.2430	-2.1803	1998.83
3.7	9.2879			1998.75
4.0	9.1840	-3.8110	-2.4413	1998.67
4.3	9.1181	-4.1476	-2.5913	1998.58
4.7	9.1341	-4.0774	-3.0427	1998.50
5.0	9.1001	-4.2616	-3.1363	1998.42
5.3	9.1731	-3.7516	-2.5464	1998.33
5.7	9.3963	-3.4586	-2.1753	1998.25
6.0	9.5252	-3.1950	-2.1549	1998.17
6.3	9.4292	-3.2686	-2.2903	1998.08
6.7	9.3520	-3.2810	-2.4933	1998.00
7.0	9.3029	-3.4246	-2.6113	1997.92
7.3	9.1952	-3.9940	-2.7433	1997.83
7.7	9.0981	-3.8096	-2.8963	1997.73
8.0	9.0851	-4.0500	-2.7793	1997.63
8.3	9.1712	-3.9136	-2.9663	1997.56
8.7	9.1646	-3.7013	-3.0063	1997.49
9.0	9.3718	-3.2362	-2.2957	1997.42
9.3	9.4268	-2.9925	-1.6898	1997.17

Depth from Top of Coral (mm)	Sr/Ca (mmol/mol)	Oxygen Isotope (permil)	Carbon Isotope (permil)	Date
9.7	9.3968	-3.2186	-1.8013	1996.96
10.0	9.2042	-3.6670	-1.9103	1996.87
10.3	9.1689	-3.6976	-1.6793	1996.75
10.7	9.2062	-3.5220	-2.0713	1996.71
11.0	9.1329	-3.9756	-2.4493	1996.67
11.3	9.2316	-3.7052	-2.5437	1996.46
11.7	9.2514	-3.3926	-2.1933	1996.40
12.0	9.4069	-2.9450	-1.5613	1996.33
12.3	9.4216	-2.9136	-1.5043	1996.17
12.7	9.3743	-3.3040	-2.3983	1996.00
13.0	9.2014	-3.6286	-2.5283	1995.83
13.3	9.1697	-3.7500	-2.8893	1995.75
13.7	9.1311	-4.1076	-2.7933	1995.63
14.0	9.1681	-3.9160	-2.5483	1995.53
14.3	9.2348	-3.5200	-2.5383	1995.47
14.7	9.3996			1995.42
15.0	9.4906	-3.4114	-2.3575	1995.21
15.3	9.3948	-3.2700	-2.4633	1995.00
15.7	9.3070	-3.4826	-2.8163	1994.89
16.0	9.2112	-3.8500	-3.1843	1994.78
16.3	9.0455	-4.0956	-3.2313	1994.67
16.7	9.0968	-3.9337	-2.8023	1994.63
17.0	9.0508	-4.1286	-2.9483	1994.58
17.3	9.1320	-4.0320	-3.0773	1994.53
17.7	9.2310	-3.8027	-3.1758	1994.47
18.0	9.3425	-3.5290	-2.9553	1994.42
18.3	9.3730	-3.2283	-2.2967	1994.33
18.7	9.4301	-3.3190	-2.1773	1994.21
19.0	9.2801	-3.4506	-2.5663	1993.92
19.3	9.2130	-3.9460	-2.5983	1993.88
19.7	9.1161	-4.0656	-3.0643	1993.71
20.0	9.0813	-4.0565	-3.2222	1993.63
20.3	9.1609	-3.8953	-2.9334	1993.58
20.7	9.2953	-3.3990	-2.0643	1993.50
21.0	9.4074			1993.42
21.3	9.4651	-3.0750	-2.1913	1993.17
21.7	9.4437	-3.1916	-2.1363	1993.04
22.0	9.3038	-3.6450	-2.4263	1992.88
22.3	9.1764	-3.7516	-2.6463	1992.81
22.7	9.1036	-4.1661	-2.8119	1992.75
23.0	9.0733	-3.9386	-2.7823	1992.63
23.3	9.1088	-4.0530	-2.9353	1992.58
23.7	9.2121	-3.9406	-3.0133	1992.54
24.0	9.3610	-3.2860	-2.5633	1992.50



Depth from Top of Coral (mm)	Sr/Ca (mmol/mol)	Oxygen Isotope (permil)	Carbon Isotope (permil)	Date
24.3	9.4637	-3.0212	-2.3133	1992.25
24.7	9.4135	-3.1050	-2.2264	1992.21
25.0	9.4822	-3.1699	-2.5432	1992.17
25.3	9.3262	-3.2568	-2.5645	1991.92
25.7	9.2766	-3.6626	-3.1063	1991.83
26.0	9.1330	-4.0030	-3.2743	1991.73
26.3	9.0986	-4.2136	-3.2843	1991.63
26.7	9.1711	-4.0060	-2.8453	1991.50
27.0	9.2142	-4.0226	-3.0763	1991.46
27.3	9.3053	-3.4070	-2.6113	1991.42
27.7	9.4284	-3.1526	-2.2013	1991.31
28.0	9.4715	-3.3510	-2.3043	1991.21
28.3	9.4114	-3.4676	-2.5303	1991.04
28.7	9.2526	-3.8240	-2.8023	1990.92
29.0	9.1843	-3.9216	-2.7623	1990.83
29.3	9.1260	-3.9851	-2.7756	1990.75
29.7	9.1412	-4.2406	-2.9843	1990.73
30.0	9.2256	-3.9100	-3.1393	1990.71
30.3	9.1455	-4.0116	-3.1663	1990.69
30.7	9.0999	-4.1280	-3.4013	1990.67
31.0	9.1772	-3.5416	-3.1603	1990.50
31.3	9.3255	-3.2010	-2.7003	1990.42
31.7	9.3178	-2.9876	-2.5273	1989.88
32.0	9.2187	-3.5590	-2.7053	1989.83
32.3	9.1606	-3.6516	-3.2363	1989.81
32.7	9.1822	-3.9130	-3.0533	1989.79
33.0	9.1352	-4.0786	-3.3083	1989.77
33.3	9.1383	-3.9380	-2.8623	1989.75
33.7	9.0743	-3.9046	-2.9873	1989.58
34.0	9.1771	-3.8780	-3.0963	1989.50
34.3	9.3277	-3.3626	-2.0663	1989.42
34.7	9.4477	-3.2210	-1.8013	1989.25
35.0	9.4611	-3.3376	-2.3923	1989.17
35.3	9.3624	-3.3103	-2.5643	1988.92
35.7	9.3087	-3.5406	-3.1363	1988.88
36.0	9.2231	-3.4449	-3.5036	1988.83
36.3	9.3111	-3.6696	-3.3503	1988.79
36.7	9.2266	-4.0300	-3.2033	1988.75
37.0	9.2259	-3.9586	-3.3693	1988.71
37.3	9.1951	-3.7555	-3.3093	1988.67
37.7	9.2727			1988.56
38.0	9.2687	-3.6150	-2.3163	1988.46
38.3	9.4192	-3.6476	-2.4923	1988.42
38.7	9.4727	-2.9916	-1.7965	1988.25

Depth from Top of Coral (mm)	Sr/Ca (mmol/mol)	Oxygen Isotope (permil)	Carbon Isotope (permil)	Date
39.0	9.4692	-3.5106	-2.1283	1988.14
39.3	9.4224	-3.3445	-2.1713	1988.03
39.7	9.2770	-3.5726	-2.5423	1987.88
40.0	9.2435	-3.5520	-2.5413	1987.87
40.3	9.1239	-3.9396	-2.8683	1987.79
40.7	9.1130	-4.1400	-3.1413	1987.58
41.0	9.1443	-3.9856	-3.4313	1987.53
41.3	9.3214	-3.2880	-2.6773	1987.42
41.7	9.3456	-3.5649	-2.9644	1987.42
42.0	9.4529	-3.4460	-3.1923	1987.25
42.3	9.4597	-3.2456	-2.9971	1987.21
42.7	9.2989	-3.5004	-3.4112	1987.00
43.0	9.2159			1986.87
43.3	9.1676	-3.9710	-3.6033	1986.83
43.7	9.1677	-4.2746	-3.7973	1986.75
44.0	9.0145	-4.0900	-3.2683	1986.63
44.3	9.1485	-4.2506	-3.1193	1986.64
44.7	9.2321	-4.1613	-3.4748	1986.61
45.0	9.1491	-4.0636	-3.0633	1986.58
45.3		-3.7840	-2.9553	1986.54
45.7	9.2621	-3.4676	-3.1149	1986.50
46.0	9.3776	-3.0510	-2.5363	1986.33
46.3	9.3874	-3.2976	-2.8043	1986.08
46.7	9.3424	-3.6280	-3.5823	1986.00
47.0		-3.6506	-3.6923	1985.90
47.3	9.1649	-3.6920	-3.4593	1985.79
47.7	9.1007	-3.9786	-3.3983	1985.71
48.0	9.1166	-4.2470	-3.5553	1985.75
48.3	9.0777	-4.2186	-3.4243	1985.71
48.7	9.0324	-4.3240	-3.6343	1985.67
49.0	9.0968	-4.2476	-3.6593	1985.63
49.3	9.0873	-3.9722	-3.1085	1985.54
49.7	9.2748	-3.5659	-2.6741	1985.45
50.0	9.4336	-3.1660	-2.4863	1985.30
50.3	9.4739	-3.0436	-2.3123	1985.21
50.7	9.4271	-3.3410	-2.8193	1985.04
51.0	9.4048	-3.1836	-2.8053	1984.98
51.3	9.3753	-3.4790	-2.8873	1984.92
51.7	9.2314	-3.9216	-3.6583	1984.79
52.0	9.2122	-3.8480	-3.7583	1984.79
52.3	9.1782	-4.1486	-3.6483	1984.75
52.7	9.0454	-3.9810	-3.2013	1984.67
53.0	9.0871	-4.1796	-3.6273	1984.58
53.3	9.2159			1984.50

Depth from Top of Coral (mm)	Sr/Ca (mmol/mol)	Oxygen Isotope (permil)	Carbon Isotope (permil)	Date
53.7	9.3083	-3.3216	-2.2233	1984.42
54.0	9.3999	-3.1990	-2.0373	1984.13
54.3	9.3697	-3.4727	-2.9933	1983.96
54.7	9.3591	-3.4810	-2.8813	1983.92
55.0	9.3552	-3.6806	-2.9378	1983.88
55.3	9.1573			1983.79
55.7	9.1389	-3.9845	-3.2377	1983.78
56.0	9.0408	-4.2603	-3.7096	1983.72
56.3	8.9937	-4.1639	-3.5060	1983.63
56.7	9.1394	-4.2430	-3.0533	1983.54
57.0	9.1402	-4.2276	-3.3633	1983.53
57.3	9.3445	-3.3011	-2.0497	1983.42
57.7	9.4756	-2.9426	-1.4783	1983.29
58.0	9.4320	-3.2680	-2.2713	1983.00
58.3	9.4058	-3.4216	-2.4843	1982.97
58.7	9.3357	-3.3660	-2.7013	1982.94
59.0	9.2855	-3.6726	-3.2463	1982.92
59.3	9.1554	-4.0490	-3.0223	1982.85
59.7	9.1161	-4.3126	-3.1993	1982.79
60.0	9.0031	-4.3817	-3.2306	1982.67
60.3	9.0653	-4.3740	-3.1763	1982.65
60.7	9.0545	-4.0456	-2.2113	1982.63
61.0	9.1510	-4.0592	-2.3687	1982.60
61.3	9.1385	-3.6366	-2.1463	1982.54
61.7	9.5236	-3.1703	-1.2686	1982.25
62.0	9.4590	-3.0652	-1.3311	1982.17
62.3	9.5011	-3.0273	-2.0508	1982.08
62.7	9.4263	-3.0696	-2.1686	1981.96
63.0	9.3373	-3.5006	-2.6883	1981.85
63.3	9.2749	-3.4766	-3.1713	1981.74
63.7	9.1327	-3.8226	-2.5903	1981.63
64.0	9.1570	-4.0397	-3.3426	1981.60
64.3	9.1414	-3.8886	-2.8363	1981.54
64.7	9.1800	-3.6300	-2.3343	1981.48
65.0	9.4467	-3.2868	-1.8761	1981.38
65.3	9.3998	-3.0780	-1.8823	1981.31
65.7	9.6123	-2.9743	-2.0412	1981.21
66.0	9.6079	-3.0370	-1.9303	1981.04
66.3	9.3885	-3.0661	-2.0970	1981.00
66.7	9.2433	-3.4450	-2.1693	1980.88
67.0	9.1626	-3.9069	-2.7306	1980.83
67.3	9.1828	-4.0219	-2.7950	1980.71
67.7	9.1524	-4.0090	-2.4682	1980.50
68.0	9.1636	-4.0616	-2.4572	1980.47



Depth from Top of Coral (mm)	Sr/Ca (mmol/mol)	Oxygen Isotope (permil)	Carbon Isotope (permil)	Date
68.3		-3.4798	-1.6598	1980.40
68.7	9.3193	-3.3800	-1.5213	1980.38
69.0	9.5056	-2.8698	-1.2844	1980.33
69.3	9.4904	-2.8564	-1.5069	1980.23
69.7	9.4768	-2.9225	-1.7685	1980.13
70.0	9.4086	-3.3960	-2.1543	1980.02
70.3	9.2654	-3.8928	-1.8693	1979.92
70.7	9.1945	-3.9940	-2.1553	1979.81
71.0	9.1146	-3.9246	-1.8543	1979.71
71.3	9.1171			1979.61
71.7	9.2099			1979.50

#### Track Shift

62.7	9.3865	-3.4009	-2.6157	1981.96
63.0	9.2548	-3.9012	-2.8271	1981.85
63.3	9.2677	-4.2679	-3.3657	1981.74
63.7	9.2011	-4.2452	-3.5111	1981.63
64.0	9.2697			1981.60
64.3	9.2417	-4.2302	-3.2491	1981.54
64.7	9.3369	-3.8189	-2.6227	1981.48
65.0	9.4299	-3.5182	-2.2751	1981.38
65.3	9.4695	-3.1469	-2.1967	1981.31
65.7	9.6369	-3.0042	-2.2451	1981.21
66.0	9.5606	-3.1069	-2.5337	1981.04
66.3	9.4308	-3.5812	-3.0091	1981.00
66.7	9.2474	-4.3609	-3.1277	1980.88
67.0	9.2472	-4.3132	-2.8081	1980.83
67.3	9.0295			1980.71
67.7	9.3793	-4.0042	-2.1441	1980.50
68.0	9.3455	-3.9649	-2.5367	1980.47
68.3	9.3607	-3.9152	-2.0151	1980.40
68.7	9.4709			1980.38
69.0	9.4369	-3.7439	-2.3467	1980.33
69.3	9.4274	-3.6882	-2.1481	1980.23
69.7	9.5387	-3.4943	-2.3356	1980.13
70.0	9.4455	-2.8642	-2.7001	1980.02
70.3	9.3088	-3.8199	-2.7057	1979.92
70.7	9.3164	-4.0842	-3.3131	1979.81
71.0	9.1761	-4.2879	-2.9587	1979.71
71.3	9.1206	-4.2262	-3.4491	1979.61
71.7	8.9876			1979.50

Depth from Top of Coral (mm)	Sr/Ca (mmol/mol)	Oxygen Isotope (permil)	Carbon Isotope (permil)	Date
72.0	9.0456	-4.3472	-3.1711	1979.40
72.3	9.3050	-4.0729	-2.3867	1979.29
72.7	9.5364	-3.4622	-1.4871	1979.19
73.0	9.4814	-3.5169	-2.1987	1979.08
73.3	9.5108	-3.9402	-2.5811	1979.06
73.7	9.4853	-3.9419	-2.5357	1979.04
74.0	9.4147	-4.0762	-2.6561	1979.02
74.3	9.2741	-4.1529	-2.5907	1979.00
74.7	9.3787	-4.2242	-2.9811	1978.97
75.0	9.3234	-4.0409	-3.0097	1978.94
75.3	9.2659	-4.2222	-3.5031	1978.92
75.7	9.1568	-4.5319	-3.9907	1978.83
76.0	9.1842	-4.3782	-3.4941	1978.75
76.3	9.1549	-4.6209	-4.0757	1978.67
76.7	9.1767	-3.9369	-2.6147	1978.56
77.0	9.3804	-3.8482	-2.6771	1978.46
77.3	9.4793	-3.5522	-2.6094	1978.35
77.7	9.4895	-3.4652	-3.0211	1978.25
78.0	9.3906	-3.4548	-3.3086	1978.00
78.3	9.2396	-4.2972	-3.7791	1977.90
78.7	9.1373	-4.4519	-3.8417	1977.79
79.0	9.1468	-4.6112	-3.0671	1977.83
79.3	9.2172	-4.5079	-3.3711	1977.76
79.7	9.2035			1977.69
80.0	9.0734	-4.2162	-3.3879	1977.63
80.3	9.1164	-4.2931	-3.3812	1977.59
80.7	9.1857	-4.2629	-2.8837	1977.56
81.0	9.1643	-3.8282	-2.9861	1977.53
81.3	9.1516	-4.0259	-3.0927	1977.50
81.7	9.3303	-3.7010	-2.3459	1977.42
82.0		-3.5019	-2.6187	1977.27
82.3	9.4238	-3.5532	-2.8331	1977.13
82.7	9.3477	-3.2749	-2.6937	1976.96
83.0	9.2212	-4.1142	-2.8871	1976.83
83.3	9.1156	-4.1019	-3.3447	1976.71
83.7	9.0678	-4.6322	-2.9679	1976.63
84.0	9.1043	-3.8729	-2.5567	1976.58
84.3	9.1855	-3.4842	-2.7941	1976.50
84.7	9.3240	-3.9189	-2.6797	1976.38
85.0	9.3486	-3.6722	-2.3001	1976.35
85.3	9.3025	-3.3553	-2.1954	1976.32
85.7	9.4205	-3.4112	-2.6341	1976.21
86.0	9.3608	-3.3759	-2.5337	1976.17
86.3	9.3781	-3.0072	-2.6059	1976.08

Depth from Top of Coral (mm)	Sr/Ca (mmol/mol)	Oxygen Isotope (permil)	Carbon Isotope (permil)	Date
86.7	9.2887	-3.3244	-3.1845	1975.96
87.0	9.1103	-3.9892	-3.6341	1975.75
87.3	9.1765	-4.4319	-3.2517	1975.73
87.7	9.0963	-4.2182	-2.6761	1975.71
88.0	9.1923	-4.0439	-2.4697	1975.50
88.3	9.3700	-3.5472	-1.9711	1975.35
88.7	9.3403	-3.5529	-2.0457	1975.31
89.0	9.4564	-2.8956	-1.3637	1975.29
89.3	9.4146	-3.2319	-1.5597	1975.21
89.7	9.4397	-3.0961	-1.7071	1975.13
90.0	9.3880			1975.02
90.3	9.1861	-4.1892	-2.6091	1974.96
90.7	9.2342	-4.0368	-3.0447	1974.91
91.0	9.0646	-4.2172	-3.0091	1974.84
91.3	9.0109	-4.6859	-3.1237	1974.79
91.7	9.0085	-4.7262	-3.3181	1974.73
92.0	8.9937	-4.7739	-3.2137	1974.67
92.3	9.1163	-3.6253	-2.3863	1974.58
92.7	9.3365	-3.6159	-1.6657	1974.50
93.0	9.3574	-3.3682	-1.5831	1974.42
93.3	9.4678	-2.7249	-1.2977	1974.33
93.7	9.3824	-3.4304	-1.7422	1974.20
94.0	9.3946	-3.8289	-1.9437	1974.05
94.3	9.3411			1973.92
94.7	9.3055	-4.0789	-2.2007	1973.89
95.0	9.1303			1973.79
95.3	9.0906	-4.4329	-3.0167	1973.78
95.7	9.1220	-4.4542	-3.6071	1973.78
96.0	9.0771	-4.2453	-2.8044	1973.72
96.3	9.0650	-4.1966	-2.4625	1973.71
96.7	9.1582	-3.6089	-1.5557	1973.54
97.0	9.2879			1973.50
97.3	9.2747	-3.4049	-1.2427	1973.42
97.7	9.5028	-2.4032	-0.5781	1973.33
98.0	9.6012	-2.9839	-1.7567	1973.17
98.3	9.2372	-3.5922	-2.8951	1972.88
98.7	9.1474			1972.79
99.0	9.1373	-3.7000	-1.4468	1972.77
99.3	9.0932	-4.7359	-2.7857	1972.75
99.7	9.0430	-4.3522	-2.2431	1972.71
100.0	9.0288	-4.3623	-2.5025	1972.63
100.3	9.1257	-4.2842	-2.5741	1972.58
100.7	9.2391			1972.50
101.0	9.3372	-3.6644	-1.8160	1972.42



Depth from Top of Coral (mm)	Sr/Ca (mmol/mol)	Oxygen Isotope (permil)	Carbon Isotope (permil)	Date
101.3	9.3730	-2.6299	-1.8687	1972.32
101.7	9.4128	-3.4002	-1.9861	1972.29
102.0	9.3551	-3.5309	-2.4147	1972.12
102.3	9.3112			1972.02
102.7	9.2537	-3.7849	-2.5057	1971.92
103.0	9.1528	-3.8802	-2.5051	1971.87
103.3	9.0854			1971.75
103.7	9.0354	-4.5332	-3.0161	1971.74
104.0	9.0169			1971.72
104.3	9.0053	-4.3212	-2.4091	1971.71
104.7	9.1092	-4.1949	-2.1847	1971.54
105.0	9.2846	-3.5460	-1.6904	1971.47
105.3	9.4920	-3.2299	-1.6307	1971.21
105.7	9.4817			1971.10
106.0	9.4248	-3.4309	-2.1487	1971.00
106.3	9.3216	-4.1122	-2.9251	1970.92
106.7	9.1975	-3.7939	-2.7137	1970.83
107.0	9.1666	-3.8152	-2.6391	1970.84
107.3	9.1077			1970.85
107.7	9.0700	-4.5042	-2.5931	1970.82
108.0	9.0403	-4.1329	-2.7417	1970.78
108.3	8.9906	-4.2412	-1.8921	1970.75
108.7	9.0217	-4.4278	-2.2382	1970.67
109.0	9.1347			1970.54
109.3	9.2576	-3.6569	-1.9737	1970.46
109.7	9.4695			1970.13
110.0	9.3485	-3.1809	-2.6287	1970.11
110.3	9.4008	-3.0452	-2.5101	1969.96
110.7	9.3535			1969.93
111.0	9.2606	-3.0282	-1.8871	1969.91
111.3	9.2542	-3.8269	-3.0187	1969.88
111.7	9.1829	-3.8532	-2.4681	1969.86
112.0	9.1548	-4.0419	-1.9607	1969.83
112.3	9.0555		-2.4236	1969.63
112.7	9.0435	-4.3249	-1.8557	1969.54
113.0	9.0672	-4.2092	-1.9281	1969.53
113.3	9.1918		-1.8974	1969.51
113.7	9.2501	-4.0212	-1.5925	1969.50
114.0	9.2586	-3.2590	-1.7481	1969.46
114.3	9.3618			1969.21
114.7	9.2170	-3.4620	-2.9498	1968.83
115.0	9.0882	-4.6052	-2.8141	1968.75
115.3	8.9951	-3.8109	-2.0757	1968.67
115.7	9.0075	-4.6292	-2.4311	1968.63

Depth from Top of Coral (mm)	Sr/Ca (mmol/mol)	Oxygen Isotope (permil)	Carbon Isotope (permil)	Date
116.0	9.0140			1968.58
116.3	9.1658	-4.4344	-2.2831	1968.54
116.7	9.1331			1968.50
117.0	9.2847	-3.7992	-1.3991	1968.46
117.3	9.3512	-3.6789	-1.5867	1968.42
117.7	9.3425	-3.4813	-1.6433	1968.38
118.0	9.3943	-3.2979	-2.3137	1968.33
118.3	9.3672	-3.4002	-2.1041	1968.29
118.7	9.4209	-3.4399	-2.0747	1968.21
119.0	9.2871	-3.5720	-2.1303	1967.99
119.3	9.2909	-3.9349	-2.6927	1967.85
119.7	9.1392	-4.4336	-2.4561	1967.79
120.0	9.0810	-4.3798	-2.3082	1967.71
120.3	9.0710	-4.4175	-2.3714	1967.67
120.7	8.9830	-4.3369	-1.8847	1967.63
121.0	9.0725	-4.3932	-2.4381	1967.58
121.3	9.4517	-3.5499	-1.6737	1967.38
121.7	9.3646	-3.4342	-1.6051	1967.21
122.0	9.4425			1967.13
122.3	9.4209	-3.1559	-1.8077	1967.04
122.7	9.3397	-3.8152	-2.6741	1966.92
123.0	9.2087	-3.9449	-2.8347	1966.89
123.3	9.1700	-4.0628	-2.2198	1966.86
123.7	9.1621	-4.4419	-2.1237	1966.83
124.0	8.9588	-4.9192	-2.6251	1966.67
124.3	8.9833	-4.1099	-1.7637	1966.58
124.7	9.0119	-4.2412	-1.7081	1966.58
125.0	9.1889	-3.9049	-1.6247	1966.52
125.3	9.2202	-3.3212	-1.5351	1966.45
125.7	9.2395	-3.2949	-2.2587	1966.38
126.0	9.2330	-3.4552	-2.2461	1966.32
126.3	9.2413	-3.4478	-1.9549	1966.25
126.7	9.1208	-4.4752	-2.5261	1966.13
127.0	9.1919	-3.7949	-2.5887	1965.75
127.3	9.0387	-4.0612	-1.9401	1965.73
127.7	9.0528	-4.9104	-1.4424	1965.71
128.0	9.0077	-4.4472	-1.5901	1965.69
128.3	8.9615			1965.63
128.7	8.9967	-4.3319	-0.7014	1965.60
129.0	9.0514	-3.7882	-0.9171	1965.58
129.3	9.1255	-3.7039	-0.5737	1965.50
129.7	9.3258	-2.9230	-0.6867	1965.42
130.0	9.4410	-3.3029	-1.4457	1965.21
130.3	9.3802	-3.1282	-1.3941	1964.96

Depth from Top of Coral (mm)	Sr/Ca (mmol/mol)	Oxygen Isotope (permil)	Carbon Isotope (permil)	Date
130.7	9.3498	-3.4059	-1.9097	1964.98
131.0	9.3319	-3.3862	-2.1201	1965.00
131.3	9.1852	-3.8739	-2.2937	1964.83
131.7	9.0802	-3.9822	-2.4871	1964.63
132.0	9.0600	-4.2081	-2.8380	1964.60
132.3	9.0361	-4.5512	-2.2551	1964.58
132.7	9.0057	-4.3459	-1.6187	1964.56
133.0	8.9901	-4.2642	-1.4641	1964.54
133.3	9.1675	-4.1976	-0.9689	1964.50
133.7	9.4434	-3.4886	-0.7808	1964.33
134.0	9.2672	-3.4129	-1.2747	1964.25
134.3	9.3218	-3.1719	-2.8050	1964.17
134.7	9.2620	-3.8471	-2.7810	1964.08
135.0	9.2413	-3.3362	-2.1741	1964.00
135.3	9.3183	-3.5462	-2.2064	1963.92
135.7	9.1921		-1.9600	1963.83
136.0	9.0397	-4.3769	-2.3417	1963.75
136.3	9.1122	-4.3528	-2.3737	1963.71
136.7	9.0307	-4.3597	-1.9768	1963.63
137.0	9.2385	-3.7572	-1.5801	1963.53
137.3	9.2246	-4.2559	-1.5927	1963.50
137.7	9.2473	-3.5392	-1.7861	1963.47
138.0	9.2929	-3.7479	-1.7307	1963.40
138.3	9.3584	-3.6172	-1.8761	1963.29
138.7	9.3466	-3.8209	-2.4047	1963.08
139.0	9.2591	-3.8758	-2.6240	1962.92
139.3	9.1645	-4.0404	-2.6408	1962.88
139.7	9.1941	-3.7492	-2.2491	1962.83
140.0	9.1037	-4.0577	-2.2982	1962.79
140.3	8.9734	-4.1092	-1.9531	1962.71
140.7	9.1692	-3.5629	-1.9147	1962.58
141.0	9.2846	-3.7492	-1.9701	1962.29
141.3	9.1425	-4.0079	-2.4917	1961.83
141.7	9.0383	-4.2672	-2.2721	1961.81
142.0	9.0454	-4.4959	-2.6207	1961.78
142.3	9.0110	-4.8422	-2.6531	1961.75
142.7	9.0138	-4.5719	-2.3947	1961.72
143.0	8.9948	-4.5432	-1.8391	1961.69
143.3	8.9367	-4.4556	-1.6171	1961.63
143.7	9.1167	-3.9546	-1.6445	1961.58
144.0	9.3272	-3.7659	-1.2097	1961.42
144.3	9.3327	-3.3413	-1.3377	1961.13
144.7	9.2888	-3.6999	-2.0117	1961.11
145.0	9.2724	-3.4192	-1.8411	1961.05



Depth from Top of Coral (mm)	Sr/Ca (mmol/mol)	Oxygen Isotope (permil)	Carbon Isotope (permil)	Date
145.3	9.2718	-3.6569	-2.2887	1960.99
145.7	9.2827	-4.0705	-2.4390	1960.93
146.0	9.2356	-3.8419	-2.5397	1960.87
146.3	9.0987	-4.2442	-2.6711	1960.81
146.7	9.0855	-5.2185	-2.3653	1960.75
147.0	9.2509			1960.73
147.3	9.1443			1960.72
147.7	9.0081			1960.71
148.0	9.0191	-4.4559	-1.3848	1960.63
148.3	9.1959	-4.3579	-1.8377	1960.50
148.7	9.3333	-3.1723	-1.4473	1960.33
149.0	9.4223	-3.4739	-1.5507	1960.21
149.3	9.3187	-3.2830	-1.7867	1960.00
149.7	9.3133	-3.0079	-1.7167	1959.92
150.0	9.2273	-4.0522	-2.3031	1959.83
150.3	9.1576	-3.1362	-1.9987	1959.79
150.7	9.1027	-3.7277	-2.3569	1959.75
151.0	8.9853			1959.71
151.3	9.0166	-3.8835	-1.2292	1959.70
151.7	9.0328	-3.6553	-1.1786	1959.70
152.0	9.0546	-3.6707	-0.3434	1959.67
152.3	9.2298	-3.4006	-0.6997	1959.50
152.7	9.4287	-3.3586	-0.5585	1959.13
153.0	9.3756	-3.1780	-1.5243	1959.00
153.3	9.2563	-3.2822	-1.8442	1958.94
153.7	9.1909	-3.5208	-2.1739	1958.88
154.0	9.0540	-4.0938	-2.2983	1958.81
154.3	9.0021	-4.5692	-2.7384	1958.75
154.7	9.0423			1958.71
155.0	8.9948			1958.67
155.3	9.0581	-4.0086	-1.1309	1958.63
155.7	9.0261	-3.4376	-0.5193	1958.58
156.0	9.3147	-3.2824	-1.2902	1958.42
156.3	9.1586	-3.9145	-1.9906	1958.36
156.7	9.1620	-4.3442	-2.3311	1958.31
157.0	9.2015			1958.25
157.3	9.1647	-4.3165	-2.8412	1958.00
157.7	9.1619	-3.4550	-2.2046	1957.79
158.0	9.0854	-4.3369	-2.7367	1957.75
158.3	8.9875	-4.1876	-2.2293	1957.71
158.7	9.0015	-4.2801	-2.5531	1957.69
159.0	9.0145	-4.0390	-1.5234	1957.67
159.3	9.0952	-4.6459	-1.8887	1957.62
159.7	9.0744	-3.2735	-1.0853	1957.58

Depth from Top of Coral (mm)	Sr/Ca (mmol/mol)	Oxygen Isotope (permil)	Carbon Isotope (permil)	Date
160.0	9.2699	-2.7909	-0.7873	1957.42
160.3	9.4601	-2.4917	-0.5568	1957.25
160.7	9.3987	-2.6623	-1.0158	1957.09
161.0	9.3426	-3.1658	-1.7824	1956.92
161.3	9.2776	-3.4287	-1.9134	1956.88
161.7	9.1325	-3.7093	-2.3787	1956.83
162.0	9.0724	-4.1191	-2.4900	1956.73
162.3	9.0434	-3.8892	-1.6071	1956.63
162.7	9.0430			1956.54
163.0	9.1303	-3.7823	-1.2208	1956.50
163.3	9.4005	-3.3593	-0.8547	1956.38
163.7	9.2644	-2.7970	-0.6377	1956.25
164.0	9.5364	-2.8414	-1.3829	1956.08
164.3	9.3657	-3.0080	-2.0477	1955.96
164.7	9.2276			1955.88
165.0	9.0678	-4.3019	-1.8457	1955.83
165.3	9.0201	-4.4022	-2.1071	1955.79
165.7	8.9822	-4.5799	-1.6087	1955.75
166.0	9.0312			1955.71
166.3	8.9561	-4.4152	-1.9851	1955.67
166.7	8.9623	-4.3099	-1.3287	1955.61
167.0	9.1803	-3.8822	-1.4771	1955.50
167.3	9.1936	-3.7269	-0.9807	1955.48
167.7	9.3783	-3.4242	-1.1951	1955.29
168.0	9.3343	-3.4799	-1.4997	1954.92
168.3	9.2942			1954.90
168.7	9.1812	-4.1549	-1.9977	1954.88
169.0	9.0900	-3.9742	-2.2191	1954.83
169.3	9.0061	-4.4528	-1.9228	1954.79
169.7	8.9769	-4.6042	-2.2801	1954.75
170.0	8.9588	-4.6559	-2.3157	1954.71
170.3	8.9500	-4.2582	-1.3731	1954.67
170.7	9.1050	-4.1729	-1.4697	1954.58
171.0	9.1161	-3.8342	-1.5371	1954.50
171.3	9.1838	-3.3889	-1.0107	1954.38
171.7	9.1910	-3.0782	-1.0591	1954.30
172.0	9.3063	-3.0789	-1.7357	1954.21
172.3	9.2272	-3.0809	-1.8475	1954.10
172.7	9.1960	-3.4379	-2.1047	1953.99
173.0	9.1539	-3.7222	-1.8961	1953.88
173.3	9.0232	-4.3265	-2.5579	1953.76
173.7	9.0500	-4.1846	-2.4614	1953.63
174.0	9.0242	-4.3969	-2.3247	1953.57
174.3	9.1039	-3.8802	-1.6231	1953.52

Depth from Top of Coral (mm)	Sr/Ca (mmol/mol)	Oxygen Isotope (permil)	Carbon Isotope (permil)	Date
174.7	9.1715	-3.6359	-1.8867	1953.46
175.0	9.2240	-3.5082	-1.5061	1953.38
175.3	9.3623	-2.9839	-1.1317	1953.29
175.7	9.3822	-3.1692	-1.7081	1953.21
176.0	9.2640	-3.4466	-2.2224	1953.04
176.3	9.2112	-3.7722	-2.7395	1952.88
176.7	9.1188	-3.5690	-1.7624	1952.82
177.0	9.1018	-4.1622	-2.6641	1952.77
177.3	8.9916	-4.7355	-2.1155	1952.71
177.7	9.0048	-4.3532	-2.0041	1952.65
178.0	9.0592	-4.2659	-1.9237	1952.58
178.3	9.1656	-3.9052	-2.1501	1952.52
178.7	9.1810	-3.5299	-2.0587	1952.46
179.0	9.2493	-3.5102	-1.4721	1952.38
179.3	9.3644	-3.3531	-1.5402	1952.29
179.7	9.4150	-3.1332	-1.5911	1952.21
180.0	9.4067	-3.1719	-1.8057	1952.10
180.3	9.2687	-3.7258	-2.6076	1951.99
180.7	9.2360	-3.8379	-2.6297	1951.88
181.0	9.1397	-4.0612	-3.2101	1951.82
181.3	9.0724		-2.6131	1951.76
181.7	9.0731	-4.2512	-3.4811	1951.69
182.0	9.0406	-4.3189	-2.3507	1951.63
182.3	9.0620	-3.9348	-2.4284	1951.51
182.7	9.3044	-3.5779	-1.8407	1951.38
183.0	9.4095	-3.6272	-1.5521	1951.32
183.3	9.4248	-3.0969	-1.2617	1951.27
183.7	9.4508	-3.0112	-1.9411	1951.21
184.0	9.3602	-3.0179	-1.5857	1951.04
184.3	9.2520	-3.4542	-2.2921	1950.88
184.7	9.3176	-3.4289	-2.0447	1950.82
185.0	9.2753	-3.2308	-2.4428	1950.75
185.3	9.1426	-3.9829	-2.9457	1950.69
185.7	9.0599		-2.3174	1950.63
186.0	9.1425	-4.2109	-2.7507	1950.59
186.3	9.1361	-4.2612	-2.6691	1950.55
186.7	9.2075	-3.9849	-2.7647	1950.50
187.0	9.2511	-3.6022	-2.5481	1950.46
187.3	9.4049	-3.1029	-1.8187	1950.34
187.7	9.4439	-3.3302	-1.9021	1950.21
188.0	9.4068	-3.4110	-2.1814	1950.04
188.3	9.3025	-3.7191	-2.4090	1949.88
188.7	9.2967	-3.7649	-2.6427	1949.80
189.0	9.1871	-3.8462	-2.8841	1949.71



Depth from Top of Coral (mm)	Sr/Ca (mmol/mol)	Oxygen Isotope (permil)	Carbon Isotope (permil)	Date
189.3	9.1731	-4.1089	-3.3667	1949.63
189.7	9.1822	-3.8662	-3.2641	1949.59
190.0	9.2572	-4.2019	-2.2617	1949.54
190.3	9.2140	-4.0862	-2.4431	1949.50
190.7	9.2786	-4.0339	-2.7877	1949.46
190.7		-3.7522	-2.3681	1949.40
191.0	9.4131	-3.4370	-1.6779	1949.33
191.3	9.5103	-3.3592	-1.5421	1949.21
191.7	9.4624	-2.3817	0.5506	1949.05
192.0	9.3566	-3.2722	-2.4181	1948.88
192.3	9.2994	-3.5049	-2.6547	1948.80
192.7	9.2308	-3.4682	-2.9931	1948.72
193.0	9.2361	-3.8519	-2.4627	1948.63
193.3	9.2327	-3.8570	-2.1826	1948.60
193.7	9.2593	-3.8374	-2.4826	1948.56
194.0	9.2515	-3.8922	-2.4521	1948.53
194.3	9.3167	-3.6869	-2.0987	1948.49
194.7	9.3432	-3.5682	-2.1331	1948.46
195.0	9.4547	-3.3693	-1.9411	1948.33
195.3	9.4499	-3.1682	-1.8481	1948.21
195.7	9.4375	-3.2029	-2.4477	1948.11
196.0	9.3964	-3.3482	-2.8001	1948.00
196.3	9.3945	-3.1959	-2.5377	1947.89
196.7	9.3045	-3.6422	-2.7121	1947.79
197.0	9.2573	-3.6209	-2.8327	1947.63
197.3	9.3399	-3.9302	-2.4001	1947.59
197.7	9.3369	-3.7649	-2.3427	1947.55
198.0	9.3600	-4.0292	-2.4361	1947.50
198.3	9.3498	-3.7509	-1.7767	1947.46
198.7	9.4354	-3.7792	-2.1471	1947.38
199.0	9.4746	-3.6411	-2.3216	1947.29
199.3	9.4652	-3.3522	-1.9581	1947.21
199.7	9.5125	-3.5119	-2.4067	1947.13
200.0	9.3738	-3.5432	-2.3671	1947.00
200.3	9.3333	-3.5379	-2.2797	1946.88
200.7	9.3245	-3.7492	-2.5961	1946.83
201.0	9.2410	-3.7389	-2.0207	1946.78
201.3	9.2440	-3.9772	-2.0871	1946.73
201.7	9.2389	-3.9449	-2.1787	1946.68
202.0	9.2015	-4.0802	-2.4571	1946.63
202.3	9.1881	-4.1379	-2.9597	1946.51
202.7	9.3249	-3.5622	-1.7161	1946.38
203.0	9.3963	-3.4839	-1.8517	1946.21
203.7	9.3555	-3.2942	-1.6941	1946.08

Depth from Top of Coral (mm)	Sr/Ca (mmol/mol)	Oxygen Isotope (permil)	Carbon Isotope (permil)	Date
204.0	9.3531	-3.5649	-2.3687	1946.02
204.3	9.3133	-3.3661	-2.3739	1945.95
204.7	9.3599	-3.1564	-2.3632	1945.89
205.0	9.3070	-3.6712	-3.0221	1945.82
205.3	9.2242	-3.9149	-2.4597	1945.76
205.7	9.2848	-3.6262	-1.8221	1945.70
206.0	9.2015	-4.0909	-2.4377	1945.63
206.3	9.2410	-3.7182	-2.8821	1945.58
206.7	9.2106	-3.8389	-2.3267	1945.53
207.0	9.2371	-3.8032	-2.1931	1945.48
207.3	9.3119	-3.7739	-2.5087	1945.43
207.7	9.4147	-3.1272	-1.7951	1945.38
208.0	9.5200	-3.3263	-2.3218	1945.21
208.3	9.4208	-3.2112	-2.1741	1945.10
208.7	9.4021	-3.3659	-2.5767	1944.99
209.0	9.3841	-3.4432	-2.6671	1944.88
209.3	9.2687	-3.7272	-2.5273	1944.83
209.7	9.2463	-3.9492	-2.4231	1944.78
210.0	9.1496	-4.1329	-2.4997	1944.73
210.3	9.1412	-4.1234	-2.7398	1944.68
210.7	9.1250	-4.2529	-2.5577	1944.63
211.0	9.1594	-4.0572	-2.7341	1944.57
211.3	9.2107	-3.8440	-2.3764	1944.52
211.7	9.3259	-3.5232	-1.8911	1944.46
212.0	9.4650	-3.3759	-1.7097	1944.33
212.3	9.4738	-3.3952	-2.0941	1944.21
212.7	9.4067	-3.4539	-2.3267	1944.13
213.0	9.3762	-3.6062	-2.5611	1944.04
213.3	9.3246	-3.6589	-2.3477	1943.96
213.7	9.3507	-3.6652	-2.1591	1943.88
214.0	9.2405	-3.9559	-2.5295	1943.79
214.3	9.1843	-4.0792	-2.2731	1943.71
214.7	9.1835	-4.0479	-2.3967	1943.63
215.0	9.3148	-3.6402	-1.9551	1943.54
215.3	9.3562	-3.4969	-1.5697	1943.46
215.7	9.4385	-3.3372	-1.5401	1943.34
216.0	9.4740	-3.2199	-1.5547	1943.21
216.3	9.4516	-3.4482	-2.5781	1943.13
216.7	9.3326	-3.5699	-2.2897	1943.05
217.0	9.3292	-3.5322	-2.5511	1942.96
217.3	9.3026	-3.8299	-2.7177	1942.88
217.7	9.2000	-4.2522	-2.7791	1942.82
218.0	9.2006	-3.9939	-2.4117	1942.75
218.3	9.1855	-4.2152	-2.9731	1942.69

Depth from Top of Coral (mm)	Sr/Ca (mmol/mol)	Oxygen Isotope (permil)	Carbon Isotope (permil)	Date
218.7	9.1548	-4.0619	-1.6047	1942.63
219.0	9.1883	-4.0982	-2.4541	1942.50
219.3	9.2987	-3.9039	-2.3177	1942.38
219.7	9.3577	-3.6702	-2.1741	1942.29
220.0	9.3431	-3.3129	-1.6357	1942.24
220.3	9.3369	-3.4272	-1.9961	1942.18
220.7	9.3715	-3.3949	-2.1027	1942.13
221.0	9.2931	-3.0282	-1.7601	1941.96
221.3	9.1549	-3.7809	-2.8747	1941.79
221.7	9.1484	-4.0172	-3.1201	1941.75
222.0	9.0956	-3.9599	-2.8937	1941.71
222.3	9.0932	-3.8872	-1.6811	1941.67
222.7	9.0764	-4.1569	-2.3877	1941.63
223.0	9.1773	-4.0261	-1.9640	1941.57
223.3	9.2328	-3.5189	-1.5617	1941.52
223.7	9.1699	-3.5432	-1.8011	1941.46
224.0	9.3704	-3.2619	-1.7417	1941.38
224.3	9.3998	-3.3462	-2.1491	1941.29
224.7	9.5036	-3.0529	-2.2747	1941.21
225.0	9.3141	-3.4672	-2.6491	1941.08
225.3	9.2784	-3.7569	-2.8937	1940.96
225.7	9.2989	-3.8372	-2.5371	1940.85
226.0	9.1834	-4.0569	-2.8277	1940.74
226.3	9.0080	-4.5170	-2.9029	1940.63
226.7	9.1068	-4.3329	-2.3867	1940.55
227.0	9.1594	-3.9862	-2.6141	1940.46
227.3	9.2876	-3.6259	-2.3387	1940.41
227.7	9.3340	-3.5322	-2.3381	1940.36
228.0	9.3948	-3.2769	-2.7067	1940.31
228.3	9.4026	-3.2102	-2.2831	1940.26
228.7	9.4141	-3.2769	-2.1257	1940.21
229.0	9.4063	-3.4642	-2.8741	1940.10
229.3	9.3847	-3.6559	-2.8887	1939.99
229.7	9.2077	-4.1102	-2.9641	1939.88
230.0	9.0811	-4.2029	-2.3577	1939.75
230.3	8.9891	-4.0582	-2.4931	1939.63
230.7	9.1997	-4.2559	-2.5737	1939.55
231.0	9.0845	-3.8832	-2.1681	1939.46
231.3	9.2645	-3.6789	-1.8337	1939.38
231.7	9.3178	-3.3432	-1.8501	1939.34
232.0	9.2901	-3.3819	-1.7037	1939.29
232.3	9.4164	-3.1482	-2.0191	1939.25
232.7	9.4165	-3.4309	-2.1957	1939.21
233.0	9.3681	-3.4612	-2.5791	1939.10



Depth from Top of Coral (mm)	Sr/Ca (mmol/mol)	Oxygen Isotope (permil)	Carbon Isotope (permil)	Date
233.3	9.3786	-3.5869	-2.7107	1938.99
233.7	9.2542	-3.8302	-2.6161	1938.88
234.0	9.1672	-4.1369	-3.0507	1938.80
234.3	9.1501	-4.0042	-3.0311	1938.71
234.7	9.0590	-4.3669	-2.9867	1938.63
235.0	9.1265	-3.8732	-2.2701	1938.54
235.3	9.1917	-3.7339	-2.0847	1938.46
235.7	9.2830	-3.4862	-2.0751	1938.38
236.0	9.3112	-3.3719	-2.2457	1938.29
236.3	9.2723	-3.3352	-2.3251	1938.21
236.7	9.2996	-3.3599	-2.3627	1938.05
237.0	9.2179	-3.6892	-2.3891	1937.88
237.3	9.1621	-3.6359	-2.3497	1937.80
237.7	9.1265	-3.9892	-2.3041	1937.71
238.0	9.2148	-3.8789	-2.0907	1937.68
238.3	9.2645	-3.9532	-2.7321	1937.66
238.7	9.0956	-4.2409	-2.8227	1937.63
239.0	9.1107	-4.2132	-2.3461	1937.55
239.3	9.2645	-3.6099	-2.4387	1937.46
239.7	9.2829	-3.5312	-2.0201	1937.38
240.0	9.3802	-3.3869	-2.3377	1937.29
240.3	9.3448	-3.4232	-1.8681	1937.21
240.7	9.3758	-3.4709	-2.5367	1937.09
241.0	9.2272	-3.6972	-2.7641	1936.96
241.3	9.2741	-3.7219	-2.8527	1936.88
242.3	9.0375	-4.3302	-1.9331	1936.63
242.7	9.1005	-4.3579	-2.4807	1936.55
243.0	9.2311	-4.0332	-2.3231	1936.46
243.3	9.4050	-2.9189	-1.4807	1936.38
243.7				
244.0	9.4819	-3.2642	-2.0281	1936.21
244.3	9.3362	-3.6269	-1.7287	1935.96
244.7	9.2719			1935.88
245.0	9.1201	-4.1809	-2.1367	1935.63
245.3	9.1476	-4.1692	-2.1091	1935.55
245.7	9.2106	-4.1319	-2.2587	1935.46
246.0	9.2745	-4.0272	-2.9381	1935.43
246.3	9.2100	-3.2129	-1.8687	1935.41
246.7	9.3490	-3.3792	-2.2321	1935.38
247.0	9.3008	-3.4939	-1.9747	1935.32
247.3	9.4147	-3.1092	-2.2371	1935.27
247.7	9.3558	-3.3349	-2.1297	1935.21
248.0	9.4191	-3.6492	-2.4281	1935.08
248.3	9.2723	-3.5309	-2.3347	1934.96

Depth from Top of Coral (mm)	Sr/Ca (mmol/mol)	Oxygen Isotope (permil)	Carbon Isotope (permil)	Date
248.7	9.2517	-3.9342	-2.7881	1934.85
249.0	9.1299	-4.4229	-2.6447	1934.74
249.3	9.1310	-4.5862	-2.8581	1934.63
249.7	9.1329	-4.0839	-2.1947	1934.55
250.0	9.2347	-3.7342	-2.6441	1934.46
250.3	9.4176	-3.2259	-1.6597	1934.21
250.7	9.3457	-3.5302	-1.4831	1934.05
251.0	9.2639	-3.8439	-1.6547	1933.88
251.3	9.1493	-3.8042	-1.6941	1933.71
251.7	9.2496	-3.9719	-1.8547	1933.63
252.0	9.1236	-4.2562	-1.6671	1933.54
252.3	9.2040	-4.0439	-1.7447	1933.49
252.7	9.2888	-3.7602	-1.7691	1933.43
253.0	9.3209	-3.5719	-1.2157	1933.38
253.3	9.3264	-3.3722	-1.6351	1933.30
253.7	9.4957	-3.5689	-1.4797	1933.21
254.0	9.3429	-3.5282	-1.9481	1933.04
254.3	9.3838	-3.6077	-1.0248	1932.96
254.7	9.2754	-3.7525	-1.2558	1932.88
255.0	9.3402	-3.6749	-2.1827	1932.80
255.3	9.2794	-3.9552	-2.1591	1932.71
255.7	9.2081	-3.8219	-2.1607	1932.63
256.0	9.4097	-3.5682	-1.6511	1932.38
256.3	9.3471	-3.5629	-1.7947	1932.30
256.7	9.4237	-3.4120	-2.3566	1932.21
257.0	9.4181	-3.6674	-1.9286	1932.08
257.3	9.2746	-3.7962	-2.2991	1931.96
257.7	9.2246	-3.7549	-2.5437	1931.88
258.0	9.1788	-3.6652	-2.2271	1931.79
258.3	9.1586		-1.7453	1931.71
258.7	9.0788	-4.0942	-2.4181	1931.63
259.0	9.1191	-3.7289	-1.4727	1931.57
259.3	9.1132	-3.6157	-1.6700	1931.51
259.7	9.3294	-3.4169	-1.4447	1931.44
260.0	9.2606	-3.5962	-1.7791	1931.38
260.3	9.4361	-3.5029	-2.1067	1931.21
260.7	9.3323	-3.5902	-2.5821	1930.96
261.0	9.1998	-4.1389	-2.8397	1930.79
261.3	9.1619	-4.1992	-2.7281	1930.71
261.7	9.1576	-3.7439	-1.7087	1930.63
262.0	9.1787		-2.2222	1930.55
262.3	9.1536	-3.8089	-2.3597	1930.46
262.7	9.3135	-3.4482	-2.2211	1930.38
263.0	9.4278	-3.4399	-2.3617	1930.29

Depth from Top of Coral (mm)	Sr/Ca (mmol/mol)	Oxygen Isotope (permil)	Carbon Isotope (permil)	Date
263.3	9.4414	-3.6412	-2.3761	1930.13
263.7	9.2904	-3.6699	-2.9377	1929.96
264.0	9.2298	-4.1602	-3.0821	1929.88
264.3	9.2209	-4.2709	-2.3017	1929.80
264.7	9.1777	-4.1762	-2.6721	1929.72
265.0	9.1469	-4.1539	-2.4097	1929.63
265.3	9.1504	-4.2022	-2.4211	1929.54
265.7	9.3457	-3.7419	-2.1977	1929.50
266.0	9.2577	-3.4068	-1.8570	1929.46
266.3	9.4363	-3.4879	-1.5927	1929.34
266.7	9.4611	-3.6004	-2.7166	1929.21
267.0	9.4226	-3.4559	-1.7217	1929.10
267.3	9.3313	-3.8042	-3.0411	1928.99
267.7	9.2127	-4.1679	-3.0587	1928.88
268.0	9.0225	-4.2762	-2.7331	1928.71
268.3	9.0453	-4.2229	-2.3027	1928.59
268.7	9.1710	-3.8543	-1.6689	1928.46
269.0	9.3563	-3.3769	-1.2887	1928.40
269.3	9.4164	-3.1722	-1.6271	1928.35
269.7	9.4352	-2.9989	0.1353	1928.29
270.0	9.3625	-3.4362	-1.3281	1928.21
270.3	9.4781	-3.6079	-1.3103	1928.13
270.7	9.2311	-3.3982	-0.8121	1927.88
271.0	9.0605	-4.1129	-1.8627	1927.63
271.3	9.0943	-4.0552	-1.7571	1927.55
271.7	9.1684	-3.6446	-1.1147	1927.46
272.0	9.3125	-3.4242	-1.2861	1927.33
272.3	9.3964	-3.3359	-0.7527	1927.21
272.7	9.3825	-3.4592	-1.3341	1927.05
273.0	9.2172	-3.8129	-1.9027	1926.88
273.3	9.1069	-4.1272	-1.9331	1926.80
273.7	9.0907	-4.1659	-2.3137	1926.72
274.0	9.0430	-4.1712	-2.6551	1926.63
274.3	9.1470	-3.9179	-1.5327	1926.55
274.7	9.2198	-3.8113	-1.6507	1926.47
275.0	9.3676	-2.9129	-0.7197	1926.38
275.3	9.4805	-3.4769	-1.3035	1926.29
275.7	9.4957	-3.2069	-1.7377	1926.21
276.0	9.3596	-3.2522	-2.3241	1925.96
276.3	9.2328	-3.7719	-1.8627	1925.88
276.7	9.1322		-2.1178	1925.80
277.0	9.0556	-4.1189	-2.1827	1925.71
277.3	9.3423	-2.8362	-0.9631	1925.63
277.7	9.0776	-4.3849	-1.9607	1925.54



Depth from Top of Coral (mm)	Sr/Ca (mmol/mol)	Oxygen Isotope (permil)	Carbon Isotope (permil)	Date
278.0	9.0992	-3.8372	-1.5951	1925.50
278.3	9.2248	-3.8409	-1.2847	1925.46
278.7	9.4241	-3.7388	-1.1992	1925.34
279.0	9.4075	-3.3569	-1.6207	1925.21
279.3	9.4345	-3.3922	-1.7921	1925.13
279.7	9.3941	-3.5189	-1.7227	1925.05
280.0	9.2838	-3.5442	-2.1721	1924.96
280.3	9.2202			1924.88
280.7	9.1153	-4.3212	-2.3471	1924.80
281.0	9.1088	-4.1297	-1.4676	1924.71
281.3	9.0974	-4.2562	-1.9941	1924.63
281.7	9.1163	-4.0989	-1.8007	1924.55
282.0	9.1265	-4.1522	-1.8671	1924.46
282.3	9.3283	-3.8239	-1.8197	1924.38
282.7	9.4019	-3.2572	-0.9071	1924.30
283.0	9.4755	-3.2439	-1.6697	1924.21
283.3	9.4387	-3.1862	-2.4661	1924.09
283.7	9.3714	-3.4499	-1.7547	1923.96
284.0	9.1795	-3.9002	-1.8821	1923.79
284.3	9.1686	-4.0389	-2.1407	1923.74
284.7	9.1450	-4.2962	-2.2861	1923.68
285.0	9.0947	-4.5722	-2.3151	1923.63
285.3	9.1115	-4.1122	-1.9301	1923.56
285.7	9.1674	-3.9539	-1.2957	1923.49
286.0	9.2165	-3.6212	-0.9981	1923.43
286.3	9.4701	-3.3149	-0.9967	1923.36
286.7	9.5058	-3.5582	-1.7561	1923.29
287.0	9.4452	-3.4959	-1.9267	1923.25
287.3	9.4045		-1.8938	1923.21
287.7	9.4233	-3.4599	-2.2317	1923.17
288.0	9.4680	-3.5322	-2.2931	1923.13
288.3	9.4192	-3.6873	-2.2875	1922.96
288.7	9.2133	-4.0949	-2.5527	1922.79
289.0	9.1851	-3.9859	-2.6707	1922.76
289.3	9.1892	-4.1982	-2.7471	1922.74
289.7	9.1094	-4.2859	-2.2267	1922.71
290.0	9.3263	-4.0892	-2.1391	1922.62
290.3	9.1002	-4.2649	-2.2557	1922.54
290.7	9.1210	-3.9522	-1.7871	1922.46
291.0	9.2830	-3.8250	-0.0677	1922.38
291.3	9.4013	-3.2222	-1.3641	1922.29
291.7	9.3199	-3.4562	-1.8029	1922.24
292.0	9.3936	-3.3352	-2.2861	1922.18
292.3	9.3932	-2.9669	-2.3607	1922.13

Depth from Top of Coral (mm)	Sr/Ca (mmol/mol)	Oxygen Isotope (permil)	Carbon Isotope (permil)	Date
292.7	9.3268	-3.6762	-2.4431	1922.05
293.0	9.3251	-3.7359	-3.0497	1921.96
293.3	9.1788	-3.7368	-2.4998	1921.88
293.7	9.1578	-4.0969	-3.1197	1921.82
294.0	9.1010	-4.0512	-2.8891	1921.75
294.3	9.0806	-4.2937	-3.0498	1921.69
294.7	9.0526	-4.1522	-2.5511	1921.63
295.0	9.1473	-3.6889	-2.0467	1921.54
295.3	9.1988	-3.6862	-1.7491	1921.46
295.7	9.3964	-3.4699	-1.3777	1921.40
296.0	9.3640	-3.3802	-1.8871	1921.33
296.3	9.3404	-3.3899	-1.9887	1921.27
296.7	9.3951	-3.6459	-2.2103	1921.21
297.0	9.3896	-3.4369	-1.9497	1921.04
297.3	9.2921	-3.9912	-1.6831	1920.88
297.7	9.2752	-3.7649	-2.4327	1920.82
298.0	9.2917	-3.8952	-2.0581	1920.75
298.3	9.3056	-3.9049	-1.9187	1920.69
298.7	9.1898	-3.6772	-1.2101	1920.63
299.0	9.3111	-3.5019	-1.4467	1920.52
299.3	9.4033	-3.3602	-1.2781	1920.42
299.7	9.4244	-3.2667	-1.8154	1920.32
300.0	9.4497	-3.5652	-1.6121	1920.21
300.3	9.3800	-3.5617	-1.6998	1920.11
300.7	9.3998	-3.4162	-1.4851	1920.00
301.0	9.4107	-4.0059	-1.6299	1919.89
301.3	9.3045	-3.8872	-1.4591	1919.79
301.7	9.3694	-3.6589	-1.3337	1919.71
302.0	9.2371	-3.9042	-1.7851	1919.63
302.3	9.2965	-3.8659	-2.1143	1919.52
302.7	9.3880	-3.3382	-0.9301	1919.41
303.0	9.4673	-3.4479	-1.4727	1919.29
303.3	9.4645	-3.3522	-1.5011	1919.21
303.7	9.4869	-3.4869	-1.5537	1919.13
304.0	9.3486	-3.7282	-1.6991	1918.96
304.3	9.2253	-3.6579	-1.5251	1918.79
304.7	9.2236	-4.0872	-1.7751	1918.71
305.0	9.1698	-4.1619	-2.3567	1918.63
305.3	9.2459	-3.9172	-2.1651	1918.57
305.7	9.1933	-4.1826	-2.3661	1918.51
306.0	9.3273	-3.7922	-1.9361	1918.44
306.3	9.4663	-3.3709	-1.2547	1918.38
306.7	9.6237	-3.1542	-0.8261	1918.21
307.0	9.3936	-3.4429	-1.1717	1917.88

Depth from Top of Coral (mm)	Sr/Ca (mmol/mol)	Oxygen Isotope (permil)	Carbon Isotope (permil)	Date
307.3	9.2988	-3.9229	-1.4297	1917.80
307.7	9.3838	-3.6417	-1.5611	1917.72
308.0	9.2196	-3.6739	-1.4611	1917.63
308.3	9.2312	-4.0799	-2.2417	1917.55
308.7	9.2999	-3.8988	-1.4744	1917.46
309.0	9.3717	-3.7119	-1.4737	1917.38
309.3	9.4931	-3.0982	-0.1541	1917.29
309.7	9.5635			1917.21
310.0	9.5166	-3.1966	-0.7977	1917.13
310.3	9.4834	-3.4699	-2.3747	1917.04
310.7	9.4212	-3.4982	-1.7001	1916.96
311.0	9.2935	-3.9787	-1.8666	1916.88
311.3	9.1582	-4.0102	-2.3771	1916.63
311.7	9.2297	-4.1603	-2.2397	1916.51
312.0	9.3557	-3.7532	-1.6371	1916.38
312.3	9.4313	-3.1279	-0.8137	1916.30
312.7	9.4836	-3.1382	-0.6241	1916.21
313.0	9.4091	-3.3489	-1.2827	1916.14
313.3	9.3709	-3.4672	-1.7951	1916.08
313.7	9.3789	-3.4999	-1.6697	1916.01
314.0	9.4015	-3.5522	-1.0501	1915.95
314.3	9.2627	-3.6739	-1.0667	1915.88
314.7	9.1900	-4.0212	-1.7391	1915.76
315.0	9.1402	-3.9149	-1.8017	1915.63
315.3	9.3069	-3.6072	-1.3871	1915.55
315.7	9.3074	-3.3929	-1.1227	1915.46
316.0	9.5024	-3.4102	-1.3391	1915.33
316.3	9.5358	-3.3219	-1.6667	1915.21
316.7	9.4371	-3.4402	-2.6011	1915.05
317.0	9.3511	-3.6109	-2.9047	1914.88
317.3	9.3289	-3.7252	-2.5111	1914.80
317.7	9.2629	-3.9799	-2.3317	1914.72
318.0	9.2134	-4.0972	-2.1901	1914.63
318.3	9.2247	-3.8099	-1.5177	1914.57
318.7	9.2563	-4.0132	-2.1311	1914.51
319.0	9.2825	-3.5869	-1.2467	1914.45
319.3	9.3267	-3.3682	-0.8371	1914.39
319.7	9.3968	-3.3089	-1.2847	1914.33
320.0	9.4017	-3.4442	-1.4511	1914.27
320.3	9.4684	-3.4109	-1.9717	1914.21
320.7	9.3327	-3.7372	-2.3431	1913.96
321.0	9.3116	-3.8779	-2.3077	1913.88
321.3	9.1957	-3.9932	-2.2291	1913.76
321.7	9.1594	-4.1719	-1.6867	1913.63



Depth from Top of Coral (mm)	Sr/Ca (mmol/mol)	Oxygen Isotope (permil)	Carbon Isotope (permil)	Date
322.0	9.1960	-4.0362	-1.5991	1913.58
322.3	9.2470	-4.0339	-1.9877	1913.54
322.7	9.4951	-3.6992	-1.2341	1913.29
323.0	9.4351	-3.6049	-1.2117	1913.26
323.3	9.4721	-3.3912	-1.2701	1913.24
323.7	9.4873	-3.5059	-1.3207	1913.21
324.0	9.4314	-3.6842	-1.6531	1913.10
324.3	9.5427	-3.9209	-1.3187	1912.99
324.7	9.3202	-3.7782	-1.0611	1912.88
325.0	9.3446	-3.8409	-1.2297	1912.82
325.3	9.2754	-4.3202	-1.4621	1912.76
325.7	9.2844	-3.7909	-1.0767	1912.69
326.0	9.2132	-4.1212	-1.7191	1912.63
326.3	9.3850	-3.8539	-1.3277	1912.46
326.7	9.4403	-3.7422	-1.1731	1912.34
327.0	9.5100	-2.3059	-1.1117	1912.21
327.3	9.3513	-3.6422	-1.7951	1912.05
327.7	9.2523	-4.1189	-2.1017	1911.88
328.0	9.1872	-4.1532	-2.2631	1911.82
328.3	9.0725	-4.4359	-2.2447	1911.76
328.7	9.0514	-4.6282	-2.2291	1911.69
329.0	8.9917	-4.8249	-2.1937	1911.63
329.3	9.0037	-4.7972	-2.2011	1911.59
329.7	9.1528	-4.4289	-2.3257	1911.55
330.0	9.1202	-4.4218	-1.5501	1911.50
330.3	9.3038	-4.3263	-1.7695	1911.46
330.7	9.4399	-3.9292	-1.4121	1911.40
331.0	9.4765	-3.6050	-1.5145	1911.33
331.3	9.5309	-3.4673	-1.4471	1911.27
331.7	9.5351	-3.3969	-1.7897	1911.21
332.0	9.4403	-3.5482	-1.8191	1911.13
332.3	9.3573	-3.6199	-1.9907	1911.05
332.7	9.3456	-3.8832	-2.0311	1910.96
333.0	9.2641	-4.3419	-2.4697	1910.88
333.3	9.0851	-4.2782	-2.8471	1910.80
333.7	8.9917	-4.4909	-2.8797	1910.72
334.0	8.9433	-4.5502	-2.5281	1910.63
334.3	8.9553	-4.3419	-2.2537	1910.55
334.7	9.1317	-3.8852	-1.6231	1910.46
335.0	9.4314	-3.3969	-1.0917	1910.37
335.3	9.4720	-3.5972	-1.4141	1910.29
335.7	9.4024	-3.3099	-1.5667	1910.21
336.0	9.5331	-3.3942	-2.0521	1910.13
336.3	9.3137	-3.8129	-2.4357	1909.96

Depth from Top of Coral (mm)	Sr/Ca (mmol/mol)	Oxygen Isotope (permil)	Carbon Isotope (permil)	Date
336.7	9.0804	-4.4036	-2.4419	1909.79
337.0	9.0076	-4.7129	-2.7847	1909.71
337.3	8.9296	-4.6062	-2.6676	1909.63
337.7	9.1096	-4.4619	-2.4617	1909.56
338.0	9.0703	-4.1932	-2.2071	1909.49
338.3	9.0309	-4.1179	-1.6787	1909.42
338.7	9.4443	-2.9302	-1.2671	1909.35
339.0	9.4862	-3.1919	-1.2017	1909.28
339.3	9.6175	-3.2952	-1.6801	1909.21
339.7	9.4612	-3.2587	-1.8490	1909.13
340.0	9.3979	-3.6292	-2.2561	1909.04
340.3	9.2874	-3.7279	-2.4637	1908.96
340.7	9.1771	-3.8692	-2.6121	1908.88
341.0	9.1285	-4.3359	-2.3637	1908.79
341.3	9.1357	-4.1052	-2.7971	1908.71
341.7	9.0842	-4.4359	-2.8327	1908.63
342.0	9.1283	-4.2862	-1.7231	1908.57
342.3	9.0968	-4.2552	-1.8371	1908.51
342.7	9.4487	-3.4002	-0.5521	1908.45
343.0	9.4854	-3.4049	-0.6057	1908.39
343.3	9.4711		-0.8309	1908.33
343.7	9.4131	-3.3169	-0.8707	1908.27
344.0	9.5395	-2.3879	-0.7157	1908.21
344.3	9.4477			1908.09
344.7	9.3235	-4.1402	-2.4561	1907.98
345.0	9.2366	-4.1616	-2.4301	1907.86
345.3	9.1749	-4.1622	-2.5891	1907.75
345.7	9.0779	-4.2669	-2.2427	1907.63
346.0	9.1546	-4.1629	-1.8779	1907.55
346.3	9.1862	-4.0159	-1.3617	1907.48
346.7	9.2982		-1.1895	1907.40
347.0	9.4169	-3.4459	-0.8287	1907.32
347.3	9.4498	-3.5842	-0.8561	1907.25
347.7	9.5145	-3.2609	-0.8767	1907.17
348.0	9.5664	-3.4102	-0.7831	1907.09
348.3	9.5185	-3.4719	-1.2047	1907.01
348.7	9.4487	-3.6452	-1.3431	1906.94
349.0	9.3825	-3.8019	-0.9297	1906.86
349.3	9.3320	-3.7932	-1.0791	1906.78
349.7	9.3098	-4.0019	-1.4737	1906.71
350.0	9.2553	-3.8322	-0.7891	1906.63
350.3	9.2785	-3.9129	-1.3117	1906.53
350.7	9.4469	-3.6352	-0.8731	1906.43
351.0	9.4819	-2.6926	0.6974	1906.33

Depth from Top of Coral (mm)	Sr/Ca (mmol/mol)	Oxygen Isotope (permil)	Carbon Isotope (permil)	Date
351.3	9.5303	-3.2242	-0.8911	1906.23
351.7	9.4331	-3.5329	-1.2687	1906.13
352.0	9.3551	-3.7932	-0.4711	1906.03
352.3	9.2945	-3.6879	-2.0767	1905.93
352.7	9.1964	-3.9082	-1.3421	1905.83
353.0	9.0865	-4.2899	-2.0567	1905.73
353.3	9.0787	-4.2802	-2.1271	1905.63
353.7	9.1290	-4.2349	-2.3387	1905.54
354.0	9.1715	-4.0882	-1.9671	1905.45
354.3	9.2409	-3.9309	-1.6467	1905.36
354.7	9.3723	-3.6222	-1.4121	1905.27
355.0	9.5716	-3.4009	-1.6817	1905.18
355.3	9.5671	-3.5899	-1.7469	1905.09
355.7	9.4520	-3.8317	-1.2798	1905.00
356.0	9.3712	-3.9862	-0.9551	1904.90
356.3	9.2987	-3.8479	-1.7107	1904.81
356.7	9.3195	-3.6862	-0.8991	1904.72
357.0	9.2426	-3.8919	-1.4747	1904.63
357.3	9.2573	-3.5882	-0.6731	1904.55
357.7	9.2791	-3.8279	-1.2327	1904.46
358.0	9.3293	-3.3212	-0.7011	1904.38
358.3	9.3831	-4.3019	-1.8557	1904.29
358.7	9.4006	-3.6122	-0.6621	1904.21
359.0	9.2960	-3.7099	0.0983	1904.17
359.3	9.4213	-3.6842	-0.4581	1904.13
359.7	9.3910	-3.7369	0.4363	1904.03
360.0	9.3688	-3.6512	-1.2881	1903.93
360.3	9.3615	-4.0049	-1.2667	1903.83
360.7	9.3329	-3.6892	-0.5721	1903.73
361.0	9.3289	-3.5119	-0.3507	1903.63
361.3	9.3706	-3.5632	-1.1651	1903.42
361.7	9.4098	-3.7340	-1.6341	1903.21
362.0	9.3612	-3.6382	-1.8521	1903.11
362.3	9.3242	-3.3629	-1.0307	1903.02
362.7	9.3102	-3.8235	-2.1399	1902.92
363.0	9.3546	-4.3839	-1.6617	1902.82
363.3	9.2675	-4.2972	-1.4441	1902.73
363.7	9.2493	-3.9559	-1.2377	1902.63
364.0	9.3251	-3.8402	-2.0191	1902.42
364.3	9.3569	-3.8919	-1.7357	1902.21
364.7	9.3215	-4.2447	-2.1822	1902.02
365.0	9.3116	-4.0859	-1.9127	1901.82
365.3	9.1694	-4.4723	-2.1869	1901.63
365.7	9.3277	-3.7179	-0.6297	1901.51



Depth from Top of Coral (mm)	Sr/Ca (mmol/mol)	Oxygen Isotope (permil)	Carbon Isotope (permil)	Date
366.0	9.4787	-3.4132	-0.8551	1901.38
366.3	9.5065	-3.1559	-0.3627	1901.32
366.7	9.4671	-3.1392	-0.7511	1901.27
367.0	9.5448	-3.2039	-0.5127	1901.21
367.3	9.5146			1901.09
367.7	9.5057	-3.4889	0.3133	1900.96
368.0	9.4510	-3.5792	0.2249	1900.83
368.3	9.3535	-3.5869	-0.9847	1900.71
368.7	9.4555		-0.1694	1900.65
369.0	9.3579	-3.4502	-0.2161	1900.60
369.3	9.3489	-3.6414	-1.0400	1900.54
369.7	9.4034	-2.9749	-0.7587	1900.43
370.0	9.4817	-3.5730	-1.3423	1900.32
370.3	9.5017	-2.9319	-0.7217	1900.21
370.7	9.4597			1900.10
371.0	9.4030	-3.3789	-1.0397	1899.98
371.3	9.1933	-3.9592	-2.0121	1899.86
371.7	9.1822	-4.1539	-1.5067	1899.75
372.0	9.1440	-3.9922	-1.3491	1899.63
372.3	9.4263	-3.3309	-1.0657	1899.29
372.7	9.4016	-3.3359	-0.7903	1899.26
373.0	9.3773	-3.2829	-1.3287	1899.24
373.3	9.4334	-3.2011	-1.1883	1899.21
373.7	9.3977	-3.4409	-2.0237	1899.17
374.0	9.4213	-3.4262	-2.1083	1899.13
374.3	9.3985	-3.5609	-2.0617	1899.02
374.7	9.2715	-3.8482	-2.8831	1898.91
375.0	9.1806	-3.9229	-2.0157	1898.79
375.3	9.1426	-3.9482	-1.6951	1898.63
375.7	9.2057	-3.8119	-1.4067	1898.57
376.0	9.3503	-3.3752	-0.8851	1898.52
376.3	9.2134	-3.5789	-1.2357	1898.46
376.7	9.4167	-3.3882	-1.3351	1898.21
377.0	9.3931	-3.2719	-1.6707	1898.10
377.3	9.3610	-3.4042	-1.9351	1898.00
377.7	9.3257	-3.5864	-2.0115	1897.90
378.0	9.2631	-4.0702	-1.7091	1897.79
378.3	9.2007	-3.7899	-1.0527	1897.71
378.7	9.1334	-4.0972	-0.8761	1897.63
379.0	9.2163	-3.9779	-1.7077	1897.59
379.3	9.2576	-4.2052	-2.4521	1897.55
379.7	9.2377	-4.0789	-1.7217	1897.50
380.0	9.2449	-3.9742	-1.3651	1897.46
380.3	9.3752	-3.6929	-1.4437	1897.40

Depth from Top of Coral (mm)	Sr/Ca (mmol/mol)	Oxygen Isotope (permil)	Carbon Isotope (permil)	Date
380.7	9.3712	-3.2732	-1.4121	1897.34
381.0	9.3593	-3.4183	-1.5882	1897.27
381.3	9.3931	-3.3242	-1.3581	1897.21
381.7	9.3923	-3.4197	-1.3567	1897.05
382.0	9.3201	-3.5437	-0.9375	1896.88
382.3	9.1850	-3.9401	-0.9416	1896.80
382.7	9.1575	-4.1362	-1.1341	1896.72
383.0	9.2168	-3.9869	-1.6797	1896.63
383.3	9.1871	-3.9194	-1.7961	1896.55
383.7	9.1678	-3.8710	-1.7603	1896.47
384.0	9.3005	-3.5482	-1.6671	1896.38

**Middle Piece Seen in Fig. 2.1**

376.7	9.4752	-3.5939	-1.7887	1898.21
377.0	9.4742	-3.3652	-1.0951	1898.10
377.3	9.2058	-3.7669	-1.8867	1898.00
377.7	9.2590	-3.7862	-1.6291	1897.90
378.0	9.1643	-4.1799	-2.1337	1897.79
378.3	9.0398			1897.71
378.7	9.0255	-4.4849	-2.1957	1897.63
379.0	9.1042	-4.4402	-2.2721	1897.59
379.3	9.1157	-3.9389	-1.8727	1897.55
379.7	9.3211	-4.0972	-2.2271	1897.50
380.0	9.1898	-3.5589	-1.7837	1897.46
380.3	9.3549	-3.5242	-1.4501	1897.40
380.7	9.4140	-3.2259	-1.3657	1897.34
381.0	9.4552	-3.2852	-1.4261	1897.27
381.3	9.4608	-3.4059	-2.1527	1897.21
381.7	9.3377	-3.7542	-2.2061	1897.05
382.0	9.2090	-3.6559	-2.3077	1896.88
382.3	9.1901	-4.0572	-2.3461	1896.80
382.7	9.1062	-4.2659	-2.3987	1896.72
383.0	9.0951	-4.1212	-2.0821	1896.63
383.3	9.0823	-4.6459	-2.4917	1896.55
383.7	9.1206	-4.2162	-2.0721	1896.47
384.0	9.3424	-3.6924	-1.2704	1896.38
384.3	9.3102	-3.6182	-1.4611	1896.32
384.7	9.3880	-3.3479	-0.8847	1896.27
385.0	9.5902	-3.1972	-0.7551	1896.21
385.3	9.5736	-3.0719	-0.5267	1896.00
385.7	9.3693	-3.2752	-0.6581	1895.79
386.0	9.3467	-3.3959	-0.6547	1895.63
386.3	9.3710	-3.3192	-0.7571	1895.38

Depth from Top of Coral (mm)	Sr/Ca (mmol/mol)	Oxygen Isotope (permil)	Carbon Isotope (permil)	Date
386.7	9.4507	-2.8899	-0.6457	1895.21
387.0	9.4217	-3.2712	-1.2051	1894.96
387.3	9.3322	-3.4039	-1.4817	1894.63
387.7	9.3899	-3.4482	-1.4621	1894.59
388.0	9.3784	-3.6249	-1.0607	1894.54
388.3	9.5414	-3.2212	-0.9761	1894.21
388.7	9.4671	-3.2399	-1.0467	1894.13
389.0	9.3949	-3.4002	-1.4781	1894.04
389.3	9.3799	-3.5099	-1.2367	1893.96
389.7	9.3148	-3.7182	-1.1841	1893.88
390.0	9.2218	-4.1469	-1.3777	1893.79
390.3	9.1591	-4.3872	-1.4801	1893.75
390.7	9.1196	-4.2599	-1.3497	1893.71
391.0	9.1120	-3.9732	-1.1711	1893.67
391.3	9.0906	-3.7739	-1.3487	1893.63
391.7	9.2239	-3.4742	-1.3141	1893.55
392.0	9.2487	-3.3309	-1.4097	1893.46
392.3	9.5254	-2.7313	1.8721	1893.21
392.7	9.3938	-2.8504	0.4696	1893.05
393.0	9.2547	-3.6562	-1.9501	1892.88
393.3	9.2596	-4.2419	-2.2137	1892.80
393.7	9.0357	-4.3492	-2.2651	1892.72
394.0	9.0455	-4.2809	-1.8477	1892.63
394.3	9.0858	-4.3122	-1.7331	1892.59
394.7	9.1139	-3.9629	-1.8497	1892.54
395.0	9.2012	-3.4642	-1.8401	1892.43
395.3	9.2651	-3.2849	-1.7687	1892.32
395.7	9.3643	-3.4042	-2.0891	1892.21
396.0	9.3113	-3.6940	-1.8378	1892.13
396.3	9.2622	-3.6532	-1.9977	1892.05
396.7	9.1810	-4.0659	-2.5327	1891.96
397.0	9.1141	-4.2102	-2.6051	1891.88
397.3	9.1060	-4.5729	-2.4437	1891.76
397.7	8.9362	-4.2992	-2.5871	1891.63
398.0	9.0742	-3.6359	-2.2177	1891.60
398.3	9.0363	-3.7222	-1.5441	1891.57
398.7	9.0888	-3.9709	-2.1357	1891.54
399.0	9.3222	-3.2592	-1.6481	1891.29
399.3	9.3063	-3.5599	-1.5247	1891.21
399.7	9.3898	-3.3572	-1.6551	1891.13
400.0	9.3541	-3.0199	-2.1157	1891.09
400.3	9.3073	-3.3542	-2.0611	1891.05
400.7	9.2124	-4.0129	-2.5477	1891.00
401.0	9.1551	-4.0642	-2.2231	1890.96



Depth from Top of Coral (mm)	Sr/Ca (mmol/mol)	Oxygen Isotope (permil)	Carbon Isotope (permil)	Date
401.3	9.1352	-4.2509	-2.4897	1890.85
401.7	9.0197	-4.3695	-2.2962	1890.74
402.0	8.9577	-4.3279	-2.3907	1890.63
402.3	9.0189	-3.8582	-1.8321	1890.55
402.7	9.1825	-3.6199	-1.5137	1890.46
403.0	9.2097	-3.4532	-1.4141	1890.38
403.3	9.3180	-3.3979	-1.6867	1890.26
403.7	9.3576	-3.5102	-2.0551	1890.13
404.0	9.3096	-3.7089	-2.1277	1890.04
404.3	9.2671	-3.9942	-1.7411	1889.96
404.7	9.1622	-3.9019	-1.7787	1889.88
405.0	9.0628	-4.3132	-1.9831	1889.79
405.3	9.0029	-4.4159	-2.2797	1889.71
405.7	8.9999	-4.2350	-1.7841	1889.63
406.0	9.0318	-4.1509	-1.8757	1889.50
406.3	9.2950	-3.6552	-1.2921	1889.38
406.7	9.2300	-3.3869	-1.0767	1889.34
407.0	9.4219	-3.1982	-1.5471	1889.29
407.3	9.3803	-3.3439	-1.8827	1889.25
407.7	9.4146	-3.1672	-1.7361	1889.21
408.0	9.3839	-3.7579	-2.4107	1889.04
408.3	9.1493	-3.9022	-2.4731	1888.88
408.7	8.9544	-4.5889	-2.2727	1888.71
409.0	9.0101	-4.4182	-1.9941	1888.67
409.3	8.9619	-4.3629	-1.6867	1888.63
409.7	9.0424	-3.9792	-1.4791	1888.55
410.0	9.2075	-3.7989	-1.1067	1888.46
410.3	9.2771	-3.3899	-0.9833	1888.38
410.7	9.4195	-3.1269	-1.1237	1888.30
411.0	9.4438	-3.0582	-1.4171	1888.21
411.3	9.3963	-3.1979	-1.7897	1888.11
411.7	9.3209	-3.8212	-2.3551	1888.00
412.0	9.2473	-4.0189	-2.0517	1887.89
412.3	9.1205	-4.4872	-2.2531	1887.79
412.7	9.0649	-3.9139	-1.9037	1887.75
413.0	9.0930	-4.4262	-1.9261	1887.71
413.3	9.0199	-4.4399	-1.8027	1887.67
413.7	8.9705	-3.6516	-2.0024	1887.63
414.0	8.9906	-3.8719	-1.4587	1887.55
414.3	9.1775	-3.4812	-1.1741	1887.46
414.7	9.2757	-3.5511	-0.7682	1887.38
415.0	9.3905	-3.0492	-0.5841	1887.32
415.3	9.4643	-3.1229	-0.8597	1887.27
415.7	9.4648	-3.3992	-1.2797	1887.21

Depth from Top of Coral (mm)	Sr/Ca (mmol/mol)	Oxygen Isotope (permil)	Carbon Isotope (permil)	Date
416.0	9.3243	-3.3889	-1.5707	1887.04
416.3	9.3111	-3.7242	-1.1321	1886.96
416.7	9.1258	-4.1439	-1.2547	1886.84
417.0	9.0801	-4.1872	-1.1641	1886.71
417.3	9.1397	-4.4198	-1.5235	1886.68
417.7	9.0542	-4.3072	-1.7031	1886.66
418.0	9.0365	-4.2609	-1.5347	1886.63
418.3	9.1614	-4.0412	-1.7871	1886.51
418.7	9.3910	-3.4369	-0.6857	1886.38
419.0	9.4979	-3.0712	-0.5821	1886.32
419.3	9.4714	-3.2469	-1.2667	1886.27
419.7	9.5893	-3.1372	-1.0121	1886.21
420.0	9.5731	-3.2639	-0.9267	1886.13
420.3	9.5018	-3.3172	-1.7261	1886.05
420.7	9.4484	-3.3909	-1.6077	1885.96
421.0	9.3324	-3.5712	-1.6991	1885.88
421.3	9.1690	-4.2532	-1.6256	1885.71
421.7	9.1174	-4.0592	-1.6501	1885.68
422.0	9.1217	-4.3619	-1.6157	1885.66
422.3	9.0821	-4.2572	-1.7181	1885.63
422.7	9.0889	-4.2749	-1.8697	1885.55
423.0	9.1195	-3.9382	-1.9091	1885.46
423.3	9.3015	-3.7399	-1.2277	1885.38
423.7	9.4818	-3.1622	-0.9351	1885.21
424.0	9.4210	-3.2359	-1.2177	1885.15
424.3	9.4523	-3.2360	-1.2635	1885.09
424.7	9.4743	-3.4359	-1.2777	1885.02
425.0	9.3603	-3.5022	-1.3871	1884.96
425.3	9.3114	-3.6209	-1.4837	1884.90
425.7	9.2752	-3.6782	-1.6821	1884.85
426.0	9.1300	-4.0221	-1.0269	1884.79
426.3	9.1094	-4.0772	-1.5411	1884.74
426.7	9.1343	-4.2269	-1.2407	1884.68
427.0	9.0844	-3.9472	-1.1541	1884.63
427.3	9.1707	-3.8129	-1.3017	1884.54
427.7	9.4449	-3.3272	-1.0231	1884.38
428.0	9.5440	-3.2429	-0.5227	1884.21
428.3	9.4771	-3.0065	-0.5623	1884.13
428.7	9.4687	-3.0199	-0.7057	1884.05
429.0	9.4725	-3.7612	-1.7551	1883.96
429.3	9.2910	-3.7779	-1.6647	1883.88
429.7	9.2348	-3.9722	-2.1321	1883.82
430.0	9.1185	-4.2379	-1.9517	1883.77
430.3	9.0464	-4.4502	-1.9441	1883.71

Depth from Top of Coral (mm)	Sr/Ca (mmol/mol)	Oxygen Isotope (permil)	Carbon Isotope (permil)	Date
430.7	9.0862	-4.3109	-2.0587	1883.67
431.0	9.0477	-4.1764	-2.1458	1883.63
431.3	9.1162	-4.2159	-2.2647	1883.55
431.7	9.2036	-3.6218	-1.5605	1883.46
432.0	9.3785	-3.3369	-1.1627	1883.38
432.3	9.4844	-3.1822	-0.8481	1883.29
432.7	9.5443			1883.21
433.0	9.5375	-3.0642	-1.3761	1883.16
433.3	9.4866	-2.9969	-1.0797	1883.12
433.7	9.4933	-3.2722	-1.5301	1883.07
434.0	9.5105	-3.3749	-1.4757	1883.02
434.3	9.3731	-3.1522	-1.7441	1882.97
434.7	9.3484	-4.0022	-1.5691	1882.93
435.0	9.2415	-4.2662	-1.0961	1882.88
435.3	9.1581	-4.0599	-1.4367	1882.82
435.7	9.1636	-3.9472	-0.7441	1882.76
436.0	9.0903	-4.0789	-1.2807	1882.69
436.3	9.0737	-4.0922	-1.5561	1882.63
436.7	9.2571	-3.8083	-1.6367	1882.51
437.0	9.3083	-3.3146	-0.7987	1882.38
437.3	9.5281	-2.8599	-0.1337	1882.30
437.7	9.6411	-2.6362	0.2509	1882.21
438.0	9.5228			1882.13
438.3	9.5265	-3.0242	-0.6771	1882.04
438.7	9.4002	-3.3219	-1.2167	1881.96
439.0	9.3071	-3.5202	-1.3311	1881.79
439.3	9.1267	-4.0079	-1.9007	1881.63
439.7	9.1599	-4.3112	-1.7471	1881.61
440.0	9.2180	-4.5039	-2.0077	1881.59
440.3	9.1659	-4.3692	-2.0151	1881.58
440.7	9.2521	-3.7429	-1.4037	1881.56
441.0	9.2783	-3.5382	-0.8041	1881.54
441.3	9.5582	-3.1299	-1.1687	1881.21
441.7	9.5306	-3.1482	-1.5221	1881.16
442.0	9.4562	-3.1179	-1.6767	1881.12
442.3	9.4591	-3.2711	-1.9602	1881.07
442.7	9.2669		-1.9301	1881.02
443.0	9.4632		-1.4436	1880.97
443.3	9.2836	-3.6819	-1.9839	1880.93
443.7	9.2261	-3.6122	-1.5631	1880.88
444.0	9.1892	-3.9663	-2.1469	1880.83
444.3	9.0829		-2.2304	1880.78
444.7	9.0833	-3.2529	-1.7147	1880.73
445.0	9.0923	-4.2732	-1.7811	1880.68



Depth from Top of Coral (mm)	Sr/Ca (mmol/mol)	Oxygen Isotope (permil)	Carbon Isotope (permil)	Date
445.3	9.0604		-1.3475	1880.63
445.7	9.1447	-4.1732	-1.6471	1880.60
446.0	9.2684	-3.7379	-1.6987	1880.57
446.3	9.1735	-3.7982	-1.9781	1880.54
446.7	9.3779	-3.4748	-1.2682	1880.48
447.0	9.4239	-3.7973	-1.7225	1880.41
447.3	9.3486	-2.9219	-1.2077	1880.34
447.7	9.4568	-3.4222	-1.4151	1880.28
448.0	9.4992	-3.2839	-1.5307	1880.21
448.3	9.4540	-3.3597	-1.7625	1880.11
448.7	9.4244	-3.0379	-1.7817	1880.00
449.0	9.3393	-3.6072	-2.8451	1879.89
449.3	9.2008	-3.8919	-2.7287	1879.79
449.7	9.1135	-4.3892	-2.4781	1879.74
450.0	9.1344	-4.0129	-1.9397	1879.68
450.3	9.0686	-4.3052	-2.7121	1879.63
450.7	9.1368	-4.1249	-1.6363	1879.60
451.0	9.0834	-3.4802	-1.5501	1879.57
451.3	9.1268	-3.6939	-1.9217	1879.54
451.7	9.4519	-3.0802	-1.2221	1879.46
452.0	9.4344	-3.3821	-2.0456	1879.37
452.3	9.4549	-3.2892	-1.9391	1879.29
452.7	9.4835			1879.21
453.0	9.3691	-3.6502	-2.4421	1879.04
453.3	9.2059	-3.8589	-2.1687	1878.88
453.7	9.1793	-4.1392	-2.3831	1878.76
454.0	9.1052	-3.6229	-2.3657	1878.63
454.3	9.1125	-4.0882	-2.4421	1878.55
454.7	9.2164	-3.7329	-1.6277	1878.47
455.0	9.3345	-3.5014	-1.4770	1878.38
455.3	9.4409		-1.2093	1878.21
455.7	9.4403		-1.8190	1878.15
456.0	9.3600	-3.4789	-2.2967	1878.08
456.3	9.2629	-3.5342	-2.4921	1878.02
456.7	9.3311	-3.8582	-2.1819	1877.96
457.0	9.2064	-3.9602	-1.7311	1877.85
457.3	9.1503	-4.3229	-2.1677	1877.74
457.7	9.1729	-4.5993	-2.8715	1877.63
458.0	9.1601	-4.0161	-2.1448	1877.55
458.3	9.2396	-3.7622	-1.7291	1877.46
458.7	9.4089	-3.4089	-1.6107	1877.38
459.0	9.4764	-3.2942	-1.3591	1877.25
459.3	9.5211	-3.4552	-1.7477	1877.13
459.7	9.4523	-3.3592	-1.7191	1877.09

Depth from Top of Coral (mm)	Sr/Ca (mmol/mol)	Oxygen Isotope (permil)	Carbon Isotope (permil)	Date
460.0	9.4653	-3.5049	-2.1547	1877.04
460.3	9.3944	-3.7416	-2.2797	1877.00
460.7	9.3362	-4.0849	-1.8107	1876.96
461.0	9.1792	-4.1162	-2.1091	1876.88
461.3	9.0727	-4.2139	-1.5277	1876.79
461.7	9.0360	-4.4412	-2.0751	1876.71
462.0	9.0920	-4.1149	-1.4947	1876.67
462.3	9.0412	-4.1722	-1.7171	1876.63
462.7	9.1606	-3.9209	-1.6557	1876.55
463.0	9.2202	-3.6922	-1.7171	1876.46
463.3	9.3915	-2.5922	0.4807	1876.34
463.7	9.4642	-3.2552	-1.5121	1876.21
464.0	9.4346	-3.4029	-1.4807	1876.10
464.3	9.4166	-3.4692	-1.7891	1876.00
464.7	9.3179	-4.1844	-1.7688	1875.90
465.0	9.1946	-4.0558	-1.7094	1875.79
465.3	9.2035	-4.2551	-1.2192	1875.74
465.7	9.2740	-4.2722	-1.5551	1875.68
466.0	9.0516	-4.2359	-2.0397	1875.63
466.3	9.1961	-4.4472	-2.1891	1875.59
466.7	9.1742	-3.7076	-1.4959	1875.54
467.0	9.4854	-3.3922	-1.1601	1875.29
467.3	9.4319	-3.3559	-1.0937	1875.24
467.7	9.4655	-3.4352	-1.3101	1875.18
468.0	9.4714	-3.3069	-1.3737	1875.13
468.3	9.4137	-3.5892	-1.3731	1875.01
468.7	9.2715	-3.7677	-1.1124	1874.88
469.0	9.1774	-3.9402	-1.0921	1874.82
469.3	9.1558	-4.0939	-1.2997	1874.76
469.7	9.1301	-4.1107	-1.7115	1874.69
470.0	9.0893	-4.6463	-2.0437	1874.63
470.3	9.2036	-3.6742	-1.7871	1874.54
470.7	9.3797	-4.1032	-1.5333	1874.38
471.0	9.4305	-3.1792	-1.3011	1874.29
471.3	9.4706	-3.7310	-1.8548	1874.21
471.7	9.3714	-3.5292	-1.9481	1874.00
472.0	9.2215	-3.6619	-2.1367	1873.79
472.3	9.1285	-4.2492	-1.4521	1873.71
472.7	9.1136	-4.2989	-2.7247	1873.63
473.0		-4.3462	-2.2411	1873.57
473.3	9.1700	-4.2489	-2.0477	1873.52
473.7	9.1523	-4.0739	-2.1767	1873.46
474.0	9.3553	-3.5699	-1.5107	1873.40
474.3	9.3528	-3.3412	-1.4691	1873.35

Depth from Top of Coral (mm)	Sr/Ca (mmol/mol)	Oxygen Isotope (permil)	Carbon Isotope (permil)	Date
474.7	9.3978	-3.5059	-1.8647	1873.29
475.0	9.3621	-3.6572	-1.9981	1873.23
475.3	9.3760	-3.4699	-2.0927	1873.21
475.7	9.2530	-3.6042	-2.4321	1872.96
476.0	9.2114	-3.8951	-2.1708	1872.92
476.3	9.1658	-3.9784	-1.2142	1872.88
476.7	9.1317	-4.1529	-1.5087	1872.83
477.0	9.0943	-4.2242	-2.2881	1872.79
477.3	9.0103	-4.2419	-2.6707	1872.63
477.7	9.0379	-4.1265	-2.4544	1872.56
478.0	9.2418	-3.7989	-1.6077	1872.49
478.3	9.4091	-3.5022	-1.5361	1872.43
478.7	9.4642	-3.3679	-1.6267	1872.36
479.0	9.4758	-3.4022	-1.9891	1872.29
479.3	9.3931	-3.5456	-2.1689	1872.21
479.7	9.5275	-3.6222	-1.9161	1872.13
480.0	9.1037	-4.3939	-1.4867	1871.79
480.3	8.8899			1871.63
480.7	9.0791	-4.2369	-2.0107	1871.51
481.0	9.2944	-3.7612	-1.8511	1871.38
481.3	9.3125		-2.0830	1871.35
481.7	9.3803	-3.3342	-1.6521	1871.31
482.0	9.3675	-3.8549	-2.1447	1871.28
482.3	9.3686	-3.6432	-2.2261	1871.24
482.7	9.4813		-3.2118	1871.21
483.0	9.3484	-4.0902	-2.2391	1870.88
483.3	9.1856	-4.1009	-2.4397	1870.80
483.7	9.1880	-4.2582	-2.7441	1870.72
484.0	9.1681	-4.1879	-1.8627	1870.63
484.3	9.2056	-3.7942	-1.3441	1870.57
484.7	9.3395	-4.0349	-2.0187	1870.52
485.0	9.2769	-3.5952	-1.7631	1870.46
485.3	9.5034	-3.1959	-1.6007	1870.34
485.7	9.5194	-3.0412	-1.3191	1870.21
486.0	9.4906	-3.1249	-1.1717	1870.12
486.3	9.4409	-3.3162	-1.5541	1870.04
486.7	9.3510			1869.96
487.0	9.4083	-3.5538	-1.3456	1869.87
487.3	9.2953	-3.7799	-1.9927	1869.79
487.7	9.2740	-4.0492	-2.4051	1869.63
488.0	9.3545	-4.0479	-2.3357	1869.46
488.3	9.5916	-3.3932	-1.4601	1869.21
488.7		-2.9827	-0.7174	1869.19
489.0	9.4709	-3.5212	-0.8171	1869.17



Depth from Top of Coral (mm)	Sr/Ca (mmol/mol)	Oxygen Isotope (permil)	Carbon Isotope (permil)	Date
489.3	9.4463	-2.8901	-0.6408	1869.15
489.7	9.6000	-2.9642	-1.6301	1869.13
490.0	9.4734			1868.96
490.3	9.0252	-4.2731	-2.8492	1868.63
490.7	9.1966			1868.57
491.0		-3.9449	-2.5727	1868.52
491.3	9.2471	-3.7742	-2.5801	1868.46
491.7	9.3711	-3.4619	-2.0227	1868.38
492.0	9.4830	-3.4812	-1.7841	1868.29
492.3	9.4378			1868.21
492.7	9.4823	-3.1899	-1.7977	1868.13
493.0	9.4277	-3.6572	-0.8821	1867.96
493.3	9.3681	-3.5859	-0.6027	1867.80
493.7	9.3078	-3.3602	-0.8841	1867.63
494.0	9.3426	-3.6936	-1.6727	1867.49
494.3	9.4261	-3.4132	-1.6001	1867.36
494.7	9.4154			1867.23
495.0	9.4506			1867.09
495.3	9.4142	-3.6949	-1.2757	1866.96
495.7	9.4127	-3.5486	-1.5503	1866.83
496.0	9.4334	-3.6998	-1.2394	1866.69
496.3	9.4277		-1.6298	1866.56
496.7	9.4018	-3.5959	-1.2337	1866.43
497.0	9.3981	-3.4271	-1.5858	1866.29
497.3	9.4540	-3.6079	-2.2937	1866.16
497.7	9.4599	-3.5212	-1.8551	1866.03
498.0	9.3483	-3.4939	-1.7197	1865.89
498.3	9.3156	-3.7102	-2.1261	1865.76
498.7	9.2603	-3.9599	-1.9327	1865.63
499.0	9.3463	-3.5392	-1.9531	1865.47
499.3	9.3060	-3.7439	-1.9667	1865.31
499.7	9.3505	-3.6257	-1.7190	1865.16
500.0	9.3838	-3.4969	-1.5377	1865.00
500.3	9.3560	-3.0684	-1.4016	1864.84
500.7	9.4215	-3.4639	-1.3377	1864.68
501.0	9.4111	-3.2642	-1.3101	1864.52
501.3	9.4397	-3.0441	-2.4130	1864.37
501.7	9.5744	-3.3889	-2.5991	1864.21
502.0	9.3519	-3.7809	-2.7637	1863.88
502.3	9.2444	-3.9852	-3.2371	1863.63
502.7	9.2755	-3.9077	-2.6982	1863.55
503.0	9.3653	-3.8102	-2.3271	1863.46
503.3	9.4344	-3.4419	-2.3097	1863.38
503.7	9.5885	-3.2112	-1.7091	1863.21

Depth from Top of Coral (mm)	Sr/Ca (mmol/mol)	Oxygen Isotope (permil)	Carbon Isotope (permil)	Date
504.0	9.5742	-3.5409	-2.1157	1863.13
504.3	9.5180	-3.5072	-3.0911	1863.04
504.7	9.4289	-3.6159	-3.0037	1862.96
505.0	9.2524	-3.9009	-2.3023	1862.79
505.3	9.2161	-4.0229	-2.1307	1862.63
505.7	9.3010	-2.9702	-0.2541	1862.52
506.0	9.3512	-3.3969	-1.5787	1862.41
506.3	9.4043	-3.4632	-1.9861	1862.30
506.7	9.4120	-3.4879	-1.5307	1862.19
507.0	9.3927	-3.5972	-0.8311	1862.07
507.3	9.4463	-3.4229	-0.8877	1861.96
507.7	9.4740	-2.9782	-0.8071	1861.85
508.0	9.4859	-3.0709	-0.2807	1861.74
508.3	9.4731	-3.1692	-0.4091	1861.63
508.7	9.4440	-3.2295	-0.5641	1861.52
509.0	9.5226	-3.1842	-0.6611	1861.41
509.3	9.5121	-3.2258	-0.4856	1861.30
509.7	9.4724	-3.3092	-0.7561	1861.19
510.0	9.4980	-2.8859	-0.3467	1861.07
510.3	9.4445	-3.3112	-0.9391	1860.96
510.7	9.4130	-3.7779	-1.8687	1860.85
511.0	9.3349	-3.8092	-1.8811	1860.74
511.3	9.3092	-3.9829	-2.5207	1860.63
511.7	9.3557	-3.7883	-2.6019	1860.57
512.0	9.4071	-3.2909	-1.7187	1860.52
512.3	9.4327	-3.2812	-1.6491	1860.46
512.7	9.4789	-2.9731	-0.9520	1860.38
513.0	9.5613	-3.3172	-0.8191	1860.29
513.3	9.4829	-3.2189	-1.1557	1860.09
513.7	9.4119	-3.2892	-0.7871	1859.88
514.0	9.3302	-3.5479	-1.4217	1859.63
514.3	9.3510	-3.4332	-1.7151	1859.55
514.7	9.3895	-3.4209	-1.4247	1859.46
515.0	9.5116	-3.2222	-1.2151	1859.21
515.3	9.4522	-3.2789	-1.0937	1859.04
515.7	9.3738	-3.4032	-0.8831	1858.71
516.0	9.4331	-3.4819	-0.6697	1858.67
516.3	9.4429	-3.6392	-1.3331	1858.63
516.7	9.3605	-4.0621	-1.1578	1858.58
517.0	9.3551	-3.5152	-1.4761	1858.54
517.3	9.3962	-3.7809	-2.1257	1858.42
517.7	9.5702	-3.0602	-1.6961	1858.29
518.0	9.5758	-3.2079	-1.1117	1858.24
518.3	9.5581	-3.2892	-0.8491	1858.18

Depth from Top of Coral (mm)	Sr/Ca (mmol/mol)	Oxygen Isotope (permil)	Carbon Isotope (permil)	Date
518.7	9.5997	-3.0848	-1.8537	1858.13
519.0	9.5276	-3.2442	-2.4471	1858.00
519.3	9.3449	-4.4109	-3.3267	1857.88
519.7	9.1976	-3.9858	-2.4908	1857.63
520.0	9.2481	-3.7119	-2.1757	1857.50
520.3	9.3337	-3.5992	-2.5111	1857.38
520.7	9.4176	-3.3481	-2.2522	1857.29
521.0	9.4188	-3.8592	-2.1331	1857.21
521.3	9.4325	-3.7234	-2.3154	1857.13
521.7	9.3108	-4.2655	-2.5790	1856.88
522.0	9.2303	-3.8399	-2.4857	1856.63
522.3	9.3674	-3.6312	-1.5691	1856.46
522.7	9.4944	-3.1119	-0.7557	1856.41
523.0	9.5368	-3.1712	-1.1981	1856.36
523.3	9.5094	-3.1329	-1.1717	1856.31
523.7	9.5304	-3.0922	-0.8321	1856.26
524.0	9.6693	-2.9769	-0.3657	1856.21
524.3	9.5897	-3.0102	-1.0171	1856.09
524.7	9.5619	-3.2159	-1.2787	1855.96
525.0	9.1599	-3.6612	-2.6351	1855.63
525.3	9.4221	-3.7699	-2.2597	1855.46
525.7	9.3917	-3.5562	-2.3071	1855.38
526.0	9.5010	-3.1199	-1.8597	1855.29
526.3	9.6720	-2.8862	-1.4261	1855.21
526.7	9.6829			1855.04
527.0	9.5179		-2.6774	1854.96
527.3	9.2861	-3.1653	-1.7183	1854.63
527.7	9.3127	-3.2802	-1.5311	1854.49
528.0	9.3511	-3.3079	-1.5187	1854.35
528.3	9.4343	-3.2202	-0.6101	1854.21
528.7	9.4051	-3.0431	-0.3334	1853.92
529.0	9.3786	-3.0582	-0.8609	1853.63
529.3	9.4196	-3.3909	-0.8597	1853.53
529.7	9.4270	-2.9452	-0.3121	1853.42
530.0	9.4751	-3.3749	-1.2727	1853.31
530.3	9.5452	-3.3112	-1.2711	1853.21
530.7	9.5294	-3.2720	-0.7838	1853.05
531.0	9.3864	-3.5962	-1.3331	1852.88
531.3	9.3060	-3.5679	-0.7907	1852.80
531.7	9.3105	-3.7152	-0.6471	1852.72
532.0	9.2801	-3.9139	-0.9737	1852.63
532.3	9.3607	-3.2850	-0.7076	1852.55
532.7	9.3874	-3.7099	-1.1947	1852.46
533.0	9.4240		-1.2668	1852.37



Depth from Top of Coral (mm)	Sr/Ca (mmol/mol)	Oxygen Isotope (permil)	Carbon Isotope (permil)	Date
533.3	9.4555	-2.9649	-1.5197	1852.29
533.7	9.3993	-3.4102	-1.4621	1852.21
534.0	9.4566	-3.9764	-2.2924	1852.13
534.3	9.3930	-3.7682	-1.7991	1852.03
534.7	9.3880	-3.7989	-2.2777	1851.93
535.0	9.2864	-4.0812	-1.2841	1851.83
535.3	9.3080	-3.9549	-2.3647	1851.73
535.7	9.2272	-3.8352	-1.9151	1851.63
536.0	9.3223	-3.5589	-1.9697	1851.54
536.3	9.4005	-3.5232	-1.9551	1851.46
536.7	9.5171	-3.2969	-1.6567	1851.38
537.0	9.5164	-3.2052	-2.1091	1851.29
537.3	9.5876	-4.5182	-2.9041	1851.21
537.7	9.4865			1850.96
538.0	9.2690	-4.0439	-2.5277	1850.71
538.3	9.2647	-3.3052	-1.7331	1850.63
538.7	9.3289	-3.7539	-1.7787	1850.42
539.0	9.5274	-3.7705	-1.4031	1850.21
539.3	9.5108	-3.3609	-1.1487	1850.07
539.7	9.4853	-3.3372	-0.9991	1849.92
540.0	9.4578	-3.3389	-0.7357	1849.77
540.3	9.4311	-3.5662	-0.9261	1849.63
540.7	9.4833	-3.0129	-0.4587	1849.49
541.0	9.4733	-3.3922	-1.3031	1849.35
541.3	9.5722	-2.9779	-0.6807	1849.21
541.7	9.4672	-3.7392	-1.3991	1848.92
542.0	9.4622	-3.9492	-0.9431	1848.63
542.3	9.5936	-3.2492	-1.6031	1848.21
542.7	9.4595	-3.3689	-1.6177	1848.05
543.0	9.3580	-4.2218	-2.0280	1847.88
543.3	9.3520	-3.8389	-1.7307	1847.76
543.7	9.1943	-3.9752	-1.8431	1847.63
544.0	9.3266	-3.8899	-1.7237	1847.50
544.3	9.4767	-3.3762	-1.2771	1847.38
544.7	9.5372	-3.2019	-1.1117	1847.30
545.0	9.5655	-3.5182	-1.1591	1847.21
545.3	9.4497	-3.3879	-0.7117	1846.92
545.7	9.4015	-3.3942	0.5179	1846.63
546.0	9.4163	-3.7639	-1.3477	1846.52
546.3	9.4721	-3.2402	-0.5331	1846.42
546.7	9.5717	-3.5149	-0.7627	1846.32
547.0	9.6487	-3.2902	-0.8421	1846.21
547.3	9.4461	-3.5449	-1.2227	1845.88
547.7	9.4363	-3.7562	-1.2781	1845.80

Depth from Top of Coral (mm)	Sr/Ca (mmol/mol)	Oxygen Isotope (permil)	Carbon Isotope (permil)	Date
548.0	9.2988	-3.9929	-1.0967	1845.71
548.3	9.2692	-4.1312	-1.8241	1845.63
548.7	9.2874	-3.8129	-0.5507	1845.59
549.0	9.3257	-3.6402	-0.9051	1845.54
549.3	9.4693	-3.3759	-1.1897	1845.42
549.7	9.5377	-3.2852	-1.2121	1845.29
550.0	9.5284	-3.2049	-1.3637	1845.13
550.3	9.4029	-3.6782	-1.7011	1845.01
550.7	9.3416	-3.3339	-1.9977	1844.88
551.0	9.1937	-4.1502	-2.0371	1844.75
551.3	9.1045	-4.2359	-1.8537	1844.63
551.7	9.1526	-4.1892	-2.0661	1844.55
552.0	9.2444	-3.8019	-1.3387	1844.46
552.3	9.4474	-3.1132	-0.9711	1844.34
552.7	9.6433	-3.0309	-1.1797	1844.21
553.0	9.6086	-3.4219	-1.9065	1844.07
553.3	9.4198	-3.0179	-1.9097	1843.93
553.7	9.2701	-3.4582	-2.2211	1843.79
554.0	9.1603	-4.0109	-1.9047	1843.71
554.3	9.1322	-4.1562	-1.8361	1843.63
554.7	9.1798	-3.8049	-1.0887	1843.54
555.0	9.3390	-3.4062	-0.7981	1843.41
555.3	9.4934	-2.9719	-0.5597	1843.29
555.7	9.5135	-3.0052	-0.5151	1843.21
556.0	9.1581	-3.8289	-1.4957	1842.88
556.3	9.2629	-3.4192	-1.8601	1842.84
556.7	9.1669	-3.8779	-2.1537	1842.79
557.0	9.0593	-4.2232	-2.1531	1842.63
557.3	9.1571	-4.0139	-1.3767	1842.55
557.7	9.2692	-3.7642	-0.5771	1842.47
558.0	9.4223	-3.2309	-0.3937	1842.38
558.3	9.5958	-2.8742	-0.6117	1842.21
558.7	9.5329	-2.9169	-1.0987	1842.07
559.0	9.3909	-3.4682	-1.1971	1841.93
559.3	9.2838	-3.9289	-1.2967	1841.79
559.7	9.1563	-4.0362	-2.0581	1841.63
560.0	9.1912	-4.1019	-1.0227	1841.52
560.3	9.2221	-3.8012	-0.7121	1841.42
560.7	9.3943	-3.3069	0.2393	1841.32
561.0	9.6080	-2.8902	-0.0361	1841.21
561.3	9.3598	-3.0519	-0.4137	1840.88
561.7	9.4986			1840.84
562.0	9.2998	-3.8599	-1.5227	1840.79
562.3	9.2722	-4.1362	-1.7751	1840.63

Depth from Top of Coral (mm)	Sr/Ca (mmol/mol)	Oxygen Isotope (permil)	Carbon Isotope (permil)	Date
562.7	9.3593	-3.5829	-1.4557	1840.49
563.0	9.5541	-3.3732	-1.4631	1840.35
563.3	9.5414	-3.3319	-1.8747	1840.21
563.7	9.5908	-3.1082	-1.2951	1840.05
564.0	9.4729			1839.88
564.3	9.3131	-3.8002	-1.4871	1839.71
564.7	9.3110	-3.9859	-1.4177	1839.54
565.0	9.4329	-3.8622	-1.7601	1839.43
565.3	9.4873	-3.4909	-1.7037	1839.32
565.7	9.4743	-3.4020	-1.3669	1839.21
566.0		-3.4019	-1.5407	1839.10
566.3	9.4874	-3.7402	-1.7661	1838.99
566.7	9.3176	-3.8249	-2.0717	1838.88
567.0	9.3503	-3.8372	-2.4881	1838.75
567.3	9.1535	-4.0859	-1.8467	1838.63
567.7	9.2177	-3.4172	-1.1821	1838.55
568.0	9.2814	-3.2199	-0.8797	1838.46
568.3	9.4728	-3.3392	-1.2351	1838.21
568.7	9.3842	-3.2289	-1.2217	1838.04
569.0	9.3575	-3.7582	-1.7851	1837.96
569.3	9.2704	-3.9699	-1.2857	1837.88
569.7	9.0952	-4.2312	-1.6651	1837.63
570.0	9.1768	-4.1119	-1.4517	1837.54
570.3	9.3037	-4.0612	-0.9781	1837.46
570.7	9.4663	-3.5659	-0.8907	1837.34
571.0	9.5463	-3.2052	-0.8791	1837.21
571.3	9.4850	-2.9909	-0.9197	1837.10
571.7	9.3788	-3.6932	-1.5261	1836.99
572.0	9.2695	-4.0029	-1.5617	1836.88
572.3	9.2307	-4.0888	-1.6108	1836.76
572.7	9.1160	-3.8719	-1.6997	1836.63
573.0	9.4930	-3.3762	-0.8751	1836.38
573.3	9.5957	-2.9079	-0.7847	1836.21
573.7	9.5654	-3.0432	-1.1411	1836.05
574.0	9.3138	-3.6079	-1.8237	1835.88
574.3	9.2054	-4.0862	-1.6811	1835.79
574.7	9.1749	-4.1259	-1.7817	1835.63
575.0	9.2557	-3.4872	-0.7831	1835.54
575.3	9.5211	-3.0169	-0.4347	1835.38
575.7	9.6515	-2.8162	-0.8821	1835.21
576.0	9.6126	-2.6569	-1.1697	1835.04
576.3	9.3488	-3.1642	-1.2751	1834.88
576.7	9.2483	-3.5089	-1.8827	1834.76
577.0	9.1044	-4.1022	-1.5171	1834.63



Depth from Top of Coral (mm)	Sr/Ca (mmol/mol)	Oxygen Isotope (permil)	Carbon Isotope (permil)	Date
577.3	9.1202	-4.1139	-1.6917	1834.55
577.7	9.3609	-3.5502	-0.8551	1834.46
578.0	9.5810	-3.1079	-1.1937	1834.21
578.3	9.5422	-2.9432	-1.1581	1834.09
578.7	9.3893	-3.2349	-1.9817	1833.96
579.0	9.2561	-3.9158	-2.0425	1833.79
579.3	9.1559	-4.1049	-2.2867	1833.63
579.7	9.3406	-3.9882	-1.6441	1833.46
580.0	9.2724	-3.8639	-1.5207	1833.33
580.3	9.3922	-3.4502	-0.9931	1833.21

#### Track Shift

580.0	9.5398	-3.3552	0.4439	1833.33
580.3	9.5768	-3.2319	0.0303	1833.21
580.7	9.4698	-3.4242	-0.1151	1833.09
581.0	9.4204	-3.6579	-0.0987	1832.96
581.3	9.3504	-3.8602	-0.4041	1832.80
581.7	9.2864	-3.6879	-0.0837	1832.63
582.0	9.3479	-3.4662	-0.0141	1832.54
582.3	9.4329	-3.5579	-0.0847	1832.46
582.7	9.5472	-3.2392	-0.0241	1832.34
583.0	9.6314	-3.2023		1832.21
583.3	9.5179	-3.7550	-0.0079	1831.92
583.7	9.3305	-3.9759	-0.7197	1831.63
584.0	9.3406	-3.7422	-0.1881	1831.55
584.3	9.3749	-3.7669	-0.0607	1831.46
584.7	9.3587	-4.1282	-0.7461	1831.38
585.0	9.3866	-3.6289	-0.2107	1831.30
585.3	9.3992	-3.3862	-0.1911	1831.21
585.7	9.4655	-3.4129	-0.3247	1831.13
586.0	9.4230	-3.7412	0.0899	1831.03
586.3	9.4921	-3.1109	0.3933	1830.92
586.7	9.3834	-3.6662	-0.2251	1830.82
587.0	9.3586	-3.6069	-0.6597	1830.71
587.3	9.3878	-3.6972	-0.8361	1830.67
587.7	9.3484	-3.2269	-0.4247	1830.63
588.0	9.3844	-3.6332	-1.2111	1830.42
588.3	9.4630	-3.4569	-1.0637	1830.21
588.7	9.4480	-3.4152	-0.3341	1830.10
589.0	9.3703	-3.6269	-0.0687	1829.98
589.3	9.3342	-3.3782	-0.0711	1829.86
589.7	9.3847			1829.75

Depth from Top of Coral (mm)	Sr/Ca (mmol/mol)	Oxygen Isotope (permil)	Carbon Isotope (permil)	Date
590.0	9.2139	-3.9422	-0.9301	1829.63
590.3	9.2774	-3.8459	-0.9597	1829.55
590.7	9.3590	-4.0672	-1.3741	1829.46
591.0	9.4130	-3.7169	-0.8037	1829.38
591.3	9.5304	-3.5012	0.2129	1829.29
591.7	9.6621	-3.3659	-0.3027	1829.21
592.0	9.5730	-3.4552	0.0809	1829.09
592.3	9.5101	-3.2259	0.2563	1828.96
592.7	9.4463	-3.5328	-1.0026	1828.84
593.0	9.4191	-3.6999	-1.3827	1828.71
593.3	9.5516	-3.9722	-1.2421	1828.68
593.7	9.4375	-3.6449	-0.5917	1828.66
594.0	9.4038	-3.5982	-0.7711	1828.63
594.3	9.5337	-3.5539	0.4403	1828.29
594.7	9.5437	-3.5212	-0.3001	1828.21
595.0	9.5342	-3.5489	-0.6757	1828.12
595.3	9.4714	-3.6002	-0.7901	1828.04
595.7	9.0976	-3.6449	-0.8437	1827.63
596.0	9.3803	-3.8892	-0.9581	1827.54
596.3	9.4283	-3.8569	-0.8757	1827.50
596.7	9.3975	-3.8812	-0.6861	1827.46
597.0	9.4343	-3.6899	-0.8667	1827.43
597.3	9.4250	-3.7922	-0.9951	1827.40
597.7	9.4328	-3.6629	-0.4647	1827.37
598.0	9.4537	-3.4512	0.1159	1827.34
598.3	9.4413	-3.6949	0.1903	1827.30
598.7	9.4733	-3.5252	0.3129	1827.27
599.0	9.4622	-3.6809	0.7523	1827.24
599.3	9.5319	-3.6332	0.6999	1827.21
599.7	9.5062	-3.6539	0.0373	1827.05
600.0	9.4003	-3.7752	-0.3541	1826.88
600.3	9.2961	-3.8129	-0.4977	1826.63
600.7	9.3646	-3.5932	-0.1001	1826.54
601.0	9.5633	-3.7639	-0.7127	1826.29
601.3				
601.7	9.4788	-3.4692	-0.4491	1826.23
602.0	9.5220	-3.3539	-0.4717	1826.19
602.3	9.5265	-3.3892	-0.6091	1826.16
602.7	9.5889	-3.7379	-1.1657	1826.13
603.0	9.3900	-3.7202	-0.9931	1825.63
603.3	9.4065			1825.52
603.7	9.5295	-3.9612	-1.7881	1825.42
604.0	9.4737	-3.7039	-1.1857	1825.31
604.3	9.5782	-3.4962	-1.1051	1825.21

Depth from Top of Coral (mm)	Sr/Ca (mmol/mol)	Oxygen Isotope (permil)	Carbon Isotope (permil)	Date
604.7	9.4414	-3.5259	-1.3967	1825.17
605.0	9.5078	-3.6202	-0.9661	1825.13
605.3	9.4118	-3.7239	-0.5927	1825.03
605.7	9.3951	-3.7789	-0.5291	1824.92
606.0	9.3803	-3.8416	-0.6146	1824.81
606.3	9.3055	-3.7712	-0.8391	1824.71
606.7	9.4364	-3.6759	-0.5697	1824.67
607.0	9.3376	-3.7032	-0.7791	1824.63
607.3	9.3792	-3.8999	-0.7547	1824.55
607.7	9.4458	-3.8442	-0.4301	1824.46
608.0	9.4436	-3.6319	-0.2277	1824.38
608.3	9.4262	-3.7889	-0.2129	1824.29
608.7	9.4516	-3.4839	0.3193	1824.21
609.0	9.4155	-3.8602	-0.3341	1824.10
609.3	9.4117	-3.7997	-0.5048	1823.99
609.7	9.3297	-4.2352	-1.2761	1823.88
610.0	9.3157	-4.1109	-1.2997	1823.83

**Bottom Piece Seen in Fig. 2.1**

607.7	9.4807	-3.8412	-1.6721	1824.46
608.0	9.4845	-3.5459	-1.0337	1824.38
608.3	9.4738	-3.1232	-0.6541	1824.29
608.7	9.6035	-3.3009	-1.1827	1824.21
609.0	9.4957	-3.5247	-1.0540	1824.10
609.3	9.4033	-3.8104	-1.7897	1823.99
609.7	9.2766	-3.9752	-1.9151	1823.88
610.0	9.1697	-4.0909	-1.3527	1823.83
610.3	9.1858	-4.0422	-1.6031	1823.78
610.7	9.1307	-4.2319	-1.7887	1823.73
611.0	9.1114	-4.2442	-2.0741	1823.68
611.3	9.0751	-4.1059	-1.6647	1823.63
611.7	9.2692	-3.9862	-1.5551	1823.55
612.0	9.3696	-3.6219	-1.1477	1823.46
612.3	9.4198	-3.7382	-1.3101	1823.38
612.7	9.5788	-3.5719	-1.1797	1823.30
613.0	9.6132	-3.3487	-1.6348	1823.21
613.3	9.4069	-3.6439	-1.8157	1822.88
613.7	9.3004	-4.0682	-1.8011	1822.63
614.0	9.3473	-3.6459	-2.2367	1822.59
614.3	9.4175	-3.5722	-0.9771	1822.55
614.7	9.3829	-3.2779	-0.9317	1822.50
615.0	9.4134			1822.46



Depth from Top of Coral (mm)	Sr/Ca (mmol/mol)	Oxygen Isotope (permil)	Carbon Isotope (permil)	Date
615.3	9.5467	-3.2949	-0.8577	1822.21
615.7	9.4329	-3.5792	-1.1771	1822.02
616.0	9.4712	-3.4882	-1.6461	1821.82
616.3	9.1488	-4.0312	-1.7461	1821.63
616.7	9.1793	-4.1549	-1.3947	1821.59
617.0	9.2208	-3.7688	-0.3221	1821.54
617.3	9.4092	-4.0609	-1.3517	1821.50
617.7	9.3204	-3.3366	-1.2947	1821.46
618.0	9.5971	-3.2490	-0.6648	1821.33
618.3	9.6794	-3.0638	-0.5006	1821.21
618.7	9.5335	-2.9296	-0.6029	1821.15
619.0	9.4645	-3.3442	-0.8701	1821.08
619.3	9.4543	-3.4939	-1.4257	1821.02
619.7	9.3972	-3.4792	-1.7041	1820.96
620.0	9.2777	-3.4759	-1.8917	1820.85
620.3	9.0680	-4.3562	-2.3511	1820.74
620.7	9.0147	-4.3079	-2.1467	1820.63
621.0	9.0810	-4.3052	-2.4201	1820.58
621.3	9.0849	-4.1379	-2.1567	1820.54
621.7	9.4394	-3.7272	-1.4461	1820.50
622.0	9.2719	-3.5189	-1.0127	1820.46
622.3	9.5330	-3.5582	-0.9951	1820.21
622.7	9.4589	-3.4389	-1.3177	1820.10
623.0	9.4794	-3.5182	-1.5261	1819.99
623.3	9.3471	-4.2309	-1.5037	1819.88
623.7	9.2991	-4.0222	-1.8951	1819.76
624.0	9.1961	-3.9519	-1.9447	1819.63
624.3	9.2008	-4.1102	-2.0601	1819.57
624.7	9.3630	-3.7229	-1.0977	1819.52
625.0	9.3553	-3.4042	-0.5511	1819.46
625.3	9.3982	-3.3679	-1.0887	1819.41
625.7	9.4491	-3.4182	-1.5421	1819.36
626.0	9.5058	-4.1029	-1.7615	1819.31
626.3	9.5116	-3.2802	-2.3671	1819.26
626.7	9.6270	-2.7699	-0.3567	1819.21
627.0	9.5063	-3.9152	-0.5111	1819.04
627.3	9.3967	-3.8994	-0.3776	1818.88
627.7	9.1385	-4.2122	-0.9671	1818.63
628.0	9.4778	-3.1479	-0.4807	1818.54
628.3	9.3601	-3.7632	-1.0671	1818.46
628.7	9.3846	-3.7049	-1.1367	1818.38
629.0	9.5345	-3.4122	-1.2011	1818.29
629.3	9.5539	-3.3737	-1.3430	1818.21
629.7	9.2626	-4.1582	-2.2451	1817.71

Depth from Top of Coral (mm)	Sr/Ca (mmol/mol)	Oxygen Isotope (permil)	Carbon Isotope (permil)	Date
630.0	9.2408	-4.3279	-2.5637	1817.67
630.3	9.2078	-4.3452	-2.6291	1817.63
630.7	9.2338	-3.3868	-1.6314	1817.60
631.0	9.2994	-3.8920	-1.7129	1817.57
631.3	9.2934	-3.9939	-1.4727	1817.54
631.7	9.3798			1817.43
632.0	9.4536	-3.5269	-1.0757	1817.32
632.3	9.4760			1817.21
632.7	9.4693	-3.3299	-0.9707	1817.13
633.0	9.3722	-3.4372	-1.7641	1817.04
633.3	9.3249	-4.1449	-1.5397	1816.96
633.7	9.1799	-4.0442	-1.7041	1816.88
634.0	9.0905	-4.2919	-1.4607	1816.80
634.3	9.0881	-4.4802	-1.8821	1816.71
634.7	9.0470	-4.3619	-1.7387	1816.63
635.0	9.0467			1816.58
635.3	9.3828	-4.5019	-1.2357	1816.54
635.7	9.2305			1816.49
636.0	9.3528	-3.8019	-1.0017	1816.44
636.3	9.3792			1816.40
636.7	9.5020	-3.3529	-0.7377	1816.35
637.0	9.5001	-3.6422	-1.3231	1816.30
637.3	9.5651	-3.4919	-1.4947	1816.26
637.7	9.5791	-3.4362	-1.4471	1816.21
638.0	9.4863	-2.9647	-1.6502	1816.08
638.3	9.3609	-4.1642	-2.0521	1815.96
638.7	9.1276	-4.1099	-2.3747	1815.88
639.0	9.2332	-4.6032	-1.9871	1815.79
639.3	9.0384	-4.6499	-1.8967	1815.71
639.7	8.9865	-4.6102	-1.7021	1815.63
640.0	9.2703	-4.0779	-0.4457	1815.60
640.3	9.1565	-4.1948	-1.2231	1815.57
640.7	9.1913	-3.8849	-1.0997	1815.54
641.0	9.3439	-3.7442	-0.6901	1815.43
641.3	9.4918	-3.3789	-1.0527	1815.32
641.7	9.5033	-3.6012	-1.3241	1815.21
642.0	9.4092	-3.6509	-1.6697	1815.00
642.3	9.2147	-4.1852	-1.5961	1814.79
642.7	9.2072	-4.5059	-1.9177	1814.74
643.0	9.0834	-4.1862	-1.4091	1814.68
643.3	9.0975	-4.3759	-1.2207	1814.63
643.7	9.0968	-4.4812	-1.3671	1814.60
644.0	9.1675	-3.9785	-1.0079	1814.57
644.3	9.2250	-3.9742	-1.3861	1814.54

Depth from Top of Coral (mm)	Sr/Ca (mmol/mol)	Oxygen Isotope (permil)	Carbon Isotope (permil)	Date
644.7	9.4049	-3.3859	-0.7424	1814.38
645.0	9.5368	-3.1512	-0.1201	1814.21
645.3	9.4612	-3.1979	-0.5427	1814.15
645.7	9.4591	-3.5572	-0.7281	1814.10
646.0	9.4815	-3.2939	-1.0927	1814.04
646.3	9.2772			1813.79
646.7	9.1721	-4.0579	-1.2077	1813.71
647.0	9.2018	-3.9522	-0.9411	1813.65
647.3	9.2811	-3.7719	-0.2417	1813.60
647.7	9.1743	-3.7282	-1.1151	1813.54
648.0	9.3391	-3.5479	-0.7407	1813.46
648.3	9.3520	-3.3892	-0.4101	1813.38
648.7	9.4680	-3.2049	-0.4527	1813.30
649.0	9.5517	-3.1284	-0.5548	1813.21
649.3	9.4840	-2.9959	-0.4947	1813.10
649.7	9.4581	-3.7602	-0.8661	1812.99
650.0	9.3233	-3.7019	-1.0577	1812.88
650.3	9.3743	-3.9012	-0.5461	1812.76
650.7	9.1917			1812.63
651.0	9.3275	-3.4982	-0.4511	1812.46
651.3	9.4527	-3.2967	-0.8118	1812.38
651.7	9.4067	-2.9683	-1.4144	1812.30
652.0	9.5651	-3.3409	-1.2617	1812.21
652.3	9.3407	-3.4692	-1.3501	1811.88
652.7	9.2188	-3.9453	-2.0880	1811.79
653.0	9.4159	-4.0818	-2.2990	1811.71
653.3	9.0867	-4.5359	-2.3297	1811.63
653.7	9.0842	-4.3512	-1.7761	1811.59
654.0	9.1594	-4.1739	-1.4357	1811.54
654.3	9.2839	-3.8242	-1.1261	1811.50
654.7	9.2506	-3.8706	-1.0437	1811.46
655.0	9.4775	-3.0072	-0.0321	1811.33
655.3	9.5553	-3.2169	-0.8377	1811.21
655.7	9.4988	-3.5632	-0.9941	1811.05
656.0	9.3818	-3.7939	-1.5947	1810.88
656.3	9.2450	-3.4402	-1.5891	1810.82
656.7	9.2081	-4.2059	-1.7107	1810.76
657.0	9.0809	-4.4962	-1.7771	1810.69
657.3	9.0204	-4.5419	-1.6817	1810.63
657.7	9.0812	-4.2782	-1.8011	1810.59
658.0	9.1079	-4.4139	-1.5907	1810.54
658.3	9.1905	-4.0012	-1.4301	1810.50
658.7	9.2992	-3.6283	-0.9579	1810.46
659.0	9.4812	-3.1562	-0.6431	1810.33



Depth from Top of Coral (mm)	Sr/Ca (mmol/mol)	Oxygen Isotope (permil)	Carbon Isotope (permil)	Date
659.3	9.4704	-3.4799	-1.4317	1810.21
659.7	9.4723	-3.4092	-1.7591	1810.10
660.0	9.3413	-3.3309	-2.0597	1809.99
660.3	9.2570	-3.9394	-2.4087	1809.88
660.7	9.1192	-4.2609	-2.4567	1809.82
661.0	9.0711	-4.5512	-2.3201	1809.77
661.3	8.9840	-4.4219	-2.2497	1809.71
661.7	9.0945	-3.9542	-1.1545	1809.67
662.0	9.0177	-4.5199	-1.4367	1809.63
662.3	9.0479	-4.4452	-1.5761	1809.55
662.7	9.2365	-3.7239	-0.9027	1809.47
663.0	9.3587	-3.2812	-0.3631	1809.38
663.3	9.5259	-3.3099	-0.6517	1809.30
663.7	9.6184	-3.0762	-0.4901	1809.21
664.0	9.4926	-3.3843	-0.9231	1809.08
664.3	9.3606	-3.6662	-1.2721	1808.96
664.7	9.2648	-4.0319	-1.3167	1808.88
665.0	9.2329	-4.3868	-2.0982	1808.79
665.3	9.1286	-4.1529	-0.8787	1808.71
665.7	9.1431	-4.1332	-0.5111	1808.63
666.0	9.2456		-0.4745	1808.54
666.3	9.3349	-3.4762	-0.2871	1808.46
666.7	9.4933	-3.5119	-0.5887	1808.34
667.0	9.5860	-3.2972	-0.5811	1808.21
667.3	9.5761			1808.11
667.7	9.5043	-3.3792	-1.3411	1808.00
668.0	9.4084	-3.7149	-1.3587	1807.89
668.3	9.2601	-3.8470	-1.7591	1807.79
668.7	9.1008	-4.5119	-1.9177	1807.71
669.0	9.0891	-4.3432	-1.9561	1807.63
669.3	9.0843	-4.3329	-1.1557	1807.59
669.7	9.1440	-4.2452	-0.9201	1807.55
670.0	9.1837	-3.9026	-1.0065	1807.50
670.3	9.3099	-3.7242	-0.5771	1807.46
670.7	9.3751			1807.38
671.0				1807.29
671.3	9.5048	-3.2652	-0.9001	1807.21
671.7	9.4325	-3.6556	-0.7825	1807.00
672.0	9.2401	-3.8002	-1.3451	1806.79
672.3	9.2374	-4.0740	-1.3291	1806.75
672.7	9.1875	-4.3502	-1.4171	1806.71
673.0	9.1958	-3.9229	-0.4837	1806.67
673.3	9.1088	-3.7293	-1.1641	1806.63
673.7		-3.7719	-0.7387	1806.51

Depth from Top of Coral (mm)	Sr/Ca (mmol/mol)	Oxygen Isotope (permil)	Carbon Isotope (permil)	Date
674.0	9.4600	-3.1256	-0.0547	1806.38
674.3	9.3903	-3.3569	-0.7367	1806.38
674.7	9.6177	-3.1032	-0.6821	1806.21
675.0	9.5443	-3.1029	-1.0017	1806.13
675.3	9.4882	-3.2362	-1.4571	1806.04
675.7	9.3930	-3.4942	-1.6875	1805.96
676.0	9.2206	-4.1002	-1.8421	1805.88
676.3	9.2061	-4.0659	-1.6127	1805.80
676.7	9.1624	-3.9472	-0.9151	1805.71
677.0	9.1258	-4.2519	-1.3002	1805.63
677.3	9.1905	-4.0232	-1.0481	1805.53
677.7	9.4399	-3.6120	-0.9747	1805.42
678.0	9.4839	-3.1759	-0.9611	1805.31
678.3	9.5112	-3.0515	-0.8457	1805.21

#### Track Shift

676.7	9.0720	-4.0962	-1.4161	1805.71
677.0	9.0445	-4.2399	-2.0417	1805.63
677.3	9.1431	-3.9922	-1.6111	1805.53
677.7	9.3740	-3.5228	-1.6943	1805.42
678.0	9.4835	-3.0502	-1.4221	1805.31
678.3				1805.21
678.7	9.2716	-3.9649	-1.8677	1804.96
679.0	9.1059	-4.1972	-1.9221	1804.71
679.3	9.0913	-4.3839	-1.6457	1804.68
679.7	9.0507	-4.5792	-1.8511	1804.66
680.0	9.0006	-4.7369	-1.4127	1804.63
680.3	9.0999	-4.0542	-1.1831	1804.59
680.7	9.1117	-4.2981	-1.4804	1804.54
681.0	9.3217	-3.7162	-1.5801	1804.37
681.3	9.4609	-3.3998	-1.4608	1804.21
681.7	9.4343	-3.0823	-1.2706	1804.16
682.0	9.4210	-3.2859	-1.1417	1804.10
682.3	9.3971	-3.3682	-1.4591	1804.05
682.7	9.4136	-3.4019	-1.3937	1803.99
683.0	9.3710	-3.6452	-1.4371	1803.93
683.3	9.1954	-4.0729	-0.9287	1803.88
683.7	9.2707	-4.0312	-1.0181	1803.82
684.0	9.1765	-3.9499	-0.9697	1803.75
684.3	9.2054	-4.2162	-1.3191	1803.69
684.7	9.1268	-4.1919	-1.0847	1803.63
685.0	9.1997	-3.9952	-1.1721	1803.54
685.3	9.3800	-3.7679	-0.9917	1803.43

Depth from Top of Coral (mm)	Sr/Ca (mmol/mol)	Oxygen Isotope (permil)	Carbon Isotope (permil)	Date
685.7	9.5012	-3.4022	-0.8371	1803.32
686.0	9.5613	-3.0799	-0.5977	1803.21
686.3	9.5528	-3.2272	-1.0621	1803.17
686.7	9.5423	-3.2339	-1.0637	1803.13
687.0	9.3319	-3.4092	-1.4041	1803.04
687.3	9.3336	-3.8489	-1.3367	1802.96
687.7	9.1552	-4.2612	-1.0831	1802.63
688.0	9.1883	-4.1919	-1.2727	1802.59
688.3	9.1816	-4.0082	-0.9421	1802.55
688.7	9.1888	-4.3649	-0.9557	1802.50
689.0	9.2599	-3.5774	-1.5198	1802.46
689.3	9.3822	-3.2599	-0.7837	1802.34
689.7	9.4513	-3.4512	-0.9711	1802.21
690.0	9.3795	-3.4639	-1.3017	1802.10
690.3	9.3726	-3.4302	-1.5771	1802.00
690.7	9.3026	-3.5119	-1.3947	1801.90
691.0	9.1640	-3.6622	-1.4171	1801.79
691.3	9.0759	-4.3653	-0.7881	1801.74
691.7	9.0577	-4.3872	-1.0194	1801.68
692.0	8.9757	-4.4150	-1.6452	1801.63
692.3	9.1522	-4.2322	-1.1601	1801.59
692.7	9.0115	-4.3299	-1.5877	1801.54
693.0	9.3311	-3.6369	-1.3577	1801.46
693.3	9.4009	-4.1163	-1.4187	1801.38
693.7	9.3588	-3.5532	-1.2601	1801.29
694.0	9.4568	-3.6259	-1.3707	1801.21
694.3	9.4454	-3.2832	-1.3541	1801.05
694.7	9.2972	-3.6269	-1.4287	1800.88
695.0	9.2204	-3.7402	-1.2971	1800.75
695.3	9.1864	-4.0629	-0.6437	1800.63
695.7	9.2392	-3.9752	-0.2721	1800.55
696.0	9.2940	-3.9209	-0.9417	1800.46
696.3	9.3937	-3.6572	-1.1801	1800.38
696.7	9.3663	-3.5699	-1.0687	1800.30
697.0	9.4803	-3.5182	-1.1291	1800.21
697.3	9.3994	-3.5589	-1.3197	1800.15
697.7	9.4341	-3.4142	-1.0391	1800.10
698.0	9.4055	-3.4439	-1.5067	1800.04
698.3	9.2778	-3.8602	-2.0131	1799.93
698.7	9.1870	-3.8899	-1.1467	1799.82
699.0	9.1722	-3.9472	-1.7401	1799.71
699.3	9.2212			1799.69
699.7	9.2236	-3.9242	-0.4631	1799.67
700.0	9.2566	-4.1439	-0.6567	1799.65



Depth from Top of Coral (mm)	Sr/Ca (mmol/mol)	Oxygen Isotope (permil)	Carbon Isotope (permil)	Date
700.3	9.1373	-4.0482	-0.8421	1799.63
700.7	9.4834	-3.4659	-0.2707	1799.29
701.0	9.4743	-3.2832	-0.1841	1799.25
701.3	9.5232	-3.1979	0.0353	1799.21
701.7	9.3894	-3.3482	-0.8281	1799.05
702.0	9.2803	-3.9349	-0.8367	1798.88
702.3	9.1517	-4.0612	-0.9321	1798.80
702.7	9.1079	-4.1329	-1.3827	1798.72
703.0	9.0306	-4.2592	-1.3351	1798.63
703.3	9.0329	-4.1811	-1.2464	1798.57
703.7	9.2060	-3.7838	-1.0642	1798.52
704.0	9.2783	-3.6999	-0.9727	1798.46
704.3	9.5140	-3.4042	-0.8611	1798.38
704.7	9.5791	-3.1409	-0.5697	1798.30
705.0	9.5961	-2.8352	-0.5981	1798.21
705.3	9.5032	-3.4839	-0.9277	1798.13
705.7	9.4024	-3.5082	-0.9481	1798.05
706.0	9.4950	-3.8269	-0.8537	1797.96
706.3	9.2989	-3.6082	-1.1161	1797.88
706.7	9.3739	-4.2209	-1.4987	1797.80
707.0	9.0658	-4.1322	-1.4291	1797.71
707.3	9.0515	-4.3293	-1.2479	1797.63
707.7	9.1131	-3.5722	-1.0771	1797.46
708.0	9.4144	-3.3028	-0.5810	1797.29
708.3	9.4861	-3.3772	-0.6951	1797.25
708.7	9.4996	-3.2859	-0.5507	1797.21
709.0	9.4249	-3.2922	-0.2531	1797.00
709.3	9.2265	-3.8079	-0.9787	1796.79
709.7	9.2084	-3.7082	-1.3241	1796.74
710.0	9.2147	-3.9009	-1.5057	1796.68
710.3	9.0764	-3.8042	-2.0891	1796.63
710.7	9.1989	-3.9639	-1.3807	1796.55
711.0	9.2810	-3.5842	-0.7111	1796.46
711.3	9.4552	-3.4069	-0.4217	1796.34
711.7	9.5744	-3.1332	-0.1981	1796.21
712.0	9.4663	-3.1569	-0.1497	1796.10
712.3	9.4783	-3.3633	-0.7449	1796.00
712.7	9.3644	-3.5299	-1.6597	1795.90
713.0	9.2972	-3.3942	-1.9161	1795.79
713.3	9.1932	-3.8049	-1.8137	1795.63
713.7	9.2902	-4.0172	-0.9571	1795.61
714.0	9.2114	-4.0289	-0.5987	1795.59
714.3	9.2647	-3.8402	-0.4341	1795.56
714.7	9.2464	-3.2859	-0.5557	1795.54

Depth from Top of Coral (mm)	Sr/Ca (mmol/mol)	Oxygen Isotope (permil)	Carbon Isotope (permil)	Date
715.0	9.3258	-3.2772	-0.7101	1795.46
715.3	9.4010	-3.0889	-0.8237	1795.34
715.7	9.4201	-3.1912	-0.9001	1795.21
716.0	9.4315	-3.1322	-0.7612	1795.10
716.3	9.3379	-3.7712	-1.4221	1795.00
716.7	9.3397	-3.6497	-0.9945	1794.90
717.0	9.2017	-3.9390	-1.4735	1794.79
717.3	9.2505	-3.6759	-0.8557	1794.74
717.7	9.0974	-3.9685	-1.2031	1794.68
718.0	9.0562	-4.0859	-1.2247	1794.63
718.3	9.1429	-3.7132	-1.3321	1794.55
718.7	9.1980	-3.6463	-1.0485	1794.46
719.0	9.4326	-3.1812	-0.9121	1794.33
719.3	9.5096	-3.1359	-0.8727	1794.21
719.7	9.4276	-3.0532	-0.7041	1794.10
720.0	9.4149	-3.2419	-1.4177	1793.99
720.3	9.2237	-3.5212	-1.4489	1793.88
720.7	9.2669	-3.7289	-0.8807	1793.82
721.0	9.4211	-3.9962	-1.5721	1793.75
721.3	9.0716	-3.9320	-1.8678	1793.69
721.7	9.0153	-4.2602	-1.7721	1793.63
722.0	9.2313	-3.6649	-1.0537	1793.46
722.3	9.2463	-3.6292	-0.9001	1793.38
722.7	9.3698	-3.4619	-0.7367	1793.29
723.0	9.3506	-3.9480	-1.3680	1793.27
723.3	9.4174	-3.2229	-0.9867	1793.26
723.7	9.3788	-3.2861	-1.2909	1793.24
724.0	9.3311	-3.4009	-1.6947	1793.23
724.3	9.4922	-3.4442	-1.6041	1793.21
724.7	9.2681	-3.6009	-1.9117	1792.96
725.0	9.1891	-4.0252	-1.2231	1792.83
725.3	8.9819	-4.1799	-2.2837	1792.71
725.7	8.9817	-4.0982	-2.1261	1792.63
726.0	9.1858	-3.4209	-1.2917	1792.46
726.3	9.4803	-3.0962	-1.5261	1792.13
726.7	9.4031	-3.1291	-1.6976	1792.08
727.0	9.3114	-3.1832	-1.1221	1792.03
727.3	9.3134	-3.4879	-1.7707	1791.98
727.7	9.2828	-3.4602	-1.8881	1791.93
728.0	9.2692	-3.7539	-1.9187	1791.88
728.3	9.6003	-3.7712	-1.5571	1791.82
728.7	9.1655	-4.1869	-1.4562	1791.76
729.0	9.0614	-4.0182	-1.4251	1791.69
729.3	8.9972	-3.9324	-1.3160	1791.63

Depth from Top of Coral (mm)	Sr/Ca (mmol/mol)	Oxygen Isotope (permil)	Carbon Isotope (permil)	Date
729.7	9.1435	-4.0820	-1.3872	1791.59
730.0	9.1469	-3.8406	-1.5164	1791.54
730.3	9.3114	-3.4922	-0.9401	1791.38
730.7	9.5104	-3.1019	-0.9217	1791.21
731.0	9.4776	-3.1882	-0.7441	1791.19
731.3	9.4576	-3.2209	-1.0137	1791.17
731.7	9.4299	-3.2582	-0.5991	1791.15
732.0	9.4818	-3.1890	-0.1981	1791.13
732.3	9.3818	-3.4053	-1.1787	1791.01
732.7	9.3078	-3.5922	0.0251	1790.88
733.0	9.1562	-4.4442	-1.0371	1790.80
733.3	9.2298	-3.9579	-1.1967	1790.71
733.7	9.0049	-4.4272	-1.8701	1790.63
734.0	9.1024	-4.1411	-1.3101	1790.55
734.3	9.3305	-3.6762	-0.8811	1790.46
734.7	9.3776	-3.4929	-0.0467	1790.38
735.0	9.2837	-3.6802	-0.7891	1790.34
735.3	9.4891	-3.3479	-0.0617	1790.30
735.7	9.4053	-3.4529	-0.9187	1790.25
736.0	9.5150	-3.4742	-1.0211	1790.21
736.3	9.4891	-3.1629	-1.0427	1790.17
736.7	9.5272		-1.2199	1790.13
737.0	9.4295	-3.6129	-1.4647	1790.07
737.3	9.3920	-3.4744	-1.3646	1790.02
737.7	9.3545	-3.6308	-1.1400	1789.96
738.0	9.2864	-3.8882	-1.9031	1789.85
738.3	9.1662	-4.0019	-1.7597	1789.74
738.7	9.1467	-4.0521	-1.6526	1789.63
739.0	9.4354	-3.7957	-1.4478	1789.21
739.3	9.3859			1789.04
739.7	9.0896	-4.1819	-1.9157	1788.63
740.0	9.1738	-3.8422	-1.7991	1788.54
740.3	9.3002	-3.6716	-1.7687	1788.46
740.7	9.3303	-3.7754	-1.4202	1788.29
741.0	9.4224	-3.3629	-1.3067	1788.21
741.3	9.3999	-3.5812	-1.4071	1788.14
741.7	9.2291	-3.6999	-1.4627	1788.08
742.0	9.2896	-3.7202	-1.5911	1788.01
742.3	9.3764	-3.9299	-1.6477	1787.95
742.7	9.2195	-3.9072	-2.2161	1787.88
743.0	9.1969	-3.9699	-2.3417	1787.75
743.3	9.0881	-3.8062	-1.5921	1787.63
743.7	9.3148	-3.4372	-1.0657	1787.46
744.0	9.4412	-3.2072	-0.6431	1787.29



Depth from Top of Coral (mm)	Sr/Ca (mmol/mol)	Oxygen Isotope (permil)	Carbon Isotope (permil)	Date
744.3	9.3018	-3.1729	-1.1317	1787.26
744.7	9.3901	-3.3421	-0.9592	1787.23
745.0	9.3337	-3.3126	-0.7405	1787.19
745.3	9.3732	-3.4052	-0.4527	1787.16
745.7	9.4607		-0.4154	1787.13
746.0	9.3395	-3.4512	-1.1241	1786.88
746.3	9.1275	-4.0091	-1.4678	1786.63
746.7	9.1445	-3.9936	-1.5852	1786.59
747.0	9.2127	-3.8822	-1.7994	1786.55
747.3	9.2326	-3.6132	-1.7571	1786.51
747.7	9.1965	-3.5959	-1.5274	1786.46
748.0	9.3431	-3.4512	-1.2291	1786.42
748.3	9.3440	-3.1569	-1.2107	1786.38
748.7	9.5236	-2.9722	-0.5431	1786.21
749.0	9.4740	-3.1529	-0.2467	1786.10
749.3	9.4682	-3.7362	-0.9151	1785.99
749.7	9.2965	-3.6242	-1.0798	1785.88
750.0	9.3178	-3.7032	-1.5951	1785.80
750.3	9.1696	-4.0129	-1.4037	1785.71
750.7	9.1050	-4.0402	-1.1751	1785.63
751.0	9.2705	-3.4809	-1.0767	1785.57
751.3	9.3553	-3.1817	-1.0098	1785.51
751.7	9.3584	-3.2189	-1.1237	1785.44
752.0	9.3280	-3.5122	-1.1881	1785.38
752.3	9.3999	-3.2719	-0.2297	1785.30
752.7	9.4996	-2.9442	-0.8063	1785.21
753.0	9.4280	-3.2986	-0.4869	1785.04
753.3	9.3385	-3.5123	-0.4112	1784.88
753.7	9.2099	-3.8109	-0.5767	1784.63
754.0	9.2339	-3.6392	-1.2571	1784.58
754.3	9.2523	-3.7289	-1.2727	1784.53
754.7	9.1924	-3.7112	-0.8271	1784.48
755.0	9.2786	-3.5519	-0.6057	1784.43
755.3	9.3997	-3.1682	-0.4261	1784.38
755.7	9.4678	-2.9629	-0.6337	1784.33
756.0	9.4496	-3.2302	-0.9321	1784.28
756.3	9.4986	-3.0819	-0.1897	1784.23
756.7	9.4420	-3.1782	-0.5891	1784.18
757.0	9.5297	-3.1499	-1.1497	1784.13
757.3	9.4724	-3.2685	-1.0876	1783.96
757.7	9.3630	-3.5649	-0.4217	1783.63
758.0	9.3787	-3.4762	-0.2501	1783.59
758.3	9.4149	-3.3032	-0.7594	1783.55
758.7	9.3468	-3.5862	-0.9041	1783.51

Depth from Top of Coral (mm)	Sr/Ca (mmol/mol)	Oxygen Isotope (permil)	Carbon Isotope (permil)	Date
759.0	9.4077	-3.3879	-0.5047	1783.46
759.3	9.4946	-3.2752	0.0219	1783.42
759.7	9.4347	-3.0673	-0.1894	1783.38
760.0	9.4626	-3.1962	0.1219	1783.29
760.3	9.5541	-2.8446	0.1219	1783.21
760.7	9.5216	-2.9864	-1.0364	1783.09
761.0	9.4108	-3.3479	-0.3397	1782.96
761.3	9.3221	-3.5514	-0.5441	1782.80
761.7	9.1873	-3.4609	-0.2087	1782.63
762.0	9.3114	-3.4939	-1.0325	1782.57
762.3	9.3502	-3.4189	-0.9861	1782.51
762.7	9.2360	-3.5872	-0.7151	1782.44
763.0	9.3754	-3.2827	-0.1817	1782.38
763.3	9.4245	-3.1472	0.4419	1782.34
763.7	9.4217	-3.1409	-0.3507	1782.30
764.0	9.3622	-3.2972	-0.1981	1782.25
764.3	9.4837	-3.2419	-0.0487	1782.21
764.7	9.3796	-3.2857	-0.1375	1782.04
765.0	9.3320	-3.7669	-0.5747	1781.88
765.3	9.2647	-3.8020	-0.6986	1781.63
765.7	9.3171	-3.6239	-0.9897	1781.60
766.0	9.2610	-3.3562	-0.5981	1781.56
766.3	9.2689	-3.6107	-0.0350	1781.52
766.7	9.3320	-3.6924	-0.1785	1781.49
767.0	9.2110	-3.7378	-0.6406	1781.45
767.3	9.2729	-3.4471	-0.3204	1781.42
767.7	9.3355	-3.4666	-0.2798	1781.38
768.0	9.4345	-3.0102	-0.3961	1781.29
768.3	9.4492	-3.1419	-0.8827	1781.21





## **Appendix E**

# **Low Resolution Record (Biennial) versus High Resolution Record (Sub-Annual) Sampling**

### **E.1 Introduction**

In Chapter 2 of this work (Goodkin et al., 2005), the BB 001 single colony calibrations are applied to a biennially sampled 225-year long record (Low Resolution Record - LRR) from the same coral. As the research continued, the sub-annual resolution sampling was extended over the length of the entire 225-year long record (High Resolution Record - HRR). Noticeable differences are found between the two Sr/Ca records (Fig. E-1), particularly during the time of maximum (~1850) and minimum (~1960) values. Applying the same calibration to these records generates large SST differences. For instance, application of the mean-annual group reconstruction, defined in Chapter 3 of this work and developed using sub-annual resolution sampling, demonstrates a 3.0°C temperature change from 1850 to 1960 for the HRR and roughly half that or 1.5°C for the LRR. Differences are large in both the values of the Sr/Ca and the long-term patterns of the records. Calibrations in this thesis were developed using sub-annual resolution records, which have better constrained age models and allow for seasonally based calibrations. As a result, it is best to draw all climatic conclusions from

the sub-annual resolution record and not the initially sampled biennial record. However, the reasons behind these differences should be investigated.

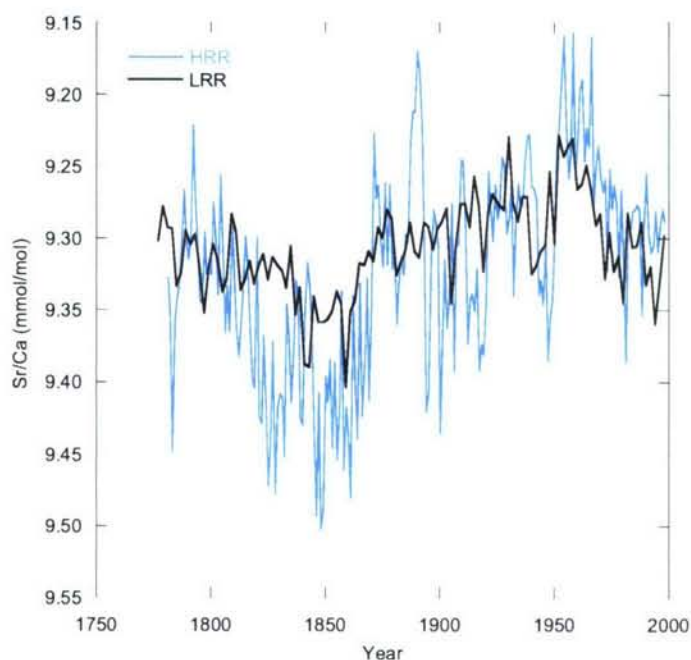


**Figure E.1:** Sr/Ca (mmol/mol) for the sub-annual resolution record (HRR-blue) and the biennial resolution record (LRR-black) from ~1780 to 1998. Large differences can be seen throughout the records and particularly during the time of maximum (~1850) and minimum (~1960) values.

## E.2 Complications of Biennial Sampling

Biennial samples were cut across theca, including two thecal walls and a narrow ambulacrum. These lines were cut between every other high-low density band interface occurring during the fall season. *Diploria labyrinthiformis* grow in a cone shaped pattern within the thecal wall with the greatest extension in summer and less extension in winter (Fig. E.2) whereas in the ambulacrum winter extension exceeds summer extension

(Cohen et al., 2004). As seen in Fig. E.2, cutting along density bands will cut through the wave patterns seen with the pink dye. If a cut were to be made through the 9/24/00, line material would be collected from as late as 1/01 and from earlier times in the summer though not as early as 6/01/00. In effect, the record will include material beyond the biennial period by 6-12 months, with the most smoothing between September and January where our cuts were made.

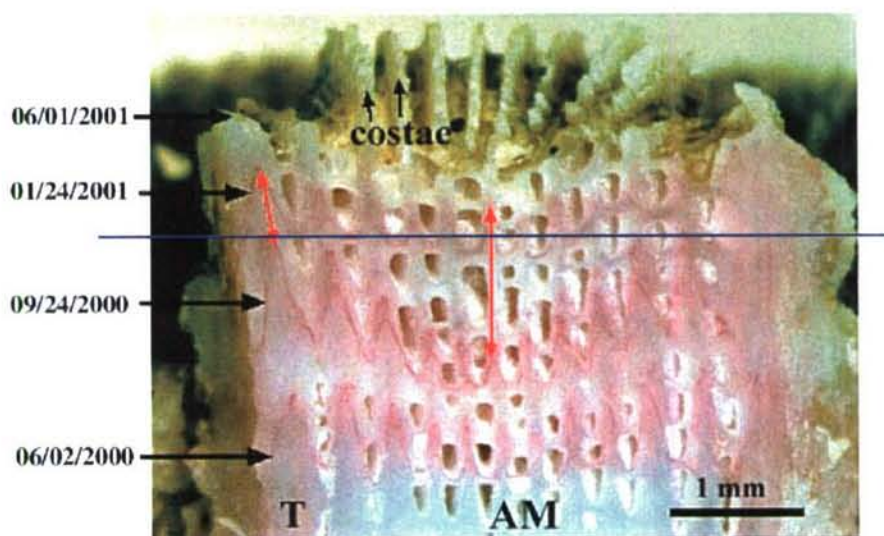


**Figure E.2:** Staining experiment conducted and published by Cohen et al. (2004) shows the cone shaped growth of a *Diploria labyrinthiformis* with varying extension in summer and winter throughout the theca-ambulacrum pairs. (Cohen et al., 2004) Blue line indicates approximately where cuts were made for the LRR record. T indicates Theca and AM indicates Ambulacrum.

Previous to the generation of the HRR, this smoothing was deemed to be minimal, but extensive smoothing of the HRR can confirm this hypothesis. For this analysis, the mean-annual Sr/Ca values of the HRR were treated with low-pass filters for three, five and seven years. As can be seen in Fig. E.3, additional smoothing beyond the biennial



bins is not shown to be significant by smoothing the HRR. Differences in max and min values are not eliminated even by a seven year smooth which is significantly more than would be expected from the growth patterns. However, smoothing does appear to better describe the 1960s period in which LRR Sr/Ca values are higher than HRR Sr/Ca values than it does the 1850s period when the relationship is reversed. The largest differences between these two periods is the growth rate which are on average 4 mm/year in the 1960s and closer to 2 mm/year in the 1850s. This relationship will be further investigated later in the text.

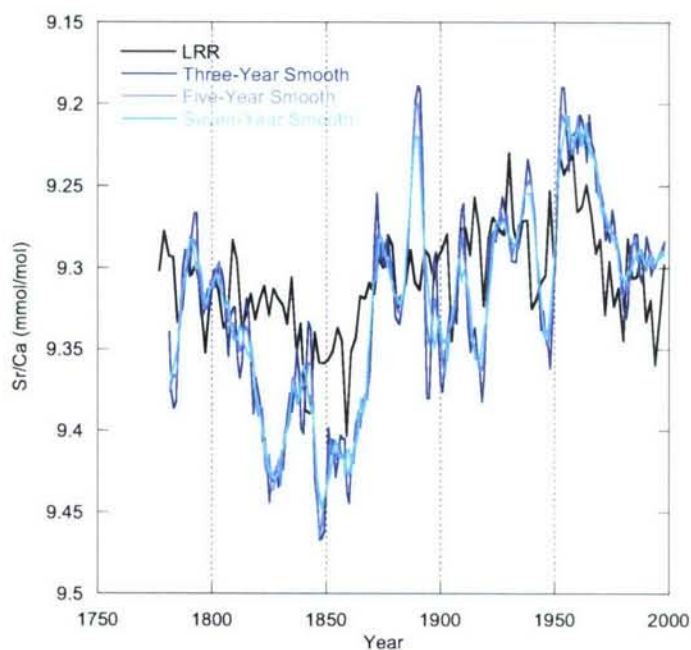


**Figure E.3:** Sr/Ca (mmol/mol) for the biennial record (LRR-black) and the sub-annual resolution record (HRR) filtered with three (dark blue), five (medium blue) and seven (light blue) year windows.

Sampling differences also arises from the incorporation of material from the ambulacrum in the LRR sampling though not the HRR samples. Samples were chosen with deliberately narrow ambulacrums and the significantly larger widths and densities of

the theca lead to the hypothesis that influence from the abulacrum is as minimal as the extended smoothing. Additionally, the effect would be to more heavily weight the winter months (Fig. E.2) than does the HRR which is not the case throughout the whole record (Fig. E.1).

### **E.3 Unaccounted Growth Influence**

Another hypothesis is that growth rate has impacts on the biennial record either through the two influences above or from factors not yet identified that are not accounted for in the sub-annual based calibration. If the relative influences of the ambulacrum and the smoothing change with growth rate, this could lead to changes in the shape and magnitude of the biennial record, though it is unlikely that they would explain the entire change in magnitude. Another possible scenario is that lower growth time periods during which samples weigh less would be increasingly effected by powder lost during cutting. While a diamond wire band saw was used to diminish sample loss, some sample was lost and could have increased as a percentage of total weight with the smaller samples. This could also increase smoothing of the record or serve to dampen winter signals lost to cutting, as the cut occurs at the fall-winter interface. As seen in Fig. E.3, the slow growth period of the early to mid-1800s appears to have larger differences in Sr/Ca than does the 1960s with an average growth rate of 4 mm/year, supporting this hypothesis.

Possible growth rate impacts were evaluated both from the Sr/Ca records and from reconstructed SSTs using the mean-annual growth-corrected group model (Chapter 3). The HRR records were binned biennially and then the LRR were subtracted. These differences were then compared to growth rates determined by the biennial record and

smoothed (Goodkin et al., 2005). Figure E.4 shows a low correlation ( $r$ ) between both the Sr/Ca anomalies (0.22) and the SST anomalies (0.33). The left panels, in which the

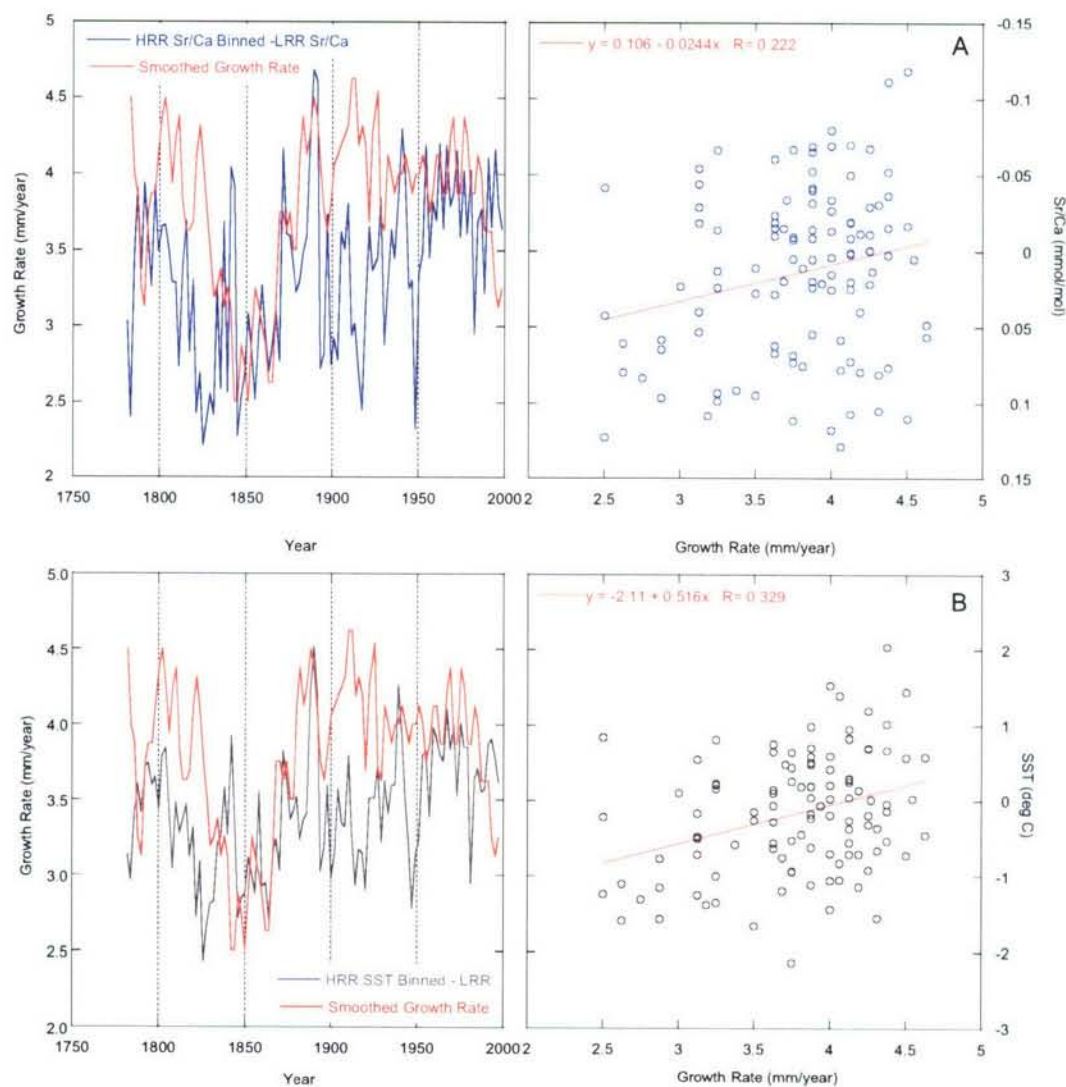


**Figure E.4:** Difference between the HRR binned biennially and the LRR compared to the mean annual smoothed growth rate (red) versus time and linearly for a) the Sr/Ca records (blue) and b) the reconstructed SST records (grey) using the mean-annual group model.



differences and growth rates are plotted versus time, show the strongest correlation for both records during the lowest growth period around 1850, lending support to the conclusion that the large discrepancies during this time may be due to impacts on low-growth periods that result either from the ambulatory or the sampling error hypothesis which cannot be described simply by the smoothing hypothesis.

#### **E.4 Inapplicability of Sub-annual Calibration to Biennial Samples**

More than one factor appears to be causing the discrepancy between the two Sr/Ca records. This conclusion indicates that when given the opportunity it is best to use a calibration sampled identically to the record to which it will be applied. Further evidence to support this conclusion is the increase in correlation between the difference of the two records and growth rate once the Sr/Ca is converted to SST (Fig. E.4). The growth rate influence becomes stronger after the growth-correction of the calibration is applied demonstrating the calibration is inappropriate.

Developing a biennial calibration raises many concerns. First, determining the calibration SST values is a challenge. Corals are cut based on high and low density bands, and it has not been determined either which month this transition occurs or if this timing remains consistent within these species through time. Smoothing beyond a biennial period is hypothesized to be occurring. Given these concerns generating an equivalent SST record is difficult. Given these caveats which will add error to any biennial calibration, SST records were binned over two year periods from November to November and correlated to the biennial Sr/Ca from 1975-1997. Three hypothesis were put forward in Chapter 2 (Goodkin et al., 2005) as to why growth rate could impact

Sr/Ca-SST relationships: 1) bulk (sub-annual) sampling biases, 2) kinetic effects and 3) convoluted skeletal architecture. Biennial sampling should eliminate concerns about summer in-filling as the samples do not get re-weighted while developing an age-model. However, skeletal architecture will effect the LRR samples as already discussed, and the hypothesis one and two could still impact a correlation. Therefore, a growth-corrected biennial model, in the form of the growth-corrected mean-annual model (Chapter 2) was generated. The exercise returns the following result:

$$\text{Sr/Ca} = -0.0389 (\pm 0.0385) * (\text{SST}) - 0.00144 (\pm 0.00081) * (\text{SST}) * (\text{Growth Rate}) + 10.3 (\pm 0.9)$$

$$(95\% \text{ conf.}, \sigma, r^2 = 0.46, F_{\text{sig}} = 0.16)$$

This is not a statistically significant relationship at the 95% confidence interval which may result from both the low number of observations (n=9) and the SST concerns expressed previously. (Note: it is more significant than a non-growth model which returns an  $r^2$  of 0.18 and an  $F_{\text{sig}}$  of 0.25.) Application of the biennial growth-corrected model to the biennial Sr/Ca record returns a result in line with magnitude of SST change seen with the SST reconstruction generated by applying the mean-annual growth-corrected group model to the HRR (Fig. E.5). Both records show a total SST change on

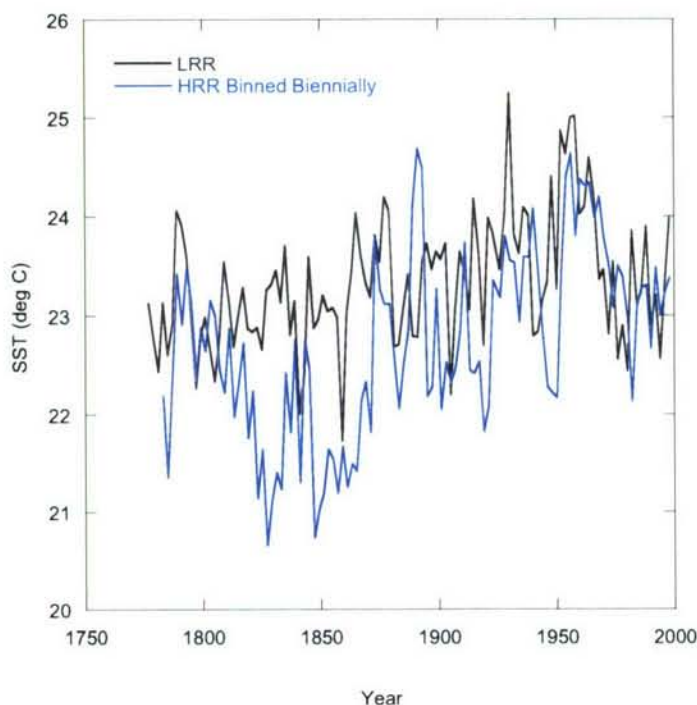


**Figure E.5:** SST reconstructed from the LRR Sr/Ca record using the biennial growth-corrected model (black) and SST reconstructed from the HRR Sr/Ca record using the group model (blue).

the order of  $\sim 3.0^{\circ}\text{C}$  from max to min. There continue to be differences mainly seen in the 1800s in the shape of the curves, where a longer period of cooling is seen in the HRR consistent with other Northern Hemisphere records (Overpeck et al., 1997; Jones et al., 1998). Further development of a biennial calibration using multiple corals could help to continue to clarify these issues, though is not necessary for the goals of this thesis.

## E.5 Results of Chapter Two

In chapter two, we used the biennially sampled record to illustrate the differences of the variously scaled calibrations/models presented. The analysis presented in this appendix calls into questions these illustrations if indeed the biennially sampled record is



not applicable. Therefore, I have redone this analysis (Fig. E.6) to demonstrate that illustration is still relevant. In this figure, reconstructions of SST from the HRR record using the BB 001 monthly and mean-annual calibrations are compared to the growth-dependent model (a and b). The monthly calibration shows an SST change of  $\sim 10^{\circ}\text{C}$  two times that of the growth-corrected model as found with the biennial record. The mean-annual calibration returns an SST change of  $7^{\circ}\text{C}$  more than 35% larger than that found with the growth-corrected model. Finally, the BB 001 growth-corrected model is compared to the group reconstruction (Fig. E.6c). The temperature changes are relatively consistent with maximum to minimum changes of  $5.3$  and  $4.9^{\circ}\text{C}$  respectively with a small shift in the absolute value of the SST through time. In conclusion, the illustration made by the biennial results hold true when the same series of calibrations are applied to the HRR data.

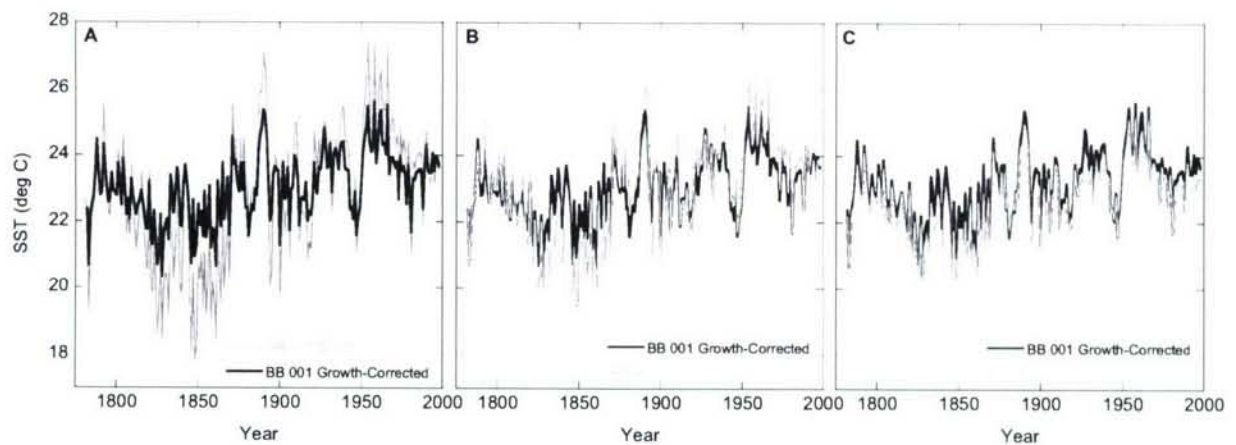


**Figure E.6:** SST reconstructions from the HRR comparing the BB 001 growth-corrected model (solid) to a) BB 001 monthly calibration (shaded), b) the BB 001 mean-annual calibration (shaded), and c) the group, growth-corrected model (shaded).

## E.6 Conclusions

The complications of using Sr/Ca to reconstruct SST have long been recognized (Devilliers et al., 1995; Alibert and McCulloch, 1997; Marshall and McCulloch, 2002; Cohen et al., 2004). This is yet another example of how carefully these records must be treated. Goodkin et al. (2005) (this work) emphasizes the importance of applying calibrations of the same temporal resolution as the samples. This analysis shows that both temporal resolution and consistent sampling regimes are critical for reconstructions in this species.

## E.7 References

- Alibert C. and McCulloch M. T. (1997) Strontium/calcium ratios in modern Porites corals from the Great Barrier Reef as a proxy for sea surface temperature: Calibration of the thermometer and monitoring of ENSO. *Paleoceanography* **12**(3), 345-363.
- Cohen A. L., Smith S. R., McCartney M. S., and van Etten J. (2004) How brain corals record climate: an integration of skeletal structure, growth and chemistry of *Diploria labyrinthiformis* from Bermuda. *Marine Ecology-Progress Series* **271**, 147-158.
- deVilliers S., Nelson B. K., and Chivas A. R. (1995) Biological-Controls on Coral Sr/Ca and Delta-O-18 Reconstructions of Sea-Surface Temperatures. *Science* **269**(5228), 1247-1249.
- Goodkin N. F., Huguenot K., Cohen A. C., and Smith S. R. (2005) Record of Little Ice Age sea surface temperatures at Bermuda using a growth-dependent calibration of coral Sr/Ca. *Paleoceanography* **20**, PA4016, doi:10.1029/2005PA001140.
- Jones P. D., Briffa K. R., Barnett T. P., and Tett S. F. B. (1998) High-resolution palaeoclimatic records for the last millennium: interpretation, integration and comparison with General Circulation Model control-run temperatures. *Holocene* **8**(4), 455-471.
- Marshall J. F. and McCulloch M. T. (2002) An assessment of the Sr/Ca ratio in shallow water hermatypic corals as a proxy for sea surface temperature. *Geochimica Et Cosmochimica Acta* **66**(18), 3263-3280.

Overpeck J., Hughen K., Hardy D., Bradley R., Case R., Douglas M., Finney B., Gajewski K., Jacoby G., Jennings A., Lamoureux S., Lasca A., MacDonald G., Moore J., Retelle M., Smith S., Wolfe A., and Zielinski G. (1997) Arctic environmental change of the last four centuries. *Science* **278**(5341), 1251-1256.



## Appendix F

### Oxygen Isotope – Salinity Relationship in Bermuda Waters

In order to investigate the assumption in Chapter Four that surface waters near Bermuda will have a  $\delta^{18}\text{O}$  – sea surface salinity (SSS) relationship similar to the global thermocline relationship of  $\delta^{18}\text{O} = 0.49 \cdot \text{SSS} - 17$  [Schmidt, 1999], two one-year time series of seawater were collected at Surf Bay Beach Bermuda (Table F.1) and at the Bermuda Atlantic Time-Series (BATs) Station (Table F.2). Each samples' salinity and  $\delta^{18}\text{O}$  was measured at WHOI and Harvard University respectively, and *in situ* temperature was taken for most samples. These samples combined with samples from the global data base were used to evaluate the relationship in this region (Figure F.1). The global database, the Surf Bay Beach and all three sources of data together return a result similar to the global thermocline relationship. The BATs site, which has the fewest samples and the smallest range of salinity, shows a steeper slope (0.86 ‰/psu). These results are not definitive as a longer time-series is required, but they do support the use of the thermocline relationship in reconstructing salinity.

**Table F.1:** Seawater measurements from Surf Bay Beach, Bermuda (32° 20' N, 64° 45' W). Water collected from the top 3 meters.

Date	Digital Date	Temperature (°C)	Salinity (psu)	$\delta^{18}\text{O}$ (‰)
07/31/2005	2005.58	29.1	36.67	1.20
10/11/2005	2005.78	26.6	36.71	1.46
11/26/2005	2005.90	23.2	36.45	1.15
01/01/2006	2006.00	20.7	36.73	1.19
01/22/2006	2006.06	20.2	36.68	1.16
03/22/2006	2006.22	16.9	36.72	1.23
04/15/2006	2006.29	20.8	36.69	1.24
05/06/2006	2006.35	23.2	36.62	1.18
06/18/2006	2006.46	25.6	36.47	1.08
07/30/2006	2006.58	28.0	36.56	1.26

**Table F.2:** Seawater measurements from BATs (31° 40' N, 64° 10' W).

Date	Digital Date	Depth (m)	Temperature (°C)	Salinity (psu)	$\delta^{18}\text{O}$ (‰)
10/12/2005	2005.78	15	25.9	36.68	1.48
12/11/2005	2005.95	15	22.8	36.71	1.27
01/31/2006	2006.08	15	20.0	36.62	1.08
02/23/2006	2006.15	15	19.3	36.63	1.19
04/06/2006	2006.26	15	19.5	36.68	1.15
06/28/2006	2006.49	15	NA	36.57	1.08
07/18/2006	2006.55	15	NA	36.59	1.28
09/06/2006	2006.68	15	NA	36.53	1.16
08/08/2006	2006.77	15	NA	36.64	1.15

**Table F.3:**  $\delta^{18}\text{O}$  and SSS measurements from global seawater oxygen-18 database.

Longitude (W)	Latitude (N)	Depth (m)	Salinity (psu)	$\delta^{18}\text{O}$ (‰)
64.00	32.00	0	36.30	1.17
64.00	32.00	0	36.40	1.05
64.00	32.00	0	36.80	1.36
64.00	32.00	0	35.40	1.01
67.98	35.99	7	36.43	1.22
64.00	32.00	18	35.40	1.05
60.82	28.08	25	36.80	1.39
60.82	28.08	500	36.30	0.89
60.82	28.08	2000	35.00	0.34
60.82	28.08	6000	34.90	0.20

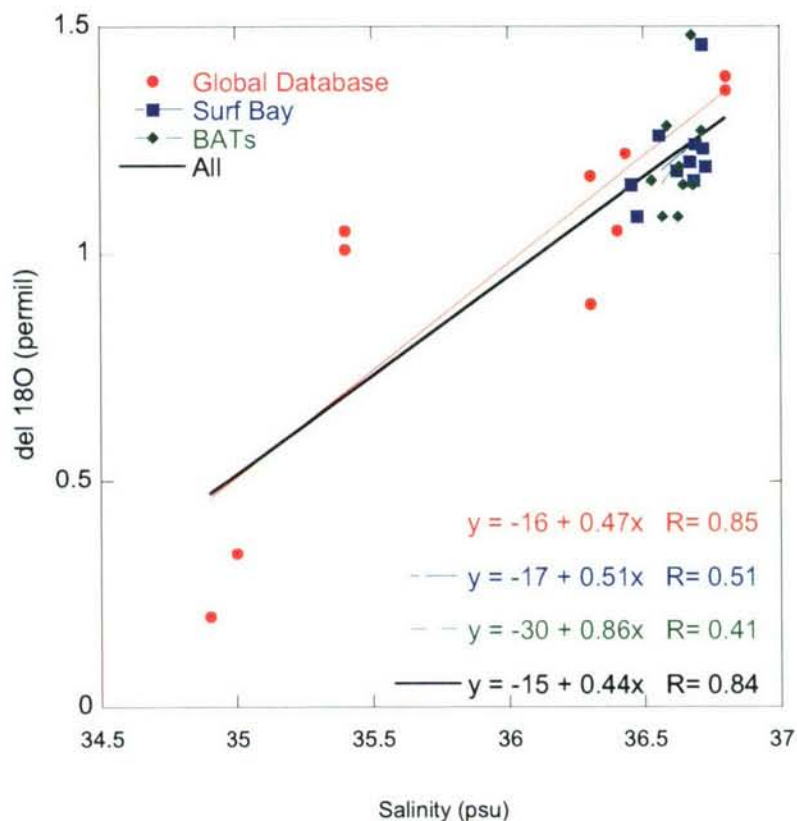


**Figure F.1:**  $\delta^{18}\text{O}$  plotted versus salinity for the global database (red circles), Surf Bay Beach (blue squares), and BATs (green diamonds). Linear regressions of the global database (red), Surf Bay (blue) and all (black) values return results in proximity to the thermocline relationship generated globally. The BATs data, with the smallest salinity range, shows a steeper slope.

## Acknowledgements

The BATs team and R. Stanley (WHOI) collected the BATs samples, and R. Stanley and D. Toole (WHOI) transported these samples. A. Emami aided in collection of the Surf Bay Samples. D. Wellwood (WHOI) performed the salinity measurements and the oxygen isotope measurements were performed in the laboratory of D. Schrag (Harvard University).

## References

Schmidt, G. A., Global Seawater oxygen-18 database, 1999.





## Appendix G

### Error Propagation on SST and SSS for Chapter Four

#### Mean Annual SST

$$(1) \quad \text{Sr/Ca} = (m_1 * (\text{ig}) + m_2 * (\text{ag}) + m_3) * \text{SST} + b$$

$$(2) \quad \text{SST} = ((\text{Sr/Ca}) - b) / (m_1 * (\text{ig}) + m_2 * (\text{ag}) + m_3)$$

$$(3) \quad \sigma_{\text{SST}}^2 = \sigma_{\text{Sr/Ca}}^2 * (\partial_{\text{SST}}/\partial_{\text{Sr/Ca}})^2 + \sigma_b^2 * (\partial_{\text{SST}}/\partial_b)^2 + \sigma_{m1}^2 * (\partial_{\text{SST}}/\partial_{m1})^2 + \sigma_{m2}^2 * (\partial_{\text{SST}}/\partial_{m2})^2 \\ + \sigma_{m3}^2 * (\partial_{\text{SST}}/\partial_{m3})^2 + 2 * \sigma_{m1-m2}^2 * (\partial_{\text{SST}}/\partial_{m1}) * (\partial_{\text{SST}}/\partial_{m2}) \\ + 2 * \sigma_{m1-m3}^2 * (\partial_{\text{SST}}/\partial_{m1}) * (\partial_{\text{SST}}/\partial_{m3}) + 2 * \sigma_{m2-m3}^2 * (\partial_{\text{SST}}/\partial_{m3}) * (\partial_{\text{SST}}/\partial_{m2}) \\ + 2 * \sigma_{m1-b}^2 * (\partial_{\text{SST}}/\partial_{m1}) * (\partial_{\text{SST}}/\partial_b) + 2 * \sigma_{m2-b}^2 * (\partial_{\text{SST}}/\partial_{m2}) * (\partial_{\text{SST}}/\partial_b) \\ + 2 * \sigma_{m3-b}^2 * (\partial_{\text{SST}}/\partial_{m3}) * (\partial_{\text{SST}}/\partial_b)$$

where:  $\sigma_{\text{Sr/Ca}}^2$  = (the standard error on the regression)<sup>2</sup>

all other  $\sigma$  are the 1-sigma error on the regression results

$$\partial_{\text{SST}}/\partial_{\text{Sr/Ca}} = 1 / (m_1 * (\text{ig}) + m_2 * (\text{ag}) + m_3)$$

$$\partial_{\text{SST}}/\partial_b = -1 / (m_1 * (\text{ig}) + m_2 * (\text{ag}) + m_3)$$

$$\partial_{\text{SST}}/\partial_{m1} = -((\text{Sr/Ca} - b) * (\text{ig})) / (m_1 * (\text{ig}) + m_2 * (\text{ag}) + m_3)^2$$

$$\partial_{\text{SST}}/\partial_{m2} = -((\text{Sr/Ca} - b) * (\text{ag})) / (m_1 * (\text{ig}) + m_2 * (\text{ag}) + m_3)^2$$

$$\partial_{\text{SST}}/\partial_{m3} = -(\text{Sr/Ca} - b) / (m_1 * (\text{ig}) + m_2 * (\text{ag}) + m_3)^2$$

**Table G.1:** Values of equation 1 parameters.

Parameter	Value	Units
$m_1$	-0.000697	(mmol/mol)(mm/year) <sup>-1</sup> (°C) <sup>-1</sup>
$m_2$	0.00304	(mmol/mol)(mm/year) <sup>-1</sup> (°C) <sup>-1</sup>
$m_3$	-0.0738	(mmol/mol)(°C) <sup>-1</sup>
$b$	10.8	(mmol/mol)

**Table G.2:** Errors and covariances ( $\sigma^2$ ) on the parameters from the regression of eqn. (1) above.

Parameter	Value	Units
Sr/Ca	$9.630 \times 10^{-4}$	mmol/mol
b	0.1858	mmol/mol
$m_1$	$1.410 \times 10^{-7}$	$(\text{mmol/mol})(\text{mm/year})^{-1}(\text{°C})^{-1}$
$m_2$	$2.615 \times 10^{-7}$	$(\text{mmol/mol})(\text{mm/year})^{-1}(\text{°C})^{-1}$
$m_3$	$3.488 \times 10^{-4}$	$(\text{mmol/mol})(\text{°C})^{-1}$
$m_1 - m_2$	$-8.787 \times 10^{-8}$	$(\text{mm/year})^{-2}(\text{mmol/mol})^2(\text{°C})^{-2}$
$m_1 - m_3$	$5.482 \times 10^{-7}$	$(\text{mm/year})^{-1}(\text{mmol/mol})^2(\text{°C})^{-2}$
$m_2 - m_3$	$-1.085 \times 10^{-6}$	$(\text{mm/year})^{-1}(\text{mmol/mol})^2(\text{°C})^{-2}$
$m_1 - b$	$-1.660 \times 10^{-5}$	$(\text{mm/year})^{-1}(\text{mmol/mol})^2(\text{°C})^{-1}$
$m_2 - b$	$9.572 \times 10^{-6}$	$(\text{mm/year})^{-1}(\text{mmol/mol})^2(\text{°C})^{-1}$
$m_3 - b$	$-8.014 \times 10^{-3}$	$(\text{mmol/mol})^2(\text{°C})^{-1}$

#### Winter-Time SST

$$(4) \quad \text{Sr/Ca} = m \cdot \text{SST} + b$$

$$(5) \quad \text{SST} = (\text{Sr/Ca} - b) / m$$

$$(6) \quad \sigma_{\text{SST}}^2 = \sigma_{\text{Sr/Ca}}^2 * (\partial \text{SST} / \partial \text{Sr/Ca})^2 + \sigma_b^2 * (\partial \text{SST} / \partial b)^2 + \sigma_m^2 * (\partial \text{SST} / \partial m)^2 + 2 * \sigma_{m-b}^2 * (\partial \text{SST} / \partial m)$$

where:  $\sigma_{\text{Sr/Ca}}^2$  = (the standard error on the regression)<sup>2</sup>  
all other  $\sigma$  are the 1-sigma error on the regression results  
 $\partial \text{SST} / \partial \text{Sr/Ca} = 1 / (m)$   
 $\partial \text{SST} / \partial b = -1 / (m)$   
 $\partial \text{SST} / \partial m = -(\text{Sr/Ca} - b) / m^2$

**Table G.3:** Values of equation 4 parameters.

Parameter	Value	Units
m	-0.0972	$(\text{mmol/mol})(\text{°C})^{-1}$
b	11.3	(mmol/mol)

**Table G.4:** Errors and covariances ( $\sigma^2$ ) on the parameters from the regression of eqn. (4) above.

Parameter	Value	Units
Sr/Ca	$1.328 \times 10^{-3}$	mmol/mol
b	0.2829	mmol/mol
m	$7.0545 \times 10^{-4}$	$(\text{mmol/mol})(\text{°C})^{-1}$
m - b	$-1.413 \times 10^{-2}$	$(\text{mmol/mol})^2(\text{°C})^{-1}$



## **Appendix H**

### **BB001 X-Radiographs**



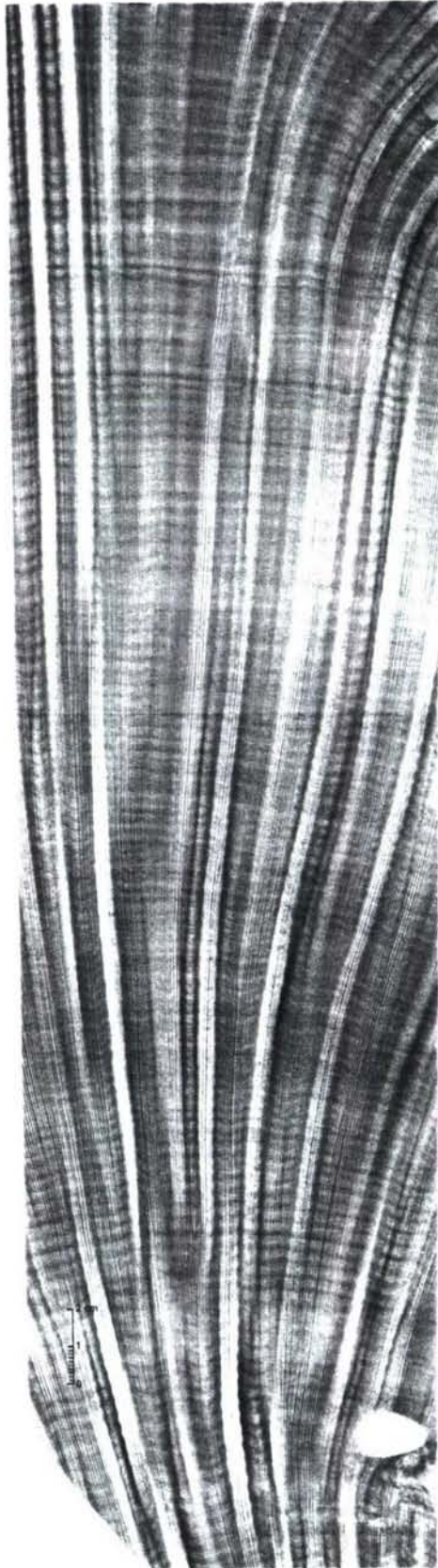
Slab 1







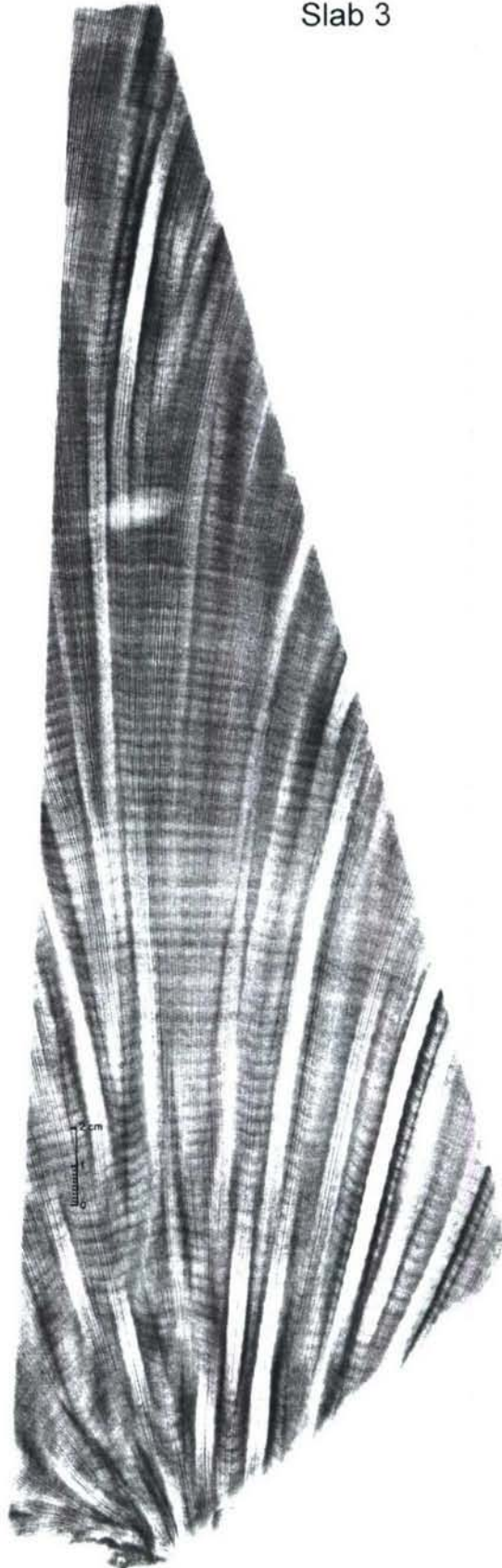
Slab 2







Slab 3





## **Appendix I**

### **Sr/Ca Calibration Data Sets**

*Mean-Annual Data*



Year	Mean-Annual Sr/Ca (mmol/mol)	Inter-annual Growth (Smoothed, mm/year)	Average Growth (mm/year)	Hydrostation S SST (deg C)	Coral ID
1997	9.315	3.49	4.22	23.115	BER 003
1996	9.303	3.32	4.22	23.014	BER 003
1995	9.273	3.42	4.22	23.097	BER 003
1994	9.303	3.31	4.22	23.381	BER 003
1993	9.307	4.01	4.22	23.204	BER 003
1992	9.341	4.00	4.22	23.130	BER 003
1991	9.347	3.89	4.22	23.264	BER 003
1990	9.285	4.02	4.22	23.522	BER 003
1988	9.352	4.01	4.22	22.850	BER 003
1987	9.308	3.67	4.22	22.573	BER 003
1985	9.272	4.12	4.22	23.263	BER 003
1984	9.312	3.76	4.22	22.901	BER 003
1983	9.276	3.98	4.22	22.980	BER 003
1982	9.262	3.71	4.22	23.324	BER 003
1981	9.345	4.26	4.22	22.805	BER 003
1977	9.293	4.47	4.22	23.285	BER 003
1976	9.295	4.58	4.22	23.352	BER 003
1996	9.301	3.24	3.20	23.014	BER 002
1995	9.247	2.45	3.20	23.097	BER 002
1994	9.258	1.67	3.20	23.381	BER 002
1993	9.279	2.45	3.20	23.204	BER 002
1992	9.221	2.93	3.20	23.130	BER 002
1991	9.263	3.22	3.20	23.264	BER 002
1990	9.194	3.03	3.20	23.522	BER 002
1988	9.312	2.97	3.20	22.850	BER 002
1987	9.247	3.00	3.20	22.573	BER 002
1985	9.192	3.50	3.20	23.263	BER 002
1984	9.277	3.72	3.20	22.901	BER 002
1983	9.278	4.23	3.20	22.980	BER 002
1982	9.234	4.18	3.20	23.324	BER 002
1981	9.258	4.32	3.20	22.805	BER 002
1977	9.216	3.31	3.20	23.285	BER 002
1976	9.189	3.55	3.20	23.352	BER 002
1997	9.331	2.97	3.82	23.115	BB 001
1996	9.350	2.97	3.82	23.014	BB 001
1995	9.316	3.08	3.82	23.097	BB 001
1994	9.293	3.08	3.82	23.381	BB 001
1993	9.331	3.19	3.82	23.204	BB 001
1992	9.345	3.13	3.82	23.130	BB 001
1991	9.333	3.35	3.82	23.264	BB 001
1990	9.321	3.30	3.82	23.522	BB 001
1988	9.348	3.41	3.82	22.850	BB 001
1987	9.327	3.85	3.82	22.573	BB 001
1985	9.266	4.07	3.82	23.263	BB 001
1984	9.305	3.96	3.82	22.901	BB 001
1983	9.326	3.68	3.82	22.980	BB 001
1982	9.280	3.90	3.82	23.324	BB 001
1981	9.336	3.85	3.82	22.805	BB 001
1977	9.281	4.45	3.82	23.285	BB 001
1997	9.319	2.03	2.15	23.115	BER 004
1996	9.347	1.97	2.15	23.014	BER 004
1995	9.364	2.05	2.15	23.097	BER 004
1994	9.344	2.17	2.15	23.381	BER 004
1993	9.414	2.38	2.15	23.204	BER 004
1992	9.374	2.40	2.15	23.130	BER 004
1991	9.325	2.59	2.15	23.264	BER 004
1990	9.280	2.54	2.15	23.522	BER 004
1988	9.278	2.49	2.15	22.850	BER 004
1987	9.278	2.65	2.15	22.573	BER 004
1985	9.253	2.98	2.15	23.263	BER 004
1984	9.297	3.00	2.15	22.901	BER 004
1983	9.238	3.10	2.15	22.980	BER 004
1982	9.287	2.79	2.15	23.324	BER 004
1981	9.389	2.88	2.15	22.805	BER 004
1977	9.279	3.16	2.15	23.285	BER 004
1976	9.281	2.68	2.15	23.352	BER 004

## Winter-Time

Winter-time				Winter-time			
Year	Sr/Ca (mmol/mol)	Hydrostation S SST (deg C)	Coral ID	Year	Sr/Ca (mmol/mol)	Hydrostation S SST (deg C)	Coral ID
1997	9.37	20.218	BER 002	1987	9.44	19.717	BER 003
1996	9.37	19.291	BER 002	1986	9.33	21.720	BER 003
1995	9.31	20.208	BER 002	1985	9.37	19.941	BER 003
1994	9.30	20.759	BER 002	1984	9.44	20.443	BER 003
1993	9.33	20.534	BER 002	1983	9.41	20.496	BER 003
1992	9.35	20.075	BER 002	1982	9.49	19.666	BER 003
1991	9.38	20.808	BER 002	1981	9.45	19.669	BER 003
1990	9.26	21.013	BER 002	1979	9.45	20.137	BER 003
1989	9.40	20.465	BER 002	1978	9.44	20.630	BER 003
1988	9.46	20.203	BER 002	1977	9.43	19.701	BER 003
1987	9.38	19.717	BER 002	1976	9.39	20.999	BER 003
1986	9.31	21.720	BER 002	1997	9.41	20.218	BB 001
1985	9.36	19.941	BER 002	1996	9.44	19.291	BB 001
1984	9.32	20.443	BER 002	1995	9.42	20.208	BB 001
1983	9.41	20.496	BER 002	1994	9.38	20.759	BB 001
1982	9.43	19.666	BER 002	1993	9.42	20.534	BB 001
1981	9.30	19.669	BER 002	1992	9.44	20.075	BB 001
1979	9.43	20.137	BER 002	1991	9.42	20.808	BB 001
1978	9.39	20.630	BER 002	1990	9.41	21.013	BB 001
1977	9.39	19.701	BER 002	1989	9.40	20.465	BB 001
1976	9.34	20.999	BER 002	1988	9.43	20.203	BB 001
1997	9.40	20.218	BER 003	1987	9.42	19.717	BB 001
1996	9.44	19.291	BER 003	1986	9.31	21.720	BB 001
1995	9.41	20.208	BER 003	1985	9.45	19.941	BB 001
1994	9.41	20.759	BER 003	1984	9.40	20.443	BB 001
1993	9.40	20.534	BER 003	1983	9.42	20.496	BB 001
1992	9.51	20.075	BER 003	1982	9.45	19.666	BB 001
1991	9.48	20.808	BER 003	1981	9.46	19.669	BB 001
1990	9.37	21.013	BER 003	1979	9.40	20.137	BB 001
1989	9.35	20.465	BER 003	1978	9.41	20.630	BB 001
1988	9.43	20.203	BER 003	1977	9.39	19.701	BB 001

<b>REPORT DOCUMENTATION PAGE</b>	<b>1. REPORT NO.</b> MIT/WHOI 2007-10	<b>2.</b>	<b>3. Recipient's Accession No.</b>
<b>4. Title and Subtitle</b> Geochemistry of Slow-Growing Corals: Reconstructing Sea Surface Temperature, Salinity and the North Atlantic Oscillation			<b>5. Report Date</b> June 2007
<b>7. Author(s)</b> Nathalie Fairbank Goodkin			<b>6.</b>
<b>9. Performing Organization Name and Address</b> MIT/WHOI Joint Program in Oceanography/Applied Ocean Science & Engineering			<b>8. Performing Organization Rept. No.</b>
			<b>10. Project/Task/Work Unit No.</b> MIT/WHOI 2007-10
			<b>11. Contract(C) or Grant(G) No.</b> (C) OCE-0402728 (G)
<b>12. Sponsoring Organization Name and Address</b> National Science Foundation			<b>13. Type of Report &amp; Period Covered</b> Ph.D. Thesis
			<b>14.</b>
<b>15. Supplementary Notes</b> This thesis should be cited as: Nathalie Fairbank Goodkin, 2007. Geochemistry of Slow-Growing Corals: Reconstructing Sea Surface Temperature, Salinity and the North Atlantic Oscillation. Ph.D. Thesis. MIT/WHOI, 2007-10.			
<b>16. Abstract (Limit: 200 words)</b> A 225-year old coral from the south-shore of Bermuda (64°W, 32°N) provides a record of decadal-to-centennial scale climate variability. The high accretion rates, longevity, and skeletal growth bands found in coral skeletons make them an ideal resource for well-dated, seasonal climate reconstructions. Coral skeletons incorporate strontium (Sr) and calcium (Ca) in relative proportions inversely to the sea surface temperature (SST) in which the skeleton is secreted. $\delta^{18}\text{O}$ of the coral skeleton changes based on both temperature and the $\delta^{18}\text{O}$ of sea water ( $\delta\text{O}_w$ ), and $\delta\text{O}_w$ is proportional to sea surface salinity (SSS). Sr/Ca was used to reconstruct winter-time and mean-annual SST, employing the first growth-corrected Sr/Ca-SST model. SSTs are ~1.5°C colder during the end of the Little Ice Age than today. SSS is fresher during that time. Winter-time SSTs at Bermuda are correlated to phases of the North Atlantic Oscillation (NAO). Using winter Sr/Ca as a proxy for temperature, we show strong coherence to the NAO at multi-decadal and inter-annual frequencies. These coral records show changes in variance in the NAO during the late 20 <sup>th</sup> century, but limited changes in the mean phase of the NAO, implying that climate change may be pushing the NAO to extremes but not to a new mean position.			
<b>17. Document Analysis</b> <b>a. Descriptors</b> Sr/Ca $\delta^{18}\text{O}$ NAO  <b>b. Identifiers/Open-Ended Terms</b>    <b>c. COSATI Field/Group</b>			
<b>18. Availability Statement</b> Approved for publication; distribution unlimited.		<b>19. Security Class (This Report)</b> UNCLASSIFIED	<b>21. No. of Pages</b> 281
		<b>20. Security Class (This Page)</b>	<b>22. Price</b>